EXPRESSION OF CHEMOKINES CXCL4 AND CXCL7 IN THE SYNOVIUM AT AN EARLY STAGE OF RHEUMATOID ARTHRITIS

By

NICHOLA JAYNE ADLARD

A thesis submitted to

The University of Birmingham

For the degree of DOCTOR OF PHILOSOPHY

School of Immunity and Infection

College of Medical and Dental Sciences

The University of Birmingham

August 2015

ABSTRACT

Identification of suitable biomarkers is growing increasingly important for the treatment of rheumatoid arthritis (RA). They can be measured in a number of different biological materials and can provide clinical information regarding prediction, diagnosis, and prognosis of disease, as well as response to therapeutics.

In this thesis, I utilised synovial biopsies collected from patients enrolled in the Birmingham Early Inflammatory Arthritis Cohort (BEACON) to test the hypothesis that detection of expression of CXCL4 and CXCL7 may be used to predict progression of early stage synovitis to RA. I found that these two chemokines, CXCL4 and CXCL7, were predominantly expressed on macrophages within the synovium of patients presenting with early synovitis. Increased CXCL4 and CXCL7 was observed in patients with early RA compared to those with a resolving disease course. However, this increase was transient as expression in treatment naive established RA patients (>12 weeks duration, <3 years duration) was comparable to uninflamed controls.

Moreover, I identified expression of a variant of CXCL4, CXCL4L1 in the rheumatoid synovium. Expression of this potent inhibitor of angiogenesis was evident in the lining layer of the synovium.

These data highlight CXCL4 and CXCL7 as potential predictors of disease outcome in patients presenting with early synovitis.

To Joseph,

“Have you ever really had a teacher? One who saw you as a raw but precious thing, a jewel that, with wisdom, could be polished to a proud shine?”

— Mitch Albom, Tuesdays with Morrie.

ACKNOWLEDGMENTS

Firstly, I wish to thank my supervisor, Dr Dagmar Scheel-Toellner, for giving me the opportunity to study at the University of Birmingham, and for all her help, support and kind words of encouragement during my PhD. I would also like to give thanks to my second supervisor, Dr Andrew Filer, as well as Prof Karim Raza for their help with obtaining the patient samples for this work. I would, also, like to thank Arthritis Research UK for funding the project.

I would like to say a huge thank you to Miss Holly Adams for all her help with collecting the biopsy samples for this work, for her support in the laboratory, for her tidy birds, and for her constant supply of tea and cake. I doubt I would have survived the past 3 years without your help. I would like to kindly acknowledge Miss Amy Wilson for her help with tissue sectioning and for all her kind words during her short time at the university. I would like to give a special thanks to members of the Rheumatology Research Group, both past and present; Dr Debbie Hardie, Mr. Philip Jones, Dr Elizabeth Clay, Miss Dominika Nanus, Dr Rachel Bayley, Mr Martin Fitzpatrick, Dr Lorraine Yeo, Miss Julia Spengler, Dr Farrah Ali, and Mr Bôzo Lugonja. I would, also, like to thank Dr Steve Watson and Miss Samantha Montague for allowing me to spend time in their laboratory to run the soluble GPVI assay.

Finally I would like to thank my fiancé, Joseph. Thank you for all of your support during my PhD. I doubt I would have made it through without you.

CONTENTS

LIST OF FIGURES

LIST OF TABLES

ABBREVIATIONS

ACR	American College of Rheumatology
ACPA	Anti-citrullinated protein antibody
ARA	American Rheumatism Association
BSA	Bovine serum albumin
βTG	β-Thromboglobulin
CD	Cluster of Differentiation
CRP	C-Reactive Protein
CTAP-III	Connective tissue activating peptide-III
DAS28	Disease Activity Score 28
DC	Dendritic cell
DMARDS	Disease modifying anti-rheumatic drugs
ELISA	Enzyme Linked Immunosorbent Assay
EULAR	European League against Rheumatism
ESR	Erythrocyte Sedimentation Rate
FCS	Foetal calf serum
FFPE	Formalin fixed, paraffin embedded
GAPDH	Glyceraldehyde-3-phosphate dehydrogenase
HBRC	Human Biomaterials Resource Centre
Mo-DC	Monocyte-derived dendritic cell
mRNA	Messenger RNA
NAP-2	Neutrophil activating peptide-2
PBS	Phosphate buffered saline
pDC	Plasmacytoid dendritic cell
PF4	Platelet factor 4
PF4V1	Platelet factor 4 variant 1
PPBP	Pro-platelet basic protein
RA	Rheumatoid arthritis
RNA	Ribonucleic Acid
RF	Rheumatoid Factor
sGPVI	Soluble glycoprotein VI

SWJ28	Swollen Joint Count 28
TJC28	Tender Joint Count 28
TLR	Toll like receptor

PUBLICATION

Yeo, L., **Adlard, N**., Biehl, M., Juarez, M., Smallie, T., Snow, M., Buckley, C. D., Raza, K., Filer, A., Scheel-Toellner, D (2015). Expression of chemokines CXCL4 and CXCL7 by synovial macrophages defines an early stage of rheumatoid arthritis. *Annals of Rheumatic Diseases*. Published Online First [9th April 2015] doi: 10.1136/annrheumdis-2014-206921.

1 INTRODUCTION

1.1 Rheumatoid arthritis

Rheumatoid arthritis (RA) is a chronic, debilitating inflammatory disease that affects approximately 1% of the world's population. The onset of disease occurs most commonly in the fifth decade of life, with increased numbers of cases being reported in females rather than males. It manifests as symmetrical painful, reddened, swollen joints (Gorman and Cope, 2008, Iwamoto et al, 2008). The joints commonly affected by RA include the wrists, knees, fingers and toes (Smolen and Redlich, 2014). Chronic joint inflammation ultimately leads to bone and cartilage degradation, deformity and disability. Further complications can arise in patients suffering from RA including cardiovascular, respiratory, musculoskeletal and neurological problems. Patients with RA are more likely to develop premature atherosclerosis and myocardial infarction than those unaffected (Karatoprak et al, 2012).

Due to the presence of autoantibodies to citrullinated proteins (ACPA) and/or Rheumatoid Factor (RF) in a large proportion of patients, RA is considered an autoimmune disease (Gorman and Cope, 2008). ACPA target proteins that have undergone post translational modification of amino acid side chains from arginine to citrulline by peptidylarginine deiminase (PAD) enzymes (Figure 1.1). Proteins that may be subject to this post translational modification include collagen, α-enolase, vimentin, and fibrin (Smolen and Redlich, 2014). RF is directed towards the Fc domain of IgG antibodies. It is present in approximately 75% of RA patients, but it is not specific for RA as it is reported in other autoimmune diseases as well as in 5% of the healthy population (Nijenhuis et al, 2004). The presence of both

autoantibodies can be found a number of years prior to the onset of clinically apparent disease. In addition to ACPA and RF, antibodies directed against carbamylated proteins (anti-CarP antibodies) may be useful predictors of RA as their presence also predates the onset of clinical symptoms (Shi et al, 2013). Carbamylation is a post translational modification involving cyanate. It results in a modification of lysine to homocitrulline (Figure 1.1) (Shi et al, 2013). Under normal conditions, cyanate is maintained in equilibrium with urea. Cyanate levels may also increase during inflammation due to the release of hydrogen peroxide and myeloperoxidase from neutrophils which drive the loss of equilibrium between thiocyanate and cyanate. A shift towards an increase in cyanate results in subsequent protein carbamylation (Trouw et al, 2013). Anti-carbamylated protein antibodies have been identified in both ACPA positive RA (49-73%) and ACPA negative RA (8-14%) patients (Jiang et al, 2014). They have also been identified in patients suffering from arthralgia (Shi et al, 2013) and juvenile idiopathic arthritis (Hissink Muller et al, 2013).

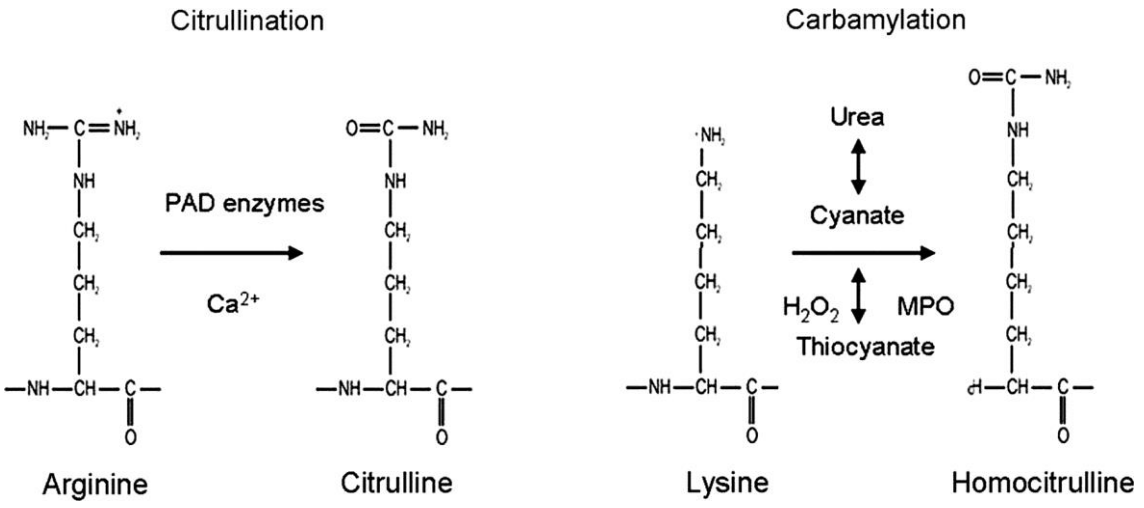

Figure 1.1 Citrullination and Carbamylation: Two post translational modifications recognised by autoantibodies. Figure from Trouw et al, 2013.

Although the exact aetiology of RA is unknown, there is strong evidence linking genetic factors, such as HLA-DR and PTPN22 (Bowes and Barton, 2008, Silman and Pearson, 2002), gender, and environmental factors, such as cigarette smoking and infectious diseases (Epstein-Barr virus, *Porphyrymonas gingivalis*, *Proteus* and *Mycoplasma*), to the pathogenesis of RA (Silman and Pearson, 2002). Pregnancy and the use of the oral contraceptive pill may be associated with a decreased risk of RA, whilst the postpartum period following pregnancy and breast feeding after the first pregnancy poses an increased risk to the development of RA (Silman and Pearson, 2002). This may indicate a role for hormones in the development of RA. Overall, the contribution of genetic factors to the risk of developing RA is approximately 60% (Bowes and Barton, 2008), whereas 40% is attributed to environmental risk factors.

Part of the heritability of RA and its association with the HLA-DR positioned on chromosome 6 (6p21.3) can be explained by the 'shared epitope' hypothesis. The 'shared epitope' is encoded by a number of different susceptibility alleles; HLA-DR4 (DRB1*0401, *0404, and *0405), HLA-DR1 (DRB1*0101 and *0102), and HLA-DR10 (DRB1*1010). In the Caucasian population the HLA-DRB1*0401 and *0404 alleles are associated with the greatest risk of RA (De Almeida et al, 2011, Gregersen et al, 1987, Pratesi et al, 2013). Individuals who are heterozygous for HLA-DRB1*0401/*0404 have been associated with suffering early onset disease that is far more severe (Bowes and Barton, 2008). Furthermore the combination of cigarette smoking and the 'shared epitope' genes further increases the risk of developing RA (Lee et al, 2007). In the Asian population, the allele associated with the greatest risk of RA is HLA-DRB1*0405. These alleles encode an amino acid sequence from position 70 to 74 (70QRRAA74, 70KRRAA74, or 70RRRAA74) in the third hypervariable region (HVR3) of the first domain of the HLA-DRβ1 chain. Alleles that offer protection against RA or that lead

to a less erosive form of RA have also been identified; HLA-DRB1*0103, *0402, *1102, *1103, *1301, *1302, and *1304. These alleles encode an amino acid sequence with a negatively charged aspartic acid residue at position 70 or encode the sequence $_{70}$DERAA$_{74}$ (Pratesi et al, 2013). The 'shared epitope' amino acid sequences are found in the MHC class II peptide binding groove and therefore may influence antigen presentation in RA.

The protein tyrosine phosphatase, non-receptor type 22 (PTPN22) gene located on chromosome 1p13 has also been associated with RA as well as in other autoimmune diseases such as type I diabetes mellitus, Hashimoto's thyroiditis, Addison's disease and systemic lupus erythematosus (SLE). A single nucleotide polymorphism (SNP) in the PTPN22 gene (Rs2476601, 1858C>T, R620W), is evident in 13.8% of RA patients compared to 8.8% of controls (Begovich et al, 2004). PTPN22 encodes a 110 kDa cytoplasmic protein lymphoid tyrosine phosphatase, known as Lyp. Lyp functions as a down regulator of effector T cell and memory T cell receptor signalling pathways through its association with the SH3 domain of Csk. Therefore the PTPN22 polymorphism may be associated with RA due to the inability of the variant Lyp phosphatase to bind Csk and down-regulate T cell activation (Begovich et al, 2004).

Although the HLA-DRB1 alleles and the PTPN22 polymorphism account for a large proportion of the genetic susceptibility to RA, several other genes have been associated with the development and severity of RA including PADI4, STAT4, PRKCQ, TRAF1/C5, CTLA4 and the 6q23 region (Bowes and Barton, 2008, Okada et al, 2014).

1.2 Early rheumatoid arthritis

With an estimated cost to the UK economy of £3.8-4.75 billion per year, RA is considered a major economic burden (NICE, UK). It is therefore essential to diagnose patients as early as possible and target expensive therapeutics to those who are most likely to respond. There is evidence to support a 'window of opportunity' hypothesis in early RA whereby patients diagnosed within 3 months of disease onset (Early RA) are more likely to benefit from treatment with disease modifying anti-rheumatic drugs (DMARDs) and various biological agents such as rituximab and etanercept than patients diagnosed later in disease (Cush, 2007). Early treatment appears to result in reduced disease activity score and the achievement of clinical remission (Demoruelle and Deane, 2012). The psychosocial consequences of disease such as work place disability leading to loss of employment as well as patient fatigue, pain and emotional stress may also be prevented by earlier treatment.

1.3 The classification of rheumatoid arthritis

The American Rheumatism Association (ARA) derived the 1987 criteria for the classification of RA. The revised criteria were drawn up based on the previous 1958 ARA criteria with the aim of simplifying and improving the specificity and sensitivity of the classification. Although classification criteria are predominantly used in clinical trials to standardise the enrolled participants, they may also be used within the clinic to aid in the routine diagnosis of RA (Cornec et al, 2012). In order to reach a diagnosis of RA using the ARA 1987 classification criteria, at least 4 out of the 7 criteria must be present and criteria 1-4 must be evident for at least 6 weeks. The criteria included morning stiffness of at least 1 hour before

improvement, arthritis of 3 or more joints, symmetric arthritis and the presence of serum rheumatoid factor (Table 1.1).

In 2010, the American College of Rheumatology / European League against Rheumatism (ACR/EULAR) collaborative group reassessed the classification criteria for RA. This was done, as the previous 1987 classification criteria were deemed too insensitive for the diagnosis of early RA. The 2010 ACR/EULAR criteria is split into 4 domains; joint involvement, serology, acute-phase reactants, and duration of symptoms. Each domain is assessed and given a score (Table 1.2). The scores from each individual domain are then combined and a classification is given. A score of ≥6/10 is regarded as 'definite' RA. An advantage of the 2010 ACR/EULAR criteria over the ARA 1987 classification criteria is the ability to identify patients at an earlier stage of disease rather than at the established stage.

Criterion	Definition
1. Morning stiffness	Morning stiffness in and around the joints, lasting at least 1 hour before maximal improvement
2. Arthritis of 3 or more joint areas	At least 3 joint areas simultaneously have had soft tisse swelling or fluid (not bony overgrowth alone) observed by a physician. The 14 possible areas are right or left PIP, MCP, wrist, elbow, knee, ankle, and MTP joints
3. Arthritis of hand joints	At least 1 area swollen (as defined above) in a wrist, MCP, or PIP joint
4. Symmetric arthritis	Simultaneous involvement of the same joint areas (as defined in 2) on both sides of the body (bilateral involvement of PIPs, MCPs, or MTPs is acceptable without absolute symmetry)
5. Rheumatoid nodules	Subcutaneous nodules, over bony prominences, or extensor surfaces, or in juxtaarticular regions, observed by a physician
6. Serum rheumatoid factor	Demonstration of abnormal amounts of serum rheumatoid factor by any method for which the result has been positive in <5% of normal control subjects
7. Radiographic changes	Radiographic changes typical of rheumatoid arthritis on posteroanterior hand and wrist radiographs, which must inclide erosions or unequivocal bony decalcification localized in or most marker adjacent to the involved joints (osteoarthritis changes alone do not qualify)

*For classification purposes, a patient shall be said to have rheumatoid arthritis if he/she has satisfied at least 4 of these 7 criteria. Criteria 1 through 4 must have been present for at least 6 weeks. Patients with 2 clinical diagnoses are not excluded. Table from Arnett et al, 1988.

Table 1.1 The American Rheumatism Association 1987 criteria for the classification of rheumatoid arthritis

	Score
A. Joint involvement	
1 large joint	**0**
2-10 large joints	**1**
1-3 small joints (with or without involvement of large joints)	**2**
4-10 small joints (with or without involvement of large joints)	**3**
>10 joints (at least 1 small joint)	**5**
B. Serology (at least 1 test result is needed for classification)	
Negative RF and negative ACPA	**0**
Low-positive RF or low-positive ACPA	**2**
High-positive RF or high-positive ACPA	**3**
C. Acute-phase reactants (at least 1 test result is needed for classification)	
Normal CRP and normal ESR	**0**
Abnormal CRP or abnormal ESR	**1**
D. Duration of symptoms	
<6 weeks	**0**
≥6 weeks	**1**

*Classification criteria for the diagnosis of rheumatoid arthritis. For a patient to be diagnosed with 'definite' RA a total score of ≥6/10 must be achieved. Table from Aletaha et al, 2010.

Table 1.2 The 2010 American College of Rheumatology/European League Against Rheumatism classification criteria for rheumatoid arthritis.

1.4 The synovium

The synovium is a thin membrane that lines the joint cavity. It is the site of synovial fluid production which acts to lubricate, maintain mobility, and provide nutrition to the cartilaginous surfaces. The synovium is divided into two regions termed; the synovial lining layer and the synovial sublining layer. The synovial lining is approximately 2-3 cell layers thick and consists of two different cell types; type A macrophage-like synoviocytes, and the type B fibroblast-like synoviocytes. In the normal synovium, the macrophage-like synoviocytes account for 10-20% of the lining layer.

The type A macrophage-like synoviocytes can be characterised by their expression of the surface markers; CD11b, CD14, CD16α, CD68, and CD163. They also express MHC class II molecules, as well as neuron-specific esterase and the cathepsins B, D, and L (Pap et al, 2000). Type A macrophage-like synoviocytes may play an important role in the presentation of antigen as well as removal of cellular debris from the joint by phagocytosis. Type B fibroblast-like synoviocytes express uridine diphosphoglucose dehydrogenase (UDPGD) required for the synthesis of hyaluronic acid, and CD55. Furthermore they express vascular cell adhesion molecule (VCAM-1), intracellular adhesion molecule (ICAM-1), β1 integrins and cadherin-11. The type B fibroblast-like synoviocytes synthesise a number of glycoproteins including lubricin, fibronectin and laminin, and furthermore during inflammation they produce a large number of inflammatory mediators including cytokines, matrix metalloproteinases and prostaglandins (Bartok and Firestein, 2010).

The synovial sublining layer is highly vascularised with a rich network of arterioles, venules and capillaries (Haywood and Walsh, 2001). It can be split into three different tissue subtypes; adipose, areolar and fibrous. The adipose tissue is largely characterised by the presence of adipocytes. Areolar tissue is the most common tissue type and is often found in larger joints. It is folded in appearance into villous projections. The fibrous sublining is poorly vascularised and often resembles fibrocartilage. The normal synovial sublining contains very few inflammatory cells. Those that are present may include $CD4^+$ and $CD8^+$ T cells and B cells.

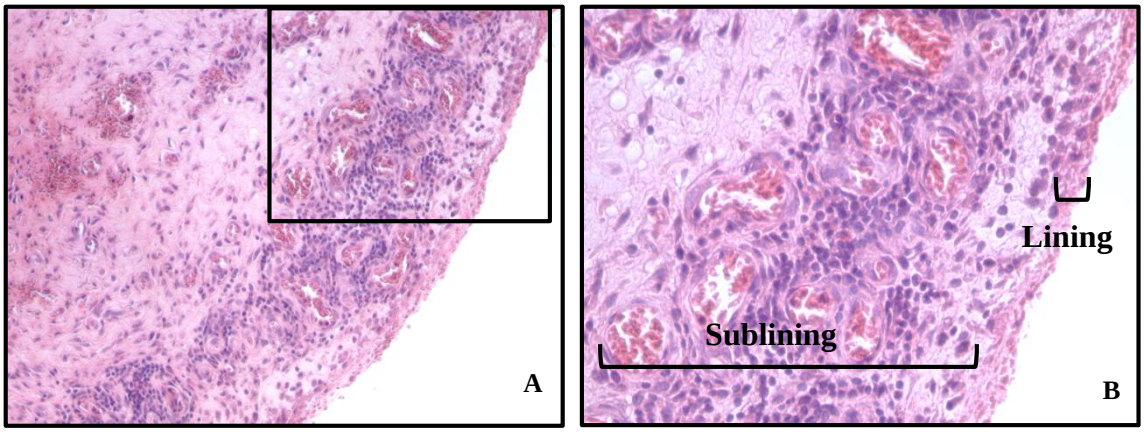

Figure 1.2 The synovium in early rheumatoid arthritis. Haematoxylin and Eosin stained synovial tissue biopsy from an early RA patient enrolled in the BEACON cohort (BX115). A large number of blood vessels surrounded by inflammatory infiltrate is evident in the sublining. Images were taken using the Nikon Eclipse E400 microscope at **A**) x200 total magnification and, **B**) x400 total magnification by Nichola Adlard and Dagmar Scheel-Toellner.

In RA, the main site of inflammation is the synovium with evidence of synovial lining hyperplasia accompanied by an infiltrate of inflammatory cells into the synovium, including T cells, B cells, plasma cells, dendritic cells (DCs), macrophages, mast cells and neutrophils (Kraan et al, 1999). The synovial lining that was once 2-3 cells layers thick can expand up to 10-20 cell layers thick (Figure 1.2). This expansion is a result of an increase in the number of both type A macrophage-like and type B fibroblast-like synoviocytes (Bartok and Firestein, 2010). In the sublining, T cells, which are predominantly $CD4^+CD45RO^+$ memory cells, are accountable for 30-50% of the infiltrating cells. $CD8^+$ T cells are also evident and are often found scattered throughout the synovium (Pratts et al, 2009). B cells numbers vary considerably between patients and may be involved in autoantibody production (Bartok and Firestein, 2010). The synovial fluid is also rich in inflammatory cells during RA, with mostly neutrophils present (Iwamoto et al, 2008). Pannus tissue, which is characteristic of RA pathology, acts like a locally invasive tumour. It is rich in type B fibroblast-like synoviocytes,

macrophages, and osteoclasts. Osteoclasts play an important role in the pathogenesis of RA by degrading bone via the production of matrix metalloproteinases (MMPs), hydrochloric acid and cathepsin K (Väänänen et al, 2000). Osteoclastogenesis is driven by the expression of RANKL and MCSF in the synovium. RANKL is expressed by synovial fibroblasts, B cells and T cells. The type B fibroblast-like synoviocytes also play a role in the degradation of cartilage via the release of a number of proteases including MMPs. Both resident and infiltrating inflammatory cells are a rich source of chemokines and cytokines, including TNFα, IL-1, IL-6, IL-17 and IL-23 (Gorman and Cope, 2008, McInnes and Schett, 2007).

1.5 Macrophages

Macrophages and monocytes belong to the mononuclear phagocytic system (Chow et al, 2011). Monocytes are small (12-20 μm in diameter) cells with kidney shaped nuclei. They are accountable for 2-8% of peripheral blood mononuclear cells. Monocytes differentiate from common myeloid progenitor cells within the bone marrow and are subsequently released into the blood whereby they circulate for 12-32 hours before migrating into tissues. Monocytes may be classified into three different subsets based on cell surface marker and chemokine receptor expression; classical, intermediate, and non-classical (Chow et al, 2011). Classical monocytes (90-95% of circulating monocytes) are $CD14^{hi}$, $CD16^{-}$, $CD64^{+}$, $CD62L^{+}$, $CCR2^{hi}$, and $CX3CR1^{low}$. They possess phagocytic and anti-microbial functions. Intermediate monocytes (2-11% of circulating monocytes) are pro-inflammatory cells that express $CD14^{hi}$, $CD16^{+}$, $CD64^{+}$, $CCR2^{low}$, and $CX3CR1^{hi}$ (Yang et al, 2014). They produce high levels of TNFα, IL-1β and IL-6. Non-classical monocytes (5-10% of circulating monocytes) are anti-inflammatory cells that produce IL-1RA. They express $CD14^{low}$, $CD16^{hi}$, $CD64^{-}$, $CCR2^{low}$, and $CX3CR1^{hi}$. As for murine monocytes, they are also classified into classical (60%

circulating monocytes), intermediate and non-classical groups (40% circulating monocytes). Murine monocyte cell surface markers differ from their human counterparts. They are grouped based on Ly6C, CD43, and CD11b expression. Murine monocytes do, however, express the same chemokine receptors, CCR2 and CX3CR1 (Chow et al, 2011).

Once in the tissue, monocytes differentiate into macrophages. Macrophages are much larger (25-50 μm in diameter) and reside in the tissue for 2-4 months. Within the tissues, macrophages are subdivided into different subpopulations based on their anatomical location. For example, macrophages within the liver are referred to as Kupffer cells, in the bone; osteoclasts, and within the central nervous system; microglia (Murray and Wynn, 2011, Zhou et al, 2014). Macrophages play an important role in both the innate and adaptive immune system. They are professional phagocytic cells that can engulf invading pathogens as well as cellular debris and apoptotic cells. Macrophages can also present processed antigen to T cells in the context of MHC class II (Gordon, 2014, Mosser, 2003).

Similar to the classification of T cells into Th1/Th2/Th17/Treg subsets, macrophages have been loosely grouped into two subsets referred to as M1 macrophages and M2 macrophages, although their phenotypes probably represent extremes of a continuous spectrum seen in humans *in vivo*. M1 macrophages, also described as classically activated macrophages, have a pro-inflammatory phenotype (Murray and Wynn, 2011). They can be induced by IFNγ, LPS, GM-CSF and TNF-α, and as a result M1 macrophages secrete a large number of pro-inflammatory mediators including cytokines; IL-1, IL-6, TNFα, IL-12, and IL-23, and chemokines; CXCL9, CXCL10 and CXCL11 (Koh and DiPietro, 2011, Li et al, 2012). M1

macrophages are extremely effective at killing intracellular pathogens through the production of reactive oxygen species (ROS) and have an enhanced ability in presenting antigen in the context of MHC class II (Cassetta et al, 2011, Mosser, 2003). M2 macrophages, or alternatively activated macrophages, are poor killers of intracellular pathogens and are also not as effective as M1 'classically activated' macrophages at presenting antigen in the context of MHC class II. M2 macrophages demonstrate an anti-inflammatory regulatory phenotype. Therefore they play important roles in the dampening of the inflammatory response, tissue repair through the release of extracellular matrix components, and in the resolution of inflammation (Murray and Wynn, 2011). M2 macrophages are induced by IL-4, IL-10, IL-13, TGF-β, M-CSF, immune complexes and glucocorticoids (Cassetta et al, 2011, Koh and DiPietro, 2011, Mosser, 2003). M2 macrophages express increased levels of cytokines; IL-4 and IL-10, and chemokines; CCL16, CCL17, CCL18, CCL22, CCL24. They also express the scavenger receptor CD163 and the mannose receptor CD206 (Li et al, 2012, Murray and Wynn, 2011). Due to the restrictive nature of the M1 and M2 classification system, macrophages may also be grouped based on their function; classically activated macrophages, wound healing macrophages and immune regulatory macrophages.

In 2012, Schulz et al described an alternative origin for tissue-resident macrophages. It is well documented that renewal of haematopoietic cells arise from the differentiation of haematopoietic stem cells (HSCs). However, in this study, it was reported that tissue macrophages in the brain, lung, liver, and epidermis in the adult mouse originate from yolk sac derived erythro-myeloid progenitors (EMPs). It was reported that yolk sac derived macrophages may co-exist with macrophages derived from HSCs. Moreover Hashimoto et al (2013) reported that tissue resident macrophages repopulate independently of monocytes.

1.5.1 Macrophages in rheumatoid arthritis

In RA, macrophages play a fundamental role in the pathogenesis of disease (Kennedy et al, 2011, Li et al, 2012). They have been found in abundance in the rheumatoid synovium and at the cartilage-pannus junction, and account for 30-40% of the cellular infiltrate (Burmester et al, 1997, Kennedy et al, 2011, Kraan et al, 1999). Although within the rheumatoid synovium, synovial macrophages have neither been classified as M1 or M2, it has been reported that both pro- and anti- inflammatory macrophages are present. However, there is an imbalance towards the pro-inflammatory phenotype rather than the anti-inflammatory phenotype (Li et al, 2012). Synovial macrophages have been shown to secrete a large variety of proinflammatory mediators that drive inflammation and exacerbate joint destruction including IL-1, IL-6, TNFα, and IL-23 as well as a host of chemokines including CXCL5, CXCL7, CXCL8, CXCL9, CXCL10, CCL2, CCL3, CCL5 and CCL18, and ROS (Li et al, 2012, Szekanecz et al, 2007). In contrast, synovial macrophages have also been shown to release a variety of anti-inflammatory mediators including IL-10, TGF-β, soluble TNF-R, and IL-1Ra (Li et al, 2012). Synovial macrophages have also been shown to release matrix metalloproteinases -1, -2 and -9 (MMP-1, MMP-2 and MMP-9) which degrade articular cartilage and bone, tissue inhibitors of matrix metalloproteinases -1 and -2 (TIMP-1 and TIMP-2), and cathepsins B, L, S and K. Synovial macrophages play a role in supporting prolonged B cell activation via the secretion of B cell stimulating factor, BLys, and the proliferation-inducing ligand, APRIL (Szekanecz et al, 2007). They also drive T cell activation via the presentation of antigen in context with MHC class II and drive Th1 cell polarisation via the release of IL-12.

Synovial macrophages have been validated as a biomarker in RA with the number of $CD68^+$ synovial macrophages in the synovial sublining being indicative of disease severity. Furthermore an increased number of macrophages have been observed in clinically affected joints as opposed to non-affected joints and the number of macrophages has been shown to correlate with radiographic progression (Burmester et al, 1997, Kennedy et al, 2011). Moreover, a reduction in the number of synovial macrophages may indicate a good response to therapy and has been reported to correlate with clinical improvement (Bresnihan et al, 2007, Haringman et al, 2005, Wijbrandts et al, 2007).

1.6 Plasmacytoid dendritic cells

In the human, there are two main populations of dendritic cell (DC); myeloid and plasmacytoid. They play an important role in the induction of the innate and adaptive immune response, induction of tolerance, and establishment of immunological memory (Mclellan and Kämpgen, 2000). Myeloid DCs, or conventional DCs as they are often described, are a population of professional antigen presenting cells (APC). They originate in the bone marrow and subsequently migrate to the non-lymphoid tissues where they are referred to as immature DCs. It is within the non-lymphoid tissues where they encounter foreign pathogens. DCs phagocytose pathogens and migrate to the lymphoid tissue whereby they present processed antigen to both $CD4^+$ and $CD8^+$ T cells in the context of major histocompatibility molecules (MHC) (Banchereau et al, 2000). Plasmacytoid dendritic cells (pDCs) are a small population (0.3-0.5% of peripheral blood mononuclear cells) of professional antigen presenting cells that are Lineage-, MHC class II^+, $CD4^+$, $CD45RA^+$, $CD123^+$/IL-3Rα^+, $ILT3^+$, $ILT1^-$, $CD303^+$/BDCA-2^+ and $CD304^+$/BDCA-4^+ (Colonna et al, 2004, Guéry and Hugues, 2013, Reizis et al, 2011). Human pDCs can be distinguished from myeloid dendritic cells (mDCs) in

that they do not express CD11c (Guéry and Hugues, 2013). However, murine pDCs do express low levels of CD11c (Swiecki and Colonna, 2010). Murine pDCs also differ from human pDCs in that they do not express the human specific pDC markers; BDCA-2, BDCA-4, ILT-7 and CD123 but instead express Siglec-H, BST-2, Ly6C and Ly49Q (Reizis et al, 2011, Swiecki and Colonna, 2010). Murine pDCs also express CD8 which may serve as a maturation and activation marker. Plasmacytoid dendritic cells were initially referred to as plasmacytoid T cells and later as plasmacytoid monocytes due to the expression of both lymphoid; CD4, and myeloid cell markers; CD68 and CD123/IL-3Rα (Swiecki and Colonna, 2010). However, in the 1990s they were finally described as plasmacytoid dendritic cells (pDCs) after it was observed that isolated cells could differentiate to dendritic cells in the presence of IL-3 or IL-3 and CD40L. Plasmacytoid DCs are key players in antiviral immunity due to their ability to produce IFNα in response to viral infection (Mclellan and Kämpgen, 2000).

Plasmacytoid dendritic cells have been identified in the foetal thymus, liver and bone marrow (Colonna et al, 2004). In the adult, pDCs are produced in the bone marrow and subsequently released into the blood (Guéry and Hugues, 2013). They arise from common dendritic cell progenitors that express CD115/M-CSFR, CD117/c-kit, and CD155/Flt3 (Guéry and Hugues, 2013). When released, they migrate to the thymus and secondary lymphoid tissues including the mucosal associated lymphoid tissue, spleen, tonsil and lymph nodes (Colonna et al, 2004). They enter the lymph nodes via the high endothelial venules (HEVs) and largely reside in areas rich in T cells (Colonna et al, 2004). Plasmacytoid dendritic cells are also recruited to sites of infection and inflammation, as well as tumours.

Plasmacytoid dendritic cells are a predominant source of type I interferons (IFNs). Type I IFNs play an important role in host defence against viral challenge (Mathan et al, 2013). They induce apoptosis in virally infected cells, prevent protein synthesis and trigger RNA degradation. Type I IFNs can also activate and recruit T cells, B cells, NK cells and mDCs (Colonna et al, 2004, Mathan et al, 2013). Furthermore, pDCs secrete a large number of cytokines; TNFα, IL-6, IL-12 and IL-10 and chemokines; CCL3, CCL4, CCL5, CXCL9, and CXCL10 (Swiecki and Colonna, 2010). Plasmacytoid dendritic cells also express the receptors for a number of chemokines including CCR1, CCR2, CCR5, CCR7, CXCR3, and CXCR4 (Colonna et al, 2004). Therefore, as well as promoting inflammation by the release of type I IFNs and cytokines such as TNFα, pDCs may also have a tolerogenic phenotype by inducing the expansion and differentiation of IL-10 secreting T regs (Kavousanki et al, 2010). Additionally pDCs produce and respond to the type III interferons: IFN λ1, λ2 and λ3 following viral challenge. The type III IFNs, like the type I IFNs, play an important role in the anti-viral response. They may also promote survival of pDCs (Yin et al, 2013).

In order for pDCs to become activated and produce type I IFNs and numerous cytokines, they must first recognise pathogen associated molecular patterns (PAMPs) expressed by the invading pathogen via the use of pattern recognition receptors (PRRs). Plasmacytoid dendritic cells express Toll-like receptor 7 (TLR7) and Toll-like receptor 9 (TLR9) (Mathan et al, 2013). Both of these are expressed intracellularly within the endosomes. Myeloid DCs do not express TLR7 and TLR9. TLR7 recognises viral uridine- or guanosine- rich single stranded RNA and synthetic compounds including imidazoquinoline, whereas TLR9 recognises unmethylated CpG motifs in single stranded DNA. Recognition of PAMPs by TLR7 and/or TLR9 leads to downstream signalling through the MyD88 adaptor protein and Btk, IRAK-4

and TRAF-6. This leads to phosphorylation and translocation of IRF-7 to the nucleus and the subsequent transcription of IFN-I. Signalling through TRAF-6 also results in cytokine and chemokine transcription via the NFκB and MAPK pathways (Guéry and Hugues, 2013).

Prior to activation pDCs are in an immature state and as a result express only low levels of MHC class II and co-stimulatory molecules, CD80 and CD86. It is at this stage where pDCs may induce anergy (Goubier et al, 2008, Guéry and Hugues, 2013, Steinman and Nussenzweig, 2002). However, upon activation pDCs upregulate MHC class II and co-stimulatory molecule expression. Plasmacytoid dendritic cells can process and present antigen to $CD4^+$ T cells. Plasmacytoid dendritic cells may also present antigen by MHC class I leading to the activation of cytotoxic $CD8^+$ T cells (Mathan et al, 2013). Furthermore, pDCs may support the differentiation of B cells to plasma cells.

1.6.1 Plasmacytoid dendritic cells in rheumatoid arthritis

In RA, pDCs have been reported in the synovial tissue nearby small and large lymphoid aggregates. They have also been reportedly found in close proximity to perivenular sites (Takakubo et al, 2008). Lande et al (2004) reported the presence of $CD123^+$, BDCA-2^+ pDCs by immunohistochemistry in the synovial tissue of RA and psoriatic arthritis (PsA) patients as well as immature pDCs in the RA and PsA synovial fluid. Plasmacytoid dendritic cells were absent in samples collected from patients with osteoarthritis (OA). In this study, pDCs within the synovial tissue expressed increased levels of CD123 compared to BDCA-2. It was suggested that the reduction of BDCA-2 staining on pDCs within the RA synovium was indicative of a mature pDC phenotype. Furthermore, Cavanagh et al (2005) identified pDCs

in synovial tissue biopsies taken from patients with RA but not in biopsies taken from healthy individuals. It was reported that pDCs were accountable for 30% of the dendritic cells within RA synovial tissue and that the numbers of pDCs were higher in the RA tissue than the synovial fluid and peripheral blood. Plasmacytoid dendritic cells express the chemerin receptor, ChemR23 (Mathan et al, 2013). Both ligand and receptor have been identified in the RA synovium, particularly the synovial lining and sublining. In a study by Kaneko et al (2011), chemerin was found to stimulate IL-6, MMP-3 and CCL2 production from fibroblast-like synoviocytes and therefore may play an important role in RA pathogenesis. The presence of chemerin in RA may also act to chemoattract pDCs to the synovium.

Richez et al (2009) identified pDCs and mDCs in the peripheral blood of RA patients who responded and failed to respond when treated with infliximab over a 14 week time period. It was shown, that both mDCs and pDCs were reduced in the peripheral blood of patients with active RA, suggesting that both mDCs and pDCs may leave the peripheral blood and reside in the synovium during inflammation. The patients that responded to infliximab treatment had increased number of mDCs in the peripheral blood. As for non-responders, the number of mDCs and pDCs in the peripheral blood did not change.

More recently, the production of tolerogenic DCs (TolDCs) are becoming an increasingly attractive therapeutic option in RA with a number of phase I clinical trials in process, including the Autologous Tolerogenic Dendritic Cells for RA trial (AUTODECRA TRIAL, clinicaltrials.gov reference NCT01352858) (Hilkens and Isaacs, 2013). TolDCs have been shown to induce anergy in antigen primed memory T cells, drive naïve T cells towards an

anti-inflammatory phenotype and in animal models of arthritis TolDCs have been shown to reduce the severity and progression of the arthritis when pulsed with type II collagen before administration (Hilkens and Isaacs, 2013). Moreover, in a phase I study carried out by Thomas et al (2011), the administration of TolDCs pulsed with four citrullinated peptide antigens to 18 RA patients was shown to be well tolerated. Harry et al (2010) have described a protocol for the generation of TolDCs using *ex vivo* monocytes taken from patients with established RA and healthy controls using dexamethasone, vitamin D3 and a TLR4 agonist. The TolDCs were reported to express high MHC class II and produce high levels of IL-10 and TGFβ but low levels of IL-12, IL-23 and TNFα. They were also shown to express low levels of co-stimulatory molecules.

1.7 Platelets

Platelets are small (2μm), anucleate disc shaped vesicles that are produced by megakaryocytes within the bone marrow (Semple et al, 2011). There are approximately 150,000-500,000 platelets per μl/blood and they have a typical life span of 7-10 days. Platelets express a number of surface receptors including P-selectin (CD62P), Fc receptors (FcγRIIA, FcεRI, and FcαRI), GPIIb/IIIa (CD41), glycoprotein VI (GPVI) and C-type lectin-like receptor 2 (CLEC-2). Platelets contain α-granules, dense granules and lysosomes which are a rich source of different inflammatory mediators and immune modulators. Platelet α-granules (200-500nm) are the most abundant granule with approximately 50-80 granules per platelet (Blair and Flaumenhaft, 2009). The α-granules are a source of over 250 biologically active mediators. Molecules that play an important role in the coagulation cascade, endothelial cell repair, and adhesion have been described (Blair and Flaumenhaft, 2009, Semple et al, 2011). Numerous chemokines and cytokines are also stored and released from α-

granules upon activation. These include, amongst many others, CXCL4, CXCL7, CCL5, TGF-β, IL-1β, IL-6 and IL-8. Additionally platelets also express the chemokine receptors; CCR1, CCR3, CCR4 and CXCR4 (Clemetson et al, 2000). Dense granules (150nm), 3-8 per platelet, contain a number of low molecular weight molecules that enhance platelet activation (Blair and Flaumenhaft, 2009). These include histamine, calcium, serotonin, adenosine diphosphate (ADP) and adenosine triphosphate (ATP) (Blair and Flaumenhaft, 2009). Platelet lysosomes contain hydrolases and are far less abundant than α- and dense granules (Nurden, 2011, Zarbock et al, 2007).

	Factor	Stored or synthesised	Reported Immune Target cells
Pleiotropic inflammatory and immune modulators	Histamine	Stored	EC, M, PMN, NK, TC, BC, E
	5-HT (serotonin)	Stored	M, MΦ
Lipid mediators	TxA_2	Synthesised	Platelets, TC, and MΦ subsets
	PAF	Synthesised	Platelets, PMN, M, MΦ and lymphocyte subsets
	SIP	Synthesised	EC, TC, BC, DC, NK, MΦ
Growth factors	PDGF	Stored	M, MΦ, TC
	TGF-β	Stored	M, MΦ, TC, BC
Chemokines	NAP2 (CXCL7) and related β-TG variants	Proteolytic cleavage of stored precursors	PMN
	PF4 (CXCL4)	Stored	PMN
	GRO-α (CXCL1)	Stored	PMN
	ENA-78 (CXCL5)	Stored	PMN
	MIP-1α (CCL3)	Stored	M, E, B, NK, TC, and DC subsets
	MCP-3 (CCL7)	Stored	M, B, NK cell , and DC subsets
Cytokines	IL-1β	Synthesised	M, EC, DC, and MΦ subsets
	HMGB1	Stored	MΦ, PMN, EC

*Abbreviations: Factors: β-TG, β-thromboglobulin; ENA-78, epithelial neutrophil activation protein-78; GRO-α, growth-regulating oncogene-α; 5-HT, 5 hydroxytryptamine (serotonin); HMGB1, high mobility group box 1; IL-1β, interleukin-1β; MCP-3, monocyte chemotactic protein-3; MIP-1α, macrophage inflammatory protein-1α; NAP2, neutrophil activating peptide 2; PAF, platelet-activating factor; PDGF, platelet-derived growth factor; PF4, platelet factor 4; SIP, sphingosine 1-phosphate; TGF-β, transforming growth factor β; TxA_2, thromboxane A_2. Target cells: B, basophil; BC, B lymphocyte; DC, dendritic cell; E, eosinophil; EC, endothelial cell; M, monocyte; MΦ, macrophage; NK, natural killer cell; PMN, polymorphonuclear leukocyte (neutrophil); TC, T lymphocyte.

Table 1.3 Inflammatory mediators and immune modulators released from activated platelets. A number of mediators are released from activated platelets including chemokines, cytokines and growth factors. This is not an exhaustive list as the platelet proteome consists of over 300 different mediators and modulators. Table from Bergmeier and Wagner, 2007.

1.7.1 Soluble Glycoprotein VI

Glycoprotein VI (GPVI) is a 60-65kDa type 1 transmembrane glycoprotein receptor expressed by platelets and megakaryocytes. GPVI is a receptor for collagen and laminin, both of which are exposed within the vessel wall upon damage. GPVI can exist as both a monomer and a dimer within the platelet plasma membrane. The GPVI monomer binds with low affinity to a specific glycine-proline-hydroxyl within collagen, whereas the dimer binds with high affinity (Al-Tamimi et al, 2011). As a result of GPVI binding to collagen, the platelet becomes activated and releases its granular contents. In order to carry out its function, GPVI is covalently linked to the Fc-receptor γ (FcRγ) chain within the platelet plasma membrane. This association is necessary as the FcRγ chain is responsible for initiation of the downstream signalling pathways upon ligand binding (Al-Tamimi et al, 2011). Patients with reduced or absent platelet GPVI may present with epistaxis, ecchymosis, gingival bleeding and menorrhagia (Moroi et al, 1989). Their platelets lack the ability to aggregate in the response to collagen.

GPVI is also found within the plasma. Soluble GPVI (sGPVI) is a marker of platelet activation. GPVI is cleaved from the plasma membrane by a disintegrin and metalloproteinase domain 10 (ADAM10) within minutes of ligand binding (Gardiner et al, 2007). Further ligands associated with the shedding of GPVI have, also, been identified. These include collagen, collagen related peptide (CRP), N-ethylmaleamide (NEM), coagulation factor X and snake toxin (Al-Tamimi et al, 2011, Wijeyewickrema et al, 2007). High shear stress may also lead to cleavage of GPVI from the plasma membrane.

GPVI has been studied as a potential diagnostic biomarker in patients with acute coronary syndrome (ACS). An increase in GPVI has been associated with poor clinical outcome in patients presenting with chest pain (Bigalke et al, 2010). Similarly an increase in GPVI has also been associated with a poor outcome in stoke patients. In contrast sGPVI is decreased in stroke patients (Wurster et al, 2013). Regulation of sGPVI has also been reported in Alzheimer's disease. Here, a decrease in sGPVI and a corresponding lower platelet count was observed in Alzheimer's disease patients when compared to healthy (Laske et al, 2008). In this study, another platelet activation marker was studied, β-thromboglobulin (β-TG). β-TG is a precursor molecule to CXCL7. Levels of β-TG were not found to be significantly different between patients and healthy controls.

1.7.2 A role for platelets in the immune response

Platelets not only play an important role in haemostasis and wound repair but are also important mediations of inflammation. They are now considered to be key immune cells with roles overlapping both innate and adaptive immune responses (Semple et al, 2011). Platelets express a number of different Toll-like receptors (TLRs) that are capable of recognising pathogen associated molecular patterns (PAMPs) and danger associated molecular patterns (DAMPs). A study by Cognasse et al (2005) identified the expression of a number of TLRs by platelets including TLR2, TLR4 and TLR9 that were found to be upregulated upon platelet activation. Platelets, therefore, have the ability to act as 'sentinels' of the immune system and are capable of responding to bacterial, viral, fungal and protozoal infection. Platelets can capture pathogens and influence killing via the release of thrombocidins and ROS. A study by Krijgsveld et al (2000) identified two thrombocidins; Thrombocidin-1 (TC-1) and Thrombocidin-2 (TC-2) are both released from the α-granules of thrombin stimulated

platelets. They were identified as C-terminal amino acid truncated forms of neutrophil activating peptide-2 (NAP-2) and connective tissue-activating peptide III (CTAP-III). Both were shown to have bactericidal effects on Gram positive and Gram negative bacteria as well as activity against the fungi, *Cryptococcus neoformans*. Platelets can form complexes with neutrophils which result in the enhancement of neutrophil chemotaxis, phagocytosis and production of ROS. Additionally, in response to infection, platelets can trigger neutrophil extracellular trap (NET) release through their expression of TLR4. This leads to the entrapment of bacteria within a complex of extracellular DNA and histones (Semple et al, 2011, Vieira-de-Abreu et al, 2012). Platelets can also play an important role in leukocyte recruitment to the site of infection/inflammation through the release of a number of different chemokines.

CD40 and CD40L belong to the TNFR/TNF superfamilies of molecules. The interaction of CD40 on a B cell with CD40L on a T cell is a necessary trigger for B cell proliferation, Ig production, isotype class switching and germinal centre formation (Renshaw et al, 1994, Splawski et al, 1993). Both CD40 and CD40L are also expressed by cells other than B cells and T cells, respectively. CD40 is expressed on monocytes/macrophages, DCs, endothelial cells, fibroblasts and neutrophils, and CD40L is expressed on basophils and mast cells (Gauchat et al, 1993). Expression of both CD40 and CD40L has also been reported on platelets (Elzey et al, 2011, Henn et al, 1998). Hence, platelets may be capable of influencing the adaptive immune response (Henn et al, 2001). Inwald et al (2003) reported the expression of CD40 on resting and activated platelets. CD40L is stored within platelet α-granules and is rapidly translocated within seconds to the platelet surface upon activation with thrombin (Henn et al, 1998). Hence, CD40L is considered a marker of platelet activation. Platelet

CD40L can also be cleaved from the platelet surface and circulate as soluble CD40L (sCD40L). Increased sCD40L has been identified in the plasma of patients with systemic lupus erythematosus (SLE), primary Sjögren's Syndrome (pSS) and RA (Sellam et al, 2009). Platelet CD40L has been shown to play a role in DC maturation, B cell isotype switching (IgM/IgD to IgG) and germinal centre formation. Platelet CD40L may also trigger endothelial cells to upregulate their expression of adhesion markers and enhance chemokine release, thus potentiating leukocyte recruitment.

Hamzeh-Cognasse et al (2008) reported a role for platelets in DC maturation. Dendritic cells cultured with platelets in a filter separated co-culture system led to an increase in DC maturation markers; CD80, CD83 and CD86 and an overexpression of IL-12 (p70). Interestingly, platelets cultured in direct contact with DCs did not lead to an upregulation of DC maturation markers or IL-12 (p70). It was suggested that platelets may release soluble mediators that trigger DC maturation. Platelets have the ability to provide the necessary co-stimulation signal to T cells through the expression of CD86 and can also influence $CD4^+$ differentiation and T cell trafficking. Zhu et al (2014) reported that platelets co-cultured with anti-CD3/CD28 stimulated $CD4^+$ T cells led to Th1, Th17 and Treg differentiation. Furthermore, Gerdes et al (2011) identified an increase in Th1 but not Th2 cytokine release when platelets were co-cultured with anti-CD3/CD28 $CD4^+$ T cells. This study also identified an increase in IL-10 and IL-17 production in the co-cultured cells. Platelets can also present antigen to $CD8^+$ cytotoxic T cells in the context of MHC class I (Chapmen et al, 2012).

1.7.3 Platelets in rheumatoid arthritis

In RA, increased levels of activated platelets have been reported in the blood as well as in the synovial fluid. High platelet counts have been observed in inflamed joints (Farr et al, 1983). Platelet-leukocyte complexes have also been observed in patients with RA, thus suggesting that platelets may aid in the recruitment and activation of leukocytes within the inflamed joint (Joseph et al, 2001). In a study by Pamuk et al (2008), blood from RA patients was shown to have increased levels of CD62P, sCD40L and circulating platelet-monocyte complexes as compared to healthy controls. In a K/BxN serum transfer model of inflammatory arthritis, mice deficient in >95% platelets were shown to have limited arthritis.

A role for platelet microparticles in the pathogenesis of RA has recently been elucidated. Pivotal work by Boilard et al (2010) used flow cytometry to demonstrate $CD41^+$ platelet microparticles in synovial fluid from RA patients. The platelet microparticles were absent in 95% of fluid samples taken from patients with OA. Likewise, Sellam et al (2009) identified platelet microparticles in the plasma of patients with pSS, SLE and RA. The numbers of platelet microparticles were shown to be significantly higher in the three different disease groups compared to healthy controls. Platelet microparticles are small vesicles (0.2-1μm) that bud off from the existing platelet. They contain an abundance of inflammatory mediators as well as a large number of platelet surface receptors including CD41, CD62P, CD40L and CXCR4. In a K/BxN serum transfer model of inflammatory arthritis, platelet microparticle release was shown to be triggered via the GPVI receptor. GPVI is a receptor for collagen. Moreover, platelet microparticles have been reported to exacerbate the inflammatory process by triggering fibroblast-like synoviocytes to release pro-inflammatory cytokines, namely IL-1. Likewise, fibroblast-like synoviocytes have also been found to trigger the release of platelet

microparticles thus creating a vicious cycle (Boilard et al, 2010, Zimmerman and Weyrich, 2010).

1.8 Chemokines

The chemokine family are a collection of small chemotactic proteins (8-15kDa) that play an important role in immune cell recruitment, activation and retention at sites of inflammation. Furthermore, chemokines are also involved in angiogenesis, tumour growth and metastasis (Lei and Takahama, 2011). To date there are approximately 50 known chemokine ligands that can be subdivided into four families based on the position of conserved terminal cysteine residues (Pease and Williams, 2006). For the purpose of nomenclature, the chemokine ligands are referred to as CCL, CXCL, XCL and CX3CL, and their corresponding receptors are CCR, CXCR, XCR, and CX3CR respectively. The two larger subfamilies are the CC chemokines, clustered on chromosome 17q, in which the cysteine residues are adjacent to one another, and the CXC chemokines clustered on chromosome 4q, in which the cysteine residues are separated by a single amino acid residue (Figure 1.3). CC chemokines are largely responsible for the chemoattraction of monocytes, DCs, lymphocytes, NK cells, basophils and eosinophils (Martier et al, 2011, Szekanecz and Koch, 2001). CXC chemokines can be subdivided into two groups based on the presence or absence of an ELR peptide motif (Glutamic acid-Leucine-Arginine). Those that are ELR^+ chemoattract neutrophils via the CXCR2 receptor, whilst ELR^- chemokines (CXCL9 and CXCL10) predominantly bind to the CXCR3 receptor and chemoattract monocytes and lymphocytes. Exceptions to this rule include CXCL4, an ELR^- chemokine that has been reported to lack the ability to chemoattract monocytes, and CXCL13, an ELR^- chemokine that does not bind the CXCR3 receptor but instead recruits B cells via the CXCR5 receptor.

ELR^+ and ELR^- CXC chemokines also differ in their angiogenic/angiostatic properties, with ELR^+ chemokines promoting angiogenesis and ELR^- inhibiting angiogenesis. One exception to this rule is CXCL12. It is an ELR^- chemokine, but promotes angiogenesis (Szekanecz and Koch, 2001, Szekanecz et al, 2003).

The smaller subfamilies are comprised of two chemokines that make up the XC family and a single chemokine, Fractalkine, which belongs to the CX3C family. The XC family contain one cysteine residue, whereas the cysteine residues in Fractalkine are separated by three amino acids (Figure 1.3). Fractalkine is a unique chemokine in that it can exist in soluble or membrane bound forms. The XC family of chemokines chemoattract only lymphocytes, whereas the CX3C member chemoattracts both lymphocytes and monocytes.

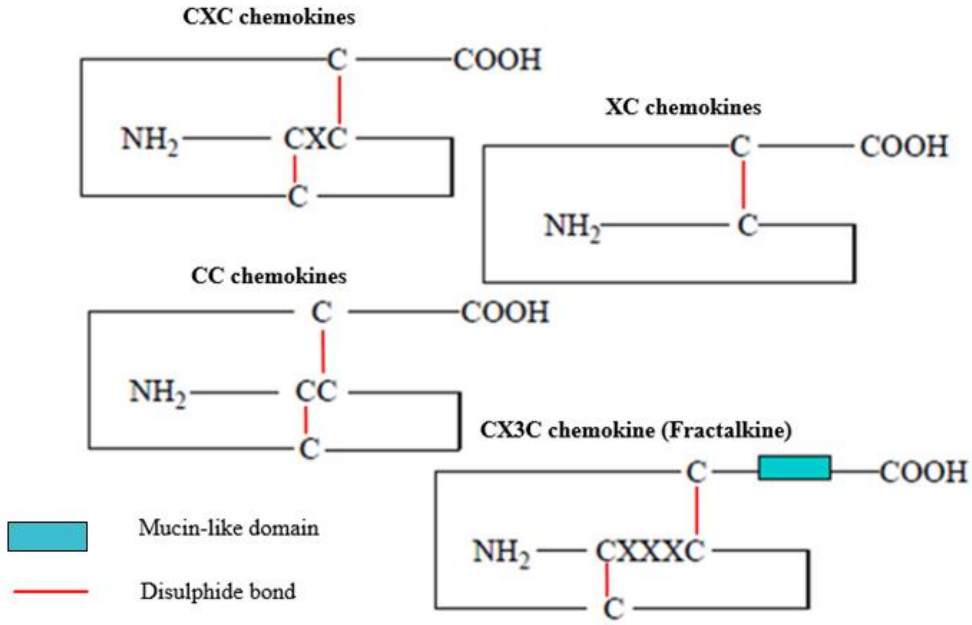

Figure 1.3 Chemokine structure. An image adapted from Wallace et al (2004) depicting the four chemokine families and their terminal cysteine residues. The mucin-like domain enables Fractalkine and, also, CXCL16 to exist as membrane bound forms. It can be cleaved from the membrane by MMPs.

Chemokines may also be subdivided into two groups based on their functional role; inflammatory or homeostatic. However, this sub-categorisation is not entirely consistent as some chemokines may have both homeostatic and inflammatory roles. Inflammatory chemokines act on cells of the innate and adaptive immune system. They play an important role in leukocyte recruitment during inflammation, cancer and autoimmune disease. Homeostatic chemokines are expressed at constitutively active levels and are largely confined to the thymus and lymphoid tissue whereby they play an important role in immune surveillance and cell trafficking during haematopoiesis. They also have a role in the initiation of the adaptive immune response within the lymph nodes, spleen and Peyer's patches (Moser et al, 2004).

1.9 Leukocyte trafficking

The trafficking of leukocytes from the circulation into the tissue occurs in four stages; (1) leukocyte rolling, (2) activation of integrins on leukocytes, (3) firm adhesion to endothelial cells, and (4) diapedesis (Springer, 1994, Tarrant and Patel, 2006).

Leukocyte rolling is mediated by selectins on the endothelium. Selectins are a family of C-type lectin, carbohydrate binding molecules of which there are three major classes; Platelet- or P-selectin (CD62P), Leukocyte- or L-selectin (CD62L), and Endothelial- or E-selectin (CD62E) (Ley, 2003). They facilitate the interactions of leukocytes with platelets and leukocytes with the endothelium (Rosen and Bertozzi, 1994). P-Selectin is evident in platelet α-granules and megakaryocytes, as well as in Weibel-Palade bodies of endothelial cells (Springer, 1994). P-selectin is not expressed on the cell surface in the resting state. However, upon activation with mediators such as thrombin, histamine or various cytokines e.g. TNFα, P-selectin is targeted to the plasma membrane whereby it functions as a cell adhesion molecule (Rosen and Bertozzi, 1994). Within minutes following an inflammatory stimulus, P-selectin is cleaved from the cell surface via proteolytic enzymes (Tarrant and Patel, 2006). E-selectin is expressed by activated endothelial cells within a few hours after the initial inflammatory stimulus (Rosen and Bertozzi, 1994). It is upregulated in the RA synovium and is thought to play an important role in inflammatory cell recruitment (Tarrant and Patel, 2005). L-selectin is expressed on the tips of the microvilli on all leukocytes apart from a particular subset of memory T cells (Schmidt et al, 2013). It plays an important role in the attachment of leukocytes to the endothelium and lymphocyte homing to the secondary lymphoid tissue via the high endothelial venules (HEVs). Upon cellular activation, like P-selectin, L-selectin is rapidly cleaved from the cell surface. The chemokine, Fractalkine, can

also serve as a selectin-like adhesion molecule. Fractalkine is an atypical chemokine since it can exist as both a soluble and a cell-bound form. It is capable of rapid capturing of leukocytes from the circulation. The interaction of leukocytes with selectins initiates cell rolling across the endothelium. As the leukocyte rolls, chemokines presented by glycosaminoglycans on the endothelial surface bind to their receptors on the surface of the leukocyte. This triggers the cell to stop and adhere. Chemokines not only trigger the cell to stop and adhere, but also lead to the activation of integrins on the leukocyte surface.

The integrins are a family of transmembrane receptors that are formed of two subunits; α and β. Thus far, there are 18 known α-subunits and 8 β-subunits which have given rise to at least 24 known α-β combinations (van der Flier and Sonnenberg, 2001). Integrins that contain a β2 subunit are largely involved in cell-cell interactions and play an important role in leukocyte function including leukocyte trafficking and phagocytosis. Whereas, those that contain a β1 subunit are involved in cell-extracellular matrix interactions and function as receptors for collagen, fibronectin (α5β1) and laminin (α6β1). Integrins on the leukocyte bind to their ligands on the endothelium and lead to firm adhesion. The integrin ligands on the endothelium include the intercellular adhesion molecules (ICAM), mucosal addressin cell adhesion molecule-1 (MAdCAM-1), platelet-endothelial cell adhesion molecule-1 (PECAM-1) and vascular cell adhesion molecule-1 (VCAM-1) (Tarrant and Patel, 2005). Integrins on leukocytes that interact with ICAM-1 and ICAM-2 include the β2 integrins, leukocyte functional antigen-1 (LFA-1) (CD11a/CD18), complement receptor type-3 (CR3, CD11b/CD18, MAC-1) and p150/95 (CD11c/CD18) (Plow et al, 2000). ICAM-1 is upregulated during inflammation whereas ICAM-2 is constitutively expressed and therefore plays a role in homeostatic leukocyte trafficking (Springer, 1994).

Following firm adhesion to the endothelium, the leukocytes migrate across the endothelial monolayer and basement membrane by a process of diapedesis, or transendothelial migration. This can occur within 90 seconds (Mamdouh et al, 2003). Predominantly, diapedesis occurs at the endothelial junctions/borders and is known as paracellular transmigration. However, it has been observed that leukocytes can also transmigrate through the endothelial cell itself by a process known as transcellular migration. Although the exact process of diapedesis has yet to be fully elucidated, it does involve the molecules PECAM-1 (CD31) and CD99 which are expressed on the leukocytes as well as the endothelial cell junctions (Mamdouh et al, 2003). Furthermore, the transmembrane immunoglobulins poliovirus receptor (CD155) and DNAX associated molecule-1 (DNAM-1/CD226) have also been shown to play a role in diapedesis (Sullivan et al, 2013). In a study by Mamdouh et al (2003), PECAM-1 was shown to recycle from the endothelial junctions to a compartment below the surface known as the 'subjunctional reticulum'. When monocytes were included in the experiments, PECAM-1 was shown to surround the monocytes during diapedesis. When monocyte PECAM-1 was blocked, the cells were unable to migrate.

More recently, novel insight into the trafficking of T cells across the endothelium has been described. Chimen et al (2015) demonstrated that B cells were able to negatively regulate the trafficking of T cells across the endothelium during inflammation and that this process was dampened in autoimmune diseases such as type 1 diabetes and RA. In response to adiponectin release and its subsequent binding to its targeted receptors, adiponectin receptor 1 (AdipoR1) and adiponectin receptor 2 (AdipoR2), B cells were shown to produce a novel 14 amino acid peptide derived from the proteolytic cleavage of 14.3.3.ζδ known as PEPtide Inhibitor of Trans-Endothelial migration or PEPITEM. Once released, PEPITEM was shown to bind to

cadherin-15 (CDH15) on the surface of the endothelium. Within the cytosol of the endothelial cells, sphingosine was subsequently phosphorylated by sphingosine kinases to produce sphingosine-1-phosphate. Sphinogsine-1-phosphate was then transported from the endothelial cell whereby it was reported to bind to sphingosine-1-phosphate receptors 1 and 4 on the surface of T cells. As a result, T cell trafficking across the endothelium was inhibited. In the context of type 1 diabetes and RA, the expression of AdipoR1 and AdipoR2 was shown to be decreased on the surface of the B cells and as a result PEPITEM release was subsequently decreased. Therefore, this led to uncontrolled trafficking of T cells into the tissues and exacerbation of disease.

1.10 Chemokine receptors in cellular trafficking

In order to exert their function, chemokines must bind to receptors. Predominantly chemokines signal via G-Protein coupled receptors (Figure 1.4). However, they may also bind and interact with glycosaminoglycans and a number of atypical decoy chemokine receptors.

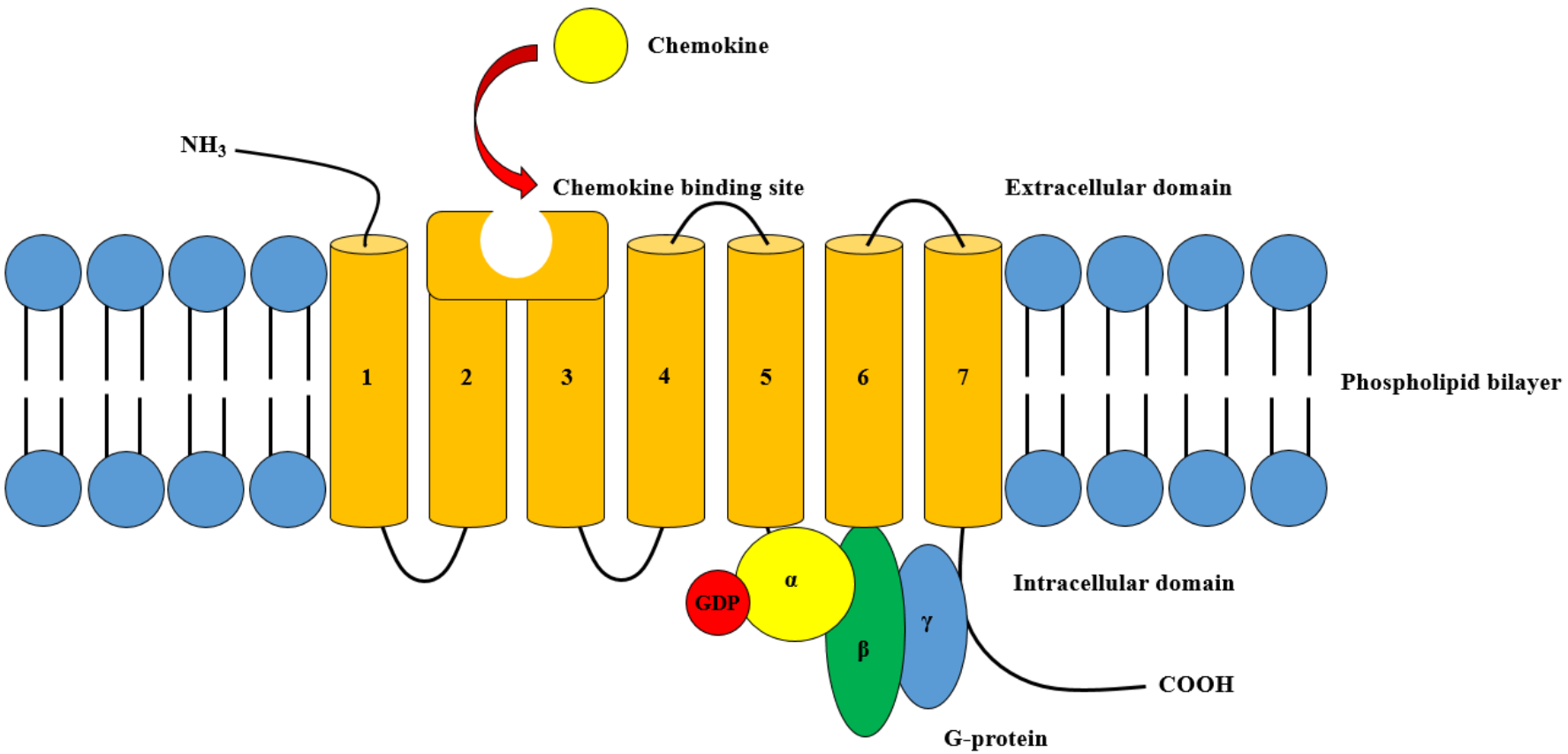

Figure 1.4 G-Protein coupled receptors. The G-protein coupled receptors are composed of a central region of seven transmembrane spanning α helices (labelled 1-7). The extracellular region consists of the N-terminus and three extracellular loops, whereas the intracellular region consists of the C-terminus and three intracellular loops. The G-protein, which is comprised of a Gα subunit and a Gβγ subunit is also found intracellularly in close proximity to the C-terminus. In its inactive form, the Gα subunit is tightly associated with GDP.

1.10.1 G-Protein coupled receptors

The G-Protein coupled receptors (GPCRs) are a large group of serpentine seven transmembrane spanning proteins coupled to heterotrimeric G proteins (Figure 1.4). The heterotrimeric G proteins are comprised a Gα subunit and a dimer of Gβ and Gγ subunits (Gβγ). In the inactive stage, the Gα subunit is associated with the Gβγ subunit. A single molecule of ADP is also bound to the Gα subunit. Upon chemokine ligand coupling to the GPCR, GDP is exchanged for GTP. This results in a conformational shape change and the dissociation of the Gα from the Gβγ subunits. The subunits are then free to modulate the activation of downstream signalling pathways. Hydrolysis of GTP to GDP by the Gα subunits GTPase activity leads to the termination of the signal and reassociation of the Gα and Gβγ subunits (Borroni et al, 2010, Kobilka, 2007, Neumann et al, 2014).

To date there are approximately 20 known G-coupled protein receptors that mediate chemokine signalling. They are grouped into CCR, CXCR, XCR and CX3CR- type receptors. Chemokines are described as being highly promiscuous as they may bind more than one chemokine receptor. For example the inflammatory chemokine CCL5 (RANTES) is capable of binding to three different receptors; CCR1, CCR3 and CCR5 (Table 1.4). Likewise, the chemokine receptor CCR3 is capable of binding five different chemokine ligands; CCL5, CCL7, CCL8, CCL13, and CCL15 (Table 1.4). However, those chemokines described as homeostatic; CCL19, CCL21, CCL25, and CXCL13, tend to be far more restrictive in the receptors they bind.

1.10.2 Chemokine interaction with Glycosaminoglycans

Chemokines not only interact with G-Protein coupled receptors but also bind to glycosaminoglycans (GAGs) with varying affinities (Comerford and Nibbs, 2005). Glycosaminoglycans are negatively charged macromolecules formed of long chains of repeating disaccharide subunits (1-25,000 subunits) (Johnson et al, 2005). Each disaccharide subunit may consist of a hexosamine and a hexose or hexuronic acid (Laguri et al, 2008). They are extremely diverse macromolecules as they can undergo extensive modifications including sulphation and acetylation. The GAGs may be subdivided into six groups; chondroitin sulphate, dermatan sulphate, keratan sulphate, heparin, heparan sulphate, and hyaluronic acid. Both heparin and hyaluronic acid are soluble glycosaminoglycans, whereas the remaining GAGs are ubiquitously expressed on the cell surface and extracellular matrix attached to a protein core. When GAGs form structures with proteins, they are known as proteoglycans (Johnson et al, 2005).

Glycosaminoglycans play an important role in retaining chemokines at their site of release and prevent chemokines from being washed away by the flow of blood (Nibbs et al, 2003). This is extremely important for the recruitment of leukocytes, as the loss of GAGs can lead to the inability of chemokines to recruit leukocytes *in vivo*. They may also regulate the presentation of chemokines to their appropriate ligands. For example, GAGs on endothelial cells may present chemokines to circulating leukocytes, thus enabling cell trafficking (Comerford and Nibbs, 2005). GAGs may also prevent chemokines from undergoing proteolytic degradation (Laguri et al, 2008).

1.10.3 The Duffy Antigen Receptor for Chemokines

The Duffy Antigen Receptor for Chemokines (DARC), or Fy antigen, was first described in 1950 after antibodies to the DARC antigen were discovered in a haemophiliac patient (Cutbush et al, 1950). DARC was initially reported as a receptor for *Plasmodium vivax* and *Plasmodium knowlesi* on the erythrocyte surface (Miller et al, 1975, Miller et al, 1976, Nibbs et al, 2003). Furthermore, it is known to be expressed by vascular endothelial cells, high endothelial venules (HEVs) of the lymph nodes and sinusoids within the spleen. Whilst in pathology, DARC has been observed in inflamed tissues such as the RA synovium (Smith et al, 2008) and psoriatic skin. In RA, DARC positivity has been observed on endothelial cells of post capillary venules but not arterioles (Patterson et al, 2002, Gardner et al, 2006). Moreover, an increase in expression of DARC was evident in patients with early RA (disease duration of <7 months) compared to those with established disease of >8.8 years.

DARC is capable of binding inflammatory chemokines, but not homeostatic chemokines, of both CC and CXC subfamilies with varying affinities (Comerford and Nibbs, 2005). Furthermore, DARC is known to bind ELR^+ angiogenic chemokines but not ELR^- angiostatic chemokines. The interaction of chemokines with DARC does not result in downstream signalling as it lacks the DRYLAIV motif on the second intracellular loop. Therefore, DARC may act to dampen the inflammatory response by acting as a chemokine decoy receptor. DARC expression on erythrocytes may also serve as a chemokine 'sink' or 'reservoir', thus regulating chemokine levels in the blood (Rot, 2005). Furthermore, DARC may play an important role in chemokine transport across the endothelial barrier (Lee et al, 2003). In a study by Lee et al (2003), CXCL1 and CXCL8 were shown to traffic across endothelial monolayers in the presence of Duffy antigen. Additionally, neutrophil recruitment was

enhanced in monolayers expressing Duffy antigen compared to those negative for Duffy antigen. In a later study by Smith et al (2008) DARC blockade was shown to inhibit the adhesion of neutrophils to endothelial cells co-cultured with RA synovial fibroblasts.

1.10.4 The D6 receptor

The D6 receptor, located on chromosome 3p21.3, was first cloned from placenta and haematopoietic stem cells in 1997 (Bonini et al, 1997, Graham et al, 2012). D6 is expressed by endothelial cells of lymphatic afferent vessels in the gut, lungs, skin and placenta. Moreover, D6 expressed has also been reported on pDCs and mDCs as well as particular subsets of B cells (Graham et al, 2012). The D6 receptor functions as a decoy and scavenging receptor by binding to a large number of inflammatory chemokines belonging to the CC family (Locati et al, 2005). It lacks the ability to trigger downstream signalling due to an alteration in the DRYLAIV motif to DRYLEIV (Graham et al, 2012, Nibbs et al, 2003).

The D6 receptor is continuously internalised via clathrin coated pits and recycled regardless of whether or not chemokine is bound. When chemokine is bound to D6 and subsequently internalised, the chemokine rapidly dissociates from the receptor due to the low pH inside the endosome. The chemokine is then targeted for degradation by the lysosomes, whilst the D6 receptor is free to recycle back to the plasma membrane (Comerford and Nibbs, 2005).

1.10.5 The CCX-CKR receptor

Although first referred to as CCR11 and thought to mediate signalling, CCX-CKR, or Chemocentryx chemokine receptor, is now described to function as a chemokine scavenging receptor as the DRYLAIV motif on the second intracellular loop required for downstream signalling is altered to DRYVAVT (Graham et al, 2012, Nibbs et al, 2003). CCX-CKR is expressed in the lung, heart and gut (Graham et al, 2012). CCX-CKR selectively binds the homeostatic CC chemokines CCL19, CCL21 and CCL25 and therefore may play an important role in the regulation of lymphoid trafficking and the triggering of the immune response (Comerford et al, 2006, Nibbs et al, 2003). It is also reported to bind the homeostatic CXC chemokine, CXCL13, but with low affinity (Comerford and Nibbs, 2005).

1.11 Chemokines in rheumatoid arthritis

Chemokines play a major role in the pathogenesis of RA. Through the recruitment, activation and accumulation of various immune cells, chemokines have been shown to contribute towards the huge inflammatory infiltrate observed in the synovium. A large number of animal studies, as well as human trials have attempted to target chemokines therapeutically in order to treat RA.

Chemokine Ligand		Chemokine Receptor
CXCL1	Growth Related Oncogene α (GROα)	CXCR1, CXCR2
CXCL2	Growth Related Oncogene β (GROβ)	CXCR2
CXCL3	Growth Related Oncogene γ (GROγ)	CXCR2
CXCL4	Platelet Factor 4 (PF4)	CXCR3B
CXCL5	Epithelial Neutrophil Activating Peptide 78 (ENA-78)	CXCR2
CXCL6	Granulocyte Chemotactic Protein-2 (GCP-2)	CXCR1, CXCR2
CXCL7	Neutrophil Activating Peptide-2 (NAP-2)	CXCR1, CXCR2
CXCL8	Interleukin-8 (IL-8)	CXCR1, CXCR2
CXCL9	Monokine Induced by IFNγ (MIG)	CXCR3
CXCL10	IFNγ Inducible Protein-10 (IP-10)	CXCR3
CXCL11	Human interferon-inducible T-cell α chemoattractant (I-TAC)	CXCR7
CXCL12	Stromal Derived factor-1 (SDF-1α/β)	CXCR4, CXCR7
CXCL13	B cell Chemoattractant-1 (BCA-1)	CXCR5
CXCL16	SCYB16, SR-PSOX	CXCR6

Table 1.4 The CXC chemokines and their receptors in rheumatoid arthritis. Table derived from Iwamoto et al, 2008, Szekanecz et al, 2003, and Szekanecz et al, 2009.

Chemokine Ligand		Chemokine Receptor
CCL1	T-cell activation gene-3 (TCA-3)	CCR8
CCL2	Monocyte Chemotactic Protein-1 (MCP-1)	CCR2
CCL3	Macrophage Inflammatory Protein -1α (MIP-1α)	CCR1, CCR5
CCL4	Macrophage Inflammatory Protein-1β (MIP-1β)	CCR5
CCL5	Regulated upon Activation, Normal T-cell Expressed, and Secreted (RANTES)	CCR1, CCR3, CCR5
CCL7	Monocyte Chemotactic Protein-3 (MCP-3)	CCR1, CCR3, CCR5
CCL8	Monocyte Chemotactic Protein-2 (MCP-2)	CCR3, CCR5
CCL13	Monocyte Chemotactic Protein-4 (MCP-4)	CCR1, CCR2, CCR3
CCL14	Hemofiltrate C-C chemokine-1 (HCC-1)	CCR5
CCL15	Hemofiltrate C-C chemokine-2 (HCC-2)	CCR3
CCL16	Hemofiltrate C-C chemokine-4 (HCC-4)	CCR2
CCL17	Thymus and activation regulated chemokine (TARC)	CCR4
CCL18	Pulmonary and Activation-Regulated Chemokine (PARC)	unknown
CCL19	Macrophage Inflammatory Protein- 3β (MIP-3β)	CCR7
CCL20	Macrophage Inflammatory Protein- 3α (MIP-3α)	CCR6
CCL21	Secondary lymphoid tissue chemokine (SLC)	CCR7

Table 1.5 The CC chemokines and their receptors in rheumatoid arthritis. Table derived from Iwamoto et al, 2008, Szekanecz et al, 2003, and Szekanecz et al, 2009.

Chemokine Ligand		Chemokine Receptor
XCL1	Lymphotactin	XCR1
CX3CL1	Fractalkine	CX3CR1

Table 1.6 The C and CX3C chemokines and their receptors in rheumatoid arthritis. Table derived from Szekanecz et al, 2003.

1.11.1 CXC chemokines in rheumatoid arthritis

A large number of CXC chemokines have been reported in biological samples from patients with RA (Table 1.4). Increased levels of both ELR^+ and ELR^- chemokines have been detected in synovial fluid, tissue and sera (Szekanecz and Koch, 2001). CXCL8/IL-8 plays an important role in the pathogenesis of RA with synovial macrophages being the major source of this chemokine. It recruits neutrophils into the synovium, thus furthering the inflammatory process. CXCL8 also promotes angiogenesis and upregulation of cell adhesion molecules in the RA joint (Iwamoto et al, 2008, Raman et al, 2011, Vergunst et al, 2005). CXCL12 plays an important role in the RA joint through the recruitment of $CD4^+$ T cells into the synovium. It prevents activation induced apoptosis of these cells leading to an accumulation within the joint (Iwamoto et al, 2008). CXCL12 and its receptor, CXCR4, have been linked to the increased survival of B cells in the synovium. Synovial fibroblasts also migrate and proliferate in response to CXCL12 (Godessart and Kunkel, 200, Gorman and Cope, 2008).

Like CX3CL/Fractalkine (described in section 1.10.4), CXCL16 can exist as either a transmembrane bound chemokine or a soluble chemokine. The transmembrane bound form of CXCL16 can act as an adhesion molecule or a scavenger receptor. Upon cleavage from the membrane by a disintegrin and metalloproteinase-10 (ADAM-10), CXCL16 can circulate as

the soluble form. CXCL16 is expressed by macrophages, T cells, B cells and DCs. CXCL16 which binds through the receptor CXCR6 is a chemoattractant for NK T cells, NK cells, activated T cells, and B cells (Nanki et al, 2005). CXCL16 and CXCR6 have both been reported in RA. Nanki et al (2005) observed an increase in CXCL16 in the RA synovium compared to the OA synovium. CXCL16 positivity was observed in both the lining and sublining layer of the RA synovium. CXCR6 was observed on $CD4^+$ and $CD8^+$ T cells in the synovium. The presence of CXCL16 was found to be associated with an accumulation of T cells within the synovium. Furthermore, in a CIA mouse model, the blockade of CXCL16 by a monoclonal antibody was shown to reduce synovial inflammation (Nanki et al, 2005).

CXC chemokines can aid in the recruitment of B cells to the inflamed synovium. B cell chemoattractant-1, CXCL13, is expressed by follicular DCs, fibroblasts and endothelial cells within the synovium of RA patients. CXCL13 has been found in germinal centre like structures within the synovial tissue (Godessart and Kunkel, 2001, Raman et al, 2011).

Chemokines that prevent angiogenesis have also been reported in the synovium of patients with RA, including CXCL9, CXCL10 and CXCL4. It has been suggested that these chemokines may play a role in the suppression of inflammation, although little evidence is available to support this suggestion.

Recently, CXCL9 and CXCL10 have been identified as potential biomarkers of disease activity in RA patients (Kuan et al, 2010). Here, the serum levels of CCL2, CCL5, CXCL8,

CXCL9 and CXCL10 were quantified in RA patients at baseline and after 12 weeks of treatment with DMARDS or biological agents. All chemokines measured, apart from CCL2, were significantly increased in patients with RA compared to healthy controls at baseline. A significant reduction in serum CXCL9 and CXCL10 was observed in patients with improved clinical activity.

1.11.2 CXCL4, CXCL4L1, and CXCL7

1.11.2.1 CXCL4

CXCL4 or Platelet Factor 4 (PF4) is predominantly a platelet derived chemokine. It is synthesised in megakaryocytes and subsequently stored in α-granules of platelets (Nurden, 2011) whereby it is accountable for 2-3% of the total protein in mature platelets. In serum, CXCL4 levels range from 0.4-1.9 μM, whereas in plasma, CXCL4 levels are 1000-fold lower (Schenk et al, 2002). When platelets become activated, CXCL4 is released alongside two chondroitin sulphate proteoglycan molecules as a tetramer complex. CXCL4 binds to CXCR3B or membrane chondroitin-sulphate, and has a multitude of different effects on various cell types (Pease and Williams, 2006). It has been shown to trigger the release of histamine from basophils and CXCL8/IL-8 from NK cells, suppress tumour growth and angiogenesis, and lead to neutrophil adhesion to the endothelium and secondary granule exocytosis (Kasper and Petersen, 2011, Petersen et al, 1999). Research has reported upregulation of CXCL4 in mDCs and pDCs following trauma (Maier et al, 2009). Furuya et al (2012) reported that in endometriosis, CXCL4 was strongly expressed on $CD68^{+}$ macrophages. Furthermore, CXCL4 has been shown to inhibit HIV-1 viral attachment and

entry into $CD4^+$ T cells and macrophages (Auerbach et al, 2012). McMorren et al (2012) also identified an anti-malarial role for CXCL4 via Duffy antigen receptor interactions.

In T cells, CXCL4 can suppress proliferation. Fleischer et al (2002) stimulated mononuclear cells with recall Ag tuberculin. The cells were then subsequently treated with varying doses of CXCL4. Here, it was observed that CXCL4 concentrations of over 0.5μM triggered a dose-dependent decrease in cell proliferation. However, in Treg cells, CXCL4 has been shown to increase cell proliferation (Liu et al, 2005). This study also reported a decrease in IL-2 mRNA expression as well as inhibition of IL-2 and IFNγ release from T cells treated with CXCL4. CXCL4 also plays a role in Th1/Th2 polarisation via the regulation of the transcription factors GATA3 and T-bet (Kasper and Petersen, 2011).

A number of different effects of CXCL4 on monocytes have been reported. Firstly, it has been shown that CXCL4 prevents monocytes from undergoing spontaneous apoptosis via a GM-CSF and TNF-α independent manner. Cultured monocytes treated over a 72 hour period with CXCL4 were also shown to differentiate into a distinct macrophage lineage. The differentiated cells were larger in size, adherent to plastic and had a macrophage-like morphology. Phenotypic changes were also observed in the differentiated in that CD14 expression was preserved, CD86 expression was increased, and HLA-DR was decreased (Scheuerer et al, 2000). It has been suggested that these CXCL4 differentiated cells should be classed as M4 macrophages (Gleissner et al, 2010). Secondly, CXCL4 has been shown to play a role in phagocytosis and ROS production in monocytes (Pervushina et al, 2004).

CXCL4 has been identified as a potential biomarker for inflammatory bowel disease (IBD). Meuwis et al (2007) identified CXCL4 alongside three other markers; myeloid-related protein (MRP8), αfibrinogen (FIBA) and haptoglobulin α2 (Hpα2), as potential discriminators of active IBD from other inflammatory diseases. Additionally, CXCL4 has been studied in patients with pancreatic adenocarcinoma. In a study by Poruk et al (2011), serum CXCL4 levels were analysed from patients with either pancreatic adenocarcinoma or chronic pancreatitis. Although serum CXCL4 levels were not shown to be significantly different between healthy individuals and patients with pancreatic adenocarcinoma, increased serum CXCL4 in the pancreatic adenocarcinoma patients was associated with a poor prognosis and shorter survival time. Interestingly, CXCL4 levels distinguished between healthy individuals and patients with chronic pancreatitis. High CXCL4 was also associated with an increased risk of venous thromboembolism in patients with pancreatic adenocarcinoma.

In RA, CXCL4 has been detected in the synovial fluid. Erdem et al (2007) compared synovial fluid levels of CXCL4 by ELISA from patients with RA, Behçet's disease (BD), Osteoarthritis (OA) and Spondyloarthritis (SpA). CXCL4 was increased in the synovial fluid from patients with RA compared to the other disease groups. CXCL4 has been identified as a potential biomarker for the prediction of response to infliximab therapy. In a study by Trocmé et al (2009), plasma samples collected from responders and non-responders to infliximab treatment were analysed. Patients who responded well to infliximab had increased plasma concentrations of apolipoprotein A-1. However, those patients who failed to respond had increased levels of CXCL4. This may suggest a role for CXCL4 in the exacerbation of inflammation in RA and aid in the identification of patients who will fail to respond to certain biologics so that the correct therapy may be targeted to the individual.

1.11.2.2 CXCL4L1

CXCL4L1 or Platelet Factor 4 variant (PF4V1) is a non-allelic variant of CXCL4 expressed in humans, rhesus monkeys and chimpanzees. There is no CXCL4L1 gene expressed in the mouse. CXCL4L1 differs from CXCL4 in a three amino acid substitution in the C-terminus; Pro58>Leu, Lys66>Glu, and Leu67>His (Figure 1.5). This region is critical for heparin interaction (Green et al, 1989). Both CXCL4 and CXCL4L1 are located on the same chromosome (chromosome 4) but are separated by the gene for CXCL1. Like CXCL4, CXCL4L1 is released from platelets but at a much lower concentration. However, unlike CXCL4, other sources of CXCL4L1 include smooth muscle cells and tumour cells. Lasagni et al (2007) reported an increase in expression of CXCL4L1 in primary cultures of human aortic smooth muscle cells (HASMCs) and human coronary smooth muscle cells (HCoSMCs) when compared to CXCL4. This study also identified the expression of both CXCL4L1 and CXCL4 in platelets, monocytes and T cells. In these cell types CXCL4 expression was greater than CXCL4L1 expression. CXCL4L1 plays an important role in the chemoattraction of activated T cells, NK cells and DCs.

In RA, CXCL4L1 gene expression was identified *in vitro* in fibroblast-like synoviocytes. However, the level of expression was much lower than observed in fibroblast-like synoviocytes cultured from osteoarthritis patients (Cagnard et al, 2005).

1.11.2.3 CXCL7

CXCL7 or neutrophil activating peptide-2 (NAP-2) is a member of a platelet derived group of proteins collectively referred to as the β-thromboglobulins (β-TG Ag) that differ in their

number of amino acids following proteolytic truncation at the N-terminus (Figure 1.5). As well as including β-TG (81 amino acids), which was the first member of this group to be described, and CXCL7/NAP-2 (70 amino acids), other members include the much larger pro-platelet basic protein (PPBP) (128 amino acids), platelet basic protein (PBP) (94 amino acids), and connective tissue activating peptide-III (CTAP-III) (85 amino acids). The family of β-TG Ag proteins are secreted as biologically inactive chemokines and therefore require proteolytic truncation to become active (Brandt et al, 1991, Brandt et al, 2000). Connective tissue activating peptide-III (CTAP-III) is the predominant inactive precursor released from activated platelets and requires cleavage by cathepsin-G like enzymes expressed by neutrophils. This occurs within 5-10 mins of release. Neutrophils can also cleave β-TG to active CXCL7/NAP-2. In serum, CXCL7 levels range from 1.6-4.8μM and within plasma levels are approximately 1000-fold lower. The receptors for CXCL7 are CXCR1 and CXCR2, both of which are expressed on neutrophils. CXCL7 is mainly responsible for chemoattraction, adhesion and transendothelial migration of neutrophils as well as their activation leading to the degranulation of lysosomal enzymes and formation of oxygen radicals (Blair and Flaumenhaft, 2009, Schenk et al, 2002). Moreover, CXCL7 has been reported to be expressed by T cells and monocytes. However, platelets are still considered the predominant source. Pillai et al (2006) reported that monocytes expressed CXCL7 when co-cultured with stromal cells. In this study $CD14^{+}$ monocytes were co-cultured with the human marrow stromal cell line HS27a. Co-culture led to an increase in the expression of CXCL7 when compared to stromal cells alone.

CXCL7 has been identified as a potential biomarker for chronic obstructive pulmonary disease (COPD) (Cazzola and Novelli, 2010, Di Stefano et al, 2009). CXCL7 was evident in

sections immunostained from the bronchial submucosa. Fibroblasts, endothelial cells and leukocytes stained positive for CXCL7. In the study by Di Stefano et al (2009), CXCL7 was significantly higher in patients with severe COPD compared to healthy controls. However, in contrast to this, a study by Dickens et al (2011) did not observe a significant difference in CXCL7 in COPD patients compared to smoker and non-smoker controls.

In lung cancer, CXCL7/CTAP-III has been identified as a potential biomarker for the prediction of early disease. A study by Yee et al (2009) identified increased CXCL7/CTAP-III in blood taken from the tumour drainage site compared to blood taken from the systemic circulation. CXCL7 decreased in the plasma following surgery to remove the tumour. However, in those patients whose cancer returned, CXCL7 did not decrease significantly. It was also shown that smokers who went on to develop lung cancer had increased levels of CXCL7 a number of years prior to clinical diagnosis. Moreover, an increase in CXCL7 has been identified in epithelial cells isolated from patients with active ulcerative colitis (Kruidenier et al, 2006). Like CXCL4, CXCL7 has also been identified as a potential biomarker for the diagnosis of early pancreatic adenocarcinoma. Matsubara et al (2011) carried out proteome screening of plasma samples collected from 24 patients with pancreatic cancer and 21 healthy controls. A significant decrease in plasma CXCL7 was identified in those patients with pancreatic cancer compared to healthy controls. By combining CXCL7 and a current biomarker used for screening pancreatic cancer, CA19-9, patients with pancreatic cancer could be distinguished from healthy controls. Additionally, Matsubata et al (2011) went on to suggest that the decrease in CXCL7 may precede the onset of pancreatic cancer and therefore serve as an early biomarker for the detection of early disease. Elsewhere, an increase in CXCL7 expression has been reported in an invasive/malignant breast cancer

cell line, MCF10CA1a.c11, compared to a pre-malignant breast cancer cell line, MCF10AT. Tang et al (2008) demonstrated that transfection of pre-malignant MCF10AT cells with CXCL7 led to a highly invasive phenotype, and treatment with an anti-CXCL7 reduced this invasiveness. Therefore it was suggested that CXCL7 expression may play an important role in breast cancer metastasis.

In RA, CXCL7 is detectable in the synovial fluid, tissue and sera. It has been reported to play a role in the proliferation of fibroblasts within the joint and to have angiogenic properties (Szekanecz et al, 2003). The uncleaved CXCL7 precursor, β-TG, has been reported at increased levels in female patients with RA compared to healthy controls (Karatoprak et al, 2012). CXCL7 expression has also been reported in PBMCs from patients with primary and secondary Sjögren's syndrome (Egerer et al, 2006).

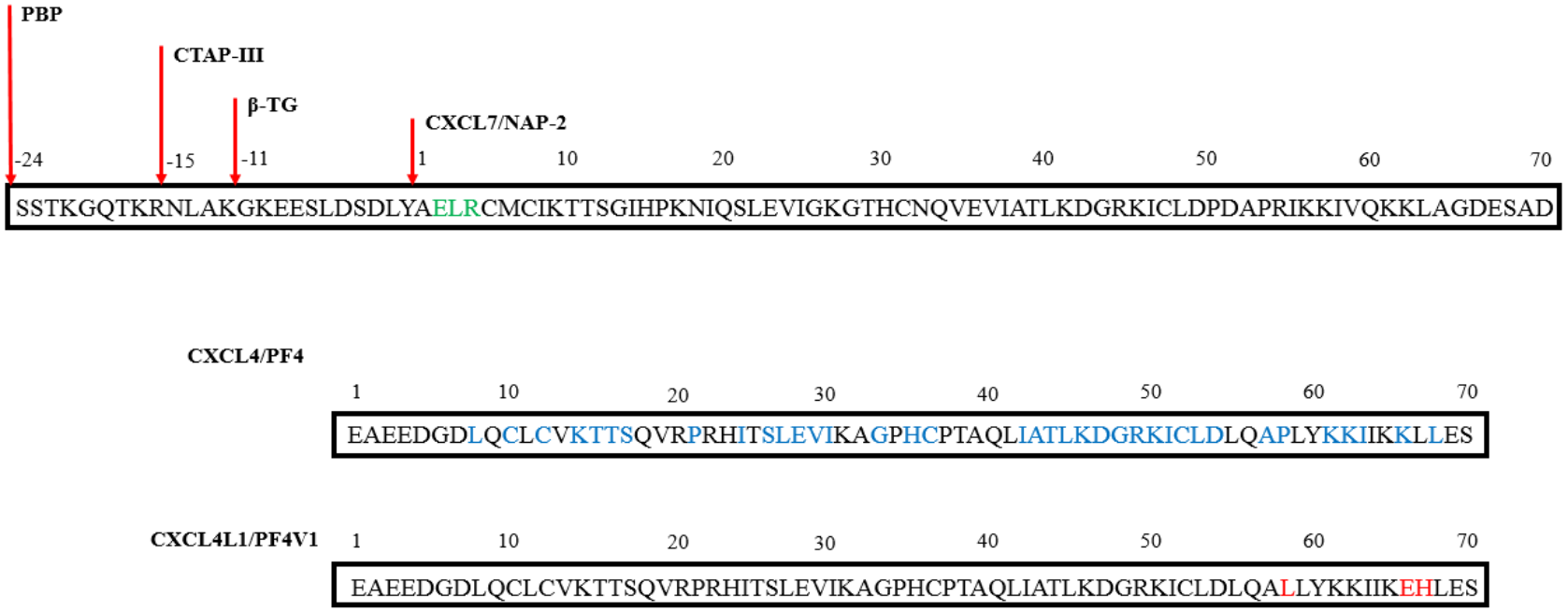

Figure 1.5 The β-Thromboglobulin family, CXCL4/PF4 and CXCL4L1/PF4V1 amino acid sequences. The numbering of the amino acid sequence commences at the N-terminus of CXCL7/NAP-2, CXCL4/PF4 and CXCL4L1/PF4V1. The red arrows indicate the proteolytic cleavage sites that give rise to CTAP-III (85 amino acids), β-thromboglobulin (81 amino acids) and the active chemokine CXCL7/NAP-2 (70 amino acids). CXCL7/NAP-2 is an ELR$^+$ chemokine (motif highlighted in green) whereas both CXCL4/PF4 and CXCL4L1/PF4L1 lack the ELR motif. The amino acids highlighted in blue in PF4 indicate sequence homologies with CXCL7/NAP-2. The amino acid sequence of CXCL4L1/PF4V1 differs from the sequence of CXCL4/PF4 in three amino acids at the C-terminus: Pro 58>Leu, Lys 66>Glu, and Leu 67>His (highlighted in red). Image adapted from Brandt et al, 2000.

1.11.3 CC chemokines in rheumatoid arthritis

Of all the CC chemokines found in the synovium, CCL2, CCL3, CCL4 and CCL5 are the most commonly described (Godessart and Kunkel, 2001 (Table 1.5). CCL2, produced by macrophages and fibroblast-like synoviocytes in the rheumatoid joint, can chemoattract a number of immune cells including DCs, NK cells, monocytes and T cells thus exacerbating the inflammatory process (Iwamoto et al, 2008, Vergunst et al, 2005). Increased levels have been detected in both synovial fluid and tissue of patients with RA (Pease and Williams, 2006). In a study carried out by Kokkonen et al (2010), CCL2 and CCL3 along with a number of other cytokines, were evident at increased levels in the peripheral blood in either anti-CCP positive or IgM-RF positive patients who went on to develop RA a number of years later. This study demonstrated the potential of pro-inflammatory cytokines and chemokines as predictive markers for RA onset. It also suggests that the immune system is activated a number of years prior to symptom onset.

In the synovial fluid, neutrophils express high levels of CCL3 which has been shown to correlate with disease severity. CCL3 is also produced by T cells, fibroblasts and monocytes and can lead to recruitment of T cells, B cells, monocytes and NK cells into the joint (Iwamoto et al, 2008). CCL5 can chemoattract a large number of different immune cells into the synovium including NK cells, monocytes and T cells (Vergunst et al, 2005). Both CCL2 and CCL5 have been linked to cartilage degradation by triggering chondrocytes to release matrix metalloproteinase-3 (MMP-3) (Iwamoto et al, 2008).

An increase in CCL20 has been reported in the synovial fluid and synovial tissue of RA patients. CCL20 recruits a number of different cell types to the synovial joint including naïve B cells, memory T cells and immature DCs. In a study by Matsui et al (2001), CCL20 expression was significantly higher in the synovium of RA patients compared to OA patients. CCL20 was evident on both synovial lining and sublining cells. The receptor for CCL20, CCR6, was also identified in the RA synovium but not OA synovium. Furthermore, *in vitro* cultured synovial fibroblasts were able to produce CCL20 in response to stimulation with IL-1β and TNFα. This would suggest that the cytokine milieu within the synovium may trigger the release of CCL20 from fibroblasts and recruit inflammatory cells to the synovial joint thus further exacerbating inflammation.

1.11.4 C chemokines in rheumatoid arthritis

Lymphotactin (XCL1) is located on chromosome 1 and is expressed by a number of cells including NK cells, $CD8^+$ and $CD4^+$ T cells. It signals through the XCR1 receptor located on the $CD141^+$ ($BDCA3^+$) subset of DCs (Lei and Takahama, 2011). Lymphotactin has been found to play a role in RA (Table 1.6). Research has reported an increase in the concentration of XCL1 in the synovial fluid compared to peripheral blood in RA patients (Raman et al, 2011). Lymphotactin is responsible for the chemoattraction of $CD45RO^+/CD45RB^-$ T cells into the inflamed joint (Borthwick et al, 1997).

1.11.5 CX3C chemokine, Fractalkine, in rheumatoid arthritis

Fractalkine has been reported in the synovial fluid, tissue and sera of patients with RA (Raman et al, 2011) (Table 1.6). A number of cells express this chemokine including DCs,

fibroblasts-like synoviocytes and interstitial macrophages (Nanki et al, 2004), whilst the receptor CX3CL1 is found on $CD4^+$ and $CD8^+$ T cells, monocytes and NK cells. Fractalkine is also expressed on endothelial cells within the RA synovium. It has been suggested to play an important role in the chemoattraction of monocytes, DCs and lymphocytes into the synovium (Iwamoto et al, 2008).

In a study carried out by Nanki et al (2004), the effect of inhibiting Fractalkine was studied using the murine collagen-induced arthritis (CIA) model. The mice were injected in the peritoneal cavity with a 500 µg/ml dose of hamster anti-mouse Fractalkine monoclonal antibody (FKN mAB) three times per week for two weeks. Treatment with FKN mAB significantly reduced the clinical arthritis score when compared to control mice injected with hamster IgG. Pannus formation, bone erosion and synovial hyperplasia were, also, markedly reduced in ankle joints harvested from the treatment group. This study demonstrated the potential of Fractalkine as a therapeutic target for the treatment of RA.

1.12 Targeting chemokines and their receptors for therapeutic benefit in patients with rheumatoid arthritis

The potential of targeting chemokines and their receptors for the treatment of RA has not been without its pitfalls. Multiple clinical trials have been carried out, most of which with limited success. A number of small molecular weight antagonists and anti-human monoclonal antibodies designed to block chemokine receptors have been tested in the past 10 years for the treatment of RA. Two CCR5 antagonists, AZD5672 (Gerlag et al, 2010) and SCH351125, have been trialled in a randomised, placebo controlled phase IIb trial and a randomised,

double blind, placebo controlled phase Ib clinical trial for the treatment of RA, respectively. Although both were well tolerated in the patients, they did not show any clinical improvement. In the case of SCH351125, there was an improvement in DAS28 in both the placebo and treatment groups (Van Kuijk et al, 2010). There was also no significant reduction in $CCR5^+$ cells in the treatment group. Similar observations were made in a double blind, placebo controlled trial of an anti-human IgG1 CCR2 monoclonal antibody (MLN1202). MLN1202 was generally well tolerated, however similar responses were seen in both the placebo and treated groups. No clinical benefit was observed (Gerlag and Tak, 2008, Vergunst el al, 2008). Moreover, a randomised, placebo controlled, proof of concept trial of a human monoclonal antibody against CCL2 led to an increase in C-Reactive Protein (CRP) and the number of macrophages in the patients given a high dose (Haringman et al, 2006). Nevertheless, the blockade of CCR1 is demonstrating far more potential (Lebre et al, 2011). Clinical benefit has been observed using a CCR1 antagonist, CP-481,715 for the treatment of RA. The number of macrophages and $CCR1^+$ cells in the synovial tissue were reduced (Gerlag and Tak, 2008).

1.13 Study background

Previous work by a member of our research group (Yeo et al, 2011) studied the expression of 117 different cytokines and chemokines from synovial tissue biopsies using TaqMan low-density real-time PCR arrays. Synovial tissue biopsies were collected by ultrasound guided biopsy from patients with synovitis of at least one joint and symptom duration of ≤ 3 months. Upon follow up, 18 months later, patient disease outcomes were determined. Patients were either grouped into those that had developed RA in accordance with the 1987 ARA classification criteria (early RA group) or those whose early synovitis had spontaneously resolved (resolving synovitis group). Synovial biopsies collected from patients with RA (1987 ARA criteria) of >3 months duration (<3 years duration) (established RA group) were also recruited as controls. All the above biopsies were collected from DMARD and glucocorticoid naiive patients enrolled in the Birmingham early inflammatory arthritis cohort (BEACON). Patients with unexplained joint pain assessed by arthroscopy in a local orthopaedic clinic without any clinically apparent or macroscopic synovial inflammation (uninflamed control group) were also included as study controls.

In order to analyse cytokine expression in the different outcome groups, a number of statistical tests and a mathematical computer model (generalized matrix relevance learning vector quantization (GMLVQ)) were applied to the real-time PCR array data. The GMLVQ model set out to categorise patients into particular outcome groups based on their cytokine data. An interesting finding from this analysis was that when the early RA outcome group was compared to the early resolving synovitis outcome group, the two cytokines shown to distinguish between the patient groups were the platelet derived chemokines, CXCL4 and CXCL7.

1.14 Hypothesis and objectives

As a result of the previous observations described in section 1.13 the principal aim of this thesis was to investigate the hypothesis that the expression of platelet derived chemokines, CXCL4 and CXCL7, in the synovium and peripheral blood could predict disease progression in patients presenting with early synovitis.

In order to study this, the primary objective was to stain synovial biopsies taken from patients enrolled in the Birmingham Early Inflammatory Arthritis (BEACON) cohort with antibodies specific for CXCL4 and CXCL7 and compare the expression data to clinical outcome.

The second objective was to address the potential of both chemokines in plasma as predictive biomarkers of disease progression in patients presenting with early synovitis. CXCL4, CXCL7 and the platelet activation marker sGPVI was assessed in plasma samples collected from patients enrolled in the BEACON cohort.

Although I initially hypothesised that an increase in CXCL4 and CXCL7 expression would be due to an increased numbers of platelets within the synovium, the current literature suggested that cells outside the megakaryocyte lineage including monocytes, macrophages, and dendritic cells express CXCL4 and CXCL7. Therefore the tertiary objective was to identify cell populations expressing both chemokines within inflamed synovial tissue. The cellular expression of CXCL4 and CXCL7 in monocytes and in vitro differentiated macrophages obtained from healthy controls was assessed by qPCR.

2 METHODS

2.1 Patient cohort: The Birmingham Early Inflammatory Arthritis Cohort (BEACON)

Patients with early synovitis were recruited via new patient clinics for early arthritis at Sandwell and West Birmingham Hospitals NHS trust, Birmingham, UK and University Hospitals Birmingham NHS Foundation Trust, Birmingham, UK. All patients gave written, informed consent. The study was approved by the Birmingham and the Black Country Research Ethics Committee (West Midlands Black Country REC 07/H1203/57). Patients were assessed by consultant rheumatologists, Dr Andrew Filer or Dr Karim Raza, and were deemed to have early synovitis based on the presence of at least one clinically swollen joint, inflammatory joint pain and/or early morning stiffness, and/or joint related soft tissue swelling for ≤3 months duration. Patients recruited to the Birmingham early inflammatory arthritis cohort (BEACON) were DMARD and glucocorticoid naïve at the time of synovial biopsy.

Synovial biopsies were obtained by ultrasound guided biopsy. Joints were first assessed using a Siemens Acuson Antares scanner (Siemens, Bracknell, UK) and multi-frequency (5-13 MHz) linear array transducers. Synovial tissue with evidence of grey scale synovitis, was collected from multiple regions within the knee, ankle or metacarpophalangeal (MCP) joints. Tissue from the knee and ankle was obtained via a single portal using custom manufactured 2.2 mm cutting edged forceps, whereas tissue from the MCP joints was obtained using a 16-gauge core biopsy needle. All biopsies were anonymised at the time of collection and were issued with a BX (biopsy) number. Blood and urine samples were also obtained from patients

enrolled in the BEACON cohort. Plasma and serum was stored at -80°C for downstream analyses. Additionally, age, sex, disease duration, CCP and RF status, ESR, CRP, global assessment of disease activity, swollen joint count, tender joint count and DAS28 status of each patient were collected upon initial assessment.

During 18 months of follow-up, patients were grouped into those that met the 1987 ARA criteria (Arnett et al, 1988), or had gone on to fulfil those criteria, those that had developed a non RA- persistent inflammatory arthritis, and those that had gone on to have a resolving synovitis. In this thesis, patients who went on to develop RA will be referred to as the 'Early RA' group, and those that went on to have a resolving synovitis will be referred to as the 'Resolving' group. Patients who went on to develop a non RA-persistent inflammatory arthritis were not studied in this context as they represent a very heterogeneous group.

In addition, synovial biopsies were obtained from patients with RA (1987 ARA criteria) of > 3 months duration (<3 years duration). Patients were DMARD and glucocorticoid naïve at the time of biopsy. In this thesis this group will be referred to as the 'Established RA' group. Synovial biopsies were also obtained from an uninflamed cohort of patients under investigation for mechanical symptoms with normal MRI appearances. This cohort was managed by Mr. Martyn Snow. Patients recruited to this group demonstrated an absence of joint inflammation clinically, with macroscopically normal synovium at the time of arthroscopy under direct vision. Synovial samples demonstrating histological evidence of inflammatory arthritis were excluded from the final cohort.

2.2 Joint replacement synovial biopsies

Synovial biopsies collected from patients with longstanding RA who had fulfilled the 1987 ARA classification criteria were used in chapters 3 and 5. Synovial biopsies were collected intra-operatively from patients undergoing joint replacement at the Royal Orthopaedic Hospital NHS trust. This cohort was kindly managed by Mr. Andrew Thomas. Patient information can be found in appendix table 8.1.

2.3 Processing of synovial biopsies

Biopsies were fixed overnight in formaldehyde and placed in pre-labelled cassettes prior to being processed using the automated Leica ASP300 tissue processor (Table 2.1). Sections were dehydrated in industrial methylated spirits (IMS) 99% alcohol, cleared in xylene and embedded in paraffin wax. This process was carried out by the Royal Orthopaedic Hospital, Birmingham, UK.

Step	Reagent	Time (mins)	Temperature (°C)
1	IMS 99% alcohol	0.45	**37**
2	IMS 99% alcohol	0.50	**37**
3	IMS 99% alcohol	0.55	**37**
4	IMS 99% alcohol	1.30	**37**
5	IMS 99% alcohol	1.30	**37**
6	IMS 99% alcohol	2.00	**37**
7	Xylene	1.00	**37**
8	Xylene	1.00	**37**
9	Xylene	2.00	**37**
10	Paraffin wax	1.00	**63**
11	Paraffin wax	2.00	**63**
12	Paraffin wax	2.00	**63**

Table 2.1 Preparation of formalin fixed paraffin embedded tissue sections using the Leica ASP300 tissue processor. Synovial biopsies, once collected, were fixed in formaldehyde before being sent to the Royal Orthopaedic Hospital (ROH) for processing and sectioning.

Following embedding in paraffin wax, 3 µm sections were cut. Sections were then air-dried in a slide drying cabinet at 65°C for a minimum of 1 hour (not overnight). One section from each block was then stained with Haematoxylin and Eosin.

2.4 Synovial fibroblasts

For the work shown in chapter 5, *in vitro* cultured fibroblasts were used in a number of experiments. Synovial fibroblasts were cultured from biopsy sections taken from patients enrolled in the BEACON cohort as well as from synovial tissue collected from patients undergoing routine joint replacement surgery at the Royal Orthopaedic Hospital. Patients recruited at the Royal Orthopaedic Hospital gave written, informed consent. The study was approved by the Birmingham and the Black Country Research Ethics Committee. For our experiments, fibroblasts from patients with early RA, established RA, resolving synovitis, joint replacement RA, or joint replacement osteoarthritis (OA) were used. Patient information can be found in appendix tables 8.4 and 8.5.

2.4.1 Fibroblast chamber slides

Fibroblast chamber slides were prepared by our lead technician, Miss Holly Adams. In brief, fibroblasts were cultured until confluent. Fibroblasts were used at passage 3, passage 4, or passage 5 depending on availability. Fibroblasts were trypsinised, counted and suspended in a volume of 0.06 x 10^6 cells/ml of complete fibroblast medium (RPMI-1640 + 10% Foetal Calf Serum (FCS) + 1% MEM Non-essential amino acids (Sigma M7145) + 1% Sodium Orthopyruvate (Sigma S8636) + 1% L-glutamine-penicillin-streptomycin (GPS)). They were then seeded in culture chamber slides (Falcon®, USA) at a density of 0.03 x 10^6 cells/well in

500 µl fibroblast medium. Slides were then cultured in an incubator set at 37°C and 5% CO_2 for 48 hrs. Following incubation, media was discarded from the chamber slides and the chamber was removed from the slide. Slides were then washed in PBS for 5 mins before being left to dry for 1 hr. Next, slides were fixed in acetone for 20 mins at 4°C and then subsequently left to dry for 5-10 mins. Slides were then stored at -80°C for downstream immunofluorescence experiments.

2.5 Immunofluorescence

Frozen synovial biopsies previously sectioned (6µm thickness), mounted, and fixed with acetone were rehydrated in PBS for 2 x 5 mins. The slides were removed from PBS and placed in a wet box and 50 µl of blocking solution (10% FCS/PBS) were added to each individual tissue section. The slides were incubated at room temperature for 30 mins. The blocking solution was then removed from the sections by gently tapping the slides and 50 µl of primary antibody was added for 60 mins. Following incubation with the primary antibodies (Table 2.2, 2.3 and 2.6), the slides were washed in PBS for 2 x 5 mins. Biotin antibody (50µl) was then added to the sections for 30 mins followed by a further wash in PBS for 2 x 5 mins. Finally the secondary antibodies (Table 2.5) were added to the sections (50 µl) and incubated for 30 mins followed by a final wash step in PBS for 2 x 5 mins. Sections were then counterstained in 10 µg/ml Hoechst 33258 pentahydrate (bis-benzimide) for 90 seconds, washed for 5 mins in PBS and mounted in 2.4% w/v 1,4- diazabicyclo [2,2,2] octane (DABCO) (Aldrich, Gillingham, England) dissolved in 90% v/v glycerol in PBS, pH 8.6 (Fisher Scientific, Loughborough, UK). Slides were visualised using the Zeiss LSM 780 Zen Confocal microscope (Zeiss, Germany), unless stated elsewhere. Analysis was carried out using Zen imaging software and Microsoft Excel.

Antibody	Isotype	Stock Concentration (if available)	Dilution	Supplier
Von Willebrand Factor (vWF)	Rabbit	NA	1 in 500	Dako
CD41	Mouse IgG1	100 μg/ml	1 in 500 1 in 370	Dako
CXCL4	Mouse IgG2b	1 mg/ml	1 in 100	Abcam
CXCL7	Mouse IgG2b	0.5 mg/ml	1 in 50	Novus Biologicals
CD68	Mouse IgG2a	30 μg/ml	1 in 25	Thermo Scientific: Pierce

Table 2.2 Primary antibodies used for the CXCL4 and CXCL7 5-colour staining panel. Antibodies were used in chapter 3.

Antibody	Isotype	Stock Concentration (if available)	Dilution	Supplier
Platelet Factor 4 variant 1	Rabbit	1 mg/ml	1 in 1200	Thermo Scientific: Pierce
hCD90/Thy1 (Clone Thy/IAI)	Mouse IgG2a	0.5 mg/ml	1 in 200	Abcam
VCAM-1 (Clone P8B1)	Mouse IgG2b	1 mg/ml	1 in 100	Millipore
Podoplanin	Mouse IgG1	NA	1 in 100	AbD Serotec
Protein Disulphide Isomerase (PDI) (RL77)	Mouse IgG2b	2.3 mg/ml	1 in 250	Abcam

Table 2.3 Primary antibodies used for the characterisation of CXCL4L1 in RA. Antibodies were used in chapter 5.

Antibody	Isotype	Stock Concentration (if available)	Dilution	Supplier
Mouse IgG1-UNLB (clone 15H6)	Mouse IgG1	1 mg/ml	*	Southern Biotechnology
Mouse IgG2a-UNLB (clone HOPC-1)	Mouse IgG2a	1 mg/ml	*	Southern Biotechnology
Mouse IgG2b-UNLB (Clone A-1)	Mouse IgG2b	1 mg/ml	*	Southern Biotechnology
Rabbit Serum	Rabbit	NA	*	Dako

Table 2.4 Isotype-matched controls used for immunofluorescence staining. The same concentration was used for the both isotype-matched controls and the primary antibodies, denoted by asterisks.

Antibody	Isotype	Stock Concentration (if available)	Dilution	Supplier
Chromeo™ 494	Goat pAb	2 mg/ml	1 in 100	Abcam
Cy™3-conjugated Streptavidin	NA	1.8 mg/ml	1 in 100	Jackson Immunoresearch
Goat anti mouse Alexa Fluor® 488	Mouse IgG1	1.7 mg/ml	1 in 300	Jackson Immunoresearch
Goat anti mouse Cy5	Mouse IgG2a	1 mg/ml	1 in 50	Southern Biotechnology

Table 2.5 Secondary antibodies used for immunofluorescence staining.

Antibody	Isotype	Stock Concentration (if available)	Dilution	Supplier
CD303 (BDCA-2) FITC	Mouse IgG1	82.5 µg/ml	1 in 100	Miltenyi Biotec
Goat anti-mouse- BIOT	Mouse IgG2b	0.5 mg/ml	1 in 50	Southern Biotechnology
Alexa Fluor® 647	Mouse Rabbit	1.4 mg/ml	1 in 800	Jackson Immunoresearch
Goat anti- mouse BIOT	Mouse IgG2a	0.5 mg/ml	1 in 50	Southern Biotechnology
Goat anti- mouse TRITC	Mouse IgG2b	1 mg/ml	1 in 100	Southern Biotechnology
Cy™5-conjugated Streptavidin	NA	1.8 mg/ml	1 in 100	Jackson Immunoresearch

Table 2.6 Additional antibodies used for immunofluorescence staining.

2.6 CXCL4 and CXCL7 measurement in plasma by ELISA

Quantitative measurement of plasma CXCL4 was assessed using a Quantikine® ELISA kit (R&D Systems, UK). Plasma CXCL7 was analysed using the ab100617- CXCL7 ELISA kit (Abcam, UK). Upon receipt, the CXCL4 ELISA was stored at 4°C and the CXCL7 ELISA was stored at -20°C.

2.6.1 CXCL4 Quantikine® ELISA

All reagents and samples were brought up to room temperature (18-25°C) before use. In order to prepare the standard curve for the assay, the recombinant human PF4 standard was first reconstituted in 900 µl dH_2O to prepare a 500 ng/ml stock solution and left to sit for 30 mins prior to use. A 50 ng/ml top standard was prepared from the stock solution by the addition of 50 µl of the stock solution to 450 µl of calibrator diluent RD6-13. The standard curve was then prepared (Table 2.7). Calibrator diluent RD6-13 was used alone as a zero (0 ng/ml) standard.

Standard (ng/ml)	Volume of standard solution (µl)	Volume of calibrator diluent: RD6-13 diluent (µl)	Concentration (ng/ml)	Standard
500	50	450	**50**	**1**
50	200	200	**25**	**2**
25	200	200	**12.5**	**3**
12.5	200	200	**6.25**	**4**
6.25	200	200	**3.13**	**5**
3.13	200	200	**1.56**	**6**
1.56	200	200	**0.781**	**7**
-	**-**	200	**0**	**Blank**

Table 2.7 Preparation of the CXCL4 Quantikine® ELISA standard curve.

Samples for the ELISA were diluted 1 in 100 or 1 in 200 in calibrator diluent RD6-13. The pre-coated ELISA plate was then prepared by adding 100 µl assay diluent RD1-15 to each well, followed by 50 µl of the standards and the diluted samples. Standards and samples were run in duplicate. After addition to the plate, the plate was incubated for 2 hrs at RT on a Denley Well Mixx 3 shaker. Following incubation, the assay plates were washed 4 times using a multi-channel pipette (400 µl each well) with 1X wash solution. Wash solution was

provided as a 25X concentrated solution in the kit. The solution was diluted with dH_2O to a 1X prior to use. After the final wash step, the plate was tapped on absorbent paper to remove any excess wash solution. Next, 200 µl anti-human PF4 conjugate was added to each well. The PF4 conjugate consisted of a polyclonal antibody specific for CXCL4 conjugated to HRP. The plate was then incubated for a further 2 hrs at RT with gentle shaking before being washed 4 times as previously described. Substrate solution (200 µl) was then added to each well and the plate was protected from light by covering with foil and left to incubate for 30 mins at RT without shaking. Prior to addition to the plate, the substrate solution was prepared by adding equal volumes of hydrogen peroxide (colour reagent A) and tetramethylbenzidine (colour reagent B). Finally, 50 µl 2 N sulphuric acid (stop solution) was added to each well. The plate was read immediately using the BioTek EL808 plate reader at 450 nm with a wavelength correction of 540 nm.

2.6.2 CXCL7 ELISA

All reagents and samples were brought up to room temperature (18-25°C) before use. In order to prepare a 50 ng/ml standard for the preparation of the standard curve, recombinant CXCL7 was reconstituted in 400 µl of assay diluent. For the preparation of the standard curve, 20 µl of the 50 ng/ml standard was diluted in 980 µl assay diluent to prepare a 1,000 pg/ml standard solution. The standard curve was then prepared (Table 2.8). Assay diluent, alone, was used as a zero (0 pg/ml) standard.

Standard (pg/ml)	Volume of standard solution (µl)	Volume of assay diluent (µl)	Concentration (pg/ml)	Standard
50,000	20	980	**1,000**	**1**
1,000	200	300	**400**	**2**
400	200	300	**160**	**3**
160	200	300	**64**	**4**
64	200	300	**25.6**	**5**
25.6	200	300	**10.24**	**6**
10.24	200	300	**4.10**	**7**
-	**-**	200	**0**	**Blank**

Table 2.8 Preparation of the ab100613- CXCL7 standard curve.

Plasma samples were diluted 1 in 5000 or 1 in 10,000 in assay diluent before addition to the assay plate. 100 µl of each standard and sample was pipetted into the appropriate wells of the pre-coated assay plate. Plates arrived pre-coated with anti-human CXCL7. The standards and samples were run in duplicate. The plate was then incubated for 2.5 hrs at room temperature with gentle shaking. Following incubation, the plate was washed 4 times with a multi-channel pipette with 1X wash solution. Wash solution was provided as a 20X concentrated solution in the assay kit. It was therefore diluted with dH_2O to a 1X wash solution prior to use. After washing, the plate was tapped against absorbent paper to remove any excess wash solution. Next, 100 µl of 1X biotinylated antibody (biotinylated anti-human CXCL7) was added to each well and incubated for 1 hour at room temperature with gentle shaking. Biotinylated antibody was provided as a lyophilized vial. To reconstitute, 100 µl of assay diluent was added to the vial. The vial was then gently mixed. Prior to use, the Biotinylated antibody was diluted 80-fold with assay diluent. The plate was washed as previously described. HRP-conjugated streptavidin solution (100 µl) was then added to the plate and incubated for 45 mins at room temperature with gentle shaking. Before use, the HRP-conjugated streptavidin

solution was diluted 200-fold. The plate was then washed. Next 100 µl of 3,3',5,5'-tetramethylbenzidine (TMB) One-Step Substrate Reagent was added to each well. The plate was incubated in the dark with gentle shaking for 30 mins. Finally, 50 µl of 0.2 M H_2SO_4 (stop solution) was added to each well. The plate was immediately read at 450 nm and 540nm using the BioTek EL808 plate reader.

2.6.3 ELISA Data analysis

The mean absorbance for each duplicate standard was calculated. The mean zero standard optical density (O.D) was subtracted from the standards and samples. A standard curve of the standard concentration against the absorbance was plotted using Prism 5 software. A line of best-fit was added and unknown serum and plasma concentrations were read from the curve.

2.7 Soluble platelet glycoprotein VI (sGPVI) measurement in human plasma by ELISA

Each well of a F96 MaxiSorp Nunc-Immuno plate (Thermo Scientific, Nunc 442404) was coated with 100 µl of 1 µg/ml (stock conc. 958 µg/ml) rabbit polyclonal anti-human GPVI extracellular domain antibody prepared in coating buffer. The coating buffer was prepared by dissolving 1 carbonate-bicarbonate buffer capsule (Sigma, C3041-100CAP) in 100 ml of ddH_2O. The plate was then covered with an adherent strip and incubated overnight at 4°C. The plate was then subsequently washed 6 times in 0.2% Tween-20 in PBS (8.18 g NaCl, 0.2 g KCl, 1.42 g Na_2HPO_4, and 0.244 g KH_2PO_4 in ~900 ml ddH_2O, pH 7.4, then volume adjusted to 1 L) before being blocked with 200 µl per well of 1% BSA in PBS for 1 hour at RT. During the blocking step, N-ethylmaleimide (NEM)-treated platelet poor plasma (PPP),

internal control and patient samples were diluted 1/20 in PBS. 5% GPVI-depleted PPP in PBS was also prepared. After blocking, the plate was washed as described previously. Next 100 µl 5% GPVI-depleted PPP was added to wells A1-A10 and B1-B10. This was followed by 100 µl NEM-PPP (1/20) (320 ng/ml) into wells A1 and B1 to prepare a 160 ng/ml standard. Wells A1 and B1 were mixed thoroughly by pipetting up and down 6 times. 100 µl from A1 and B1 was then transferred to wells A2 and B2 (80 ng/ml standard) using a multi-channel pipette. This process was repeated until wells A10 and B10. 100 µl was discarded from wells A10 and B10. 100 µl of each sample and control was added to duplicate wells of the plate. The plate was then incubated for 1 hour at RT before being washed 6 times with 0.2% Tween-20/PBS. Next 100 µl 1 µg/ml (stock conc. 1.17 mg/ml) monoclonal mouse anti-human GPVI antibody (1A12) prepared in PBS was added to each well of the plate. The plate was then incubated for 1 hour at RT before being washed 6 times with 0.2% Tween-20/PBS. 100 µl of 2.6 µg/ml (stock conc. 1.3 g/L) polyclonal rabbit anti-mouse Immunoglobulins/HRP (Dako, UK) was added to each well. The plate was then incubated for a further 1 hour at RT before being washed for the final time as described previously. Finally, 100 µl of Super Signal ELISA PICO chemiluminescent substrate (1:1 Luminol/Enhancer solution and Stable Peroxide Solution) (Thermo Scientific, PIE 37069) was added to each well of the plate. The plate was incubated for 1 min at RT before being read at 425 nm using the Wallac VICTOR^2 1420 multi label counter (PerkinElmer Life Sciences).

2.8 Peripheral blood mononuclear cell isolation

Peripheral blood was collected from healthy donors into ethylenediaminetetraacetic acid (EDTA)-containing tubes (3µl EDTA per 1ml blood) and subsequently diluted at a 1:1 ratio

with RPMI-1640 supplemented with 1% GPS. The diluted blood was then layered on to Ficoll-Paque at a 1:3 blood to Ficoll ratio (GE Healthcare, UK). Tubes were centrifuged for 30 mins at 290 x g (acceleration: 0, brake: 0). Following centrifugation, peripheral blood mononuclear cells (PBMCs) were carefully removed at the Ficoll-Paque interface with a sterile pasteur pipette. The PBMCs were then washed twice in RPMI-1640 + 1% GPS by centrifugation for 6 mins at 300 x g (acceleration: 9, brake: 9). Supernatant was removed between washes and fresh medium was added. The cells were then counted using a haemocytometer and used in downstream experiments.

2.9 $CD14^+$ cell isolation

2.9.1 Magnetic labelling

Isolated PBMCs were first centrifuged at 290 g for 10 mins and the supernatant was removed. The cell pellet was resuspended in 80µl MACs buffer per 10^7 cells. To this, 20µl of CD14 magnetic beads were added (Miltenyi Biotec, UK). The cells were incubated for 15 mins at 4°C. Following this, the cells were washed in 1-2ml of MACs buffer per 10^7 at 290 g x 10 mins. The cell pellet was then resuspended in 500µl per 10^8 cells.

2.9.2 Magnetic separation

An LS column (Miltenyi Biotec, UK) was placed in the magnetic field of the MACs separator. The column was prepared by rinsing through with 3ml of MACs buffer. The cell suspension was then added to the column and the flow-through was collected as waste. The column was then washed with 3 x 3ml MACs buffer. The column was then removed from the

magnetic separator and placed over a collection tube. 5ml of MACs buffer was then added to the column and the flow through was collected. The flow through contains the $CD14^+$ cell fraction. The cells were subsequently counted and purity checked using the Cyan Flow Cytometer (Beckman Coulter, UK).

2.10 Cell sorting of monocyte and platelet complexes

Peripheral blood mononuclear cells (PBMCs) were isolated from healthy donors by Ficoll-Paque. Cells were sorted into three populations; $CD14^+$ $CD41^-$, $CD14^+$ $CD41^+$ intermediate, and $CD14^+$ $CD41^+$ using the MoFlo™ cell sorter (Beckman Coulter). The cell sorter was kindly operated by Mr Roger Bird, a cell sorting and analysis expert, based at The University of Birmingham.

	Dilution	Antibody Clone	Supplier
Surface antibodies			
Monoclonal mouse anti-human CD41, platelet glycoprotein IIb/FITC	1 in 50	5B12	Dako
Anti-human CD14 PE-CY7	1 in 100	61D3	ebioscience
Isotype-matched control antibodies			
Mouse IgG1κ Iso control FITC	1 in 250	P3.6.2.8.1	ebioscience
Mouse IgG1κ Iso control PE-CY7	1 in 100	P3.6.2.8.1	ebioscience
Compensation antibodies			
Anti-human CD14 PE-CY7	1 in 50	61D3	ebioscience
Anti-human CD14 FITC	1 in 50	61D3	ebioscience

Table 2.9 Surface antibodies, isotype-matched control antibodies and compensation antibodies used during the cell sort.

To prepare the isolated PBMCs for the cell sort, the wells of a round-bottomed 96-well plate were coated with 180 µl FCS. The plate was incubated on the bench for 10 mins at RT before the FCS was removed by gently tapping the plate on absorbent paper. The isolated PBMCs were resuspended in FCS and added to the plate. For the cell sort, the number of cells added to each well was dependent on the number of PBMCs isolated from each donor. The plate was then centrifuged at 290 g (acceleration: 9, brake: 9) for 4 mins at 4°C in order to pellet the cells. The supernatant was then removed and 100 µl of the prepared surface antibodies and isotype-matched control antibodies (Table 2.9) diluted in MACs buffer (phosphate buffered saline (PBS) supplemented with 0.5% bovine serum albumin (BSA) and 2 mM EDTA) were added to the appropriate wells. For compensation, cells were stained with either anti-human CD14 FITC or anti-human CD14 PE-CY7 (Table 2.9). The cells were then incubated for 30 mins at 4°C. Cells were then washed by adding 50 µl of MACs buffer to each well, followed by centrifugation at 290 g for 4 mins at 4°C. Supernatant was removed, and the cells were resuspended in 150 µl MACs buffer before being transferred to FACs tubes containing 400 µl MACs buffer. The stained cells were then stored protected from light at 4°C for approximately 30 mins prior to the cell sort. Following the cell sort, cells were stored briefly on ice. For qPCR experiments, the sorted cells from the $CD14^+$ $CD41^-$, $CD14^+$ $CD41^+$ intermediate, and $CD14^+$ $CD41^+$ populations were centrifuged for 4 mins at 894 g. The supernatant was then removed and the cells were resuspended in 350 µl RLT buffer. Lysed cells were then stored at -80°C ready for RNA isolation. For downstream cell culture experiments, $CD14^+$ $CD41^-$ cells were centrifuged for 4 mins at 894 g, the supernatant was removed, and the cells were resuspended in 1 ml RPMI-1640 + 10% heat inactivated FCS (Hi FCS) + 1% GPS.

2.10.1 *In vitro* monocyte differentiation

Following the cell sort, the $CD14^+$ $CD41^-$ cell population was seeded in a 96 well-plate at 3.37 x 10^4 cells/well in RPMI-1640 + 10% Hi FCS + 1% GPS in a volume of 200 µl/well. Cells were differentiated to macrophages under M1, M2 or Mo-DC culture conditions (Table 2.11). Cells were cultured in an incubator set at 37°C and 5% CO_2 for 6 days. After 6 days, the differentiated cells were treated with 10 ng/ml LPS for 6 hrs or 24 hrs or left unstimulated. Isolated CD14+ monocytes used in work shown figure 4.1 were seeded in a 6 well-plate at 1 x 10^6 cells/well in RPMI-1640 + 10% Hi FCS + 1% GPS in a volume of 1000 µl/well. They were then subsequently differentiated under M1, M2 or Mo-DC culture conditions as described (Table 2.10).

	Media	**Cytokine (Peprotech, UK)**	**Cytokine concentration (ng/ml)**
M1	RPMI + 10% Hi FCS +1% GPS	GM-CSF	10
M2	RPMI + 10% Hi FCS +1% GPS	M-CSF	10
Mo-DC	RPMI + 10% Hi FCS +1% GPS	GM-CSF	25
		IL-4	25

Table 2.10 Culture of $CD14^+$ $CD41^-$ cells under M1, M2 and Mo-DC culture conditions. GM-CSF, M-CSF and IL-4 (stock conc. 100 µg/ml) were supplemented into 10 ml RPMI + 10% Hi FCS + 1% GPS. For cells cultured under M1 conditions, GM-CSF was added to the media, for M2 conditions M-CSF was added, and for Mo-DC, both GM-CSF and IL-4 were added.

Supernatants were collected from cells cultured under M1, M2 or Mo-DC conditions and TNFα levels were analysed using a TNFα sandwich ELISA MAX™ Deluxe set (Biolegend, UK). Upon analysis of the results there was no significant difference in TNFα between the cultured subsets. Therefore I was reluctant to refer to the M1, M2 and Mo-DC cultured cells

as terminally differentiated populations. Furthermore, due to time restraints I was unable to carry out additional phenotyping experiments of these cell populations.

2.11 RNA extraction

RNA was extracted from monocytes and *in vitro* differentiated macrophages using the Qiagen RNeasy Mini Kit. A DNAse step was also included in the protocol in order to remove contaminating genomic DNA. To begin, cells that had been lysed in RLT buffer and subsequently stored at -80°C were thawed and homogenized by vortexing for 1 min. To the lysate, an equal volume of 70% ethanol was added to each sample and mixed well. The sample (up to 700µl) was then transferred to an RNeasy spin column, placed in a 2ml collection tube and centrifuged for 15 secs at 6708 g. The flow through was discarded and the collection tube was reused. If the sample exceeded 700µl, then the previous step was repeated until all the sample had been passed through the column.

In order to carry out the DNAse step, 350µl Buffer RW1 was added to the column, centrifuged for 15 secs at 6708 g and the flow through was discarded. Meanwhile, 10µl DNase I stock solution was added to 70µl Buffer RDD (80µl per sample required). The DNase I/Buffer RDD mix was then added to the membrane of the column and incubated for 15 mins at room temperature. After 15 mins, 350µl Buffer RW1 was added to the column, centrifuged for 15 secs and the flow through was discarded.

500µl of Buffer RPE was added to the column, centrifuged for 15 secs, and the flow through was discarded. This step was then repeated, but centrifuged for 2 mins. The RNeasy spin column was then placed in a 1.5ml collection tube. 30µl of water was added to the column membrane and centrifuged for 1 min to elute the RNA.

2.12 Reverse Transcription

In order to carry out reverse transcription from RNA to cDNA, the Superscript® VILO™ cDNA synthesis kit from Invitrogen was used. 5X VILO™ reaction mix (containing random primers, dNTPs and MgCl2), 10X Superscript® Enzyme mix and RNA (up to 2.5µg) were combined in order to create a total reaction volume of 20µl. The reaction was performed on a Thermocycler for 10 mins at 25°C, 2 hours at 42°C and 5 mins at 85°C. Following this, the cDNA was stored at -20°C.

2.13 PCR (cDNA) clean-up

PCR (cDNA) clean-up was carried out using the NucleoSpin Extract II kit (Macherey-Nagal, UK) in order to remove contaminating buffers and enzymes used during the reverse transcription protocol. The first step was to combine 1 volume of cDNA sample with 2 volumes of buffer NT. This was then loaded on to a NucleoSpin extract II column placed over a collection tube. The column was centrifuged for 1 min at 11,000 g. The flow through was discarded and 600µl of buffer NT3 was added to the column. The column was then centrifuged again at 11,000 g for 1 min. The flow through was discarded and the column was centrifuged at 11,000 g for 2 mins to remove any excess buffer. The column was then placed into a clean 1.5 ml eppendorf and 15-50 µl of Elution buffer NE was added. The elution

buffer was incubated on the column for 1 min. The column along with the collection tube was centrifuged for 1 min at 11,000 g to collect the cDNA.

2.14 Quantitative PCR

In order to carry out quantitative PCR (qPCR), a total reaction volume of 20µl was prepared per sample. 10 µl SensiFAST™ Lo-ROX kit (2X PCR mastermix) (Bioline, UK), 1 µl forward primer, reverse primer and probe (Life Technologies, UK) (Table 2.11), 4 µl RNase free water and 5 µl cDNA. In chapter 5, qPCR was carried out in a 384 well plate, rather than a 96 well plate. As a result, the master mix was adjusted; 5 µl 2X TaqMan® PCR master mix (Applied Biosystems, UK), 0.5 µl forward primer, reverse primer and probe (Life Technologies, UK) (Table 1.3), 3.5 µl RNase free water and 1 µl cDNA.

Gene	Assay ID	Assay	Supplier
ACTB	Hs99999903_m1	TaqMan® Gene Expression assay	Life Technologies
ITGA2B	Hs01116228_m1	TaqMan® Gene Expression assay	Life Technologies
PF4	Hs00427220_g1	TaqMan® Gene Expression assay	Life Technologies
PF4V1	Hs01891271_s1	TaqMan® Gene Expression assay	Life Technologies
PPBP	Hs00234077_m1	TaqMan® Gene Expression assay	Life Technologies

Table 2.11 TaqMan® Gene Expression assays used in this study.

RT PCR was carried out using the Stratagene MX3000P qPCR machine. Reactions were incubated at 50°C for 2 mins, 95°C for 10 mins, 95°C for 15 secs (45 cycles) and 60°C for 1 min. The genes of interest were quantified relative to the housekeeping gene, β-actin, by fold change in the gene expression. The formula, power (2,-ΔCt) was used. In chapter 5, an alternative qPCR machine was used, the Applied Biosystems 7900 qPCR machine.

2.15 In Situ Hybridization

In Situ Hybridization was carried out using the QuantiGene® ViewRNA ISH Tissue 1-Plex Assay kit (Panomics, Italy). The kit was comprised of three units; the QuantiGene ViewRNA ISH Tissue 1-Plex Assay Kit (QVT0050), the QuantiGene View RNA Chromogenic Signal Amplification Kit (QVT0200), and the QuantiGene View RNA Type 1 Probe Set. Each kit was designed to be sufficient for 24 assays. However, reagent volumes were adjusted to achieve a greater number of assays.

Three different QuantiGene View RNA Type 1 Probe Sets were used for the experiments:

- Positive control probe: GAPDH
- Negative control probe: BACILLUS SUBTILIS, dapB
- Target probe: Pro-platelet basic protein (PPBP)/ Chemokine (C-X-C motif) ligand 7

The assay was split into two parts, spread over the course of two days. The first part involved the sample preparation and hybridization of the target probe (day 1), and the second part involved signal amplification and detection (day 2).

2.15.1 Part 1: Sample preparation and hybridization of the target probe

Prior to commencing the assay, the hybridization system/tissue culture incubator was set at 40 ± 1°C with 0% CO_2, and the dry incubator was set at 60 ± 1°C. Slides were labelled and placed in a slide rack. The rack of slides was then transferred to the dry incubator and baked for 60 mins. During this time, the following reagents were prepared;

- 2L 1X Phosphate Buffered Saline (PBS) 1 tablet/100ml ddH_2O (Oxoid/Thermo Scientific, UK)
- 100ml 100% ethanol, 100ml 95% ethanol, and 100ml 70% ethanol (VWR chemicals, UK)
- 2L wash buffer: 1.5L ddH_2O, 18ml wash component 1, and 5ml wash component 2. Adjust to final volume of 2L with ddH_2O
- 500ml 1X pretreatment Solution: 5 ml 100X pretreatment solution and 495ml ddH_2O
- 100ml storage buffer: 30ml wash component 2 and 70ml ddH_2O

1X PBS, ethanol, pretreatment solution and storage buffer were prepared using HyPure™ Molecular Biology Grade Water (HyClone®) (Thermo Scientific, UK).

During the baking step, the probes were thawed, mixed and briefly centrifuged and placed on ice. 10ml 1X PBS and the probe set diluent QF were pre-warmed to 40°C. Following the baking the step, the sections were de-waxed in 100ml xylene (VWR chemicals, UK) for 5 mins x 3, and then subsequently rehydrated in 100ml 100% ethanol for 5 mins, 95% ethanol for 5 mins, and 70% ethanol for 5 mins. Slides were then removed from the rack, and air dried for 5 mins. A hydrophobic barrier was drawn around the tissue sections to prevent the spread of reagents across the slide (Vector Laboratories, UK). When dry, the slides were loaded into a slide rack and placed in the pre-warmed 1X pretreatment solution (85-90°C). Slides were incubated for the desired time, 10 mins, as determined by the optimisation experiments (Table 2.12). Following pretreatment, the slides were removed from the solution and submerged in 100ml ddH_2O. Slides were washed for 1 min with frequent agitation and then transferred to 1X PBS.

Tonsil	Slide	Heat pre-treatment	Protease digestion	Quantigene ViewRNA probe set
S077007	1	5	10	GAPDH
S077008	2	10	10	GAPDH
S077009	3	10	20	GAPDH
S077010	4	5	10	PPBP
S077011	5	10	10	PPBP
S077012	6	10	20	PPBP
S077013	7	5	10	*Bacillus subtillis* dapB
S077014	8	10	10	*Bacillus subtillis* dapB
S077015	9	10	20	*Bacillus subtillis* dapB

Table 2.12 Optimisation protocol for determining appropriate heat pre-treatment and protease digestion times for the Quantigene ViewRNA ISH Tissue 1-Plex Assays. Optimisation of the In Situ Hybridization experiments was carried out using 4µm cut sections from formalin-fixed, paraffin-embedded (FFPE) tonsil biopsies. Sections were obtained from the Human Biomaterials Resource Centre (HBRC): Biobank (University of Birmingham, UK). Each probe; GAPDH, PPBP, and *Bacillus subtillis* dapB, was tested using three different heat pre-treatment and protease digestion combinations. Slides 1, 4 and 7, had 5 mins heat pre-treatment and 10 mins protease digestion. Slides 2, 5, and 8, had 10 mins heat pre-treatment and 10 mins protease digestion. Slides 3, 6, and 9, had 10 mins heat pre-treatment and 20 mins protease digestion. Following the optimisation experiments a heat pre-treatment time of 10 mins and a protease digestion time of 10 mins was used for all experiments.

Next, the protease solution was prepared by diluting the protease solution 'Protease QF' 1:100 in pre-warmed 1X PBS (Table 2.13). The solution was scaled according to the number of slides run per experiment. The protease solution was briefly vortexed.

Working Protease Solution	
Reagent	**Volume**
Protease QF	2µl
1X PBS (pre-warmed to 40°C)	198µl
Total volume	**200µl**

Table 2.13 Preparation of the working protease solution for the protease digestion step of the In Situ Hybridization. Volumes were scaled up depending on the number of slides run during each experiment.

The 1X PBS was removed from the slides by gently tapping onto laboratory tissue. The slides were then placed in a wet box and 200µl of protease solution was added to each section. The sections were then covered with a square of parafilm to enable the protease solution to spread across the entire section and to prevent drying. The slides were then transferred to the hybridization system and incubated at 40 ± 1°C for the desired time, 10 mins, as determined during the optimisation experiments (Table 2.12). Following the protease digestion step, the parafilm was removed from the section and the working protease solution was tapped off the slide onto laboratory tissue. The slides were washed in 100ml 1X PBS for 1min x 2 and then fixed in 100ml 4% formaldehyde/Formalin solution (Sigma Aldrich, UK) for 4 mins at RT . The slides were then washed, once more, with 100ml 1X PBS for 1 min with frequent agitation.

Meanwhile, the probes for the In Situ Hybridization were prepared (Table 2.14). Probes were diluted 1:50 in pre-warmed probe set diluent QF. The solution was scaled according to the number of slides run per experiment. The probes were briefly vortexed.

Working Probe Set Solution	
Reagent	**Volume**
Probe Set Diluent QF (pre-warmed to 40°C)	196µl
Quantigene ViewRNA TYPE 1 probe set	4µl
Total Volume	**200µl**

Table 2.14 Preparation of the working probe set solution for In Situ Hybridization. Volumes were scaled up depending on the number of slides run during each experiment.

The 1X PBS was removed from the slides by gently tapping onto laboratory tissue. The slides were then placed in a wet box and 200µl working probe set solution was added to each section. Each section was covered with a square of parafilm. The slides were then transferred to the hybridization system and incubated at 40 ± 1°C for 3 hrs. Following incubation, the working probe set solution was tapped off the slide, excess solution was removed with PBS and the slides were washed in 100ml wash buffer for 2 mins x3. Slides were then transferred into 100ml storage buffer. Slides were stored overnight at RT.

2.15.2 Part 2: Signal amplification, detection and visualisation

The hybridization system/tissue culture incubator was set at 40 ± 1°C with 0% CO_2. Prior to commencing part 2, both the Amplifier Diluent QF and Label Probe Diluent QF were pre-warmed to 40°C. The PreAmp1 QF and Amp1 QF were thawed and placed on ice until use. The Label Probe-AP was placed on ice, and the Fast Red tablets, Naphol buffer and AP enhancer solution was brought to RT.

Slides were removed from the storage buffer and washed in 200ml wash buffer for 2 mins x 2 with frequent agitation. Meanwhile, the PreAmp1 solution was prepared (Table 2.15). The PreAmpl 1 QF solution was diluted 1:100 in pre-warmed Amplifier Diluent QF. The solution was scaled according to the number of slides run per experiment. The probes were mixed by gentle inversion.

Working PreAmp1 Solution	
Reagent	**Volume**
Amplifier Diluent QF (pre-warmed to 40°C)	198µl
PreAmp1 QF	2µl
Total Volume	**200µl**

Table 2.15 Preparation of the working PreAmp1 solution for In Situ Hybridization. Volumes were scaled up depending on the number of slides run during each experiment.

Following the wash step, the slides were removed from the wash buffer and tapped on laboratory tissue. 200µl working Pre Amp 1 solution was added to each tissue section. Slides were then transferred to the hybridization system and incubated at 40 ± 1°C for 35 mins. Slides were tapped on laboratory tissue and washed in 100ml wash buffer for 3 mins x 3 with constant agitation. Next, the working Amp1 solution was prepared by diluting the Amp1 QF 1:100 in pre-warmed Amplifier Diluent QF (Table 2.16). The solution was scaled according to the number of slides run per experiment. The probes were mixed by gentle inversion.

Working Amp1 Solution	
Reagent	**Volume**
Amplifier Diluent QF (pre-warmed to 40°C)	198µl
Amp1 QF	2µl
Total Volume	**200µl**

Table 2.16 Preparation of the working Amp1 solution for In Situ Hybridization. Volumes were scaled up depending on the number of slides run during each experiment.

Slides were removed from the wash buffer, tapped on laboratory tissue and transferred to a wet box. 200µL working Amp1 solution was added to each section. The slides were then transferred to the hybridization system and incubated at 40 ± 1°C for 22 mins. Following

incubation, the working Amp1 solution was tapped off the slides and the slides were washed in 100ml wash buffer for 3 mins x 3 with constant agitation. During the wash steps the Label Probe-AP solution was prepared by diluting the Label Probe AP 1:1000 in pre-warmed Label Probe Diluent QF (Table 2.17). The solution was mixed by gentle inversion.

Working Label Probe-AP Solution	
Reagent	**Volume**
Label Probe Diluent QF (pre-warmed to 40°C)	999µl
Label Probe-AP	1µl
Total Volume	**1000µl**

Table 2.17 Preparation of the working Label Probe-AP solution for In Situ Hybridization.

The slides were removed from the wash buffer, tapped on laboratory tissue and transferred to a wet box. 200µl working Label Probe-AP was added to each section. The slides were then transferred to the hybridization system and incubated at 40 ± 1°C for 22 mins. Following incubation, the Label Probe-AP solution was tapped off the slides and the slides were washed in 100ml wash buffer for 2 mins x 4 with constant agitation. Slides were removed from the wash buffer, and placed face up on laboratory tissue. Immediately 200µl AP-Enhancer solution was added to each tissue section and incubated for 5 mins at RT. During this incubation the Fast Red substrate was prepared. To a 1.5ml tube, 1.25ml Naphol buffer and ¼ Fast Red tablet was added. The solution was then vortexed at high speed to dissolve the tablet. After 5 mins, the AP-Enhancer solution was removed from the sections. The slides were transferred to a wet box and 200µl Fast Red substrate was immediately added to each tissue section. The slides were then transferred to the hybridization system and incubated at 40± 1°C for 30 mins. The Fast Red substrate was removed from each section by washing in 100ml 1X

PBS for 1 min. The sections were then counterstained using 3µg/ml DAPI prepared in PBS. 200µl DAPI was added to each section for approximately 1 min. Excess DAPI was removed from each section and the slides were washed in 100ml ddH_2O. The sections were then removed from the ddH_2O and left to air dry for 20-30 mins. Sections were subsequently mounted in 1 drop of Vectamount™ AQ aqueous mounting medium (Vector Laboratories Ltd, UK). Coverslips (22mm x 40 mm rectangular) were placed on top of the mountant and the slides were left to dry at RT until visualisation.

2.15.3 In Situ Hybridization visualisation

Sections stained during the optimisation experiments were first visualised using the Zeiss LSM 780 Zen Confocal microscope at x40 and later x63 objective magnification/total magnification x400 and x630. Gain and threshold settings were adjusted so that the background staining on the negative probe, *Bacillus subtillis* dapB, was minimal. A background of <1 dot/10 cells was deemed acceptable by Affymetrix/Panomics. Images were subsequently taken of the GAPDH sections and finally the target probe, PPBP sections.

Coverslips were then removed from the slides by soaking in 1X PBS for 3-5 hours. The sections were counterstained using Haematoxylin for 30 seconds before being washed gently in tap water to 'blue' the Haematoxylin. Sections were then re-mounted in Vectamount™ as described previously. Images were taken using the Nikon Eclipse E400 microscope.

2.15.4 Immunofluorescence following In Situ Hybridization

Coverslips were removed from the sections by soaking in 1X PBS for 3-5 hours. The slides were then washed 3 x 5 mins in PBS with gentle shaking. Sections were blocked in 2% BSA/0.1% Triton-X/PBS for 1 hour at RT. Following this, the blocking solution was removed from the sections by gently tapping on laboratory tissue. Immediately 100µl primary antibody prepared in the blocking solution was added. The slides were then incubated overnight at 4°C in a wet box. The following day, slides were transferred to PBS and washed 3 x 5 mins with gentle shaking. 100µl of secondary antibody prepared in the blocking solution was then added to each section and incubated for 2 hours at RT in a wet box. The slides were then washed as described previously and subsequently counterstained with 3µg/ml DAPI for 1 min. Finally, slides were washed for 1 min in dH2O and re-mounted in Vectamount™. Images were taken using the Zeiss LSM 780 Zen Confocal microscope at x400 total magnification.

3 CXCL4 AND CXCL7: POTENTIAL PREDICTORS OF DIAGNOSTIC OUTCOME IN EARLY INFLAMMATORY ARTHRITIS?

3.1 INTRODUCTION

The National Institutes of Health Biomarkers Definitions Working Group defines a biomarker as 'a characteristic that is objectively measured and evaluated as an indicator of normal biological processes, pathogenic processes, or pharmacologic responses to a therapeutic intervention'. Biomarkers are extremely powerful tools that can be utilised in a number of clinical applications including the prediction of both diagnosis and prognosis of disease (Mayeux, 2004, Perlis, 2011, Tesch et al, 2010). Biomarkers are predominantly measured in tissue and biological fluids including serum, plasma, urine, bronchoalveolar lavage, sputum and cerebrospinal fluid (Schrohl et al, 2008). In RA, biomarkers include autoantibodies (e.g. RF and anti-CCP), various cytokines and chemokines, proteases, collagen degradation products, markers of inflammation (e.g. ESR and CRP) and genetic polymorphisms (e.g. shared epitope and PTPN22) (Tesch et al, 2010). Clinical assessment by X-ray, ultrasound, and Magnetic Resonance Imaging (MRI) are examples of imaging biomarkers that are commonly used in the diagnosis and monitoring of disease progression in RA (Tesch et al, 2010). Assays that measure more than one biomarker at a time are also becoming increasingly attractive (O'Hurley et al, 2014, Rifai et al, 2006). The opportunity to offer personalised medicine and improve patient care may also be made a possibility with the use of biomarkers. They may be used to assess patients who are most likely to respond to certain therapeutics, to establish safety and dosing regimens, and to identify any patients likely to suffer from adverse

events. Moreover, biomarkers may be used within clinical trials as determinants of clinical and surrogate endpoints (Tesch et al, 2010).

In this chapter I sought to determine CXCL4 and CXCL7 protein expression within the rheumatoid synovium. This body of work was influenced by previous findings within our research group suggesting that CXCL4 and CXCL7 mRNA expression in synovial tissue biopsies could distinguish patients with early RA from those with resolving synovitis. I systematically addressed the suitability of both chemokines as predictive markers of outcome in patients presenting with early synovitis at our early arthritis clinics. Using synovial biopsies collected by ultrasound guided biopsy, I stained sections with antibodies specific for CXCL4, CXCL7, vWF, CD41 and CD68 by immunofluorescence. I also explored the potential of both chemokines as predictive biomarkers in plasma samples collected from patients enrolled in the BEACON cohort.

3.2 RESULTS

3.2.1 CXCL4 and CXCL7 expression at the protein level in the rheumatoid synovium

I first set out to stain rheumatoid synovial tissue sections taken from patients who had undergone joint replacement with CXCL4 and CXCL7 alongside CD41 (GPIIb) and von Willebrand Factor (vWF). Here I observed CXCL4 (Figure 3.1 A) and CXCL7 (Figure 3.1B) expression at the protein level in the tissue. CXCL4 and CXCL7 expression was observed outside the vasculature. Platelets stained with the surface marker CD41 were also detectable in the tissue. Although platelets were mainly detectable in the blood vessels, there were also a number found outside the vessels. Co-localisation of both CXCL4 and CXCL7 with CD41 was limited in the rheumatoid synovium. It was predominantly observed in thrombi.

The specificity of the CXCL7 antibody was confirmed by a blocking with the CXCL7 peptide. In brief the antibody was incubated overnight with increasing concentrations of CXCL7 peptide. The CXCL7-peptide complex was then used to stain a section of rheumatoid synovium from a patient who had undergone joint replacement. The anti-CXCL7 staining was successfully inhibited when incubated with the CXCL7 peptide (see appendix, Figure 8.1).

A

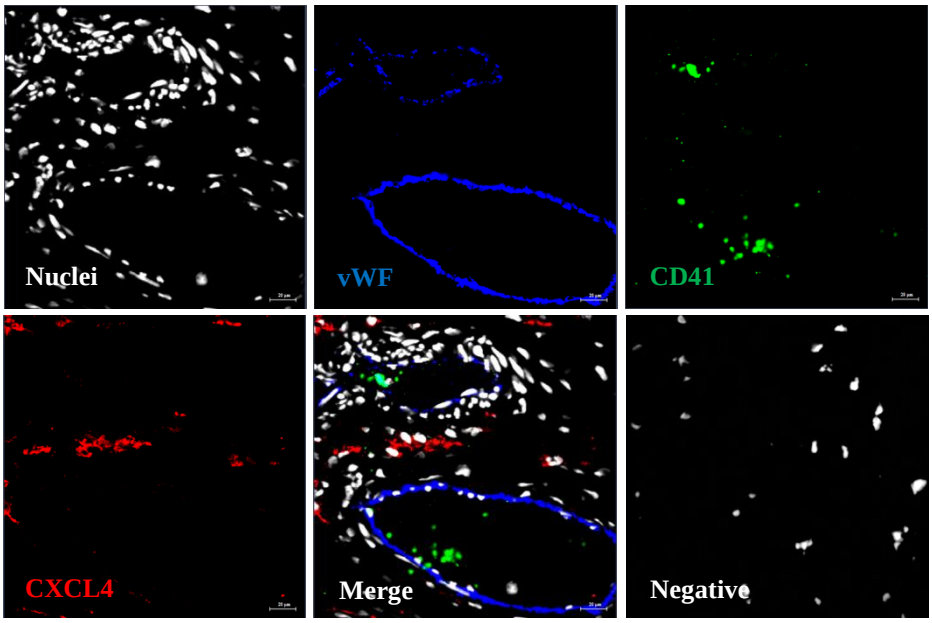

B

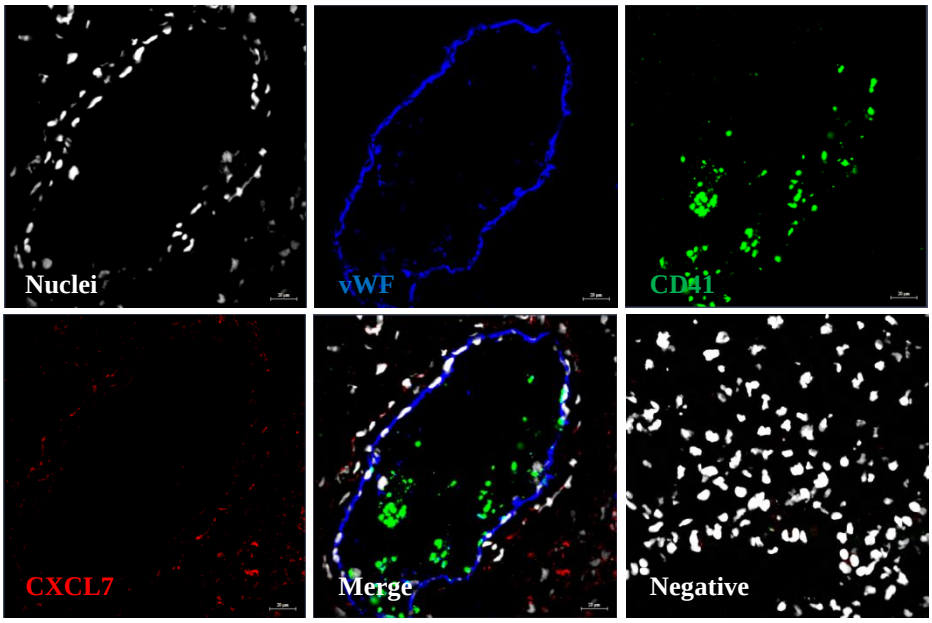

Figure 3.1 Staining of the rheumatoid synovium with antibodies specific for CXCL4/CXCL7, CD41 and vWF. Sections of rheumatoid synovium taken from patients who had undergone joint replacement were stained with antibodies specific for **A**) CXCL4 (red) or **B**) CXCL7 (red) alongside CD41 (green), and vWF (blue). Nuclei were counterstained with Hoechst 33258 (grey). Images were taken at x400 total magnification using the Zeiss LSM 510-UV confocal. Tissue sections were stained alongside isotype matched controls which were negative. CXCL4 (n=7), CXCL7 (n=6). Scale bar: 20µm.

3.2.2 CXCL4 and CXCL7 staining on CD68 positive macrophages and plasmacytoid dendritic cells

Synovial biopsies taken from patients who had undergone joint replacement due to longstanding RA and subsequently stained with the macrophage specific marker CD68, clearly identified macrophages as an abundant cell population within the rheumatoid synovium (Figure 3.2). As the CXCL4 and CXCL7 staining described in the previous section was largely observed outside the vasculature and was not predominantly localised to platelets, I decided to stain rheumatoid synovium with antibodies specific to CXCL4 and CXCL7 alongside CD68. I observed co-localisation of both CXCL4 (Figure 3.3A) and CXCL7 (Figure 3.3B) with CD68 (pink/purple staining). Moreover, not all $CD68^+$ stained cells were $CXCL4^+$ or $CXCL7^+$, and vice versa.

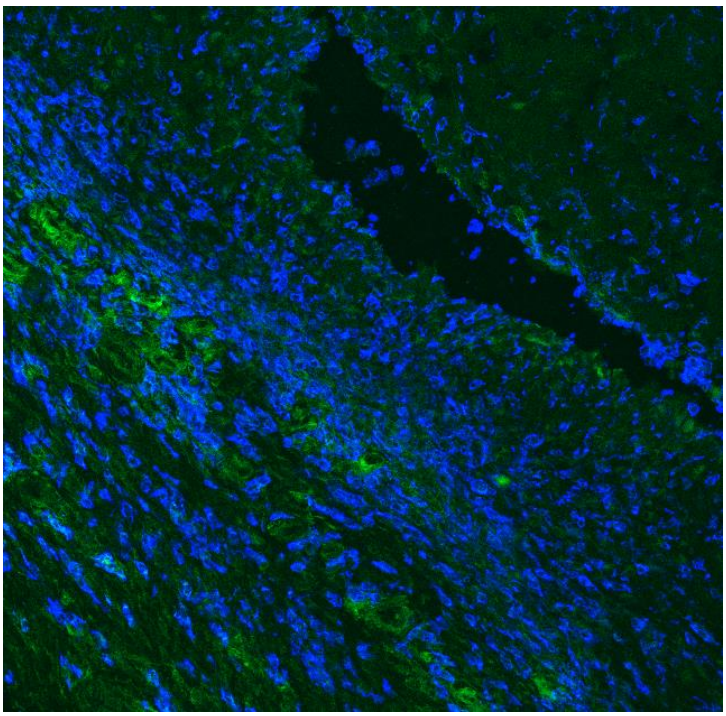

Figure 3.2 Staining of the rheumatoid synovium with an antibody specific for CD68. A section of synovium taken from a patient with long standing rheumatoid arthritis who had undergone joint replacement was stained with antibodies specific for CD68 (blue) and as a contrast CD248 (green). Sections were stained and images were taken at x400 total magnification using the Zeiss LSM 780 confocal by Dr. Jennifer Marshall.

During the course of these experiments, it was reported that increased CXCL4 expression in the plasma of patients with systemic sclerosis and scleroderma was attributed to expression by plasmacytoid DCs (Van Bon et al, 2014). In response to these observations, I stained rheumatoid synovial tissue taken from patients undergoing joint replacement with BDCA-2, an antibody specific for pDCs, alongside CXCL4 and CXCL7. I observed co-localisation of CXCL4 with BDCA-2 in the rheumatoid synovium (Figure 3.4). However, not all cells positive for CXCL4 were also positive for BDCA-2. Co-localisation of CXCL7 with BDCA-2 was not observed in the majority of rheumatoid synovium analysed. Moreover, CXCL4 and CXCL7 was not found to co-localise with CD1c, BDCA-2 and CD123 in tonsils (data not shown). As a result macrophages, rather than pDCs, may be the predominant source of both chemokines in rheumatoid arthritis.

A

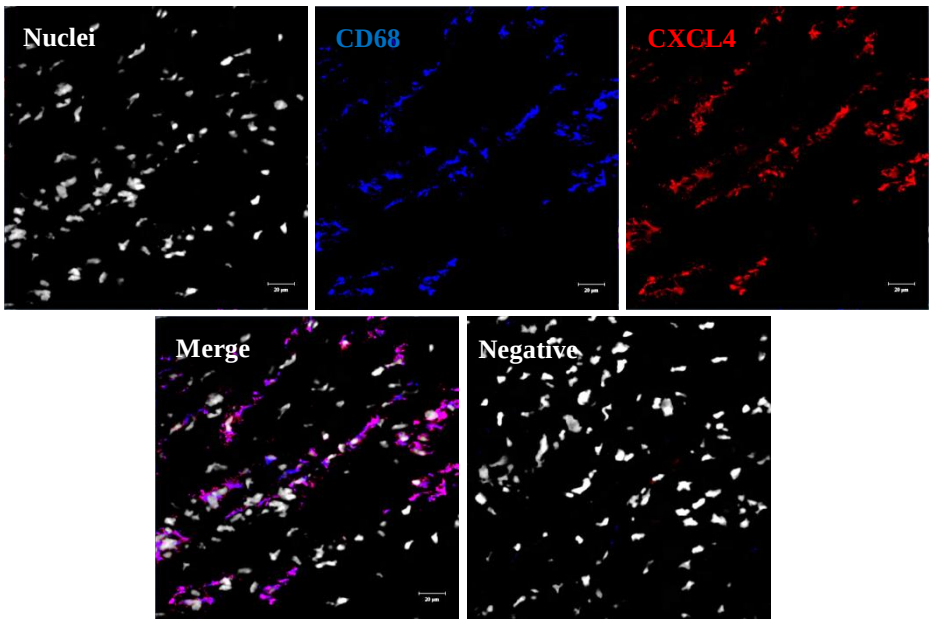

B

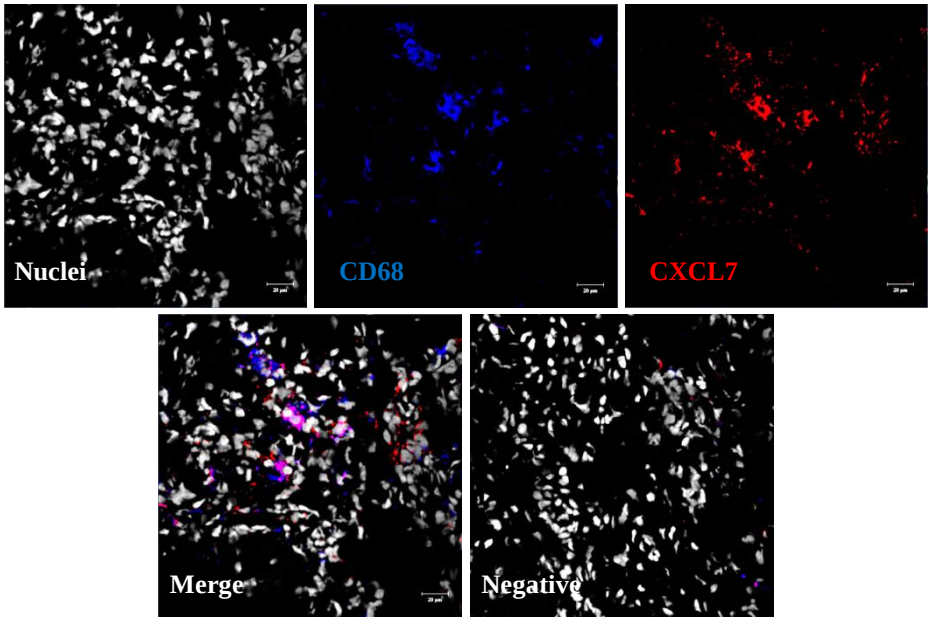

Figure 3.3 Staining of the rheumatoid synovium with antibodies specific for CXCL4/CXCL7 and CD68. Sections of rheumatoid synovium taken from patients who had undergone joint replacement were stained with antibodies specific for **A**) CXCL4 (red) or **B**) CXCL7 (red) alongside CD68 (blue). Nuclei were counterstained with Hoechst 33258 (grey). Images were taken at x400 total magnification using the Zeiss LSM 510-UV confocal. Tissue sections were stained alongside isotype matched controls which were negative (n=5). CXCL4 (n=5), CXCL7 (n=5) Scale bar: 20µm.

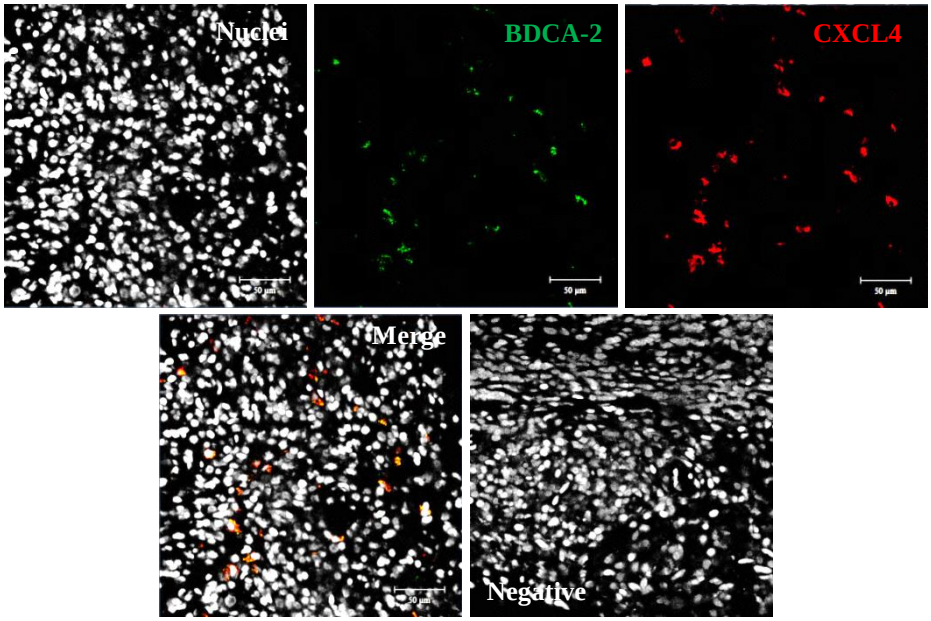

Figure 3.4 Staining of plasmacytoid dendritic cells in the rheumatoid synovium with antibodies specific for CXCL4 and BDCA-2. Sections of synovium from RA patients who had undergone joint replacement were stained with antibodies specific for BDCA-2 (green) and CXCL4 (red) (n=6). Nuclei were counterstained using Hoechst 33258 (grey). Sections were stained alongside isotype matched controls which were negative. Images were taken at x400 total magnification using the Zeiss LSM 780 Zen confocal. Scale bar: 50µm.

3.2.3 Expression of CXCL4 and CXCL7 within the synovium of patients enrolled in the BEACON cohort

I sought to determine the expression of CXCL4 and CXCL7 at the protein level within synovial biopsies taken from four different patient groups; established RA patients (symptom duration >12 weeks, <3 years), early RA patients (symptom duration <12 weeks), resolving synovitis patients, and uninflamed controls (Table 3.1, Appendix Table 8.2). All biopsies were taken from individuals naive for DMARDs and glucocorticoids. Each synovial biopsy was stained with antibodies specific for CXCL4 (Figure 3.5 A) or CXCL7 (Figure 3.5 B), CD68, CD41 and vWF. Co-staining of CXCL4 or CXCL7 with CD68 and CD41 enabled us to identify CXCL4 or CXCL7 staining on macrophages and platelets, respectively. Co-staining sections with vWF and both chemokines enabled us to distinguish positive staining inside and outside the synovial vasculature. A section from each patient was also stained for CXCL4 alongside BDCA-2. All sections were stained alongside isotype matched negative controls.

A

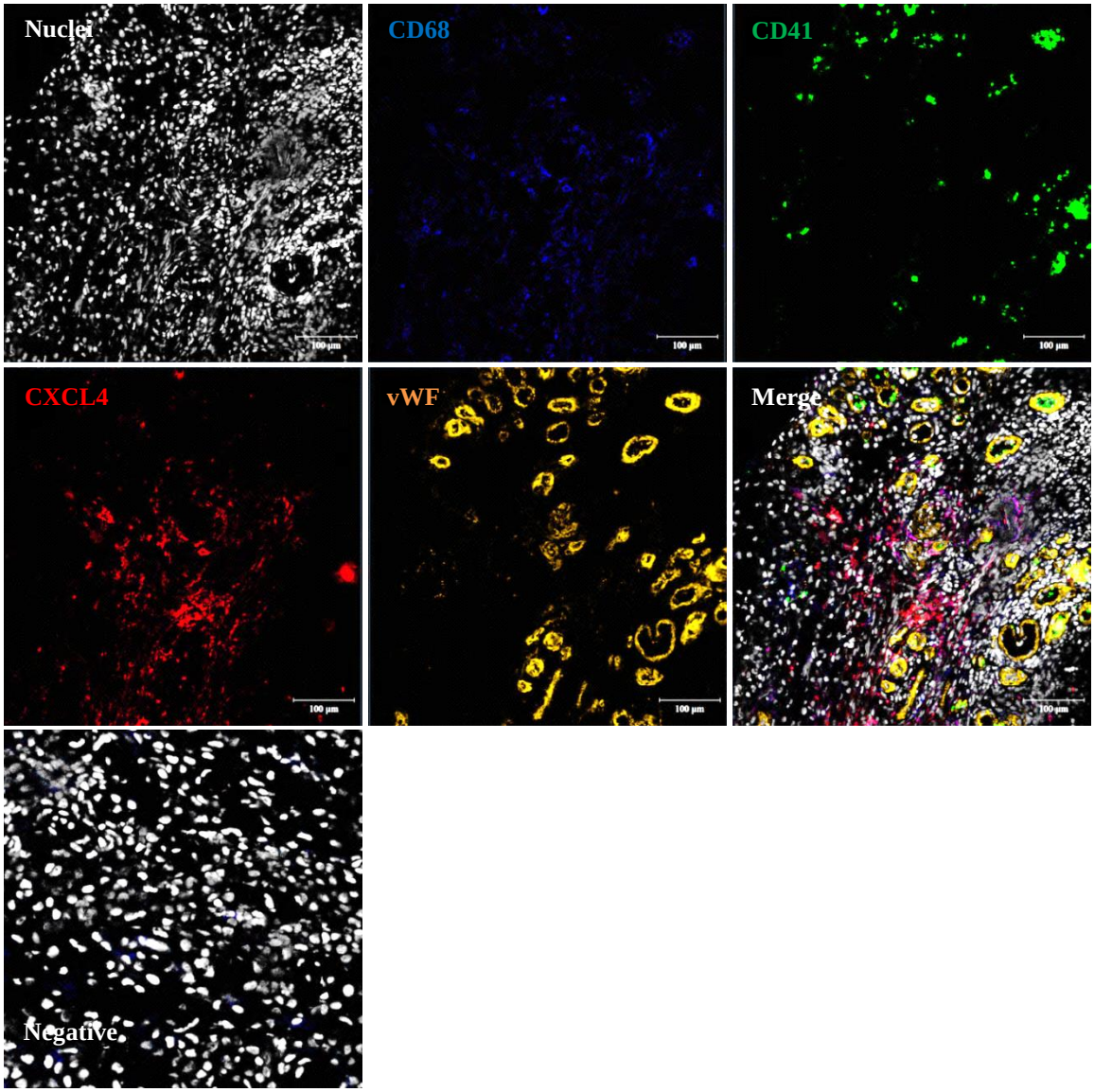

B

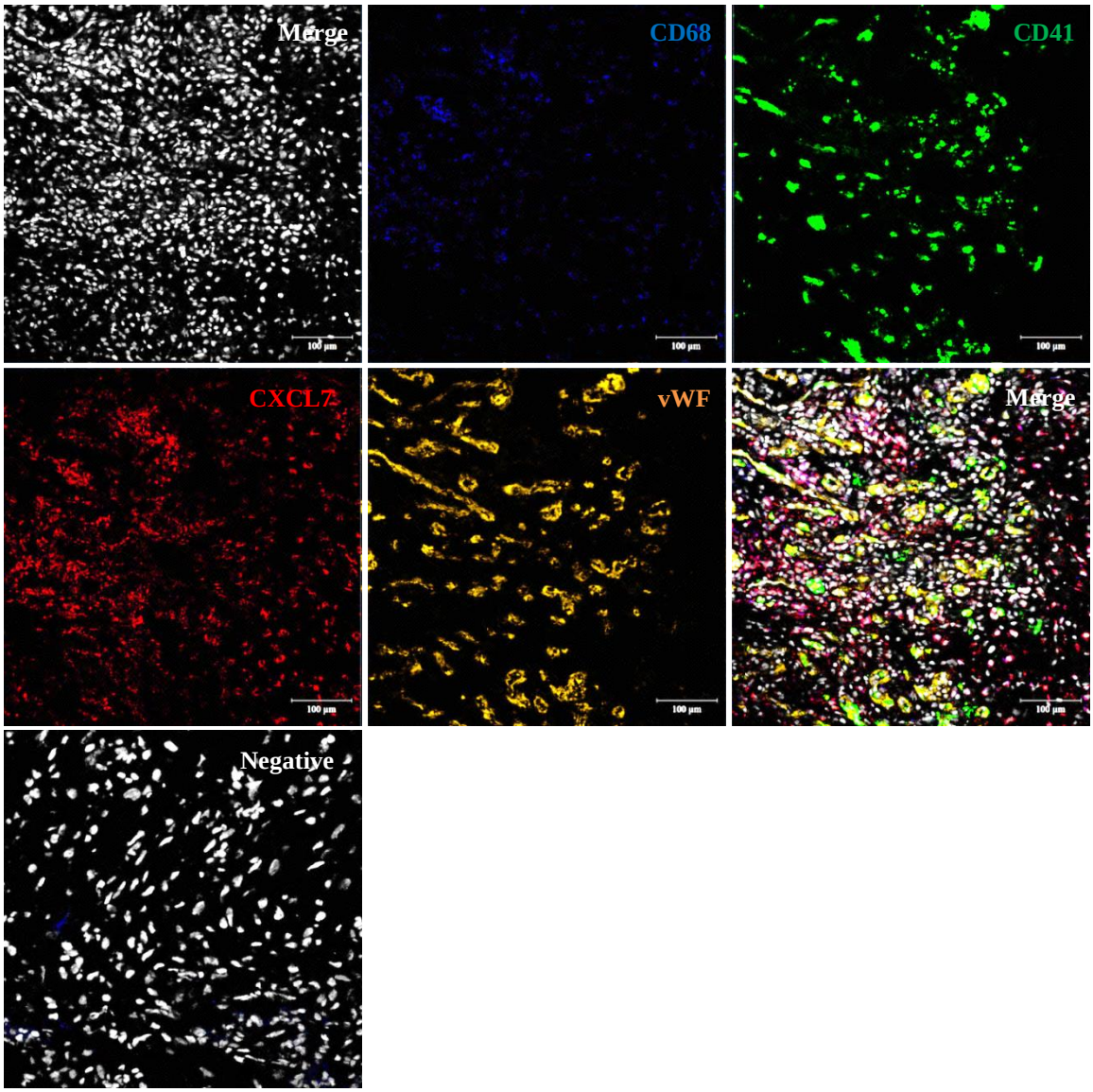

Figure 3.5 Synovial tissue section from an early RA patient stained with antibodies specific for CXCL4 or CXCL7, CD68, CD41 and vWF. Tissue sections were stained with antibodies specific for **A**) CXCL4 (red) or **B**) CXCL7 (red), CD68 (blue), CD41 (green) and vWF (orange). Nuclei were counterstained using Hoechst 33258 (grey). Sections were stained alongside isotype matched controls which were negative. 2 x 2 tile scans were taken at x400 total magnification using the Zeiss LSM 780 Zen confocal. Co-staining of CXCL4 or CXCL7 with CD68 and CD41 identified CXCL4 or CXCL7 expression on macrophages and platelets, respectively. Co-staining with vWF distinguished between CXCL4 or CXCL7 expression inside and outside the vasculature. Scale bar: 100µm.

CXCL4 and CXCL7 were expressed in the synovium of all patient groups analysed. $CD41^+$ platelets were predominantly evident inside the vasculature as opposed to outside. Co-localisation of CXCL4 and CXCL7 with $CD68^+$ macrophages was observed in the synovium. However, not all CXCL4 and CXCL7 positive cells were also $CD68^+$ and vice-versa. Co-localisation of $CD41^+$ platelets with CXCL4 and CXCL7 was also observed, however this was largely evident in thrombi within blood vessels. No co-localisation of CXCL4 and CXCL7 with $CD41^+$ platelets was observed outside the vasculature. BDCA-2^+ cells were not observed in the sections.

3.2.4 Quantification of CXCL4 and CXCL7 in tissue sections from established RA patients, early RA patients, resolving synovitis patients and uninflamed controls (BEACON cohort)

CXCL4 and CXCL7, CD68, CD41, and vWF immunofluorescence was quantified in synovial biopsies from established RA patients (n=11), early RA patients (n=10), resolving synovitis patients (n=9) and uninflamed controls (n=9) using the Zeiss LSM 780 Zen confocal and the Zen 2010 software. There was no statistically significant difference in the acute phase markers; CRP (Kruskall-Wallis p=0.2059) and ESR (Kruskall-Wallis p=0.1370) between the patient groups. Although a small number of patients who went on to develop a non RA-persistent inflammatory arthritis were stained with the antibody panel, they were not included in the quantification analysis as they represented a very heterogeneous group (psoriatic arthritis n=2, sarcoidosis n=1, ankylosing spondylitis n=1, unclassified n=1). Please refer to table 3.1 and appendix table 8.2 for further patient demographics and clinical characteristics. For each biopsy an 8 x 8 overview scan (0.7 zoom) was first taken at x400 total magnification. Using the position tool on the Zen 2010 software, 5 or 6 regions were then

selected from the overview scan to 2 x 2 tile scan (5% overlap, 0.0080 rotation) at x400 total magnification. To avoid experimental bias when selecting regions from the large overview to tile scan, the CXCL4/CXCL7 channel (ChS2-T3) was turned off. Prior to analysis, each 2 x 2 tile scan was stitched together using the processing function within the software. This resulted in each tile scan being recognised as a single image.

	Uninflamed	Resolving arthritis	Early RA	Established RA	Early non-RA
Number	9	9	10	11	5
Symptom duration (weeks); median (IQR)	na	6 (3-7)	7 (4.8-9.3)	45 (16-53)	7 (2-8.5)
Female; n (%)	4 (44)	3 (33)	5 (50)	6 (55)	2 (40)
Age, years; median (IQR)	41 (31-43)	37 (33-65)	58 (50-65)	62 (57-65)	41 (37-56)
RF and/or anti-CCP positive; n (%)	na	0 (0)	4 (40)	6 (55)	1 (20)
Global disease-related variables					
CRP; median (IQR)	na	8 (13-13.5)	26 (7.5-58)	10 (0-79)	25 (18.5-54)
ESR; median (IQR)	na	18 (5.5-51)	19 (4.75-39.25)	50 (34-70)	44 (24-73.5)
DAS28; median (IQR)	na	4.1 (3.4-5.7)	4.7 (3.8-5.8)	5.2 (4.6-7.5)	4.8 (4.1-6.4)
Biopsied joint-related variables					
Joint biopsied					
Ankle; n (%)	0 (0)	2 (22)	2 (20)	3 (27)	2 (40)
Knee; n (%)	9 (100)	7 (78)	7 (70)	8 (73)	3 (60)
MCP joint; n (%)	0 (0)	0	1 (10)	0 (0)	0 (0)

Early non-RA group; psoriatic arthritis n=2, sarcoidosis n=1, ankylosing spondylitis n=1, unclassified n=1.

CCP, cyclic citrullinated peptide; RF, rheumatoid factor; CRP, C-reactive protein; ESR, erythrocyte sedimentation rate; DAS28, Disease Activity Score in 28 joints; MCP, metacarpophalangeal; na, not available.

Table 3.1 Demographic and clinical characteristics of study participants used for the detection of CXCL4 and CXCL7 by immunofluorescence.

To quantify the immunofluorescence signal for CXCL4 and CXCL7, CD68, CD41 and vWF, areas of tissue were selected using the overlay function within the Zen 2010 software (Figure 3.6A). Any areas of tissue that were folded or damaged were excluded from the analysis. Pixel counts were then obtained using the histogram function within the software for each individual channel; CXCL4 and CXCL7 (ChS2-T3), CD68 (Ch2-T1), CD41 (ChS1-T2) and vWF (Ch2-T4). The pixel counts for the nuclei channel (Ch1-T1) were not included in the analysis (Figure 3.6B). The pixel counts were then exported into Microsoft Excel. Here, the total number of pixels for each channel from intensity 30 to 255 was calculated. This value was then divided by the area [µm x µm] to give the number of pixels per μm^2 area. The mean values for the number of pixels per μm^2 area were calculated from the 5-6 2 x 2 tile scans and subsequently plotted on graphs (Figure 3.7).

A

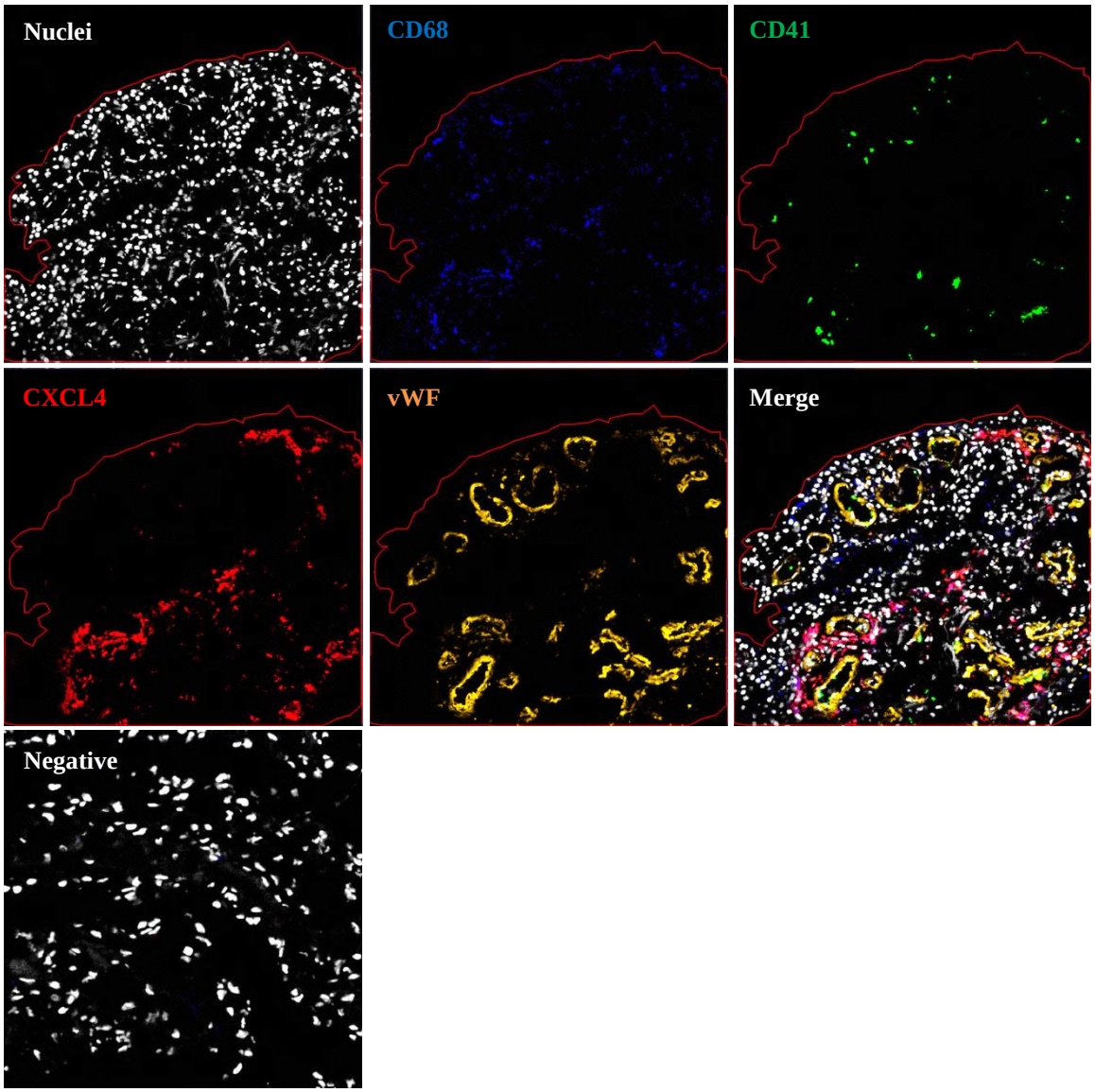

B

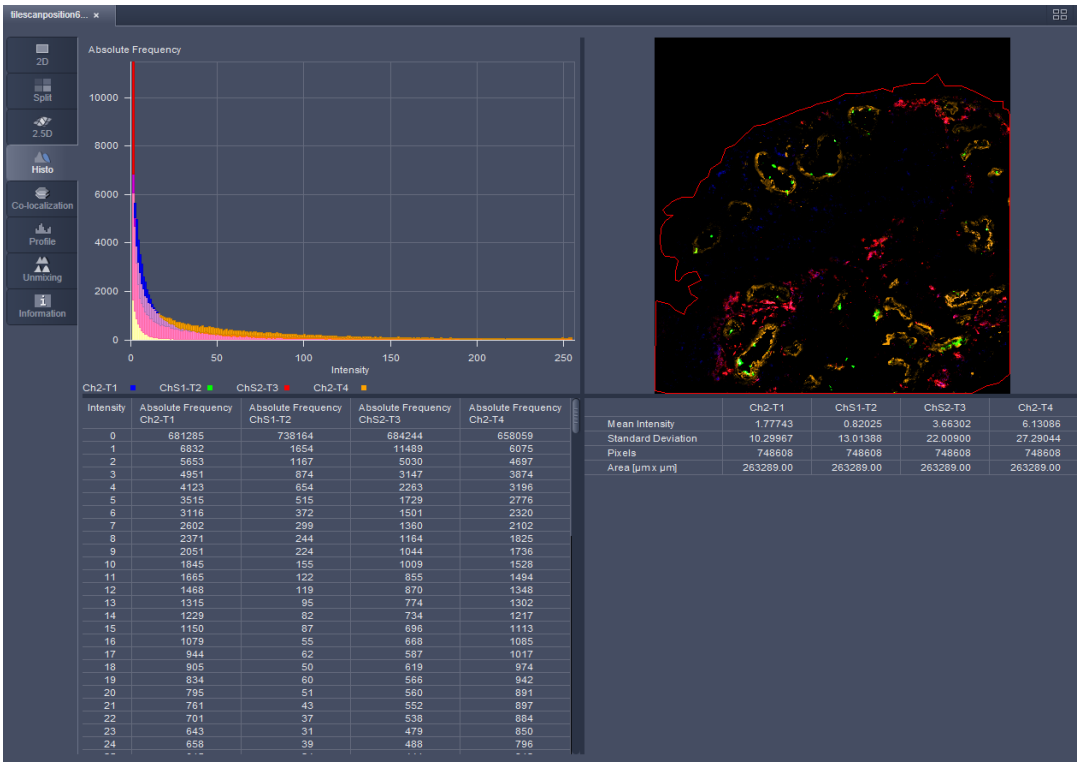

Intensity	Absolute Frequency Ch2-T1	Absolute Frequency ChS1-T2	Absolute Frequency ChS2-T3	Absolute Frequency Ch2-T4
0	681285	738164	684244	658059
1	6832	1654	11489	6075
2	5653	1167	5030	4697
3	4951	874	3147	3874
4	4123	654	2263	3196
5	3515	515	1729	2776
6	3116	372	1501	2320
7	2602	299	1360	2102
8	2371	244	1164	1825
9	2051	224	1044	1736
10	1845	155	1009	1528
11	1665	122	855	1494
12	1468	119	870	1348
13	1315	95	774	1302
14	1229	82	734	1217
15	1150	87	696	1113
16	1079	55	668	1085
17	944	62	587	1017
18	905	50	619	974
19	834	60	566	942
20	795	51	560	891
21	761	43	552	897
22	701	37	538	884
23	643	31	479	850
24	658	39	488	796

	Ch2-T1	ChS1-T2	ChS2-T3	Ch2-T4
Mean Intensity	1.77743	0.82025	3.66302	6.13086
Standard Deviation	10.29867	13.01388	22.00900	27.29044
Pixels	748608	748608	748608	748608
Area [µm x µm]	263289.00	263289.00	263289.00	263289.00

Figure 3.6 Quantification of CXCL4 and CXCL7 protein expression within synovial tissue biopsies using the Zen 2010 software. A) Synovial tissue section taken from an early RA patient. The tissue section was stained with antibodies specific for CXCL4 (red), CD68 (blue), CD41 (green), and vWF (orange). Nuclei were counterstained using Hoechst 33258 (grey). Sections were stained alongside isotype matched controls which were negative. 2 x 2 tile scans were taken at x400 total magnification using the Zeiss LSM 780 Zen confocal. To carry out the analysis, tissue sections were drawn around using the overlay function within the Zen 2010 software. Any areas of tissue that were badly damaged or folded were excluded from the analysis. **B**) A screen shot taken from the Carl Zeiss Zen 2010 software. By using the histogram function within the software, pixel counts for each channel were obtained: CD68 (Ch2-T1), CD41 (ChS1-T2), CXCL4/CXCL7 (ChS2-T3) and vWF (Ch2-T4). Pixel counts from the nuclei channel (Ch1-T1) were not included in the analysis. Results from both tables shown in **B**) were exported into Microsoft Excel. The total number of pixels within each channel from intensity 30 to 255 was calculated. This number was then divided by the area [µm x µm] to give the number of pixels per μm^2 area.

CXCL4 expression within synovial biopsies was significantly higher in patients with early RA as compared to established RA patients (Mann Whitney p=0.001) and resolving synovitis patients (Mann Whitney p=0.043) (Figure 3.7A). Likewise, for CXCL7, expression was significantly higher in the early RA patient group as compared to established RA (Mann Whitney p=0.004) and resolving synovitis patients (Mann Whitney p=0.010) (Figure 3.7B). No significant differences in the expression of CXCL4 and CXCL7 were observed in biopsies taken from different synovial joints (Figure 3.9). CXCL4 expression within the synovial biopsies correlated with CXCL7 expression (Spearman r=0.7557, p<0.0001) (Figure 3.7). No correlation was observed for CXCL4 and CXCL7 with erythrocyte sedimentation rate (ESR), C-reactive protein (CRP), Disease Activity Score 28 (DAS28), swollen joint count 28 (SWJ28) and tender joint count 28 (TJC28). No significant difference in CXCL4 and CXCL7 expression was observed when data was split based on the patients RF status (positive or negative) (CXCL4 Mann Whitney p=0.6669, CXCL7 Mann Whitney p=0.5468) or anti-CCP status (positive or negative) (CXCL4 Mann Whitney p=0.3910, CXCL7 Mann Whitney p=0.5235). Furthermore, no significance was observed when CXCL4 and CXCL7 expression from the early RA group (CXCL4 Mann Whitney p=0.1714, CXCL7 Mann Whitney p=0.1714) and established RA group (CXCL4 Mann Whitney p=0.9307, CXCL7 Mann Whitney p=0.6623) were split based on anti-CCP status (Figure 3.10). However, it is important to note that upon splitting patients based on anti-CCP status, this resulted in reduced patient numbers in each group. Therefore, in the future, increasing patient numbers may allow this question to be addressed with appropriate power.

CXCL4 expression within the synovial biopsies correlated with CD68 expression (Spearman r=0.4741, p=0.0023) (Figure 3.11A). However, CXCL7 expression within the synovial

biopsies did not show a correlation with CD68 (Spearman r=0.2006, p=0.2208) (Figure 3.11B). CXCL4 and CXCL7 expression did not correlate with CD41 expression in the synovial biopsies (CXCL4: Spearman r= 0.07975, p= 0.6293, CXCL7: Spearman r= -0.0431, p=0.7944) (Figure 3.11C and Figure 3.11D).

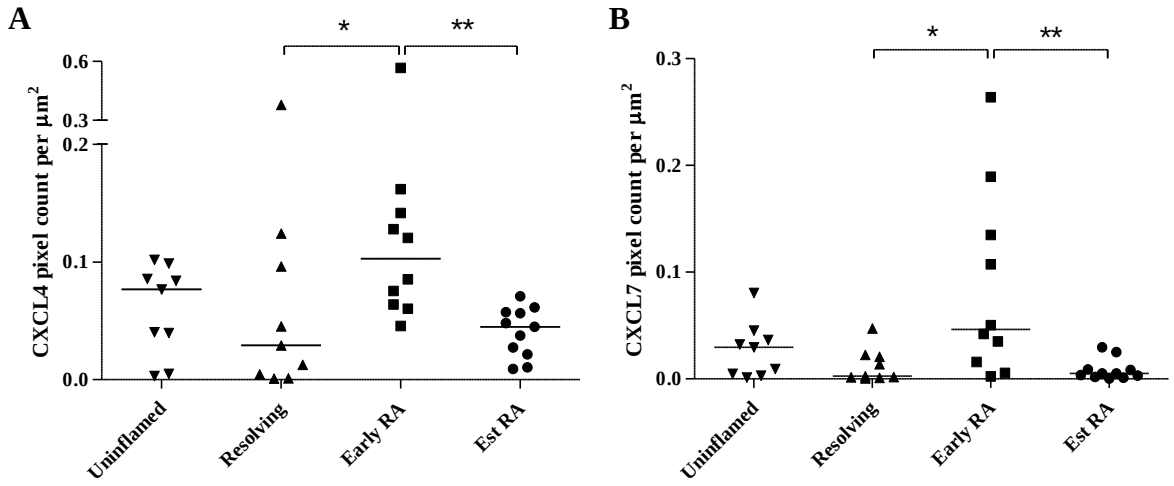

Figure 3.7 CXCL4 and CXCL7 protein quantification within synovial biopsies taken from uninflamed controls and patients enrolled in the BEACON cohort. CXCL4 (**A**) and CXCL7 (**B**) protein expression was quantified in synovial biopsies taken from uninflamed controls (n=9), resolving synovitis patients (n=9), early RA patients (n=10) and established RA patients (n=11) by calculating the number of pixels per μm^2 from 5-6 2x2 tile scans taken at x400 total magnification. Significance was calculated using a Mann-Whitney test. The median value is indicated by a horizontal bar.

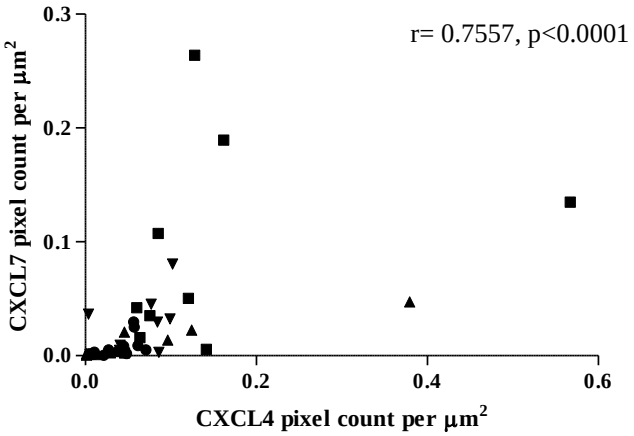

Figure 3.8 Correlation of synovial CXCL4 and CXCL7 expression in uninflamed controls and patients enrolled in the BEACON cohort. The CXCL4 pixel count per μm^2 was plotted against the corresponding pixel count per μm^2 for CXCL7. Upside down triangles indicate uninflamed controls, triangles indicate resolving synovitis patients, squares indicate early RA patients, and circles indicate established RA patients. The Spearman's correlation coefficient 'r' value and p value are shown.

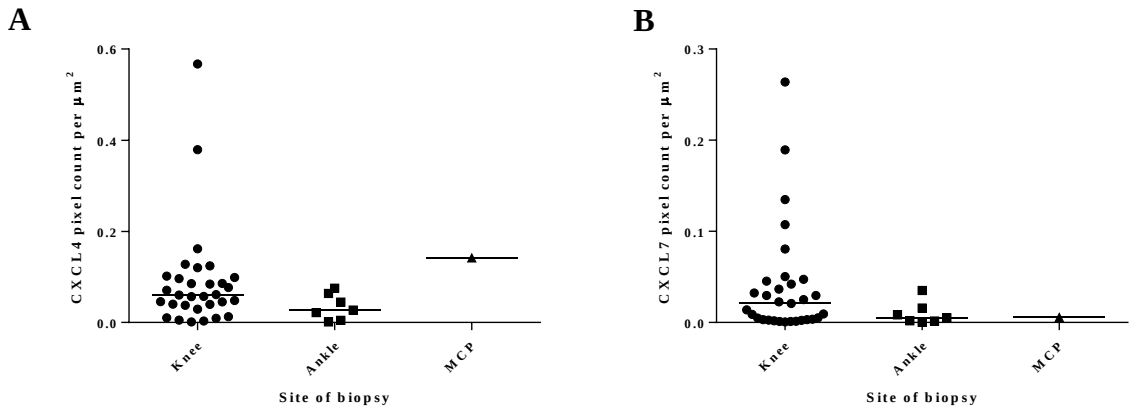

Figure 3.9 CXCL4 and CXCL7 expression in synovium taken from different sites of biopsy. For this study, synovial biopsies were either obtained from the knee, ankle or MCP joint. To observe any probable influence of the site of biopsy on the expression of CXCL4 and CXCL7, the pixel count per μm^2 for **A**) CXCL4 and **B**) CXCL7 were divided based on the site of biopsy. The median value is indicated by a horizontal bar.

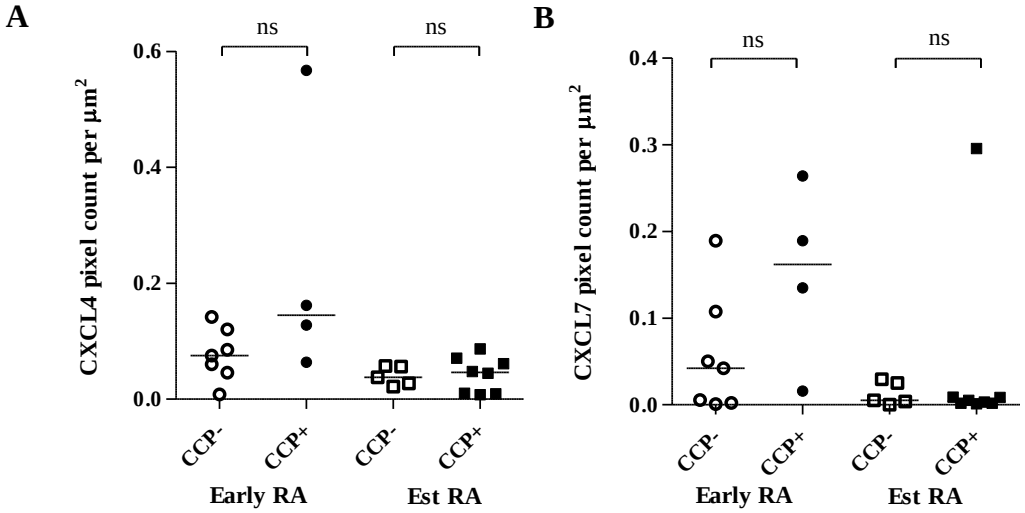

Figure 3.10 CXCL4 and CXCL7 protein quantification from patients with anti-CCP positive/negative early RA or established RA. The anti-CCP status was obtained for each patient included in this study. The CXCL4 and CXCL7 quantification results for early RA patients and established RA patients were split into either CCP negative or CCP positive groups. Figures **A**) and **B**) show the quantification of CXCL4 and CXCL7, respectively, in anti-CCP negative and positive early RA patients. The median value is indicated by a horizontal bar.

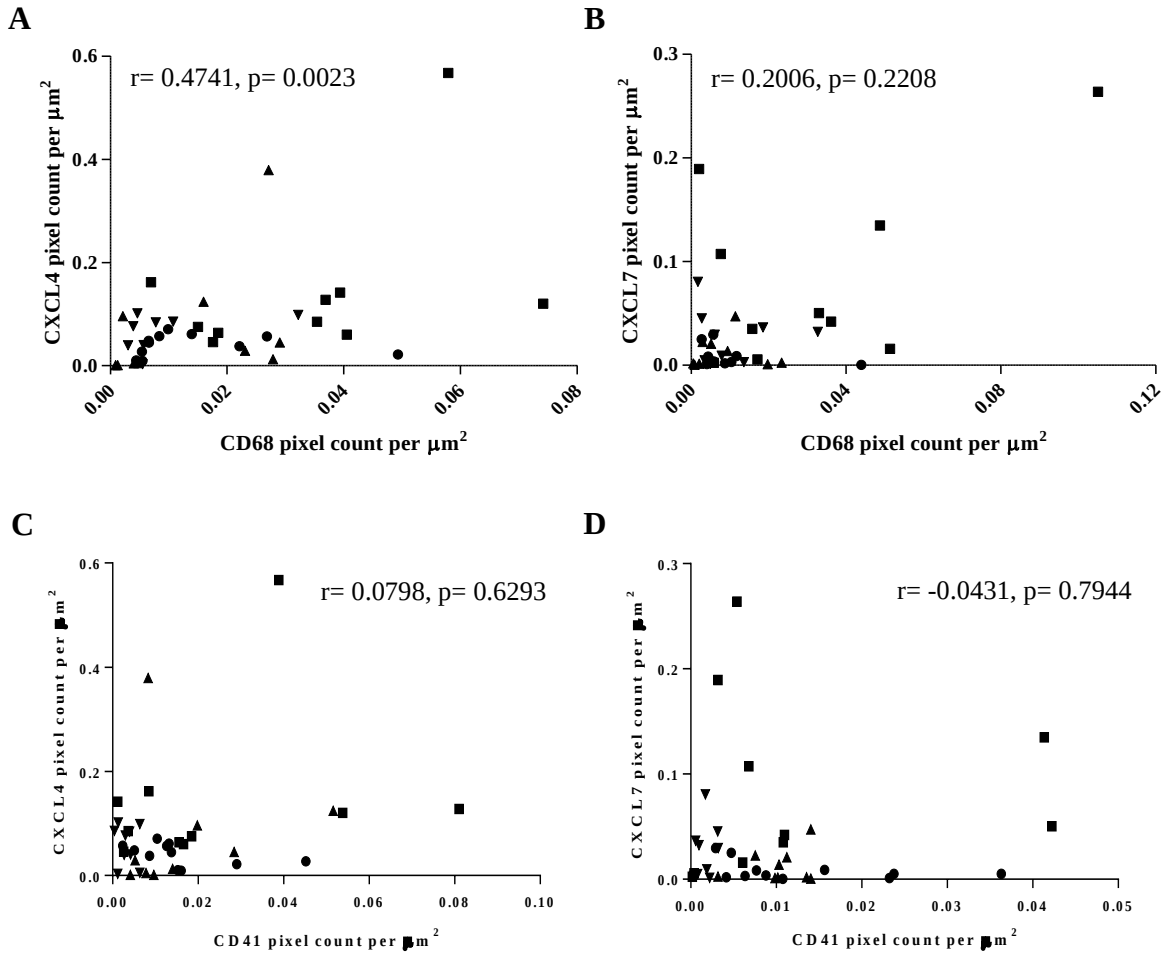

Figure 3.11 Correlation of synovial CXCL4 and CXCL7 with CD68 and CD41 expression in uninflamed controls and in patients enrolled in the BEACON cohort. The CD68 and CD41 pixel counts per μm^2 were plotted against the corresponding pixel counts per μm^2 for CXCL4 and CXCL7. **A** and **C** display CD68 and CD41 plotted against CXCL4, respectively. **B** and **D** display CD68 and CD41 plotted against CXCL7, respectively. Upside down triangles indicate uninflamed controls, triangles indicate resolving synovitis patients, squares indicate early RA patients, and circles indicate established RA patients. The Spearman's correlation coefficient 'r' value and p value are shown.

3.2.5 Quantification of CXCL4, CXCL7 and CD41 inside and outside the synovial vasculature

As I observed a large proportion of CXCL4 and CXCL7 outside as opposed to inside the vasculature, I set out to quantify this. In addition I also quantified the $CD41^{+}$ platelet staining inside and outside the vasculature. Similar to the quantification technique described previously, I used the overlay function within the Zen Software, but this time I identified each blood vessel as a region of interest (Figure 3.12). The pixel counts from within these regions were then exported and subsequently subtracted from the total tissue quantification result.

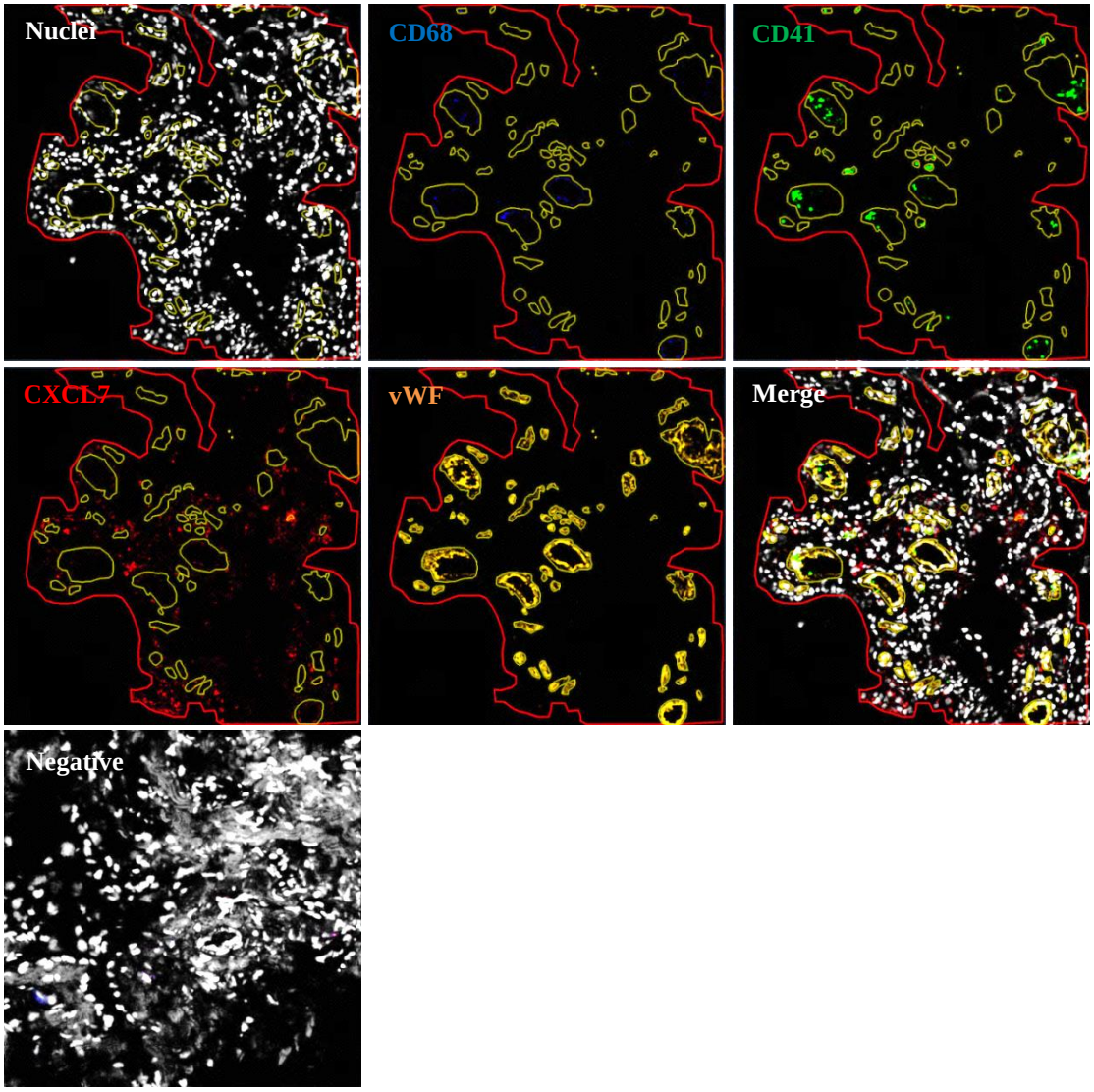

Figure 3.12 Quantification of CXCL4 and CXCL7 protein expression inside and outside the vasculature within synovial tissue biopsies using the Zen 2010 software. Resolving synovitis tissue section stained with antibodies specific for CXCL7 (red), CD68 (blue), CD41 (green) and vWF (orange). Nuclei were counterstained with Hoechst 33258 (grey). Sections were stained alongside isotype matched controls which were negative. 2 x 2 tile scans were taken at x400 total magnification using the Zeiss LSM 780 Zen confocal. Quantification of CXCL4 and CXCL7 inside and outside the vasculature was calculated using the Carl Zeiss Zen 2010 software. For each image, the channels for CXCL4/CXCL7 (ChS2-T3), CD68 (Ch2-T1), CD41 (ChS1-T2) and nuclei (Ch1-T1) were turned off. Using the vWF (Ch2-T4) channel only, each vessel was drawn around using the overlay function (yellow 'closed poly-lines'). Pixel counts for each channel were then exported to Microsoft Excel. The total number of pixels within each channel from intensity 30 to 255 was calculated. This number was then divided by the area [µm x µm] to give the number of pixels per μm^2 area inside the vasculature. To calculate staining outside the vasculature, quantification within the vessels was subtracted from the total quantification.

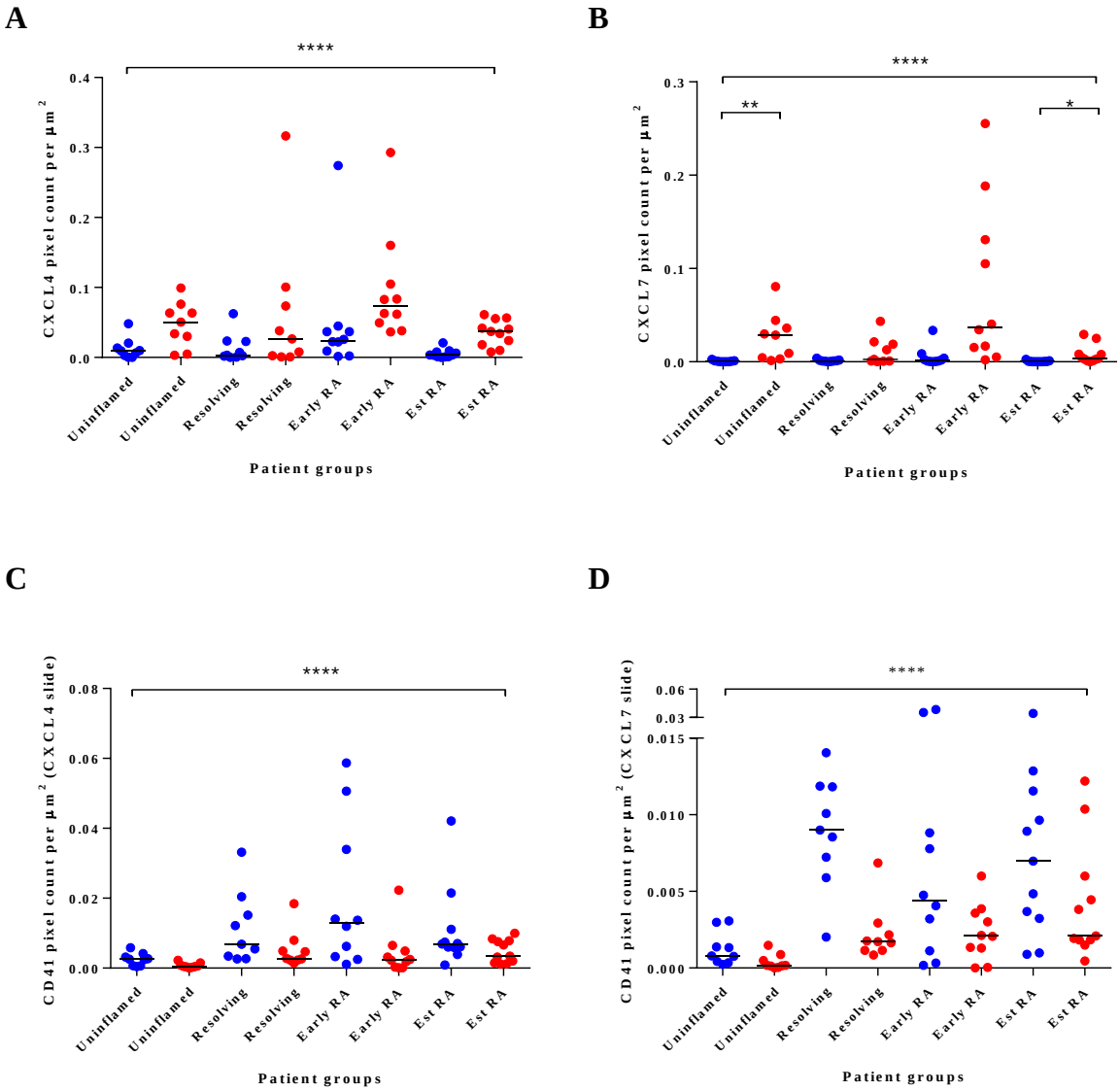

Figure 3.13 CXCL4, CXCL7 and CD41 quantification inside and outside the vasculature. The numbers of CXCL4 (**A**), CXCL7 (**B**), and CD41 (**C** and **D**) pixels per µm^2 area were calculated inside (blue dots) and outside (red dots) the vasculature for uninflamed controls, resolving synovitis patients, early RA patients and established RA patients. A Kruskall Wallis (****p=0.0001) test followed by a Dunn's post-test for multiple comparisons was carried out (**p=0.01, *p=0.05). The median value is indicated by a horizontal bar.

There was an increase in CXCL4 outside the vasculature as opposed to inside the vasculature in the early RA patients, established RA patients, resolving synovitis and uninflamed controls (Kruskall-Wallis $p<0.0001$) (Figure 3.13A). CXCL7 was increased outside the vasculature in the early RA patients and the uninflamed controls but not the resolving synovitis or established RA patients (Figure 3.13B). A Kruskall-Wallis test ($p<0.0001$) followed by a Dunn's post-test for multiple comparisons identified a significant increase in CXCL7 outside the vasculature as opposed to inside in the uninflamed ($p=0.01$) and established RA groups ($p=0.05$) (Figure 3.13B).

In contrast to the chemokine staining which was predominantly found outside the vasculature, quantification of $CD41^+$ staining resulted in a clear trend with the majority of platelets found inside the vasculature as opposed to outside in the synovium (Kruskall Wallis $p<0.0001$) (Figure 3.13C and Figure 3.13D). Differences between the quantification of CD41 on the CXCL4 stained sections and the CXCL7 stained sections may indicate differences in the scanning positions.

3.2.6 Investigation of plasma CXCL4, CXCL7 and sGPVI in the BEACON cohort

In order to investigate the potential of peripheral blood levels of CXCL4 and CXCL7 as predictors of disease outcome in patients presenting with synovitis (<12 week symptom duration and >12 week symptom duration), the concentrations of CXCL4 and CXCL7 in plasma samples were quantified by ELISA. Plasma sGPVI was also assessed as a marker of platelet activation. Samples were obtained from patients attending the early arthritis clinics at the Sandwell and West Birmingham Hospital. Patients were assessed by the consultant rheumatologist Dr Karim Raza and samples were collected by Mr Biruk Asfaw. Upon collection, samples were transferred to and processed by The University of Birmingham staff members, Miss Holly Adams and Mr Philip Jones at the Queen Elizabeth Hospital, Birmingham. Plasma samples were stored at -80°C prior to ELISA analysis. Please refer to table 3.2 and appendix table 8.3 for patient clinical characteristics.

Furthermore, I carried out sample analysis for CXCL4 and CXCL7 in serum samples collected from patients in the BEACON cohort. The concentration of both chemokines ranged from 4-20 μg/ml in the serum. A number of sample results exceeded the assay cut off of 20 μg/ml. Interestingly, patients with psoriatic arthritis had significantly increased CXCL7 concentrations compared to early resolving synovitis patients (Dunn's post-test *$p \leq 0.05$). CXCL7 in early RA patients was comparable to that observed in established RA and resolving synovitis patients (data not shown)

	RA	Unclassified Inflammatory arthritis	Psoriatic arthritis	Inflammatory arthralgia
Number	12	15	8	19
Symptom duration (weeks); median (IQR)	39 (11-170)	22 (17-104)	19 (8-46)	18 (13-43)
RF positive and/or CCP positive; n (%)	7 (58)	3 (20)	2 (25)	5 (26)
Global disease-related variables				
CRP; median (IQR)	7 (0-20.5)	6 (0-30)	5 (0-13.75)	6 (2-12)
ESR; median (IQR)	30 (7.25-31)	13 (2-32.5)	10.5 (2.75-36.5)	5 (2-20)
TJC 28; median (IQR)	5 (3-8)	3 (1-7)	5.5 (3-16)	1 (1-5)
SJC 28; median (IQR)	2 (1-5)	2 (1-4)	3 (0-14)	0 (0-0)

Inflammatory arthralgia group; Inflammatory arthralgia n=17 and palindromic rheumatism n=2.

CCP, cyclic citrullinated peptide; RF, rheumatoid factor; CRP, C-reactive protein; ESR, erythrocyte sedimentation rate; TJC 28, Tender Joint Count of 28 joints; SJC 28, Swollen Joint Count of 28 joints.

Table 3.2 Clinical characteristics of study participants used for the detection of CXCL4 and CXCL7 in plasma by ELISA.

3.2.6.1 CXCL4 in the plasma

The concentration of CXCL4 in the plasma was quantified in 53 patients enrolled in the BEACON cohort. Two patients had a CXCL4 result outside the assay range and were therefore excluded from the analysis; of those patients excluded from the analysis, one had persistent arthritis, and the other inflammatory arthralgia with an unknown outcome. Samples from these patients will be run at a higher dilution in future experiments. CXCL4 was also assessed in 10 healthy controls.

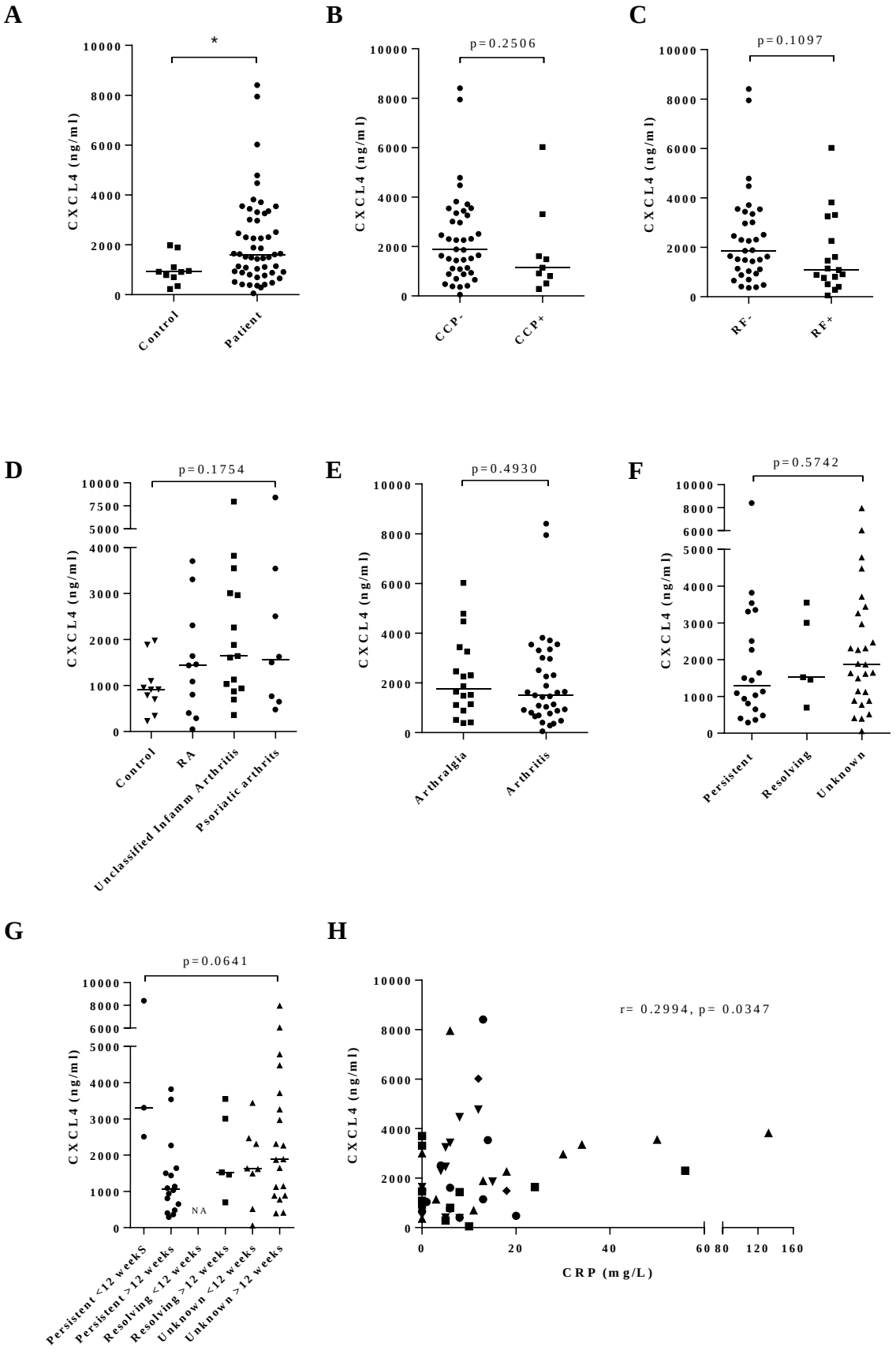
A
*
CXCL4 (ng/ml)
10000
8000
6000
4000
2000
0
Control
Patient
B
p=0.2506
CCP-
CCP+
C
p=0.1097
RF-
RF+
D
p=0.1754
7500
5000
4000
3000
2000
1000
Control
RA
Unclassified Infamm Arthritis
Psoriatic arthritis
E
p=0.4930
Arthralgia
Arthritis
F
p=0.5742
Persistent
Resolving
Unknown
G
p=0.0641
NA
Persistent <12 weeks
Persistent >12 weeks
Resolving <12 weeks
Resolving >12 weeks
Unknown <12 weeks
Unknown >12 weeks
H
r= 0.2994, p= 0.0347
CRP (mg/L)
0
20
40
60
80
120
160

Figure 3.14 CXCL4 in plasma samples from BEACON cohort patients and healthy controls. A) CXCL4 was quantified in plasma samples collected from patients enrolled in the BEACON cohort (n=53) and healthy controls (n=10) using a Quantikine® ELISA (R&D systems, UK). Patient results were divided into **B**) anti-CCP negative (n=40) and anti-CCP positive groups (n=9), and **C**) RF negative (n=35) and RF positive groups (n=17). Patients whose anti-CCP and RF status was unknown were excluded. In **D** the CXCL4 plasma concentrations were split in accordance with disease diagnosis. Patients were split into those with a diagnosis of RA (n=11), unclassified inflammatory arthritis (n=15), or psoriatic arthritis (n=8). In **E** the CXCL4 plasma concentrations were split into those patients with a disease diagnosis of arthritis (n=35) vs those with inflammatory arthralgia or palindromic rheumatism (n=18). In **F**, CXCL4 plasma concentrations were divided based on patient outcome. Patients were split into those with persistent disease (n=20), resolving disease (n=5) or an unknown outcome (n=27). In **G**, CXCL4 plasma concentrations in patients with either persistent disease, resolving disease or an unknown outcome were split according to disease duration at the time of sample collection. Patients were split into <12 weeks symptomduration and >12 weeks symptom duration. In **H** the CRP result for each patient was plotted against the corresponding CXCL4 plasma concentration. Here, upside down triangles indicate patients with inflammatory arthralgia, triangles indicate patients with unclassified inflammatory arthritis, squares indicate patients with RA, circles indicate those with psoriatic arthritis, and diamonds indicate patients with palindromic rheumatism. The Spearman's correlation coefficient 'r' value and p value are shown. Significance was calculated using a Mann-Whitney test for **A**, **B**, **C**, and **E**. A Kruskall-Wallis test followed by a Dunn's post-test for multiple comparisons was used to calculate significance in **D**, **F** and **G**. The Kruskall-Wallis p value is shown. The median value is indicated by a horizontal bar.

CXCL4 was expressed in the plasma of both patients and healthy controls. CXCL4 was significantly increased in patient samples compared to healthy controls (Mann-Whitney p=0.0343) (Figure 3.14A) and correlated weakly with CRP (Spearman r=0.2994, p=0.0347, Figure 3.14H) but not ESR (data not shown). Next, plasma CXCL4 results were split into those with anti-CCP negative or positive disease, and those with RF negative or positive disease (Figure 3.14B and 3.14C). An anti-CCP result of >7 and a RF result of >20 was classified as positive. No statistically significant differences between the anti-CCP negative and anti-CCP positive patients (Mann-Whitney p=0.2506), and the RF negative and RF positive patients was observed (Mann-Whitney p=0.1097).

No significant difference in CXCL4 was observed when patients with RA were compared to those with a different diagnosis (unclassified inflammatory arthritis, inflammatory arthralgia, palindromic rheumatism, or psoriatic arthritis) and the healthy controls (Figure 3.14D). Moreover, no statistical significance was observed when the results were split into patients diagnosed with arthritis versus inflammatory arthralgia and palindromic rheumatism (Figure 3.14E). Due to the low number of patients with palindromic rheumatism (n=2) they were grouped with the patients with inflammatory arthralgia. Division of CXCL4 results based on patient outcome (persistent and resolving synovitis) was not significant (Figure 3.14F), however there was a trend towards an increase in CXCL4 in patients presenting with <12 weeks symptom duration who went on to a persistent outcome (Figure 3.14G). 52% of patient outcomes were unknown at the point of analysis, therefore this result may change as new patient information becomes available.

3.2.6.2 CXCL7 in the plasma

The concentration of CXCL7 in the plasma was quantified in 49 patients enrolled in the BEACON cohort. Six patients had a CXCL7 result outside the assay range and were therefore excluded from the analysis; of those patients excluded from the analysis, three patients were diagnosed with inflammatory arthralgia with an unknown outcome, one patient was diagnosed as having persistent RA, one patient with persistent psoriatic arthritis, and the other patient with unclassified inflammatory arthritis. Samples from these patients will be run at a higher dilution in future experiments. CXCL7 was also assessed in 9 healthy controls. One healthy control had a CXCL7 result outside the assay range and was therefore excluded from the analysis.

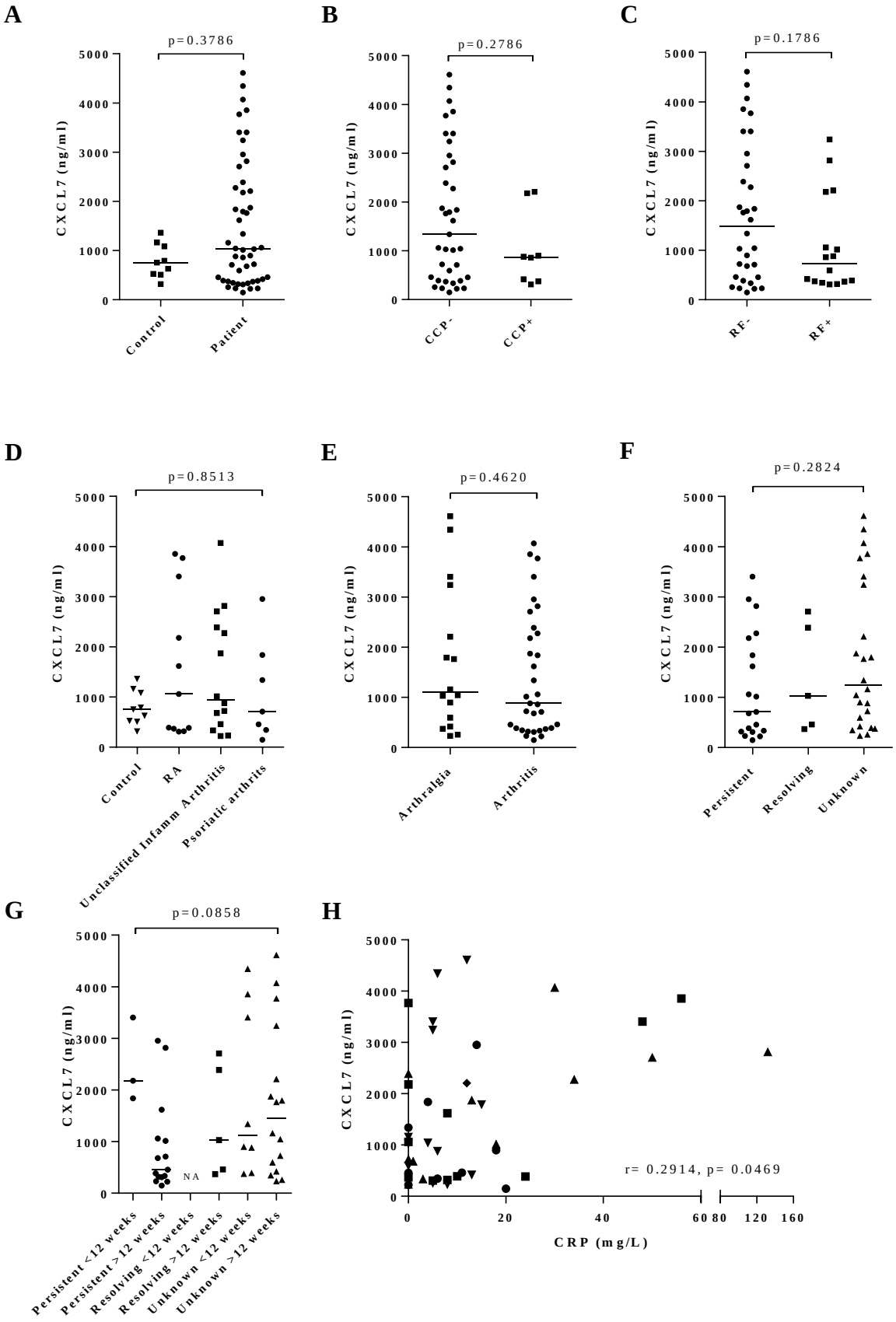
A
p=0.3786
CXCL7 (ng/ml)
5000
4000
3000
2000
1000
0
Control
Patient
B
p=0.2786
CXCL7 (ng/ml)
CCP-
CCP+
C
p=0.1786
CXCL7 (ng/ml)
RF-
RF+
D
p=0.8513
CXCL7 (ng/ml)
Control
RA
Unclassified Infamm Arthritis
Psoriatic arthritis
E
p=0.4620
CXCL7 (ng/ml)
Arthralgia
Arthritis
F
p=0.2824
CXCL7 (ng/ml)
Persistent
Resolving
Unknown
G
p=0.0858
CXCL7 (ng/ml)
NA
Persistent <12 weeks
Persistent >12 weeks
Resolving <12 weeks
Resolving >12 weeks
Unknown <12 weeks
Unknown >12 weeks
H
CXCL7 (ng/ml)
r= 0.2914, p= 0.0469
0
20
40
60
80
120
160
CRP (mg/L)

Figure 3.15 CXCL7 in plasma samples from BEACON cohort patients and healthy controls. A) CXCL7 was quantified in plasma samples collected from patients enrolled in the BEACON cohort (n=49) and healthy controls (n=9) by ELISA (Abcam, UK). Patient results were divided into **B**) anti-CCP negative (n=37) and anti-CCP positive groups (n=8), and **C**) RF negative (n=32) and RF positive groups (n=16). Patients whose anti-CCP and RF status were unknown were excluded. In **D** the CXCL7 plasma concentrations were split in accordance with disease diagnosis. Patients were split into those with RA (n=10) versus those with unclassified inflammatory arthritis (n=14) or psoriatic arthritis (n=7). In **E** the CXCL7 plasma concentrations were split into those patients with a disease diagnosis of arthritis (n=33) vs those with inflammatory arthralgia or palindromic rheumatism (n=16). In **F**, CXCL7 plasma concentrations were divided based on patient outcome. Patients were split into those with persistent disease (n=19), resolving disease (n=5) or an unknown outcome (n=24). In **G**, CXCL7 plasma concentrations in patients with either persistent disease, resolving disease or an unknown outcome were split according to symptom duration at the time of sample collection. Patients were split into <12 weeks symptom duration and >12 weeks symptom duration. In **H** the CRP result for each patient was plotted against the corresponding CXCL7 plasma concentration. Here, upside down triangles indicate patients with inflammatory arthralgia, triangles indicate patients with unclassified inflammatory arthritis, squares indicate patients with RA, circles indicate those with psoriatic arthritis, and diamonds indicate patients with palindromic rheumatism. The Spearman's correlation coefficient 'r' value and p value are shown. Significance was calculated using a Mann-Whitney test for **A**, **B**, **C**, and **E**. A Kruskall-Wallis test followed by a Dunn's post-test for multiple comparisons was used to calculate significance in **D**, **F** and **G**. The Kruskall-Wallis p value is shown. The median value is indicated by a horizontal bar.

CXCL7 was expressed in both patients and healthy control plasma, however no significant difference was observed (Mann-Whitney p=0.3786) (Figure 3.15A). Like the results obtained in the CXCL4 ELISA, no significant difference between the anti-CCP negative and anti-CCP positive patients (Mann-Whitney p=0.2786), and the RF negative and RF positive patients was observed (Mann-Whitney p=0.1786) (Figure 3.15B and 3.15C). Grouping of CXCL7 results based on disease diagnosis and outcome was not statistically significant, however there was a trend towards an increase in CXCL7 in patients with a symptom duration of <12 weeks who went on to a persistent outcome (Figure 3.15D, E, F and G). Moreover CXCL7 weakly correlated with CRP (Spearman r=0.2914, p=0.0469, Figure 3.15H), but not ESR (data not shown).

When comparisons were made between plasma CXCL4 and CXCL7, a significant strong positive correlation (Spearman r= 0.8931, p<0.0001) was observed (Figure 3.16).

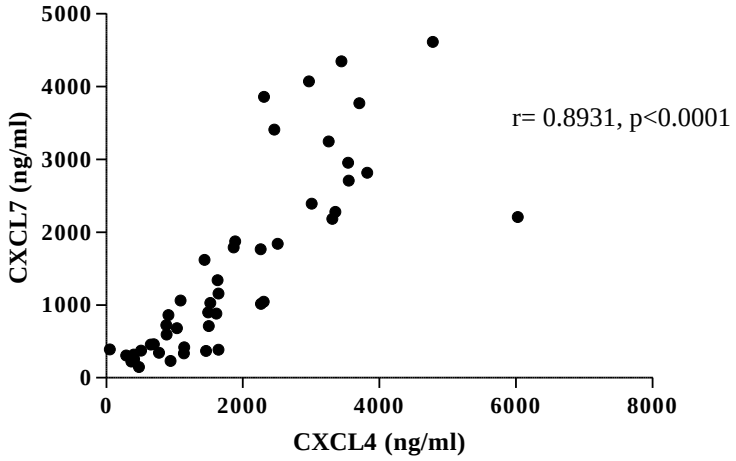

Figure 3.16 Correlation of plasma CXCL4 and CXCL7 in patients enrolled in the BEACON cohort. The plasma CXCL4 results were plotted against the CXCL7 plasma results. The Spearman's correlation coefficient 'r' value and p value are shown.

3.2.6.3 sGPVI in the plasma

The concentration of sGPVI in the plasma was quantified in 53 patients enrolled in the BEACON cohort. Two patients had a sGPVI result outside the assay range and were therefore excluded from the analysis; of those patients excluded from the analysis, one patient was diagnosed with persistent unclassified inflammatory arthritis, and the other was diagnosed with inflammatory arthralgia. sGPVI was also quantified in 6 healthy controls.

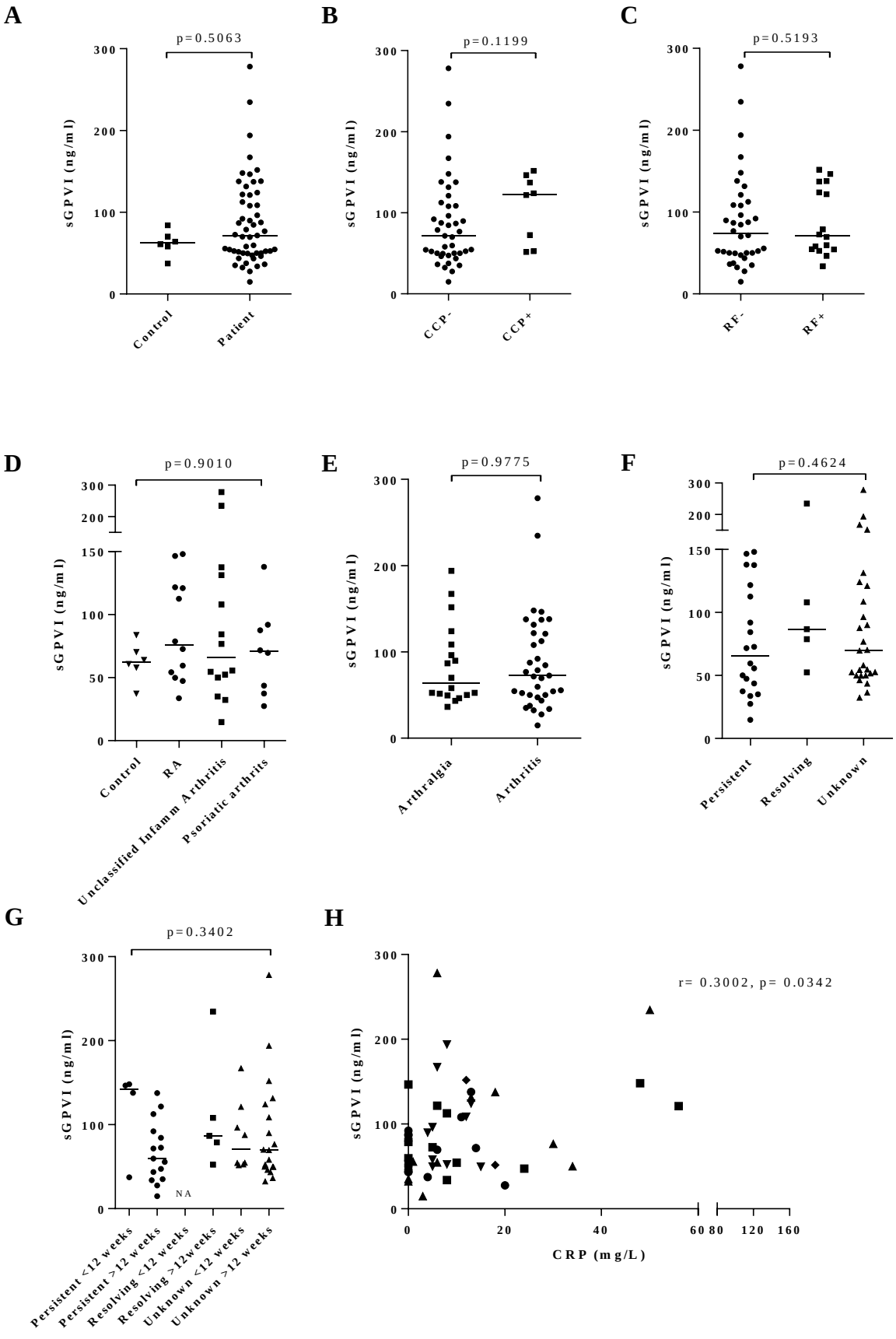
A
p=0.5063
sGPVI (ng/ml)
300
200
100
0
Control
Patient
B
p=0.1199
sGPVI (ng/ml)
300
200
100
0
CCP-
CCP+
C
p=0.5193
sGPVI (ng/ml)
300
200
100
0
RF-
RF+
D
p=0.9010
sGPVI (ng/ml)
300
200
150
100
50
0
Control
RA
Unclassified Infamm Arthritis
Psoriatic arthritis
E
p=0.9775
sGPVI (ng/ml)
300
200
100
0
Arthralgia
Arthritis
F
p=0.4624
sGPVI (ng/ml)
300
200
150
100
50
0
Persistent
Resolving
Unknown
G
p=0.3402
sGPVI (ng/ml)
300
200
100
0
NA
Persistent <12 weeks
Persistent >12 weeks
Resolving <12 weeks
Resolving >12weeks
Unknown <12 weeks
Unknown >12 weeks
H
r= 0.3002, p= 0.0342
sGPVI (ng/ml)
300
200
100
0
0
20
40
60
80
120
160
CRP (mg/L)

Figure 3.17 sGPVI in plasma samples from BEACON cohort patients and healthy controls. A) sGPVI was quantified by ELISA in plasma samples collected from patients enrolled in the BEACON cohort (n=53) and healthy controls (n=6). The ELISA method was published by Al-Tamimi et al, 2009. Patient results were divided into **B**) anti-CCP negative (n=41) and anti-CCP positive groups (n=8), and **C**) RF negative (n=36) and RF positive groups (n=16). Patients whose anti-CCP and RF status were unknown were excluded. In **D** the sGPVI plasma concentrations were split in accordance with disease diagnosis. Patients were split into those with RA (n=12), unclassified inflammatory arthritis (n=14) or psoriatic arthritis (n=8). In **E** the sGPVI plasma concentrations were split into those patients with a disease diagnosis of arthritis (n=35) vs those with inflammatory arthralgia or palindromic rheumatism (n=18). In **F**, sGPVI plasma concentrations were divided based on patient outcome. Patients were split into those with persistent disease (n=20), resolving disease (n=5) or an unknown outcome (n=27). In **G**, sGPVI plasma concentrations in patients with either persistent disease, resolving disease or an unknown outcome were split according to symptom duration at the time of sample collection. Patients were split into <12 weeks symptom duration and >12 weeks symptom duration. In **H** the CRP result for each patient was plotted against the corresponding sGPVI plasma concentration. Here, upside down triangles indicate patients with inflammatory arthralgia, triangles indicate patients with unclassified inflammatory arthritis, squares indicate patients with RA, circles indicate those with psoriatic arthritis, and diamonds indicate patients with palindromic rheumatism. The Spearman's correlation coefficient 'r' value and p value are shown. Significance was calculated using a Mann-Whitney test for **A**, **B**, **C**, and **E**. A Kruskall-Wallis test followed by a Dunn's post-test for multiple comparisons was used to calculate significance in **D**, **F** and **G**. The Kruskall-Wallis p value is shown. The median value is indicated by a horizontal bar.

No significant difference in the concentration of sGPVI in the patients and the healthy controls was observed (Mann-Whitney, p=0.5063) (Figure 3.17A). There was a trend towards an increase in sGPVI in anti-CCP positive patients compared to anti-CCP negative patients, although this was not significant (Mann-Whitney p=0.01199) (Figure 3.17B). There was no significant difference in the concentration of sGPVI in the RF negative and RF positive patients (Mann-Whitney p=0.51931) (Figure 3.17C). Like, the CXCL4 and CXCL7 results, grouping of sGPVI results based on disease diagnosis and outcome was not statistically significant, however there was a trend towards an increase in sGPVI in patients with <12 weeks symptom duration who went on to develop a persistent outcome (Figure 3.17 D, E, F and G). Yet again sGPVI correlated weakly with CRP (Spearman r=0.3002, p=0.0342, Figure 3.17H) but not ESR (data not shown). Furthermore, a significant positive correlation was observed for sGPVI and both CXCL4 (Spearman r=0.4910, p=0.0002) (Figure 3.18A) and CXCL7 (Spearman r=0.4588, p=0.0011) (Figure 3.18B).

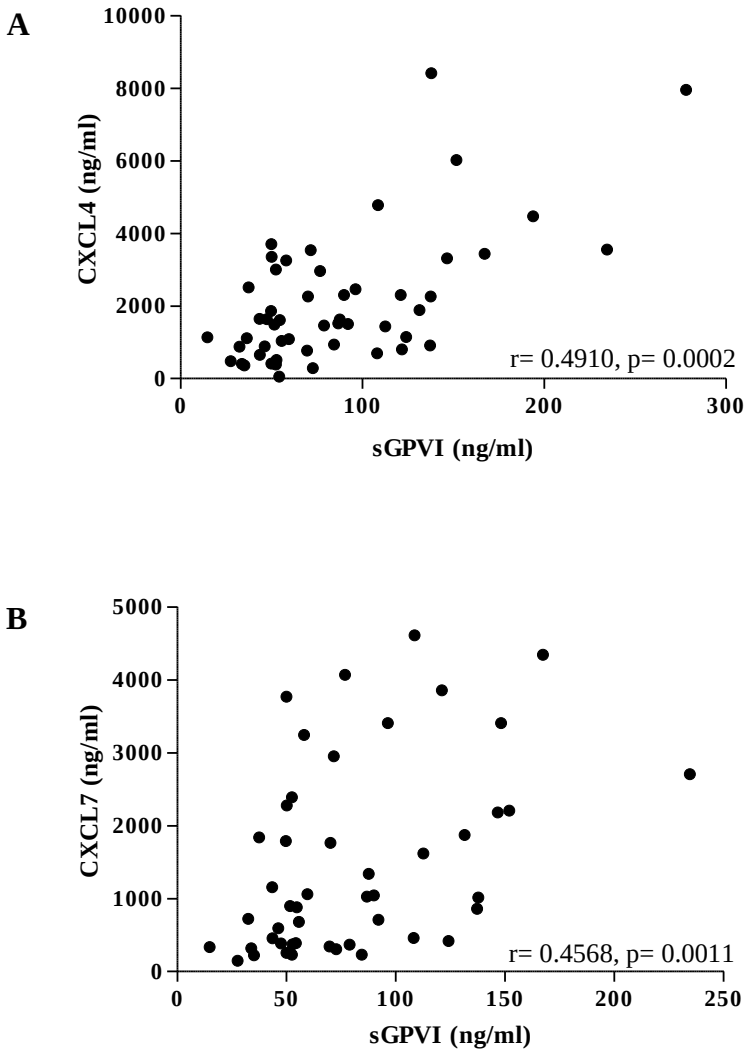

Figure 3.18 Correlation of plasma sGPVI with CXCL4 and CXCL7 in patients enrolled in the BEACON cohort. Correlation of plasma **A**) sGPVI and CXCL4, and **B**) sGPVI and CXCL7 are shown. The Spearman's correlation coefficient 'r' value and p value are shown for both plots.

3.3 DISCUSSION

Biomarkers for early diagnosis and progression, disease severity, and response to therapy are pivotal in RA. In this chapter I have identified two chemokines, CXCL4 and CXCL7, which were transiently increased in the synovium of patients with early RA. As a result, both CXCL4 and CXCL7 may be considered as interesting potential biomarker candidates in biopsy sections for the prediction of RA in patients presenting with early synovitis. Chemokines are an attractive choice for potential biomarkers with a number of studies presenting evidence for their use in prostate cancer (Blum et al, 2008), cancer metastasis (Kakinuma and Hwang, 2006) and SLE (Rovin et al, 2005). Recent studies have also reported on the use of CXCL4 and CXCL7 as potential biomarkers for IBD and COPD, respectively (Cazzola and Novelli, 2010, Di Stefano et al, 2009, Meuwis et al, 2007).

Although biomarkers are becoming increasingly attractive, they are not without their disadvantages. Firstly, the development of biomarkers is extremely costly and time-consuming. Before a biomarker can be used within the clinic, they require thorough analytical and clinical validation. This is not only difficult due to the large number of samples required, but also validation requires collaboration between scientists, clinicians, pharmaceutical companies and regulatory bodies. Strict guidelines must be in place for sample collection, transportation and storage (Mayeux, 2004, Schrohl et al, 2008). Secondly, if the biomarker is to be detected within tissue, for example by immunohistochemistry, the method for sample handling, fixation and processing, choice of antigen retrieval, antibody selection and detection method, and interpretation of results must be standardized so that it can be carried out efficiently across multiple locations. If this is done early in the development process, then the

biomarkers have an increased chance of gaining approval (O'Hurley et al, 2014). Moreover, the collection of biopsy samples may be difficult and not as easily accessible as blood or urine.

It was the work carried out by Yeo et al (2011) in our research team that initially drew our attention to CXCL4 and CXCL7 in the context of RA. Within this study, expression of CXCL4 and CXCL7 at the mRNA level was increased in patients with early RA compared to those with established RA, resolving synovitis and uninflamed controls. Further analysis of the cytokine mRNA expression data by a mathematical based computer model; 'generalized matrix relevance learning vector quantization (GMLVQ)' enabled the division of patient cytokine profiles into categories based on the contribution of individual mRNA results. GMLVQ is an extremely useful model as it can use large data sets to predict diagnosis and identify novel biomarker targets (Biehl et al, 2013). When comparisons between the early RA and the resolving synovitis category were made, the two cytokine mRNA results shown to contribute most to the categorisation were CXCL4 and CXCL7. This highlighted the importance of CXCL4 and CXCL7 in the classification of disease.

As a result of the previous mRNA findings, I analysed the expression of CXCL4 and CXCL7 at the protein level in synovial biopsies taken from patients enrolled in the BEACON cohort. Within this chapter I observed expression of CXCL4 and CXCL7 in synovial biopsies taken from patients with early RA, established RA, and resolving synovitis. Furthermore, I also observed expression of both chemokines in uninflamed controls. Upon quantification of CXCL4 and CXCL7 in the synovial biopsies, I observed significantly higher expression of

both CXCL4 and CXCL7 in patients with early RA compared to those with a resolving synovitis. This increase reflected a transient phase in early RA, as results observed in the established RA patients were significantly lower. Furthermore the increased expression of both CXCL4 and CXCL7 in the early RA patients was not influenced by anti-CCP status. As a result, CXCL4 and CXCL7 may play an important role during the earliest stage of inflammation in RA and may enable us to distinguish those patients who are likely to develop RA from those whose synovitis is likely to resolve. Studies have suggested a pro-inflammatory and angiogenic role for CTAP-III, the pre-cursor molecule to CXCL7, in RA, with levels of the chemokine evident in the sera, synovial fluid and tissue (Szekanecz and Koch, 2001). CXCL7 is known to chemoattract neutrophils and activate their granule release. Therefore, an increase in CXCL7 in early RA may drive increased neutrophil recruitment to the synovium, thus driving early pathogenesis. I can hypothesise that the increase in the angiostatic chemokine, CXCL4, in early disease may be a means of trying to prevent or minimise the first signs of inflammation and angiogenesis, but as inflammation spreads throughout the joint, the effect of CXCL4 is outweighed by other mediators within the joint. A study by Wooley et al (1997) reported an anti-inflammatory role for CXCL4 in models of experimental arthritis. Here, a CXCL4 peptide sequence (CT-112) was delivered to a type II collagen induced arthritis model either as a prophylactic or a therapeutic. When the peptide was given as a prophylactic, the development of type II collagen induced arthritis was prevented and when given as a therapeutic the progression of disease was reduced.

Both CXCL4 and CXCL7 are still considered to be, predominantly, platelet derived chemokines. Therefore I initially hypothesised that CXCL4 and CXCL7 in the synovium would be due to the presence of platelets. An increased number of platelets were observed

inside the vasculature as opposed to outside the vasculature in the synovium. However, apart from the co-localisation of platelets with both chemokines in thrombi within blood vessels, I did not observe co-localisation of CXCL4 and CXCL7 with platelets outside the blood vessels and furthermore CXCL4 and CXCL7 was not found to correlate with CD41 expression. In addition to this, the expression of CXCL4 and CXCL7 was increased outside the vasculature as opposed to inside. Moreover, I observed co-localisation of CXCL4 and CXCL7 with $CD68^+$ macrophages in the synovium. I observed weak positive correlation of CXCL4 with CD68, however I did not observe the same for CXCL7 with CD68. Increasing the sample number, eliminating any outliers, or increasing the number of images taken from each section may rectify this in the future. From this I may hypothesise that both chemokines are not solely platelet derived. In agreement, Schaffner et al (2005) reported that both CXCL4 and CXCL7 were not restricted to the megakaryocyte lineage and that in fact monocytes expressed both chemokines. In this study they detected CXCL4 expression in monocytes by Western blot, qPCR, immunofluorescence and ELISA. Using a Pf4-Cre mouse model, Calaminus et al (2012) also reported that CXCL4 was no longer restricted to the megakaryocyte lineage but that both myeloid and lymphoid lineages were a source. The expression of CXCL4 and CXCL7 in monocytes and macrophages will be further explored in the next chapter.

Our interest in pDCs and CXCL4 expression arose from the patent filed by Radstake in 2010 and the more recent publication by van Bon et al (2014). Van Bon et al (2014) reported an increased plasma level of CXCL4 in patients with systemic sclerosis compared to patients with SLE, hepatic fibrosis, ankylosing spondylitis and healthy controls. An increase in CXCL4 mRNA expression was reported in pDCs isolated from patients with systemic sclerosis compared to controls. Moreover, CXCL4 protein was expressed in pDCs within the

circulation and the skin. Furthermore, studies have reported the expression of both CXCL4 and CXCL7 in pDCs and mDCs. Maier et al (2009) reported the expression of CXCL4 in both DC subsets and observed a correlation with injury severity score in patients with trauma. Piqueras et al (2006) also reported the expression of both CXCL4 and CXCL7 in pDCs and mDCs. In this study, the host response to influenza virus infection was reported. Interestingly, CXCL4 expression was downregulated in pDCs and mDCs following viral exposure, whereas CXCL7 was released following infection resulting in neutrophil recruitment. Furthermore, CXCL4 released from pDCs has identified as a potential biomarker for systemic sclerosis (van Bon et al, 2014).

In this chapter, I identified co-localisation of CXCL4 with the pDC marker BDCA-2 in rheumatoid synovium taken from patients who had undergone joint replacement (Figure 3.3). Staining for CXCL7 alongside BDCA-2 was less convincing. Upon staining of synovial biopsy sections taken from patients enrolled in the BEACON cohort, I did not observe any co-localisation of CXCL4 with BDCA-2. Moreover, it was often extremely difficult to locate BDCA-2 positive cells within the sections. In our work I used antibodies specific for the pDC marker, BDCA-2. However in hindsight this may not have been the best marker to use in labelling rheumatoid synovium. Immature pDCs express BDCA-2 and BDCA-4 and a number of studies have suggested that both markers are downregulated upon entry into tissue. The marker CD123 is predominantly used as a marker for both immature and mature pDCs. However, other than being found on pDCs it is also expressed on mast cells, macrophages, and basophils amongst many others.

When visualising some of the patient's synovial biopsy sections, I did observe $CD41^+$ staining on the membrane of particular cells. Occasionally I observed this staining on $CD68^+$ cells, thus suggesting that platelets could possibly attach to the macrophage membrane. I, also, observed CD41 positive staining on the membrane of other cells. It is possible that these cells could be mast cells as a study carried out by Berlanga et al (2005) reported that mast cells express the CD41 integrin. Mast cells have been reported in the synovial fluid and tissue of patients with RA and they are often found at sites of cartilage degradation. Therefore it is quite possible that the CD41 positive staining I observed on the membrane of unidentified cells could be mast cells. One way to test this would be to stain for mast cell markers such as CD203c and FcεRIα. It is also possible that CXCL4 and CXCL7 observed on the macrophages may be a result of their interactions with platelet microparticles. Platelet microparticles are known to contain an abundance of inflammatory mediators, and have been shown to contribute to the exacerbation of inflammation in RA (Boilard et al, 2010).

In this chapter I identified a significant increase in the plasma concentration of CXCL4 in patients from the BEACON cohort compared to healthy controls. However, the CXCL4, CXCL7 and sGPVI plasma results must be given careful consideration before any firm conclusions are drawn. I analysed sGPVI as a marker of platelet activation in our samples. Al-Tamimi et al (2009) published the method for the measurement of sGPVI in human plasma. In this published method, the measurement of sGPVI in plasma was not affected by the use of different anti-coagulants used during blood collected such as acid-citrate-dextrose, trisodium citrate or EDTA. However, the method used to obtain the plasma samples differed greatly from what was done in this chapter. Al-Tamimi et al (2009) used twice spun platelet poor plasma (blood centrifuged at 100g for 20 mins, followed by centrifugation of platelet rich

plasma at 300g for 15 mins. In this method, plasma was also further centrifuged to remove platelet microparticle contamination (platelet poor plasma centrifuged at 8000 g for 2 mins, then ultracentrifuged at 10,000g for 1 hr). Plasma samples used in my study were processed from blood collected from patients enrolled in the BEACON cohort. All samples were processed by a laboratory technician using standard operating procedures routinely carried out by our laboratory. Blood was centrifuged once at 3000rpm for 10 mins, before being stored first at -20°C, and then at -80°C. As plasma samples were obtained from the BEACON cohort a number of years prior to the onset of this study, unfortunately due to time constraints I was unable to collect new samples from the cohort and process them as described in the published method. Al-Tamimi et al (2009) established a normal range of sGPVI in healthy control plasma; 18.9 ± 4.1 ng/ml (mean ± stdev), range 11-24 ng/ml, however in my study the range of sGPVI in healthy control plasma was 62.4 ± 15.4 ng/ml (mean ± stdev), range 37.4-84.0 ng/ml. Hence, it is possible that the results obtained in this study may be attributed to platelet or platelet microparticle contamination, and therefore I must consider this when evaluating my results. Furthermore, as sGPVI is an indicator of platelet activation, the positive correlation observed between sGPVI, CXCL4 and CXCL7 may be explained by increased platelet activation in these samples (Figure 3.17). Moreover, I must also consider the duration of time from blood collection to sample processing as this can have a detrimental effect on the results obtained. Jackman et al (2011) reported that levels of certain plasma cytokines increased or decreased depending on whether the sample was processed immediately, after 24 hours, 48 hours and 72 hours. For example, the concentration of IL-8/CXCL8, TNFα and IL-1β were all found to increase as the time to processing increased in trauma patients, whereas the concentrations of CXCL10, IL-12 (p40), and CX3CL1 were found to decrease. Now, although, all of the samples used within my study were processed within 24 hours, there was

often a delay of ~1-4 hours between sample collection and processing. This may have resulted in differences in the concentrations of CXCL4, CXCL7 and sGPVI. Similarly, agitation of samples during the shipping process may have led to platelet activation and a subsequent increase in both chemokines and sGPVI concentrations.

A final analysis of the use of plasma levels of CXCL4 and CXCL7 is not yet possible, as I am still awaiting disease outcomes from a proportion of patients. However, the data so far suggest that neither of these cytokines allows prediction of patient outcome if measured in plasma. This may be due to a larger contribution of platelet derived chemokines in the plasma, compared to the macrophage linked expression in the tissue. I did however, observe a positive correlation of both CXCL4 and CXCL7 with the acute phase protein CRP, suggesting that plasma CXCL4 and CXCL7 expression may be a marker for early inflammatory disease, but not prediction of patient outcome.

4 CXCL4 AND CXCL7 EXPRESSION WITHIN THE MONOCYTE LINEAGE

4.1 INTRODUCTION

Macrophages play a pivotal role in driving the pathogenesis of RA through their release of a large array of both pro- and anti-inflammatory mediators. Moreover increased numbers of macrophages in the synovium are associated with severe disease, whilst a reduction in macrophages in response to therapy has been shown to predict a positive outcome.

Although I initially thought that platelets were the sole producers of CXCL4 and CXCL7, I was surprised when I observed co-localisation of CXCL4 and CXCL7 with what appeared to be $CD68^+$ macrophages in the rheumatoid synovium. As a result, I sought to explore this further. Firstly, I investigated the expression of CXCL4 and CXCL7 at the mRNA level in monocytes and in vitro differentiated macrophages cultured under M1 and M2 conditions. I also studied the expression of both chemokines in cells cultured under monocyte-derived DC conditions. In order to eliminate the risk of contaminating platelets during our mRNA analysis, I devised a cell sorting strategy to obtain $CD14^+$ $CD41^-$ cells from healthy donors. These cells were then used for downstream differentiation protocols.

In this chapter, I also sought to validate an in situ hybridization method for use by us and a number of other groups within our rheumatology department. For our work, I sought to validate the method for the detection of CXCL7/PPBP single RNA molecules with the overall

aim of detecting CXCL4 in a similar way once I had the method up and running. Upon trying to validate the method, I ran into a number of problems which required troubleshooting. Although in the end I was not entirely satisfied with the method for the detection of our target of interest in the rheumatoid synovium, I obtained more promising results in tonsil tissue.

4.2 RESULTS

4.2.1 CXCL4 and CXCL7 mRNA expression in monocytes and in vitro differentiated macrophages

Within chapter 3 I described co-localisation of CXCL4 and CXCL7 with the marker for macrophages, CD68, at the protein level within the rheumatoid synovium. Following on from these observations I sought to determine the expression of CXCL4 and CXCL7 at the mRNA level in healthy donor $CD14^+$ monocytes, and monocytes differentiated to macrophages and monocyte derived dendritic cells (Mo-DCs) under M1, M2 and Mo-DC culture conditions established in Birmingham by Prof. Andrew Clark's team.

mRNA coding for CXCL4 and CXCL7 was expressed in all four cell populations. Both CXCL4 and CXCL7 mRNA expression was significantly higher in $CD14^+$ monocytes compared to the cells cultured under M1, M2 and Mo-DC conditions. There was no statistically significant difference in CXCL4 and CXCL7 mRNA expression between the cells cultured under M1, M2 and Mo-DC conditions as assessed by the Dunn's multiple comparison test (Figure 4.1).

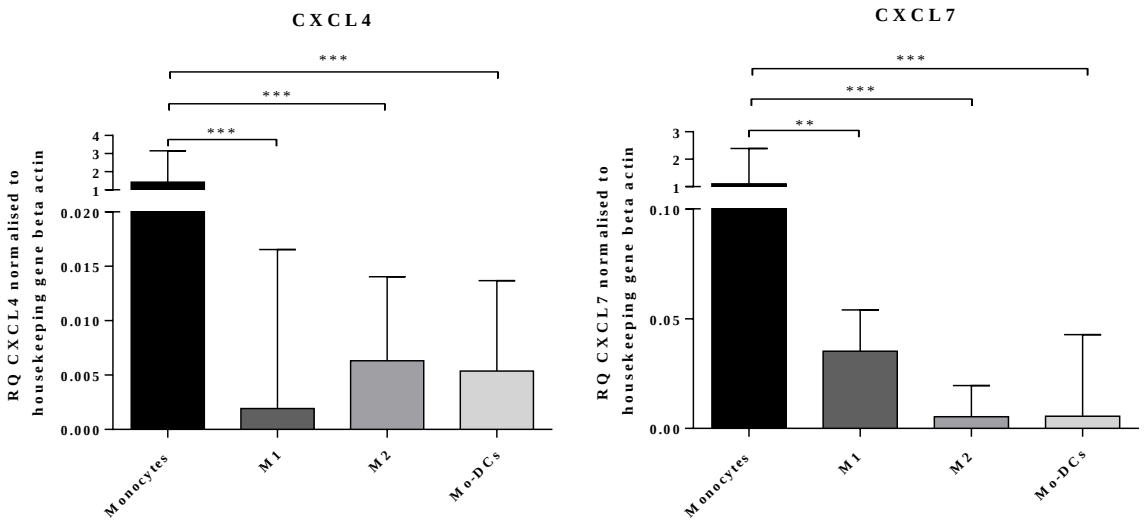

Figure 4.1 CXCL4 and CXCL7 mRNA expression in CD14$^+$ monocytes differentiated to macrophages and monocyte-derived dendritic cells (Mo-DC) under M1, M2 and Mo-DC culture conditions. PBMCs were isolated from peripheral blood taken from healthy donors using Ficoll-Paque. CD14$^+$ monocytes were isolated via positive selection using CD14$^+$ conjugated magnetic beads (Miltenyi Biotec, UK). Monocytes were seeded in a 6 well-plate at 1 x 10^6 cells/well in RPMI-1640 + 10% Hi FCS + 1% GPS in a volume of 1000 µl/well. Cells were differentiated to macrophages and Mo-DCs under M1 (10 ng/ml GM-CSF), M2 (10 ng/ml M-CSF), and Mo-DC (25 ng/ml GM-CSF and 25 ng/ml IL-4) culture conditions for 6 days. Monocytes were also immediately lysed in RLT lysis buffer following the isolation to act as a control. CXCL4 and CXCL7 mRNA expression in monocytes (black bar) and cells cultured under M1 (dark grey bar), M2 (medium grey bar) and Mo-DCs (light grey bar) conditions was assessed using the Stratagene MX3000p qPCR machine. Gene expression was normalised to the housekeeping gene, beta actin. The results show median + interquartile range (IQR) of 5 independent experiments. Statistical significance was calculated using the Kruskall-Wallis test followed by the Dunn's multiple comparison test; **p≤0.01, ***p≤0.001.

As I observed increased expression of both CXCL4 and CXCL7 mRNA in CD14$^+$ monocytes, I was concerned that the expression could be largely due to platelet contamination following the cell isolation, as monocytes can bind platelets on their surface. Therefore I established a cell sorting method to isolate CD14$^+$ monocytes with or without CD41$^+$ platelets (Figure 4.2). CXCL4, CXCL7 and CD41 mRNA was expressed in the CD14$^+$ CD41$^-$, CD14$^+$ CD41$^+$

intermediate, and $CD14^+$ $CD41^+$ cell sorted populations. CXCL4 mRNA expression was significantly increased in the $CD14^+$ $CD41^+$ population compared to the $CD14^+$ $CD41^-$ population (Kruskall Wallis followed by Dunn's multiple comparison test $p \leq 0.001$) (Figure 4.2D). Likewise, CXCL7 mRNA expression was also significantly increased in the $CD14^+$ $CD41^+$ population compared to the $CD14^+$ $CD41^-$ population (Dunn's multiple comparison test $p \leq 0.001$). CXCL7 was also significantly increased in the $CD14^+$ $CD41^+$ intermediate population compared to the $CD14^+$ $CD41^-$ population (Dunn's multiple comparison test $p \leq 0.01$) (Figure 4.2E). CD41 mRNA was also expressed in all three sorted populations. CD41 mRNA was significantly increased in the $CD14^+$ $CD41^+$ population compared to the $CD14^+$ $CD41^-$ (Dunn's multiple comparison test $p \leq 0.001$) and $CD14^+$ $CD41^+$ intermediate populations (Dunn's multiple comparison test $p \leq 0.05$) (Figure 4.2F).

A

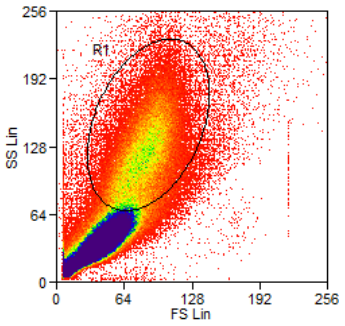

Gated on monocytes (R1)

B

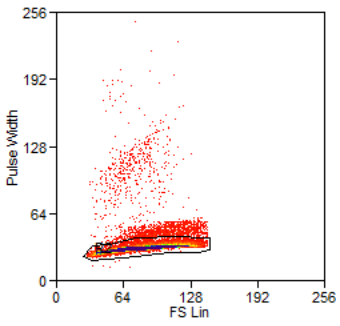

Gated to exclude cell doublets (R2)

C

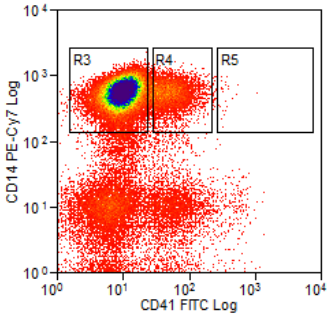

Gated on three populations;

1) **$CD14^+$ $CD41^-$ (R3)**
2) **$CD14^+$ $CD41^+$ intermediate (R4)**
3) **$CD14^+$ $CD41^+$ (R5)**

D

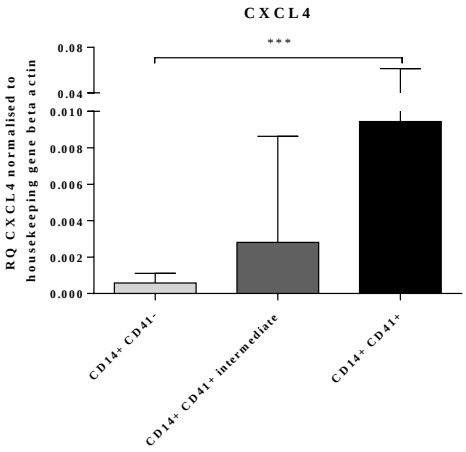

E

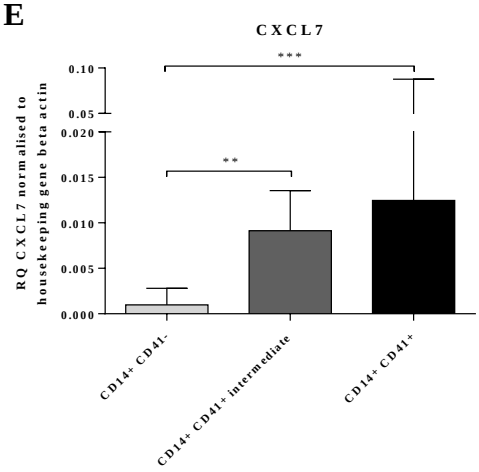

F

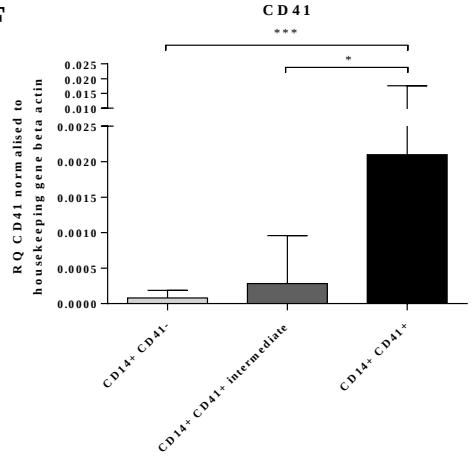

Figure 4.2 Cell sorting protocol for $CD14^+$ monocytes with or without $CD41^+$ platelets and subsequent analysis of CXCL4, CXCL7 and CD41 mRNA expression. PBMCs were isolated from peripheral blood collected from healthy donors using Ficoll-Paque. Cells were fluorescently labelled with antibodies specific for CD14 and CD41 and subsequently sorted into three different cell populations using the MoFlo™ cell sorter operated by Mr. Roger Bird. Cells were gated on the monocyte population as determined by forward scatter versus side scatter (**A**) before being gated by forward scatter versus pulse width to exclude cell doublets (**B**). The cells were then sorted into $CD14^+$ $CD41^-$ (R3), $CD14^+$ $CD41^+$ intermediate (R4), and $CD14^+$ $CD41^+$ (R5) populations (**C**). The purity of the sort was routinely above 95%. Dot plots were generated using Summit v4.3 software. CXCL4 (**D**), CXCL7 (**E**) and CD41 (**F**) mRNA expression was assessed using the Stratagene MX3000p qPCR machine. Gene expression was normalised to the housekeeping gene, beta actin. The results show median + IQR of 5 independent experiments. Light grey bar; $CD41^+$ $CD41^-$ population, dark grey bar; $CD14^+$ $CD41^+$ intermediate population, and black bar; $CD14^+$ $CD41^+$ population. Statistical significance was calculated using the Kruskall-Wallis test followed by the Dunn's multiple comparison test; *$p \leq 0.05$, **$p \leq 0.01$, ***$p \leq 0.001$.

Finally, I studied the effect of 6 hour and 24 hour LPS (10 ng/ml) stimulation on the expression of CXCL4, CXCL7 and CD41 on $CD14^+$ $CD41^-$ cells differentiated to macrophages and Mo-DCs under M1 (GM-CSF), M2 (M-CSF) and Mo-DC (GM-CSF and IL-4) culture conditions. I observed significantly higher CXCL4 mRNA expression in $CD14^+$ $CD41^-$ monocytes compared to unstimulated cells cultured under M1 conditions (Dunn's multiple comparison test $p \leq 0.01$). CXCL4 mRNA expression was higher in the cells cultured under M2 conditions compared to those cultured under M1 and Mo-DC conditions. Furthermore there was significantly more CXCL4 mRNA expressed in the M2 cultured cells following 6 hrs of LPS stimulation compared to the Mo-DCs stimulated with LPS for 6 hrs (Dunn's multiple comparison test $p \leq 0.05$). Cells cultured under Mo-DC conditions and left unstimulated expressed greater CXCL4 mRNA than those following stimulation with LPS (Figure 4.3A).

CXCL7 mRNA was expressed in $CD14^+$ $CD41^-$ monocytes and monocytes differentiated to macrophages and Mo-DCs under M1, M2 and Mo-DC culture conditions. Cells differentiated under M1 conditions had significantly more CXCL7 mRNA expression following 6 hrs LPS stimulation than cells differentiated under M2 conditions and stimulated for 6 hours (Dunn's multiple comparison test $p \leq 0.05$). Cells differentiated under Mo-DC conditions and stimulated for 6 hrs expressed the greatest level of CXCL7 mRNA (Figure 4.3B).

A potential confounder may be that, although I used the $CD14^+$ $CD41^-$ sorted cell population during these experiments, CD41 mRNA was still detectable in this population as well as in cells following differentiation under M1, M2 and Mo-DC conditions. Therefore further

experiments must be performed before drawing a firm conclusion. CD41 mRNA expression was significantly higher in the unstimulated Mo-DC cultured population compared to the M1 (Dunn's multiple comparison test $p \leq 0.01$) and M2 cultured populations (Dunn's multiple comparison test $p \leq 0.001$). Also, significantly higher CD41 mRNA expression was also observed in Mo-DCs stimulated for 6 hrs with LPS compared to M2 cultured cells stimulated for 6 hrs (Dunn's multiple comparison test $p \leq 0.01$) (Figure 4.3C). I currently have no method to determine whether the CD41 mRNA expression indicates a remainder of platelet derived contamination, although in the future I could explore the potential of other platelet or platelet microparticle markers. However, residual platelet contamination should be equal in the individual samples, unless platelet survival in culture was affected by the Mo-DC culture condition. As the expression pattern of CD41 differs from that of CXCL4 and CXCL7, it is unlikely that the higher expression of CXCL4 in the M2 stimulated macrophages can be explained by residual platelets.

A

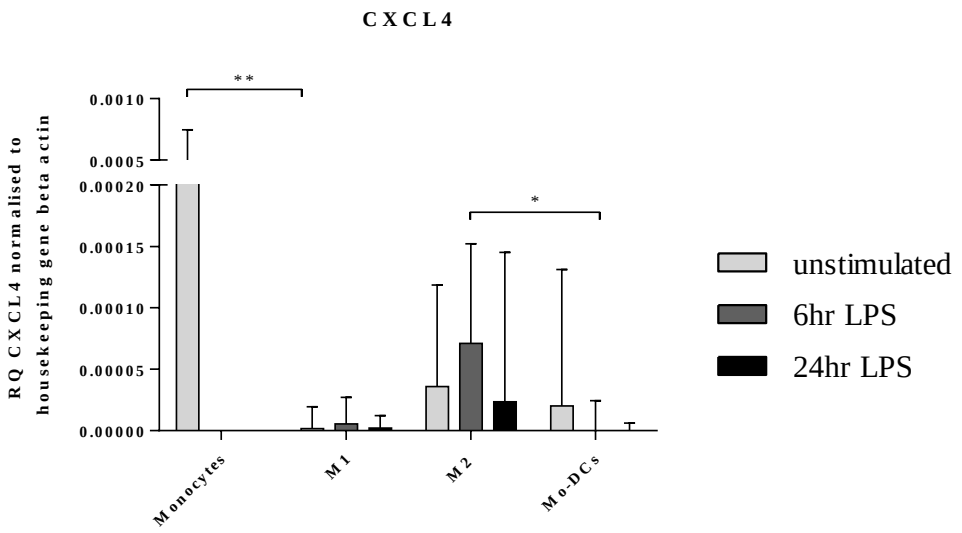
CXCL4
RQ CXCL4 normalised to housekeeping gene beta actin
0.0010
0.0005
0.00020
0.00015
0.00010
0.00005
0.00000
**
*
Monocytes
M1
M2
Mo-DCs
unstimulated
6hr LPS
24hr LPS

B

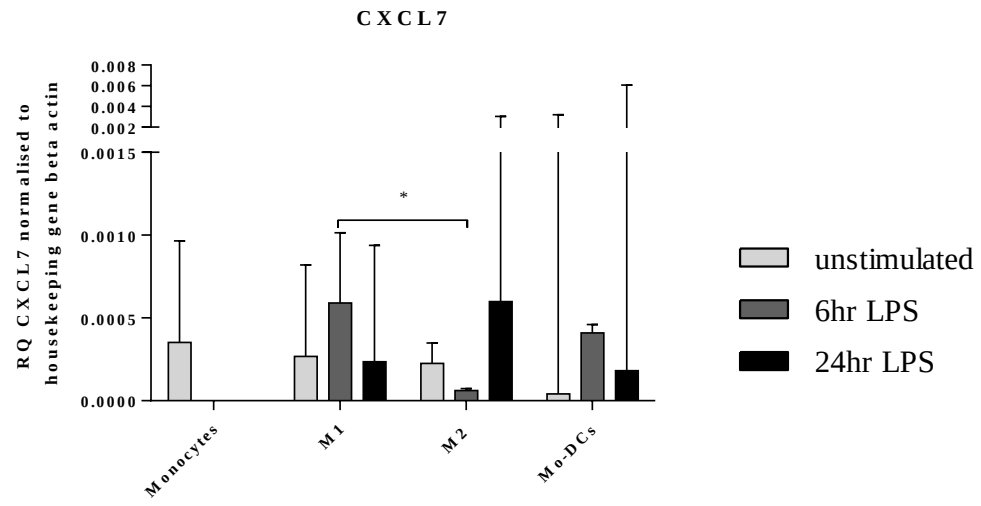
CXCL7
RQ CXCL7 normalised to housekeeping gene beta actin
0.008
0.006
0.004
0.002
0.0015
0.0010
0.0005
0.0000
*
Monocytes
M1
M2
Mo-DCs
unstimulated
6hr LPS
24hr LPS

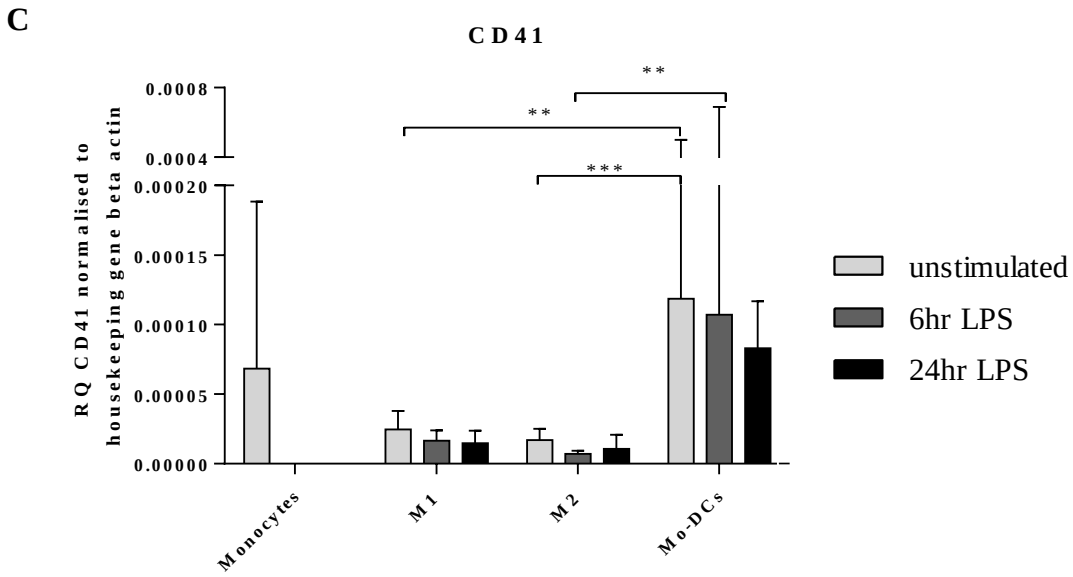

Figure 4.3 CXCL4, CXCL7 and CD41 mRNA expression in CD14^{+} CD41^{-} monocytes differentiated under M1, M2 and Mo-DC conditions and subsequently stimulated with LPS. CD14^{+} CD41^{-} sorted cells were seeded in a 96 well-plate at 3.37 x 10^{4} cells/well in RPMI-1640 + 10% Hi FCS + 1% GPS in a volume of 200 µl/well. Cells were differentiated to macrophages under M1, M2 or Mo-DC culture conditions and subsequently stimulated with 10 ng/ml LPS for 6 hours (dark grey bar) or 24 hours (black bar). Undifferentiated CD14^{+} CD41^{-} monocytes were also immediately lysed in RLT lysis buffer following the cell sort to act as a control. **A**) CXCL4, **B**) CXCL7 and **C**) CD41 mRNA expression was assessed using the Stratagene MX3000p qPCR machine. Gene expression was normalised to the housekeeping gene, beta actin. The results show median + IQR of 5 independent experiments. Statistical significance was calculated using the Kruskall-Wallis test followed by the Dunn's multiple comparison test; *p≤0.05, **p≤0.01, ***p≤0.001.

4.2.2 Detection of CXCL7 by In Situ Hybridization

I set out to validate an In Situ Hybridization method for the detection of PPBP/CXCL7 (target probe), GAPDH (positive control), and *Bacillus subtilis* dapB (negative control) as I sought to identify the exact source of the chemokine message within the tissue. Due to a shortage of early RA formalin fixed paraffin embedded (FFPE) sections I decided that it was best to set up the In Situ Hybridization method using human tonsil tissue FFPE sections. In order to carry out the In Situ Hybridization I used the QuantiGene® ViewRNA In Situ Hybridization Tissue 1-Plex Assay from Affymetrix/Panomics.

The QuantiGene® View RNA In Situ Hybridization Tissue 1-Plex Assay method was optimised using human tonsil FFPE sections cut and mounted by the Human Biomaterials Resource Centre (HBRC): Biobank (University of Birmingham, UK). Sections were viewed using the Zeiss LSM 780 Zen confocal. Initially I set out to visualise the sections by light microscopy, following Haematoxylin and Eosin staining of the sections. However, observing any signal was difficult following this method. During the initial experiments, optimisation of the heat pre-treatment and protease digestion steps was carried out. Sections were either heat pre-treated for 5 mins followed by protease digestion for 10 mins, heat pre-treated for 10 mins followed by protease digestion for 10 mins or heat pre-treated for 10 mins followed by protease digestion for 20 mins. The sections displayed good tissue morphology following all combinations of heat pre-treatment and protease digestion. The GAPDH (positive control) probe was evident in the FFPE tonsil sections. The majority of GAPDH signal was observed within germinal centres of the tonsil. Sections probed for *Bacillus subtilis* dapB (negative control) were predominantly negative. The level of background was deemed acceptable if <1 dot was evident per 10 cells. PPBP/CXCL7 (target probe) expression was barely evident in

the tonsil sections. This was comparable to what was observed in FFPE tonsil sections stained by immunofluorescence with an antibody specific to CXCL7. Following the optimisation I decided to go ahead with a heat pre-treatment time of 10 mins and a protease digestion time of 10 mins (Figure 4.4).

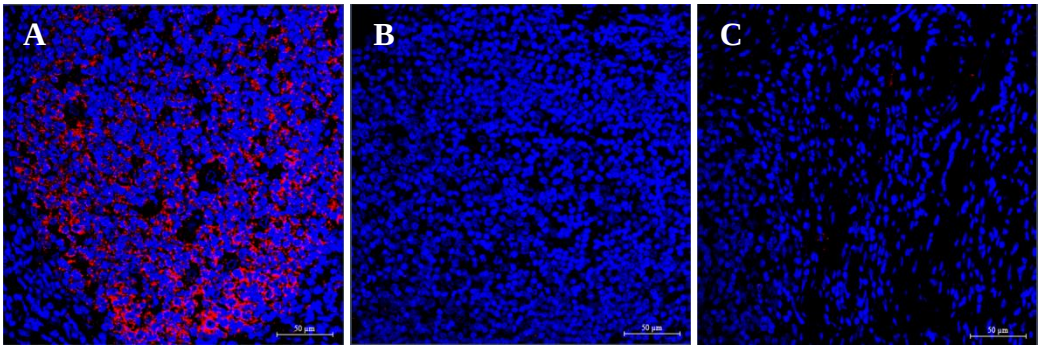

Figure 4.4 In Situ Hybridization of FFPE human tonsil. In Situ Hybridization was carried out using the QuantiGene® ViewRNA ISH Tissue 1-Plex Assay (Panomics/Affymetrix) for the presence of GAPDH (positive control probe) (Image A), *Bacillus subtilis* dapB (negative control probe) (Image B), and PPBP (target probe) (Image C). Sections underwent heat pre-treatment for 10 mins and protease digestion for 10 mins. Sections were viewed on the Zeiss LSM 780 Zen confocal. Images were taken at x400 total magnification. Probe-red, DAPI stained nuclei-blue.

Following on from my initial experiments in the tonsil tissue and prior to moving on to the early RA sections, I wanted to address whether or not I could carry out immunofluorescence staining with an antibody specific to CD68 after the In Situ Hybridization method. Establishment of this method would enable me to identify the cellular localisation of the RNA signal and thus support my data at the protein and mRNA level. Using a section of tonsil tissue previously used for In Situ Hybridization I was able to stain $CD68^+$ macrophages. I did not observe any co-localisation of the GAPDH probe with CD68 (Figure 4.5).

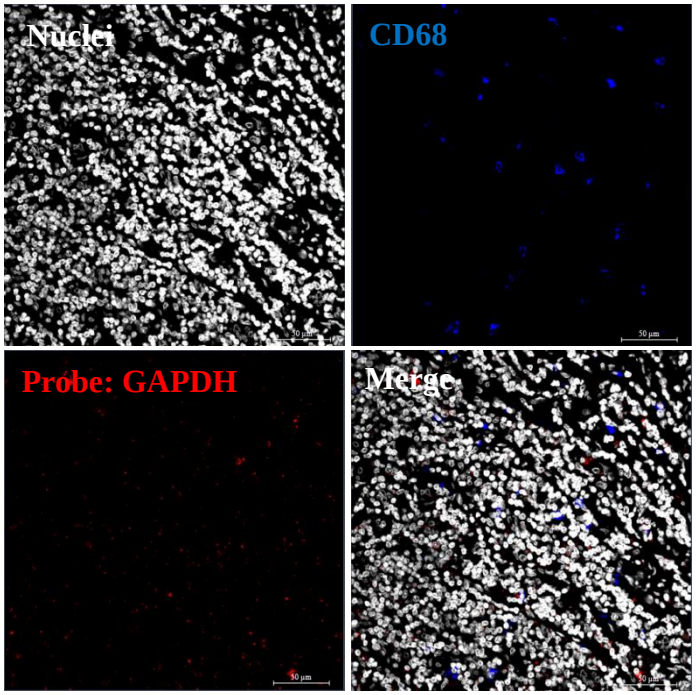

Figure 4.5 Immunofluorescence following the QuantiGene® ViewRNA ISH Tissue 1-Plex Assay in FFPE tonsil tissue. Following In Situ Hybridization, Immunofluorescence with an antibody specific for CD68 (blue) was carried out in FFPE human tonsil tissue. The image above was taken from a section previously probed for GAPDH (positive control probe (red)). Sections were viewed on the Zeiss LSM 780 Zen confocal. Images were taken at x400 total magnification.

Next I carried out In Situ Hybridization method in early RA sections. I decided to use the early RA sections as I observed an increase in CXCL7 protein expression by immunofluorescence in this patient group. First of all, as the numbers of sections were extremely limited I decided to trial the In Situ Hybridization method on three RA FFPE sections (positive, negative, and target probe) from one patient. In this experiment I observed expression of GAPDH and PPBP/CXCL7. I observed a large proportion of the PPBP/CXCL7 target probe signal outside the nuclei. However, some positive staining was observed within the nuclei. Positive staining was observed on the *Bacillus subtilis* dapB negative control; however I initially deemed the level of staining acceptable. On further inspection of the slides,

I identified non-specific binding on the glass slide. This gave rise to an increased background signal and therefore I was hesitant regarding the PPBP/CXCL7 result (Figure 4.6).

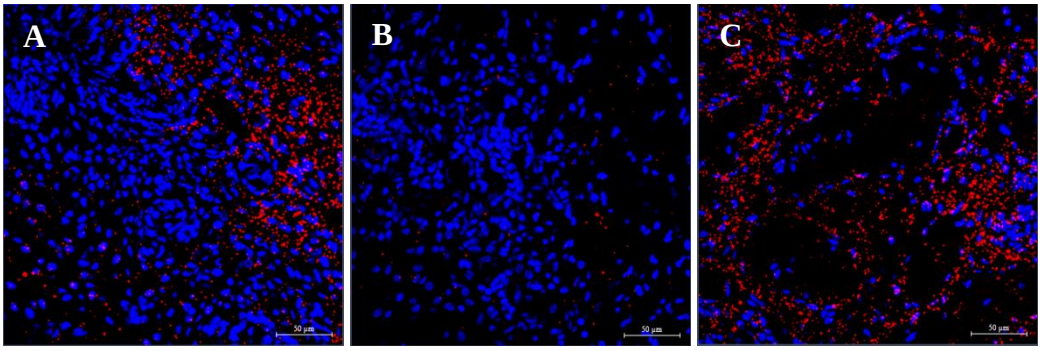

Figure 4.6 In Situ Hybridization of FFPE early RA tissue. In Situ Hybridization was carried out using the QuantiGene® ViewRNA ISH Tissue 1-Plex Assay (Panomics/Affymetrix) for the presence of GAPDH (positive control probe) (Image A), *Bacillus subtilis* dapB (negative control probe) (Image B), and PPBP (target probe) (Image C). Sections underwent heat pre-treatment for 10 mins and protease digestion for 10 mins. Sections were viewed on the Zeiss LSM 780 Zen confocal. Images were taken at x400 total magnification. Probe-red, DAPI stained nuclei-blue.

In order to try and address this issue, I adjusted the In Situ Hybridization method. I had the synovial biopsy sections cut and mounted on the recommended glass slides; Leica non-clipped X-tra slides by The Royal Orthopaedic Hospital NHS Foundation Trust (Birmingham, UK). I increased the number of xylene steps to ensure the full removal of paraffin and prolonged the wash times by 1 min following hybridization with the pre-amplifier and amplifier solutions. On first trying the adjusted protocol on tonsil sections (sections from the Biobank), the glass background was reduced. I observed expression of GAPDH, again predominantly within the germinal centres, and limited expression of *Bacillus subtilis* dapB in the sections as described previously. However, when I repeated the method in the early RA sections, the GAPDH and PPBP/CXCL7 signal was absent and I observed an increase in the glass background.

Next, I sought to determine whether or not the duration of tissue fixation in formaldehyde had any effect on the absence of the signal observed in the previous experiments in the early RA tissue. Some synovial biopsies used in the previous experiments, once collected, were fixed in formaldehyde for weeks if not months before being processed into paraffin and sectioned. Therefore synovial biopsies were collected and fixed for a maximum of 24 hours before being processed into paraffin and sectioned. I observed an increase in the GAPDH signal in the section fixed in formaldehyde for a maximum of 24 hours (Figure 4.7). *Bacillus subtilis* dapB signal was low. The section with a prolonged fixation time in formaldehyde had an increased *Bacillus subtilis* dapB signal. I did observe, again, an increase in glass background on the section probed with GAPDH. This was not observed on the section probed with *Bacillus subtilis* dapB. Moreover, blocking sections with 1% BSA/PBS did not eliminate the glass background issue.

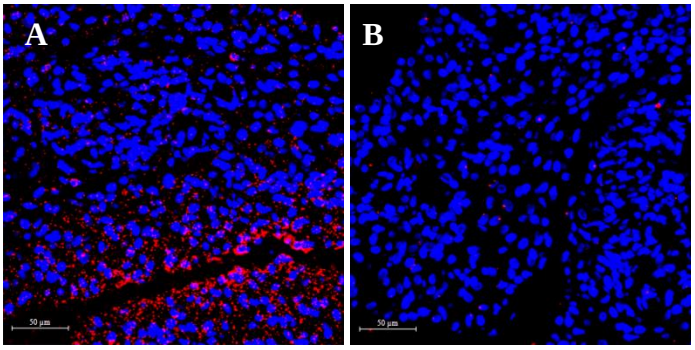

Figure 4.7 In Situ Hybridization of sections fixed and processed within 24 hours of collection (BX149B). Sections were probed for GAPDH (A and B) and *Bacillus subtillis* dapB (C and D). Sections were viewed on the Zeiss LSM 780 Zen confocal. Images were taken at x400 total magnification. Probe-red, DAPI stained nuclei-blue.

In conclusion, I validated the In Situ Hybridization method for the detection of the positive control probe, GAPDH, and the negative control probe, *Bacillus subtillis* dapB, in the tonsil sections. I was also able to design and perform an immunofluorescence protocol for the detection of CD68 within the tissue following the In Situ Hybridization method. Although I took multiple steps to validate the method for use in the RA tissue sections, I failed to eliminate non-specific binding of the probe to the glass slide. I was therefore unable to quantify and study the localisation of the CXCL7/PPBP target probe in the RA tissue.

4.3 DISCUSSION

In this chapter, I investigated the expression of CXCL4 and CXCL7 mRNA outside of the megakaryocyte lineage. The data supported my findings at the protein level in chapter 3, whereby I observed co-localisation of CXCL4 and CXCL7 with the macrophage marker, CD68. Here, I reported CXCL4 and CXCL7 mRNA expression in monocytes isolated from healthy controls. Furthermore, upon differentiation under M1, M2 and Mo-DC conditions *in vitro* I observed expression of both CXCL4 and CXCL7 mRNA in these cell populations, although relative mRNA quantification was significantly lower than observed in the freshly isolated monocytes (Figure 4.1). Within this chapter I was very reluctant to refer to the M1, M2 and Mo-DC cultured cells as terminally differentiated populations as the supernatants taken from cultured cells did not differ significantly in their TNFα levels. Therefore I referred to these populations as being cultured under M1, M2 and Mo-DC conditions.

Although there is no clearly defined marker that distinguishes between the M1 and M2 macrophage subsets, there have been several studies that outline a panel of markers than may be useful. M1 macrophages express high levels of pro-inflammatory mediators including TNFα, IL-1, IL-6, and IL-12 whilst M2 macrophages express high levels of anti-inflammatory mediators including IL-1RA, IL-10, and TGFβ. Additionally M2 macrophages can be characterised by their expression of the mannose receptor CD206 and the scavenger receptor CD163 on their surface, whilst M1 macrophages express increased levels of MHC class II and CD80/CD86 (Stöger et al, 2012). Furthermore M1 and M2 macrophages can be distinguished from one another by their metabolism of L-arginine. M1 macrophages upregulate nitric oxide synthase (iNOS) whilst M2 macrophages upregulate arginase 1 (Hao et al, 2012). Therefore in

the future, any cells differentiated in culture would be assessed using a number of these different markers to confirm their phenotype either by qPCR or flow cytometry.

My findings are in agreement with a study by Pertuy et al (2015). They studied the recombination of platelet factor 4 *(Pf4)-cre* in the Pf4-cre transgene mouse. Here, the expression of PF4/CXCL4 was not only reported in the megakaryocyte lineage but also in a small population of circulating leukocytes. *Pf4-cre* recombined cells were evident in all organs examined in the study including the heart, kidney, liver, stomach, brain and lung. Interestingly, the Pf4-cre recombined cells were identified as murine macrophages as they stained positive with an antibody specific for the surface marker F4/80. In humans, F4/80 is expressed by eosinophils, not macrophages (Murray and Wynn, 2011). F4/80 is a pan macrophage marker for macrophages in the mouse. Similar to our findings that not all CXCL4 positive cells were positive for CD68 and vice versa, Pertuy et al (2015) reported that not all F4/80 positive cells demonstrated *Pf4-cre* recombination. Therefore it was suggested that expression of PF4 was in a particular subset of macrophages. In our results I observed greater expression of CXCL4 mRNA in the cells differentiated to macrophages under M2 conditions (Figure 4.3A) compared to M1 and Mo-DC conditions. Therefore, I speculate that the F4/80 positive population expressing *Pf4-cre* observed by Pertuy et al (2015) may belong to the M2 macrophage subset. Moreover, the F4/80 negative cells expressing recombined *PF4-cre* are unlikely to be dendritic cells as they were negative for CD11c. However, as CD11c is a marker for mDCs as well as monocytes and macrophages (Murray and Wynn, 2011), it would have been interesting for this report to have stained with a more specific marker for pDCs, especially in light of the publication by van Bon et al (2014) which identified CXCL4 expression by pDCs in patients with systemic sclerosis. In support of my

findings, Schaffner et al (2005) reported the expression of CXCL4 in human monocytes. An increase in CXCL4 mRNA expression was observed in monocytes in response to thrombin stimulation. Moreover Mo-DCs were also found to express CXCL4 mRNA following thrombin stimulation, but not as high as observed in monocytes.

Likewise, the expression of CXCL7 has also been reported outside the megakaryocyte lineage. This is not surprising as the gene for CXCL4/PF4 is located only 5.3kb upstream of CXCL7/PBP. A recent study by Smith et al (2015) identified elevated levels of pro-platelet basic protein (PPBP) in human monocyte derived macrophages in patients with allergic bronchopulmonary aspergillosis and chronic cavitary pulmonary aspergillosis. PPBP mRNA expression was higher in the disease groups compared to healthy controls. In a study by El-Gedaily et al (2004) human mononuclear phagocytes were reported to transcribe and translate PPBP. Furthermore, PPBP mRNA expression was found to be negatively regulated by IL-4 and IL-10. Glucocorticoids were also found to have a negative effect on PPBP mRNA expression in monocytes and platelets. Interestingly, El-Gedaily et al (2004) reported that LPS stimulation of monocytes did not increase PPBP mRNA expression but instead decreased expression. This finding may support my results, as I observed a decrease in CXCL7 mRNA expression following 6 hours of LPS stimulation in monocytes differentiated to macrophages under M2 culture conditions compared to the unstimulated cells. However, CXCL7 mRNA expression increased following 24 hours of LPS stimulation in this population. Furthermore, El-Gedaily et al (2004) reported that NAP-2 release into the supernatant from stimulated monocytes was not substantial, and therefore it was suggested that PPBP and its cleavage products may play a role in intracellular functions such as anti-microbial activity. As a result, the expression of CXCL4 and CXCL7 by macrophages may result in extra care needing to be

taken when studying the function of megakaryocytes in animal models, especially where inflammatory cells are present (Pertuy et al, 2015).

It has also been reported in a number of studies that platelets may form complexes/aggregates with other immune cells within the circulation and trigger inflammation. Joseph et al (2001) carried out a study looking at the formation of platelet-leukocyte complexes in the peripheral blood of patients with systemic lupus erythematosus (SLE), primary antiphospholipid syndrome (PAP) and RA. Here, it was reported, that within the peripheral blood of patients with RA, there was a significant increase in platelet-granulocyte and platelet-monocyte complexes compared to healthy controls. They also reported an increase in circulating platelet-lymphocyte complexes, although this was not significant compared to controls. Pamuk et al (2008) also reported an increase in circulating platelet-monocyte- and platelet-neutrophil-complexes within the peripheral blood of patients with RA compared to controls. I was able to demonstrate that monocytes were capable of forming complexes with platelets using flow cytometry. These complexes were observed upon cell sorting from freshly isolated PBMCs and also positively selected isolated $CD14^+$ monocytes. A similar method was described by Jung et al (2014). I observed expression of CXCL4, CXCL7 and CD41 mRNA on $CD14^+$ $CD41^-$ monocytes. This suggests that monocytes are a source of both chemokines at the mRNA level. Furthermore, when $CD41^+$ platelets were included in the sorted populations, the expression of CXCL4, CXCL7, and CD41 mRNA was significantly higher. Hence, this would suggest that although monocytes express CXCL4 and CXCL7 in the blood, platelets are still the predominant source of both chemokines. Interestingly in the $CD14^+$ $CD41^-$ sorted population, I did observe a low level of CD41 mRNA expression. This may indicate that my gates were set too large or it is quite possible that platelet microparticles may

have been attached to the surface of the monocytes. Although I did not have the opportunity to look for monocyte-platelet complexes in the peripheral blood from patients with RA, I did observe $CD41^+$ staining on the membrane of certain cells within the synovium. This could suggest that the formation of monocyte-platelet complexes in the peripheral blood may also be evident in the synovium of RA patients. This may also be a potential mechanism of how platelets leave the circulation and enter the synovium.

In Situ Hybridization allows the visualisation of target RNA at the single cell level in frozen and paraffin embedded tissue without disruption of the tissue architecture. The technique offers higher specificity when compared to qPCR and has an advantage in that it can be coupled with immunohistochemistry and immunofluorescence for identification of cell populations expressing the target RNA (Reichard et al, 2006). In this chapter, I set out to validate a method for In Situ Hybridization for the detection of single CXCL7/PPBP RNA molecules within the rheumatoid synovium. As CXCL7/PPBP target probes were commercially available from Affymetrix/Panomics, I initially set about validating the method using this probe alongside positive and negative controls with the overall aim of designing my own CXCL4/PF4 target probe once the method worked. I was also keen on establishing the method within our laboratory so that it could be utilised by other members of our research group for different targets of interest. Overall, I was generally satisfied with the In Situ Hybridization method in tonsil sections and moreover I was able to carry out immunofluorescence with an antibody specific for CD68 following In Situ Hybridization (Figure 4.5) whilst still retaining good tissue architecture. I observed strong positive control GAPDH and minimal negative control *Bacillus subtilis* dapB RNA signal. Interestingly I observed GAPDH signal predominantly targeted to germinal centres within the tonsil tissue.

This was not a result I was anticipating as I expected GAPDH to be found across the entire tissue (Figure 4.4A). Similar to my observations in tonsil sections by immunofluorescence I was not surprised by the low levels of PPBP/CXCL7 in this tissue detected by In Situ Hybridization. However, upon moving to rheumatoid synovium sections in which I had previously observed high expression of CXCL7 by immunofluorescence, I struggled to produce an In Situ Hybridization result that I was satisfied with. The main issue I encountered when moving from the tonsil sections to the synovium was the increase in glass slide background and although I tried multiple optimisation protocols to try and eliminate this issue, I was unable to distinguish a positive result over background. To conclude, although I detected a positive signal for GAPDH in the tonsil, further work must be performed to fully validate the In Situ Hybridization method for use in the synovial tissue.

5 CHARACTERISATION OF CXCL4L1 EXPRESSION IN THE RHEUMATOID SYNOVIUM

5.1 INTRODUCTION

In the work shown in chapter 3, I observed CXCL4 expression within the synovium of patients with early RA, established RA, and early resolving synovitis. Expression was also observed in uninflamed controls. During this study I became aware of the variant form of CXCL4 which differs in only three amino acids; Proline58>Leucine, Lysine66>Glutamic acid, and Leucine67>Histidine, within the C-terminus (Green et al, 1989). The variant is referred to as CXCL4L1 or platelet factor 4 variant (PF4V1). CXCL4L1 is expressed predominantly by thrombin stimulated platelets, smooth muscle cells and tumour cells (Struyf et al, 2004). It functions as a potent inhibitor of endothelial cell migration and angiogenesis (Vandercappellen et al, 2011).

Angiogenesis is the development of new blood vessels from pre-existing vessels. It is involved in physiological processes such as embryogenesis, wound healing and the female reproductive cycle. It is also a key player in tumour growth and metastasis, RA, psoriasis, and diabetic retinopathy amongst many others (Friis et al, 2013). Angiogenesis is regulated by a balance between both angiogenic and angiostatic factors. Angiogenic factors promote angiogenesis and include vascular endothelial growth factor (VEGF), fibroblast growth factor-1 (FGF-1), fibroblast growth factor-2 (FGF-2), platelet derived growth factor (PDGF), epidermal growth factor (EGF), insulin-like growth factor (IGF), hepatocyte growth factor (HGF) and the angiopoietins 1-4 (Ang 1-4). A large number of cytokines and chemokines

also drive angiogenesis. These include; TGFβ, TNFα, IL-1, IL-6, IL-13, IL-15, IL-18, and the ELR^+ CXC chemokines. They are released when tissue becomes injured, diseased or hypoxic. CXCL4L1 is an angiostatic factor.

Currently, there is very little known about CXCL4L1 in the context of RA. Thus far a single study exists that briefly describes the expression of CXCL4L1 at the mRNA level in vitro fibroblast-like synoviocytes from OA and RA patients (Cagnard et al, 2005). However, as of yet there is no research regarding the expression of CXCL4L1 at the protein level within the RA synovium.

In this chapter, the primary objective was to determine whether or not the antibody used for the CXCL4 study was indeed specific for CXCL4 and was not detecting CXCL4L1. Interesting preliminary data led me to study the expression of CXCL4L1 at the protein level in the rheumatoid synovium alongside markers for synovial fibroblasts. Furthermore, I progressed on to study the expression of CXCL4L1 at the protein and mRNA level in *in vitro* cultured fibroblasts. I hypothesised that expression of CXCL4L1 in the synovium and cultured fibroblasts would explain the pathology observed in rheumatoid arthritis.

The normal synovium can be subdivided into two regions; the synovial lining layer and the synovial sublining layer. The synovial lining is 2-3 cell layers thick and consists of type A macrophage-like synoviocytes and type B fibroblast-like synoviocytes. Type B fibroblast-like synoviocytes produce hyaluronan, a constituent of synovial fluid, whilst type A macrophage-

like synoviocytes clear debris from the joint. The sublining is relatively acellular, with a small number of scattered blood vessels, fibroblasts, lymphocytes, and macrophages (Smith, 2011). Capillaries, venules and arterioles, as well as the lymphatics are positioned within the sublining (Smith, 2011). In RA, it is the synovial fibroblasts that are thought to play a key role in driving RA progression and the persistence of inflammation (Filer, 2013). They produce a large array of different inflammatory cytokines, chemokines, angiogenesis mediators, serine proteases, matrix metalloproteinases and cathepsins, and as a result exhibit an aggressive and invasive phenotype (Pap et al, 2000). Rheumatoid synovial fibroblasts (RA-SFs) produce CCL2, CCL3, CCL5, CCL20, CCL21, CXCL1, CXCL5, CXCL8, CXCL10, CXCL12, and CXCL13 which drive leukocyte recruitment to the synovial joint and retention of leukocytes within the synovium. They release IL-15 and IL-16. RA-SFs are highly invasive and are often characterised by their large pale nuclei, rounded shape, abundant cytoplasm, and prominent nucleoli (Pap et al, 2000). On activation they upregulate expression of adhesion molecules and as a result are capable of attaching to cartilage. Müller-Ladner et al (1996) reported that RA-SFs were capable of invading healthy human cartilage when engrafted into the severe combined immunodeficiency (SCID) mouse, whereas fibroblasts taken from OA, skin and healthy donors showed very little if any invasive growth. This study also identified the expression of cathepsins B, D, and L at the site of invasion, as well as VCAM-1. RA-SFs also produce MMP-1 and MMP-3 which drive cartilage degradation. Moreover, Lefevre et al (2009) described the potential of RA-SFs to spread disease to unaffected joints using healthy cartilage co-implanted subcutaneously into SCID mice alongside RA-SFs and detecting migration of RA-SFs into contralaterally implanted cartilage. RA-SFs produce RANKL which promotes osteoclast formation and drives bone erosion. They also release DKK-1 which inhibits osteoblast function, thus preventing the repair of bone erosions. Additionally,

synovial fibroblasts have been shown to protect $CD4^+$ T cells from undergoing spontaneous apoptosis (Salmon et al, 1997). In the study by Salmon et al (1997), synovial fibroblasts co-cultured with $CD4^+$ T cells isolated from peripheral blood and synovial fluid were shown to inhibit apoptosis via the upregulation of Bcl-xL. Moreover, factors released by synovial fibroblasts were also effective.

A number of different markers can be used to define fibroblast subpopulations in the RA synovium (Table 5.1). Within this chapter, I used CD90 (Thy-1), protein disulphide isomerase (PDI) and vascular cell adhesion molecule (VCAM-1) to aid in the study of the expression of CXCL4L1 in the rheumatoid synovium and *in vitro* cultured fibroblasts.

Name	Synonyms	Geographical marker	Role in disease
CD55	DAF	Lining layer subpopulation	Interacts with macrophage CD97
VCAM-1	CD106	Lining layer subpopulation	Adhesion via VLA-4
Cadherin-11		Lining layer	Homotypic adhesion
Gp38	Podoplanin	Lining layer and lymphatics	Invasiveness in cancer
FAP	Fibroblast activation protein	Lining layer subpopulation in RA	Resistant to cancer chemotherapy
CD90	Thy-1	Sublining layer and endothelial cells	Cell adhesion via Mac-1
CD248	Endosialin	Sublining layer and pericytes	Invasiveness in cancer, angiogenesis

Table 5.1 Markers of fibroblast subpopulations in the RA synovium. Table from Filer, 2013.

CD90 was originally identified on mouse thymocytes and as a result is also referred to as thymocyte differentiation antigen-1 (Thy-1). CD90 (Thy-1) is a 25-35 kDa cell surface glycoprotein that is anchored to the membrane via glycosylphosphatidylinositol. CD90 (Thy-1) is expressed by mesenchymal, haematopoietic and keratinocytic stem cells as well as fibroblasts, neuronal cells and activated endothelial cells. It functions in inflammation and wound healing by playing a role in the synthesis and release of cytokines, growth factors and extracellular matrix constituents. It also plays a role in cell-matrix and cell-cell adhesion. CD90 (Thy-1) is expressed in the synovium of RA patients (Saalbach et al, 1999). It is used as a marker of the synovial sublining and endothelial cells.

Protein disulphide isomerase (PDI) is a 55 kDa member of a large family of thiol-disulphide oxidoreductases. It is expressed in the lumen of the endoplasmic reticulum whereby it plays a role in the synthesis and folding of proteins. Protein disulphide isomerase is a non-catalytic β-subunit of prolyl-4-hydroxylase. It is involved in the biosynthesis of collagen triple helix formation. It is responsible for the hydroxylation of proline residues within collagen (Appenzeller-Herzog and Ellgaard, 2008, Wilkinson and Gilbert, 2004). Prolyl-4-hydroxylase also plays a role in the regulation of hypoxia inducible factors (Myllyharju, 2003). Prolyl-4-hydroxylase and PDI can be used as fibroblast markers (Hirohata et al, 2001).

Vascular cell adhesion molecule-1 (VCAM-1/CD106) is 100-105 kDa member of the immunoglobulin family. VCAM-1 is expressed by the endothelium in response to inflammatory stimuli such as cytokines. It is involved in leukocyte trafficking via the α4β1 integrin and retention of said leukocytes at sites of inflammation. VCAM-1 also plays

important roles in embryogenesis, angiogenesis, B cell development, and B cell and T cell activation (Carter et al, 2002, Reparon-Schuijt et al, 2001). In RA, VCAM-1 is expressed by fibroblast-like synoviocytes in the lining layer, chondrocytes and endothelial cells (Carter et al, 2002). Tak et al, (1995) also reported the expression of VCAM-1 in lymphocyte aggregates and diffuse leukocyte infiltrates in RA patients of <1 year disease duration. Sublining fibroblasts do not express VCAM-1. Therefore, VCAM-1 is often used as a marker to distinguish between fibroblasts of the synovial lining and sublining.

Other markers used for fibroblast identification within the rheumatoid synovium, although not used in this chapter, include CD55, cadherin-11, Fibroblast activation protein (FAP), CD248 and podoplanin (gp38) (Table 5.1) (Filer, 2013). Cadherin-11; a molecule involved in cell-cell adhesion, and development and organisation of the synovium (Lee et al, 2007) CD55; a negative regulator of the complement system (Hoek et al, 2010), and FAP; a potential promoter of extracellular matrix degradation reported to co-localise with MMP-1 and MMP-13, are all expressed within the synovial lining layer (Bauer et al, 2006). CD248 is a type I transmembrane glycoprotein expressed by pericytes and sublining fibroblasts. CD248 has been reported in RA and PsA synovium but not in healthy synovium (Maia et al, 2010). In RA, podoplanin (gp38) has been observed early in disease as well as in established destructive disease. It is expressed by both lining and sublining fibroblasts within the rheumatoid synovium (Del Rey et al, 2014, Ekwall et al, 2011).

5.2 RESULTS

CXCL4L1 differs from CXCL4 in a three amino acid substitution in the C-terminus. I was therefore concerned that the antibody used for the CXCL4 study may also bind to CXCL4L1. Therefore to address these concerns I set out to analyse protein expression of CXCL4L1 in the synovial tissue of patients with RA. An antibody specific for CXCL4L1 was titrated for immunofluorescence by staining synovial tissue section cut from biopsies taken from patients with RA that had undergone joint replacement. My initial observations identified CXCL4L1 predominantly within the lining layer of the RA synovium (Figure 5.1).

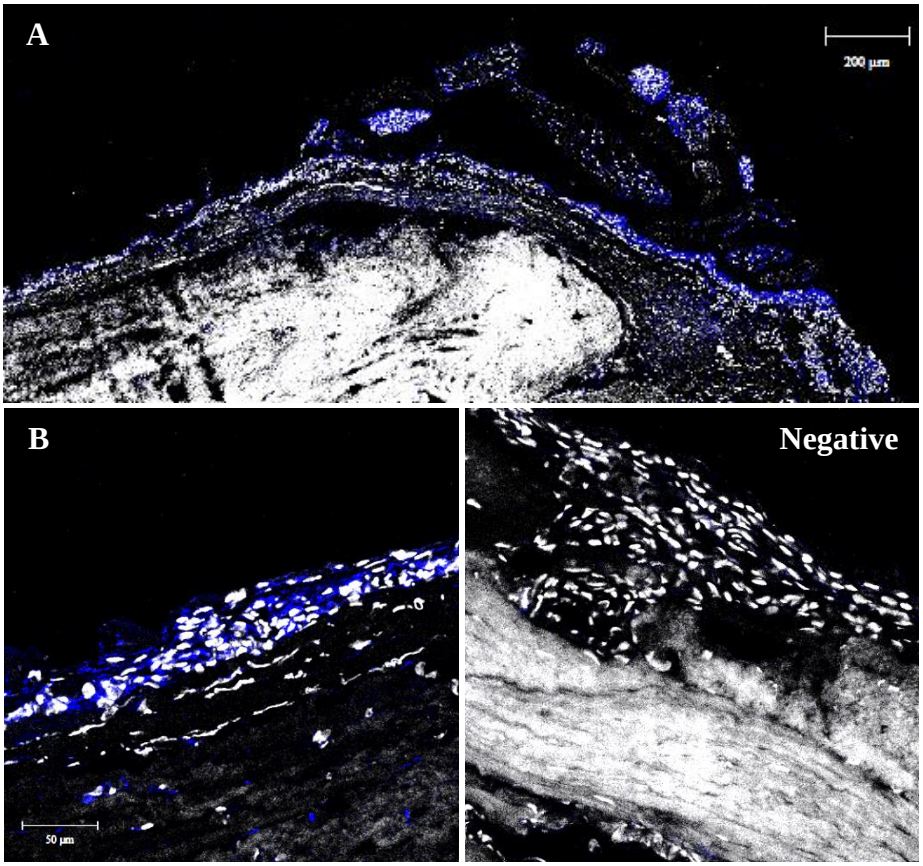

Figure 5.1 CXCL4L1 staining of the rheumatoid synovium (H03.12). Sections of rheumatoid synovium taken from patients who had undergone joint replacement was stained with an antibody specific for CXCL4L1 (blue). Nuclei were counterstained with Hoechst 33258 (grey). Image A depicts an 8 x 8 (0.7 zoom) overview tile scan taken using the Zeiss LSM 780 Zen confocal. Image B represents a selected region from the overview tile scan. Images were taken at x400 total magnification. Tissue sections were stained alongside an isotype matched control. The isotype matched controls were negative. Scale bar: A 200µm and B: 50µm.

Next, I double stained synovial tissue with antibodies specific for CXCL4 and CXCL4L1 to test whether there was an overlap in the staining pattern indicating possible cross-reactivity (Figure 5.2). Expression of both CXCL4 and CXCL4L1 was observed in the RA synovial tissue. CXCL4 and CXCL4L1 co-localisation was extremely limited. Positive staining for CXCL4 and CXCL4L1 was largely segregated within the synovial tissue. Likewise, in the

tonsil tissue, that I had available, CXCL4L1 and CXCL4 did not co-localise (data not shown). Therefore cross-reactivity between the two antibodies was deemed unlikely.

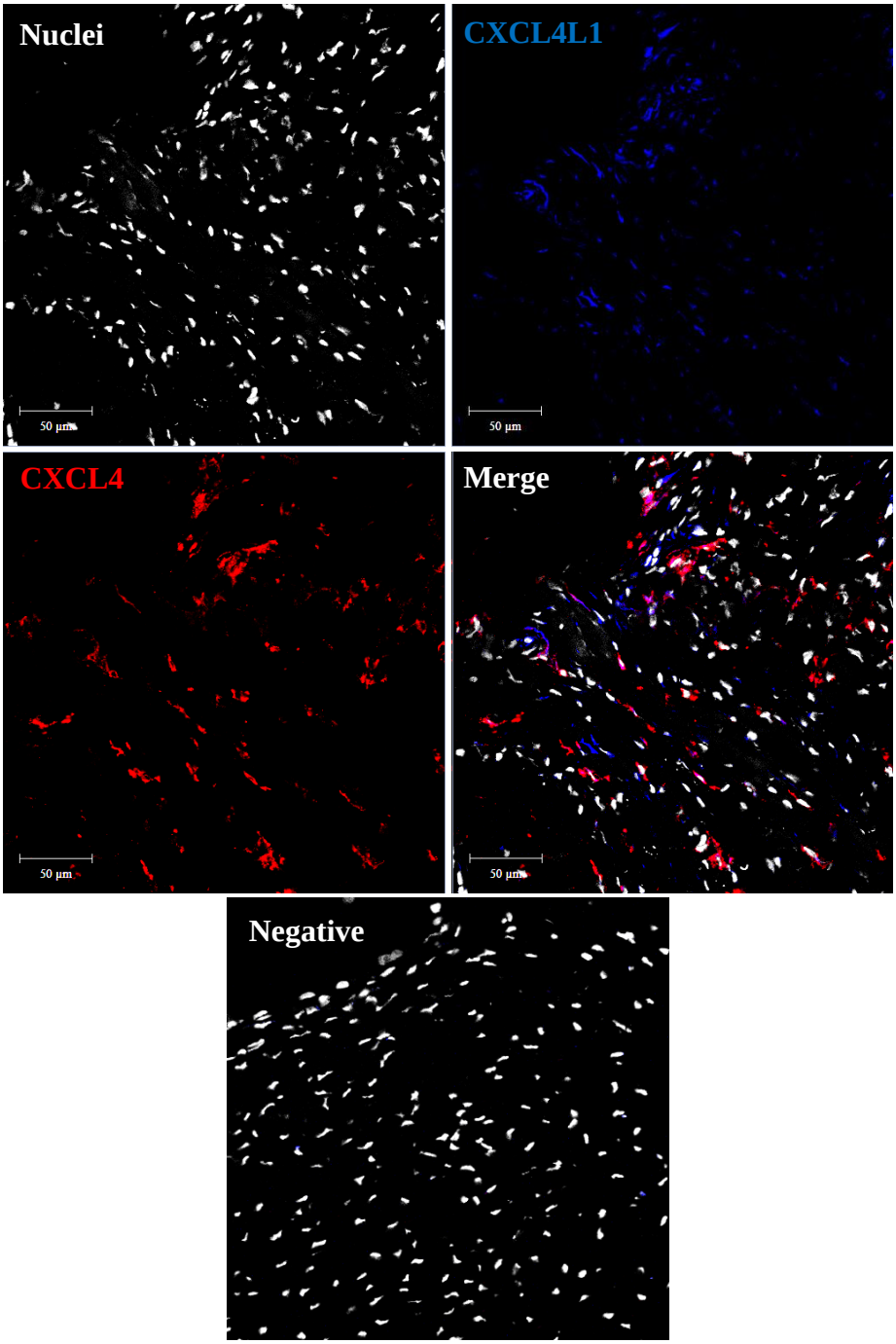

Figure 5.2 CXCL4L1 and CXCL4 staining of the rheumatoid synovium (H03.11). Sections of rheumatoid synovium taken from patients who had undergone joint replacement were stained with antibodies specific for CXCL4L1 (blue) and CXCL4 (red). Nuclei were counterstained with Hoechst 33258 (grey). Images were taken at x400 total magnification using the Zeiss LSM 780 Zen confocal. Tissue sections were stained alongside isotype matched controls which were negative (n=5). Scale bar: 50µm.

Next, I sought to determine whether or not CXCL4L1 was evident within the lining layer or the sublining of the RA synovium. For this purpose I stained RA synovial sections with antibodies specific for VCAM-1 and CD90. VCAM-1 and CD90 aid in distinguishing the lining layer of the synovium from the sublining layer, respectively. RA synovial tissue sections were stained with antibodies specific for CXCL4L1 alongside VCAM-1 and CD68 or CXCL4L1 and CD90. No co-localisation of CXCL4L1 with CD68 was observed. CXCL4L1 was evident in the lining layer of the synovium, as defined by the presence of VCAM-1(Figure 5.3 and Figure 5.4). CXCL4L1 and CD90 staining was largely distinct. However, co-localisation of CXCL4L1 and CD90 was evident in the areas where the sublining was adjacent to the lining layer (Figure 5.5 and Figure 5.6).

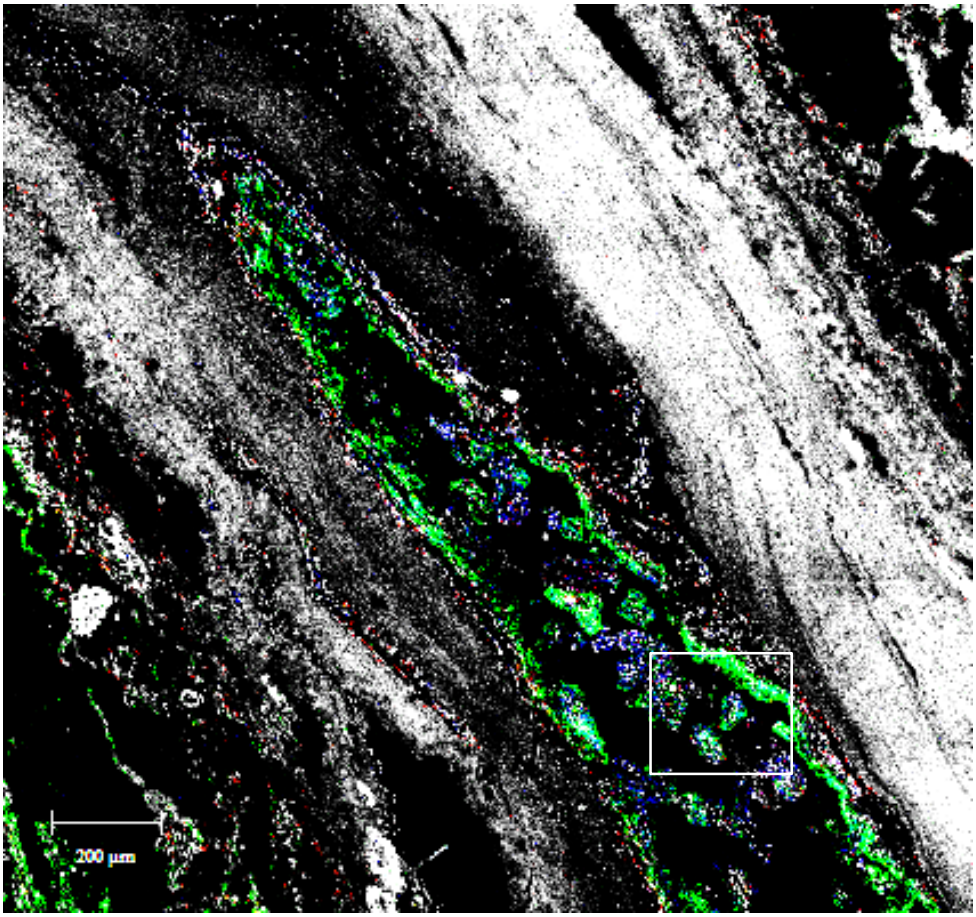

Figure 5.3 CXCL4L1, VCAM-1 and CD68 overview scan of the rheumatoid synovium (H03.12). Sections of rheumatoid synovium taken from patients who had undergone joint replacement were stained with antibodies specific for CXCL4L1 (blue), VCAM-1 (green), and CD68 (red). Nuclei were counterstained with Hoechst 33258 (grey). An 8 x 8 (0.7 zoom) overview tile scan was taken using the Zeiss LSM 780 Zen confocal. An area of interest was selected from the overview scan as depicted by the white box. This area was then scanned. It is shown in Figure 1.3. Scale bar: 200µm.

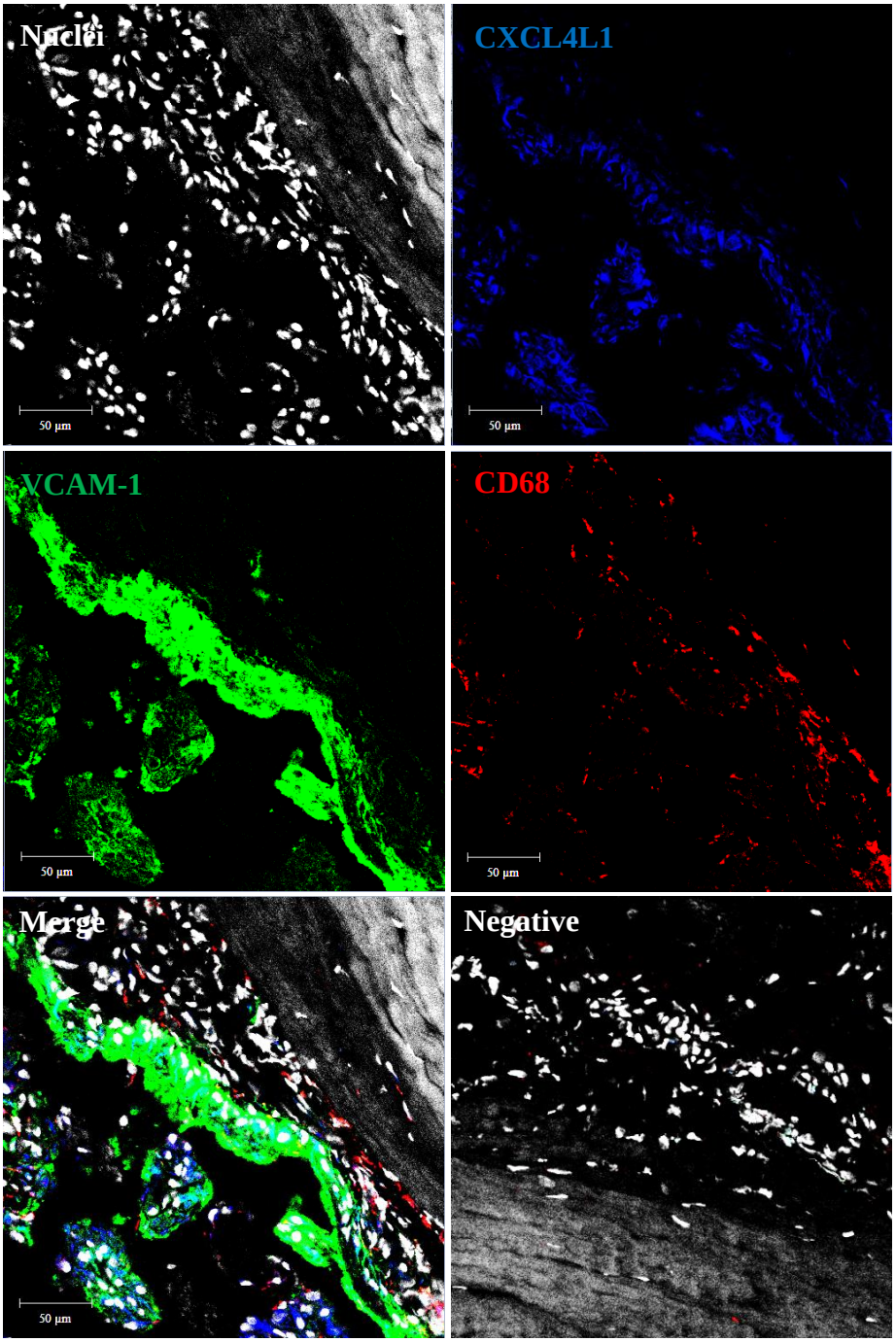

Figure 5.4 CXCL4L1, VCAM-1, and CD68 staining of the rheumatoid synovium (H03.12). Sections of rheumatoid synovium taken from patients who had undergone joint replacement were stained with antibodies specific for CXCL4L1 (blue), VCAM-1 (green), and CD68 (red). Nuclei were counterstained with Hoechst 33258 (grey). Images were taken at x400 total magnification using the Zeiss LSM 780 Zen confocal. Tissue sections were stained alongside isotype matched controls which were negative (n=5). Scale bar: 50µm.

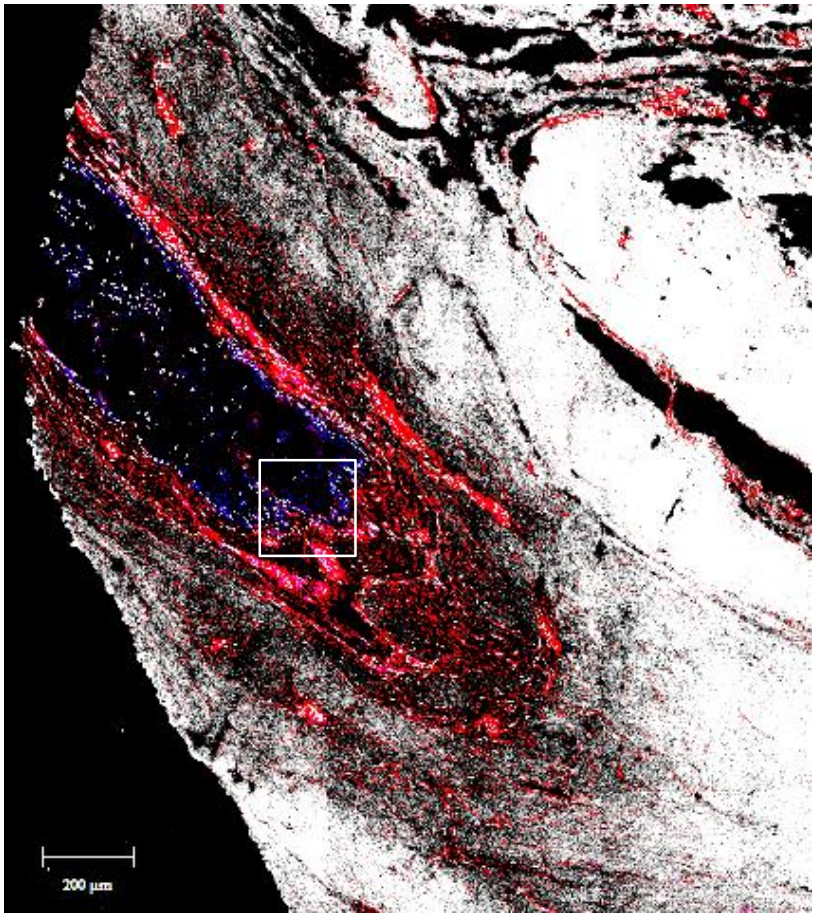

Figure 5.5 CXCL4L1 and CD90 overview scan of the rheumatoid synovium (H03.12). Sections of rheumatoid synovium taken from patients who had undergone joint replacement were stained with antibodies specific for CXCL4L1 (blue) and CD90 (red). Nuclei were counterstained with Hoechst 33258 (grey). An 8 x 8 (0.7 zoom) overview tile scan was taken using the Zeiss LSM 780 Zen confocal. An area of interest was selected from the overview scan as depicted by the white box. This area was then scanned. It is shown in Figure 1.5. Scale bar: 200µm.

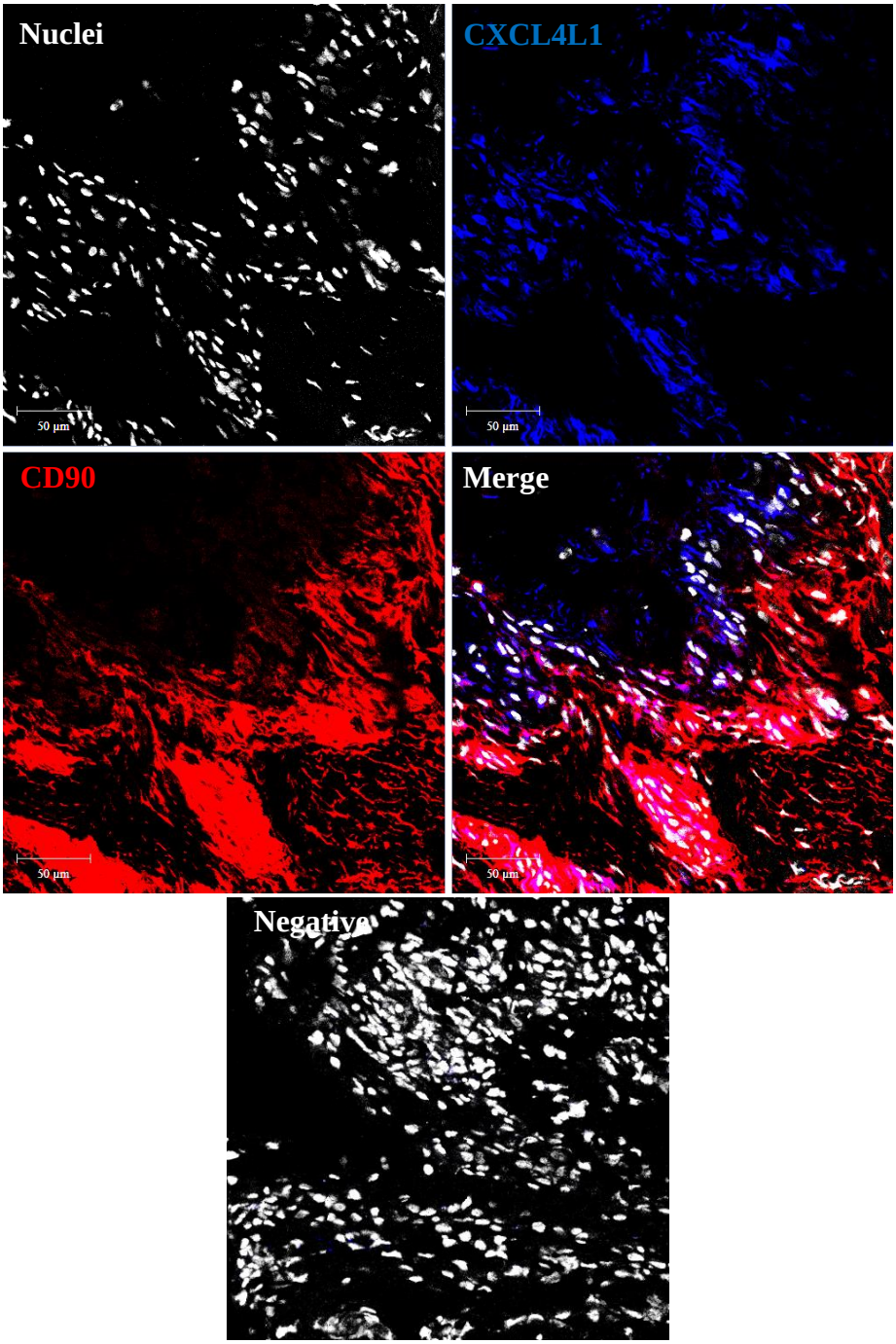

Figure 5.6 CXCL4L1 and CD90 staining of the rheumatoid synovium (H03.12). Sections of rheumatoid synovium taken from patients who had undergone joint replacement were stained with antibodies specific for CXCL4L1 (blue) and CD90 (red). Nuclei were counterstained with Hoechst 33258 (grey). Images were taken at x400 total magnification using the Zeiss LSM 780 Zen confocal. Tissue sections were stained alongside isotype matched controls which were negative (n=5). Scale bar: 50µm.

As my results indicated that CXCL4L1 was largely expressed within the lining layer, but not associated with $CD68^{+}$ macrophages, I decided to stain RA sections with a fibroblast marker. RA sections were stained with antibodies specific for CXCL4L1 and protein disulphide isomerase (PDI). Co-localisation of CXCL4L1 with PDI was observed within the tissue, however not all CXCL4L1 positive cells stained for PDI and vice versa (Figure 5.7).

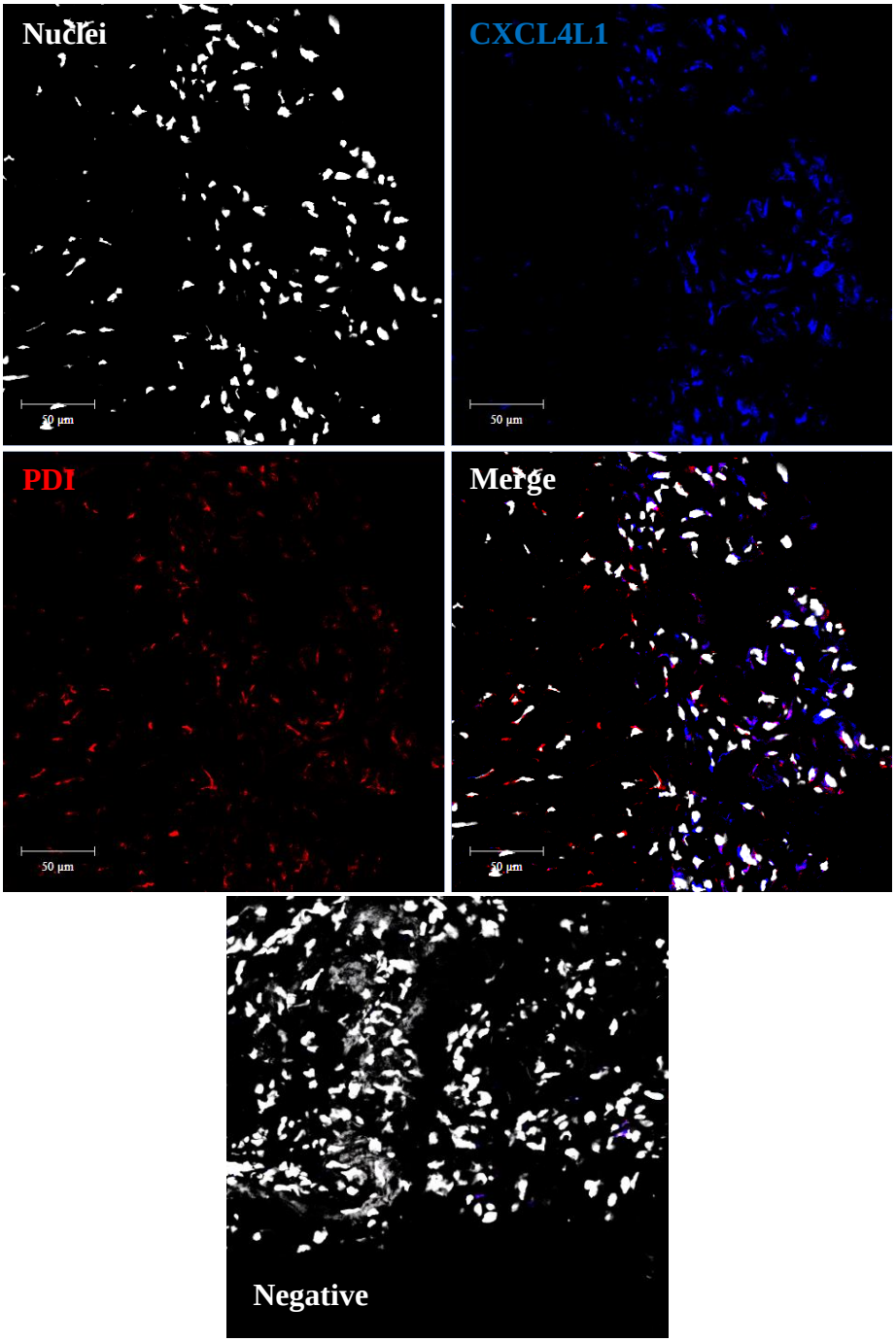

Figure 5.7 CXCL4L1 and protein disulphide isomerase (PDI) staining of the rheumatoid synovium (H07.6). Sections of rheumatoid synovium taken from patients who had undergone joint replacement were stained with antibodies specific for CXCL4L1 (blue) and PDI (red). Nuclei were counterstained with Hoechst 33258 (grey). Images were taken at x400 total magnification using the Zeiss LSM 780 Zen confocal. Tissue sections were stained alongside isotype matched controls which were negative (n=4). Scale bar: 50µm.

To follow up on these data and to formally establish expression of CXCL4L1 by synovial fibroblasts, I stained *in vitro* cultured synovial fibroblasts. Chamber slide cultures were prepared from in *vitro* cultured synovial fibroblasts from 5 different patient groups; mainly from patients with osteoarthritis (Figure 5.8) and late stage RA from tissue extracted from joint replacement surgery. As a pilot experiment I also used a small number of samples from treatment naïve patients from the Birmingham Early Arthritis Cohort (BEACON). These were grouped into patients with early RA <12 weeks symptom duration, patients with established RA (>12 weeks, <3 years symptom duration) and patients with resolving disease. Fibroblasts were stained with antibodies specific for CXCL4L1 and PDI (Figure 5.8). The majority of cultured fibroblasts from all 5 patient groups expressed CXCL4L1 and PDI. The detection of PDI expression in the cultured cells clearly identified the cells as fibroblasts. CXCL4L1 and PDI protein expression was quantified using the Zen 2010 software (Figure 5.9). In order to do this, 5-7 x400 total magnification images were obtained from each chamber slide. Regions were drawn around individual fibroblasts using the overlay function within the Zen 2010 software. Individual pixel counts were then obtained from the selected regions and exported to Microsoft Excel. Here, a mean of the pixel count per μm^2 area was calculated. Overall these data suggest that *in vitro* cultured synovial fibroblasts homogeneously express CXCL4L1. As these cells are likely to be a mixture of fibroblasts derived from lining and sublining, the data would suggest that the restriction of CXCL4L1 expression to the lining layer in the intact tissue is lost in culture. There was no clear difference in CXCL4L1 in cultured fibroblasts derived from patients with OA or RA or any of the groups of the BEACON cohort.

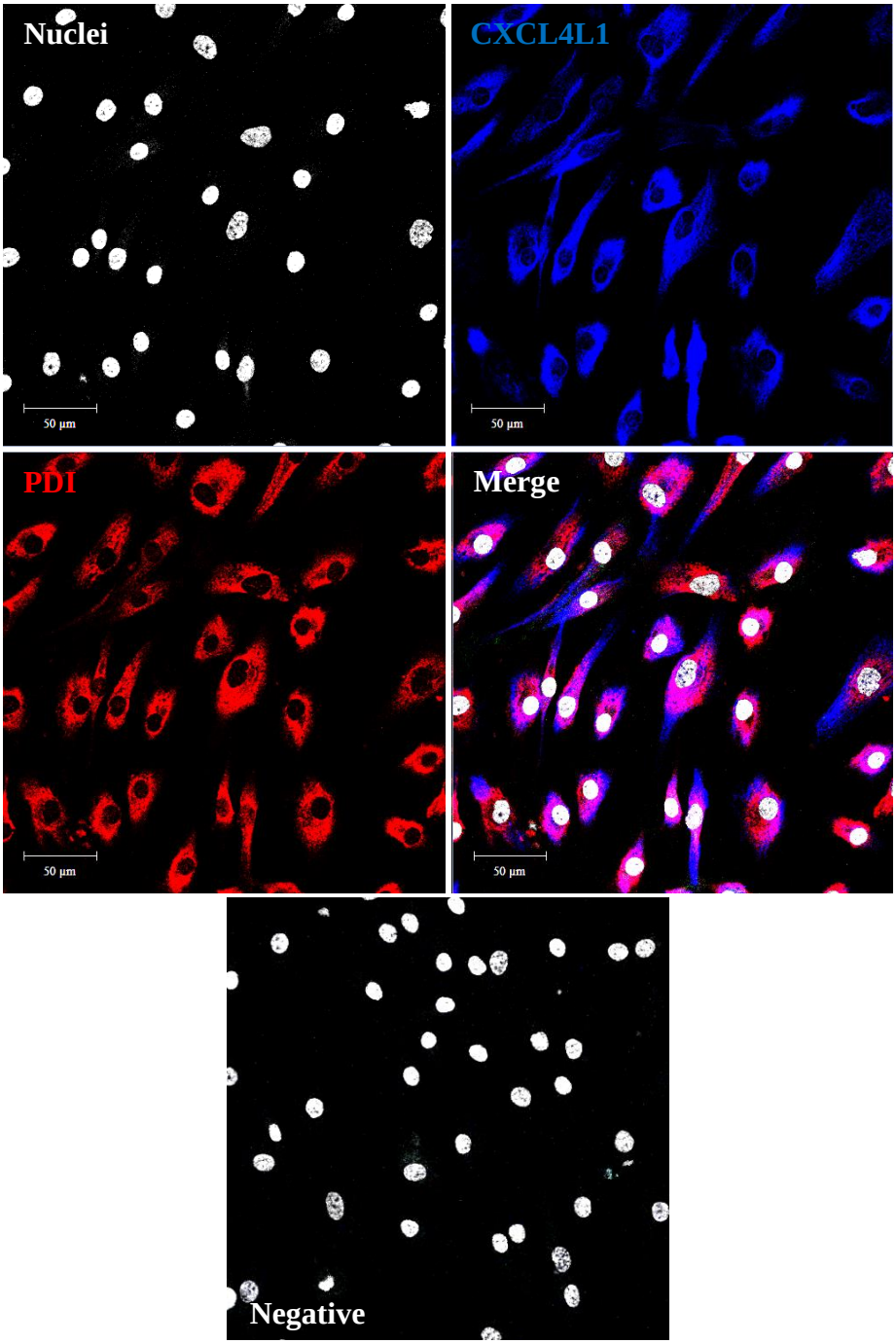

Figure 5.8 CXCL4L1 and protein disulphide isomerase (PDI) staining of *in vitro* cultured fibroblasts (ST01SY). A chamber slide of *in vitro* cultured fibroblasts taken from a patient with osteoarthritis was stained with antibodies specific for CXCL4L1 (blue) and PDI (red). Nuclei were counterstained with Hoechst 33258 (grey). Images were taken at x400 total magnification using the Zeiss LSM 780 Zen confocal. Tissue sections were stained alongside isotype matched controls which were negative. Scale bar: 50µm.

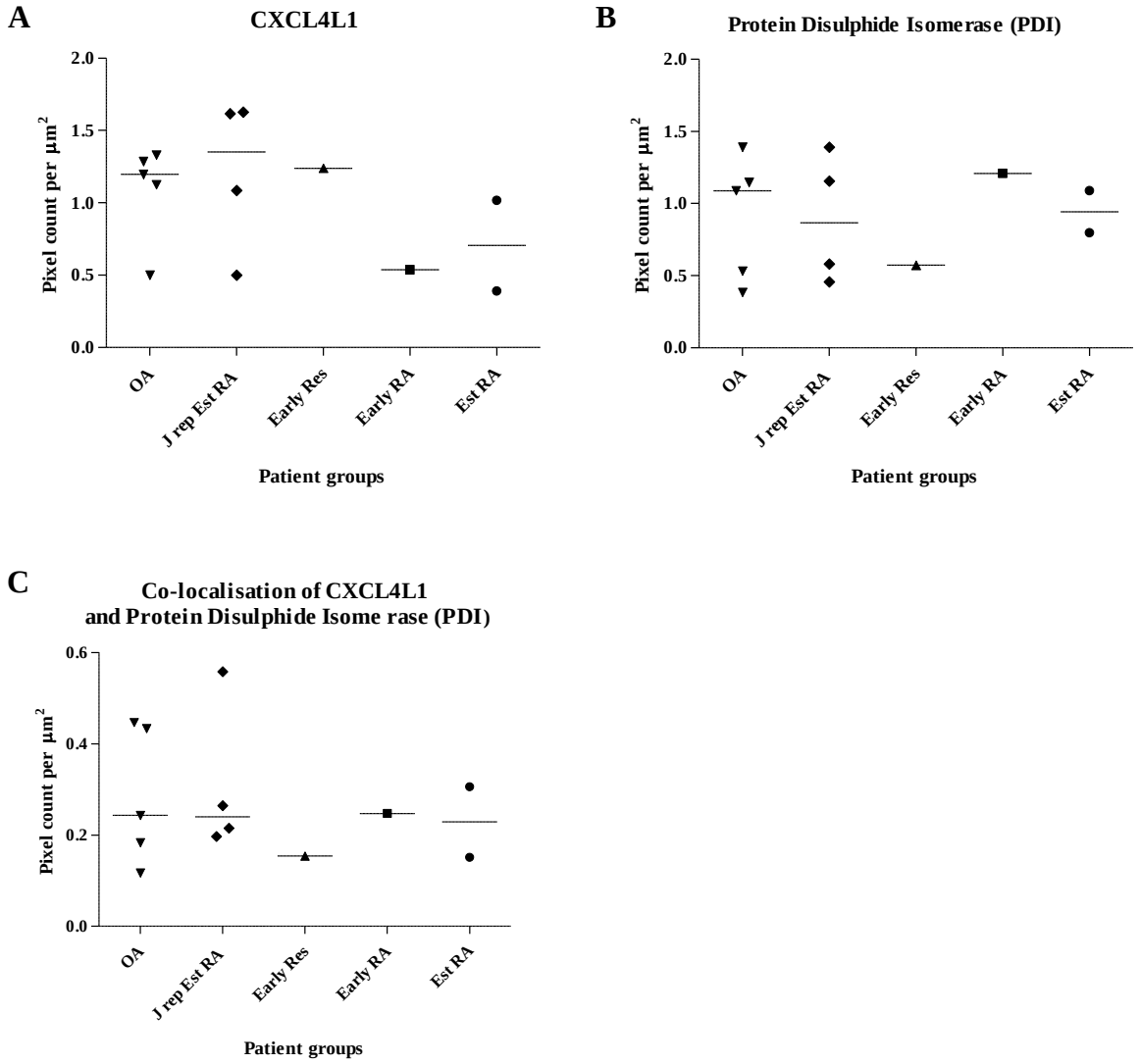

Figure 5.9 Quantification of CXCL4L1 and protein disulphide isomerase expression in *in vitro* cultured fibroblasts. A) CXCL4L1 and **B**) PDI expression was calculated using the Zen 2010 software. Individual fibroblasts were drawn around using the overlay function in the Zen 2010 software. Pixel counts were exported and transferred to Microsoft Excel. A formula was applied to calculate the number of pixels per μm^2 area. Co-localisation of **C**) CXCL4L1 and PDI was calculated by applying a formula within the Zen 2010 software that calculated the number of pixels in the CXCL4L1 channel overlaid by the number of pixels in the PDI channel. Fibroblasts were cultured from osteoarthritis (OA) and long standing RA (J rep Est RA) patients who had undergone joint replacement. Moreover fibroblasts were cultured from synovial biopsies taken from patients enrolled in the BEACON cohort; early resolving synovitis (Early Res), early RA (<12 weeks symptom duration) and established RA (Est RA) (>12 weeks, <3 years symptom duration).

Finally, I studied the expression of CXCL4L1 at the mRNA level in fibroblasts taken from patients with joint replacement RA (n=5) and fibroblasts taken from individuals that had undergone synovial biopsy due to unexplained joint pain with no obvious signs of inflammation (n=5). The latter were used as controls. Fibroblasts were treated with or without TNFα for 72 hours. CXCL4L1 mRNA was expressed by untreated control fibroblasts and joint replacement RA fibroblasts (Figure 5.10). CXCL4L1 mRNA expression was significantly increased in both control fibroblasts and joint replacement RA fibroblasts following treatment with TNFα (Wilcoxon matched pairs signed rank test ***$p \leq 0.001$). No significant difference in CXCL4L1 mRNA expression was observed between TNFα treated control fibroblasts and TNFα treated joint replacement RA fibroblasts (Mann Whitney, non-significant $p=0.4194$). Moreover these was no significant difference in fold-induction of CXCL4L1 observed between the joint replacement RA fibroblasts and the control fibroblasts (Mann Whitney, $p=0.222$).

I would therefore conclude from this set of experiments that TNFα is a strong inducer of CXCL4L1 expression. This response is independent of whether the fibroblasts were derived from patients with or without inflammatory joint conditions.

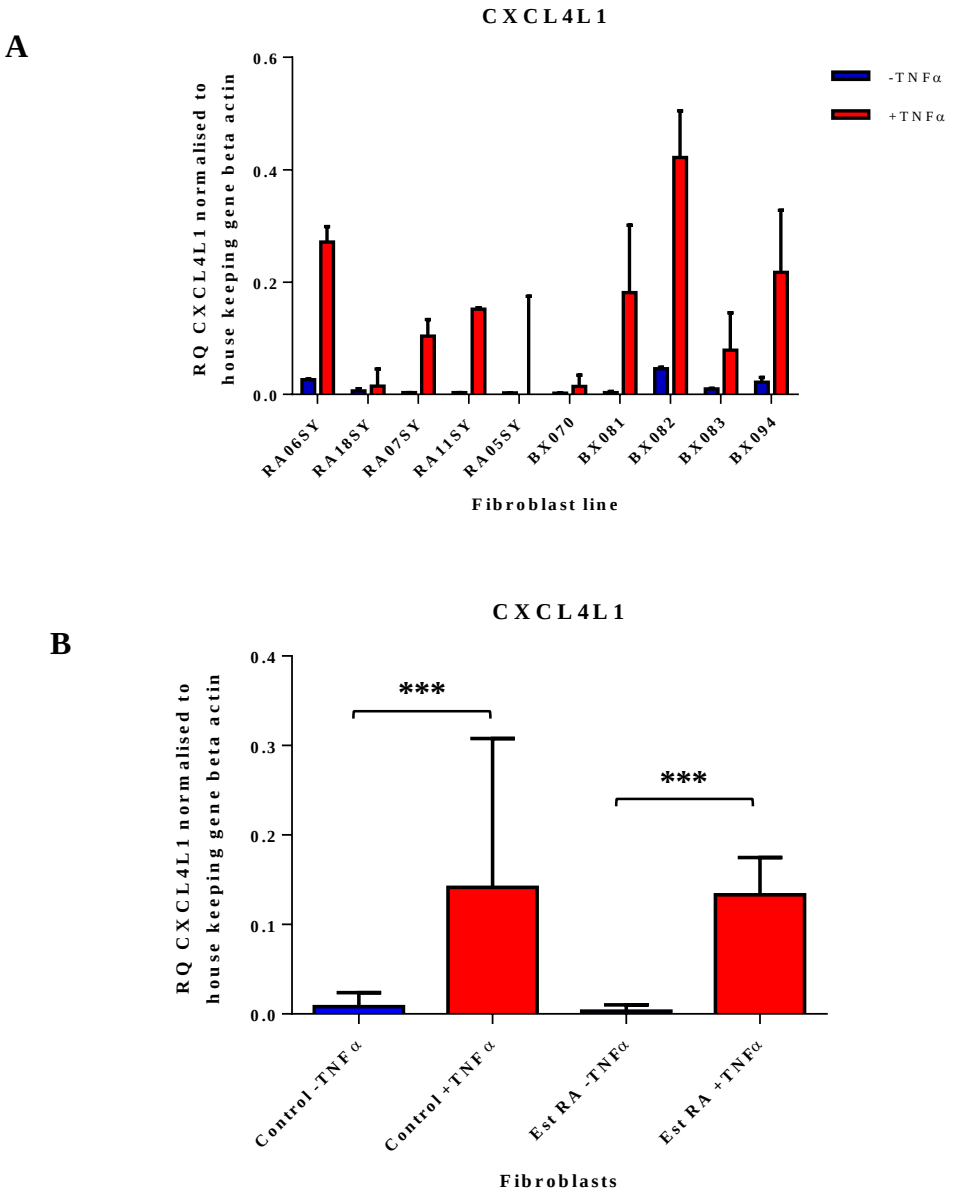

Figure 5.10 mRNA expression of CXCL4L1 in *in vitro* cultured control and RA fibroblasts treated with or without TNFα. A) 5 fibroblast cell lines from healthy controls (denoted by BX) and 5 fibroblast cell lines from patients with RA (joint replacement-established RA) (denoted by RA) were treated with or without 10 ng/ml TNFα for 72 hours. Relative quantification (RQ) of mRNA expression for CXCL4L1 was determined by normalisation to the housekeeping gene beta actin. In **B**) results shown in **A**) were grouped into healthy control fibroblasts treated with or without TNFα and RA fibroblasts (joint replacement-established RA) treated with or without TNFα. cDNA for this experiment was a kind gift from Miss Dominika Nanus. Significance was calculated in **B**) using a Wilcoxon matched pairs signed rank test (*** $p \leq 0.001$). Error bars represent the IQR.

5.3 DISCUSSION

In this chapter, I have identified the expression of CXCL4L1 at the protein level within synovial biopsies taken from patients with RA, and as far as I am aware this is the first study to do so. Although I have little information regarding the function of CXCL4L1 in RA, I can hypothesise based on pre-existing literature that it may play an important role in the regulation of both angiogenesis and lymphangiogenesis.

As mentioned previously, angiogenesis plays a pivotal role in the pathogenesis of RA. Angiogenesis within the rheumatoid synovium can exacerbate synovitis by promoting the ingress of leukocytes into the tissue and by driving pannus growth. The number of blood vessels within the rheumatoid synovium has been shown to correlate with the number of infiltrating leukocytes, synovial hyperplasia and joint tenderness. As a result, angiogenesis has been considered to be an early event that drives RA progression. Within the rheumatoid synovium, fibroblasts, lymphocytes, macrophages and mast cells have been shown to produce angiogenic factors, thus driving angiogenesis. Most notably are the synovial fibroblasts that have been shown to upregulate their expression of VEGF and FGF-1 in response to the cytokine milieu during inflammation. The formation of new blood vessels can also deliver nutrients and oxygen to the growing synovium. The synovial joint is highly hypoxic and as a result, overexpression of the transcription factors hypoxia inducible factors- 1 (HIF-1) and -2 (HIF-2) have been reported in the rheumatoid synovium. HIFs are known to upregulate VEGF release, as well as CXC chemokines, MMPs, and TNFα converting enzyme (TACE). VEGF has been reported at increased levels in synovial fluid and synovial tissue. Increased serum levels have been shown to correlate with CRP, ESR and swollen joint counts as well as being

associated with an increase in joint damage as assessed by radiological progression (Sone et al, 2001). An RA disease duration of >12 years was also associated with higher VEGF levels than controls. However, levels did not correlate with markers of disease activity.

CXCL4L1 is a potent inhibitor of angiogenesis, tumour growth and metastasis. Vandercappellen et al (2010) studied the effect of the COOH-terminal peptide of CXCL4L1 (CXCL4L1/PF-4var$^{47-70}$) and CXCL4 (CXCL4/PF-4$^{47-70}$) on monocyte and lymphocyte chemotactic activity, endothelial cell motility and proliferation, and anti-tumour and angiostatic activity. Both peptides were found to lack monocytic THP-1 cell and activated T cell chemotactic activity. A 5-fold lower dose of CXCL4L1/PF-4var$^{47-70}$ was required to inhibit endothelial cell motility and proliferation whilst angiogenesis as assessed by tube formation in Matrigel assays was also significantly reduced in CXCL4L1/PF-4var$^{47-70}$ treated assays compared to CXCL4/PF-4$^{47-70}$. Furthermore in this study, the effect of CXCL4L1/PF-4var$^{47-70}$ and CXCL4/PF-4$^{47-70}$ on B16 melanoma tumour development, growth and apoptosis was assessed. Here, nude mice were injected subcutaneously with B16 melanoma cells and subsequently treated three times per week with either 1μg CXCL4L1/PF-4var$^{47-70}$, 1μg CXCL4/PF-4$^{47-70}$, or 1μg of control buffer. In mice treated with CXCL4L1/PF-4var$^{47-70}$, tumour growth was reduced when compared to control treated mice. Upon sacrifice, tumours dissected from the CXCL4L1/PF-4var$^{47-70}$ treated mice were significantly smaller in volume and weight compared to control treated mice. A lower number of small and medium sized tumour blood vessels was also observed compared to controls. Moreover, tumour cell apoptosis was also increased in CXCL4L1/PF-4var$^{47-70}$ treated tumours. Mice treated with CXCL4/PF-4$^{47-70}$ did not show any significant differences in tumour development, final tumour volume and weight, and tumour cell apoptosis when compared to controls. Struyf et al

(2011) also reported that human adenocarcinoma cell growth was inhibited in the SCID mouse model when treated with 0.1 µg of either native CXCL4 or recombinant CXCL4L1 over an 8 week period. It was also identified that in CXCR3$^{-/-}$ animals, treatment with CXCL4L1 was no longer able to reduce tumour growth or size. More recently, Van Raemdonck et al (2014) described the angiostatic, tumour inflammatory and anti-tumour effects of CXCL4/PF-4$^{47-70}$ and CXCL4L1/PF-4var$^{47-70}$ in a human epidermal growth factor (EGF)-dependent breast cancer model. Interestingly, administration of the CXCL4/PF-4$^{47-70}$ peptide led to a better reduction in tumour growth than when CXCL4L1/PF-4var$^{47-70}$ was given.

Osteosarcoma cells stimulated with IL-1β, TNFα and IL-17A have been reported to express CXCL4L1. Positive staining for CXCL4L1 has also been observed in tissue biopsies taken from leiomyosarcoma, liposarcoma and colon adenocarcinoma patients. In the study by Verbeke et al (2010), CXCL4L1 was identified in the upper crypts of normal colon and in the tumour cells, fibroblasts, endothelial cells and inflammatory cells of colon adenocarcinoma. Furthermore, in a study by Vandercappellen et al (2007) CXCL4L1 was produced by monocytes *in vitro* in response to various inflammatory stimuli including LPS, IL-1β, Con A, PMA and thrombin. However, upon differentiation to macrophages after 5 days of culture, CXCL4L1 was not produced following stimulation. Moreover, CXCL4L1 remained undetectable in isolated neutrophils. Conversely, CXCL4 was produced by both monocytes and macrophages. Following stimulation, the levels of CXCL4 were much lower in macrophages than monocytes. Neutrophils also produced CXCL4, but at extremely low levels regardless of stimulation. In this chapter, I did not observe CXCL4L1 expression in CD68^{+} macrophages in the rheumatoid synovium.

In this chapter, I identified the expression of CXCL4L1 predominantly within the synovial lining of RA patients with established disease. This area was void of any blood vessels. Given the tumour-like characteristics of the rheumatoid synovium as it expands and invades nearby cartilage, I can speculate that CXCL4L1 attempts to counteract this tumour-like behaviour by inhibiting the growth of new blood vessel formation which provide nutrients and oxygen to the expanding synovium. Furthermore the expression of an angiostatic chemokine may be produced constitutively within the lining layer may act to prevent bleeding into the synovial joint space following mechanical pressure and friction, and maintain its barrier function. However, due to the abundance of angiogenic mediators in the synovium during disease, these may outweigh the angiostatic effects of CXCL4L1 and shift the balance towards angiogenesis which drives the exacerbation of disease. Pablos et al (2003) studied the expression of the angiogenic chemokine CXCL12 in the synovium of patients with either rheumatoid arthritis or osteoarthritis, and healthy controls. CXCL12 staining was observed in all synovial biopsies. Within the healthy synovium, CXCL12 expression was observed in a single cell layer in the lining. One the other hand, in the rheumatoid synovium, CXCL12 expression was observed in the hyperplastic lining. Positive staining was also observed in the perivascular areas of the sublining, as well as in blood vessels. Blood vessels in the healthy synovium did not express CXCL12. In a study carried out by Verbeke et al (2010), CXCL4L1 was reported to counterbalance CXCL12, as well as CXCL8 expression, in oesophageal and colorectal cancers. Moreover in this chapter, I identified synovial fibroblasts as a source of CXCL4L1 at the mRNA and protein level. In the *in vitro* cultured cells, I was unable to distinguish cells originating from lining layer from sublining derived synovial fibroblasts. The homogenous expression of CXCL4L1 in the *in* vitro cultured cells could either suggest that the lines were

only derived from lining layer fibroblasts, or more plausibly, that the restricted expression I have observed in the synovium is deregulated *in* vitro.

Prats et al (2013) studied the role of CXCL4L1 in angiogenesis, metastasis and lymphangiogenesis and identified a synergistic role for CXCL4L1 and fibstatin, an endogenous anti-angiogenic molecule derived from fibronectin, in the inhibition of tumour lymphangiogenesis and metastasis. Fibstatin, endostatin, and CXCL4L1 were able to inhibit angiogenesis and invasion of the inguinal draining lymph nodes, but were unable to prevent tumour development at the early stages. Additionally, the administration of the CXCL4L1/PF-4var$^{47-70}$ peptide or CXCL4/PF-4$^{47-70}$ peptide was reported to inhibit lymphatic endothelial cell proliferation (Van Raemdonck et al, 2014).

In conclusion, I have identified CXCL4L1, a potent angiostatic chemokine and the variant form of CXCL4, in the rheumatoid synovium. CXCL4L1 expression within the synovium was distinct from CXCL4. CXCL4L1 was identified in the synovial lining as indicated by its distinct localisation alongside VCAM-1 and its expression may explain the absence of blood vessels in the lining layer. Furthermore in this chapter, I have demonstrated that *in vitro* cultured synovial fibroblasts express CXCL4L1 mRNA and upregulate this expression upon stimulation with TNFα. Future work will be important to study the functional role of CXCL4L1 in RA and to address its therapeutic potential.

6 DISCUSSION

6.1 Early arthritis and outcome prediction

In this thesis, I took advantage of the well-established Birmingham early inflammatory arthritis cohort (BEACON) to test whether the chemokines CXCL4 and CXCL7 could be potential biomarkers to allow prediction of progression of early synovitis to RA or spontaneously resolving disease. This body of work was novel in that CXCL4 and CXCL7 had not been previously explored in early synovitis and the prediction of outcome in synovitis, largely due to the preconception that both CXCL4 and CXCL7 were considered mainly platelet derived chemokines and that platelet involvement in RA had been overlooked until fairly recently when Boilard et al (2010) studied the role of platelet microparticles in RA pathogenesis. Here, I demonstrated an increase in both CXCL4 and CXCL7 at an early stage of disease and moreover this expression was lower in patients with a resolving disease course. Furthermore, I was able to demonstrate that both chemokines were not limited to the megakaryocyte lineage as previously thought, but instead were largely expressed by macrophages.

$CD68^+$ macrophages are key drivers of disease pathogenesis in RA (Kennedy et al, 2011, Li et al, 2012). Moreover, they have been identified as a biomarker within the synovium for monitoring the early response to therapy (Bresnihan et al, 2007, Haringman et al, 2005, Wijbrandts et al, 2007). In this thesis, CXCL4 and CXCL7 expression within the synovium was found to co-localise and correlate with $CD68^+$ macrophages. Moreover at the mRNA level, isolated monocytes cultured under M1, M2 and Mo-DC culture conditions were found

to express CXCL4 and CXCL7. It will be interesting in the future to investigate whether these particular macrophages derive from circulating monocytes that leave the blood and subsequently enter the synovium, or if they are locally dividing cells that can proliferate independently of HSCs (Schulz et al, 2012, Hashimoto et al, 2013). Both CXCL4 and CXCL7 did not correlate with CD41 expression in the synovium, and furthermore co-localisation of CXCL4 and CXCL7 with CD41 was largely confined to thrombi within blood vessels. Despite the current literature identifying CXCL4 expression and production by pDCs in early scleroderma and systemic sclerosis, I rarely observed such co-localisation in our cohort (van Bon et al, 2015).

CXCL4 and CXCL7, both of which are located on chromosome 4, have a diverse array of functions. CXCL4 plays an important role in pro- and anti-coagulation, inhibition of megakaryopoiesis, inhibition of angiogenesis, tumourigenesis and metastasis, and promotion of the inflammatory response (Wang and Huang, 2013). CXCL4 can drive differentiation of monocytes towards a distinct population of macrophages, deemed the M4 population. Moreover CXCL4 can inhibit monocyte apoptosis, enhance phagocytosis, and increase production of ROS (Gleissner et al, 2010, Pervushina et al, 2004, Scheuerer et al, 2000). In T cells, CXCL4 drives the proliferation of $CD4^+$ $CD25^+$ T cells whilst inhibiting proliferation of $CD4^+$ $CD25^-$ T cells. Furthermore, CXCL4 can influence intracellular signalling pathways within T cells through the downregulation of the Th1 cytokine IFNγ and the upregulation of Th2 cytokines IL-4, IL-5 and IL-13 (Fleischer et al, 2002, Kasper and Petersen, 2011, Liu et al, 2005). Additionally, CXCL4 has been shown to trigger the release of histamine from basophils, and IL-8 from NK cells (Kasper and Petersen, 2011, Petersen et al, 1999). CXCL7 can drive neutrophil chemoattraction, adhesion and transendothelial cell migration, and

activation (Blair and Flaumenhaft, 2009, Schenk et al, 2002). In this thesis, both CXCL4 and CXCL7 were expressed within the synovium at the early stage of disease. This expression appeared to be transient, as in established disease, the expression of CXCL4 and CXCL7 was lower and was comparable to those patients with a resolving disease course. These findings have to be taken in context, as these outcome groups were made up of different individuals; no investigators as yet possess the tissue resource to examine progression of disease longitudinally within a patient cohort. I can conclude that the presence of both chemokines may act to exacerbate and drive early inflammation.

CXCL4, an ELR^- chemokine, was the first angiostatic chemokine to be identified. CXCL4 can inhibit endothelial cell proliferation and migration through interaction with FGF-2 and VEGF. In this thesis, I identified CXCL4L1, a potent inhibitor of angiogenesis, in the rheumatoid synovial lining layer. The structure of CXCL4L1 differs from CXCL4 in three amino acids within the C-terminus (Green et al, 1989). Conversely, CXCL7, an ELR^+ chemokine, is angiogenic. I may speculate that within the synovium, increased CXCL4 and CXCL4L1 production may act to counterbalance the angiogenic effects of CXCL7. Furthermore, as CXCL4L1 was largely found in the synovial lining, it may explain the lack of blood vessels observed in this region.

The diagnosis of RA regularly involves assessment of patient history, examination of the affected joints, routine laboratory tests such as the measurement of RF and ACPA, and the analysis of synovial fluid through joint aspiration. The requirement for routine synovial biopsy collection by blind needle biopsy, arthroscopy or ultrasound guided biopsy, which are

generally safe and well-tolerated procedures, are often not considered a high priority (Gerlag and Tak, 2005, Kane et al, 2002, Vordenbäumen et al, 2009). A significant number of synovial biopsies are collected within clinical practice by orthopaedic surgeons when infection is suspected. When infection is suspected, for example by *Neisseria gonorrhoeae* or *Mycobacterium tuberculosis,* a synovial biopsy can aid in the differential diagnosis. Often aspirated synovial fluid and peripheral blood samples will give rise to a negative culture, whereas the tissue itself may stain positive by stains such as Gram and Ziehl Neelsen. Alternatively, staining of the biopsy may reveal crystal deposition within the synovium thus leading to a diagnosis of gout or pseudogout. The presence of malignant cells within the synovium can also be identified and can indicate primary tumour or metastasis (Gerlag and Tak, 2005, Vordenbäumen et al, 2009).

In patients who fulfil the 1987 ARA/ACR criteria for RA, synovial biopsies may not be required. However, the prediction of disease outcome is growing increasingly important in patients presenting with early synovitis or undifferentiated arthritis. The term undifferentiated arthritis is given to those patients whose symptoms do not fulfil specific criteria. Not only is it important to identify patients who are likely to develop RA and therefore target therapies accordingly and at the earliest possible stage to reduce eventual progression to joint destruction, it is also important to identify those whose arthritis is likely to resolve as this occurs in 30-50% of patients, therefore eliminating the need for treatment with DMARDs which may result in more harm than good (Van de Helm-van Mil et al 2007). Therefore, as a result, the collection of synovial biopsies may be beneficial in these patients.

A large number of early arthritis cohorts have been established worldwide with the aim of capturing patients within the first stages of disease onset. Cohorts include the Leiden Early Arthritis cohort established in The Netherlands, the French ESPOIR cohort study, and the Canadian early arthritis cohort (CATCH). Although it is generally accepted that there is a 'window of opportunity' for the treatment of disease, there is still often a delay between patients visiting their general practitioner, being referred to a rheumatologist, and subsequently being enrolled into a cohort. Therefore the time course of what is referred to as 'early arthritis' can often differ between the different cohorts. An advantage of enrolling patients into early arthritis cohorts is that a large number of samples can be taken and stored for further analysis including serum, plasma, urine and whole blood for DNA analysis. These samples enable us to develop strategies to predict disease outcome and identify prognostic markers in RA. Van de Helm-van Mil et al (2007) utilised the Leiden early arthritis cohort, which has enrolled over a thousand patients since 1993, to develop a prediction rule for disease outcome in patients with undifferentiated arthritis. In this study a number of clinical variables including age, sex, CRP, anti-CCP status, tender joint count and swollen joint count were able to predict the development of RA in patients presenting with undifferentiated arthritis. The results presented in this thesis have the potential to become useful additions to this prediction rule, particularly if combined with other novel discriminating tissue variables. However, it may be difficult to implement immunofluorescence staining of synovial biopsies for CXCL4 and CXCL7 in clinical practice. Detection of CXCL4 and CXCL7 in the plasma would be more acceptable in clinical practice. Unfortunately, the differences identified between the patient groups at the biopsy level were not reflected in plasma.

In order to eliminate sampling error and experimental bias during the quantification of immunofluorescence, it is recommended that at least six synovial biopsies are taken from each joint to be assessed. In this thesis, sections were comprised of multiple biopsies taken from a single joint during ultrasound guided biopsy (Bresnihan et al, 2005, Gerlag and Tak, 2005). The site of biopsy did not result in significant differences in CXCL4 and CXCL7 expression. To quantify CXCL4 and CXCL7 within the joint, I selected areas of tissue at random in order to eliminate any experimental bias. Moreover, I selected these areas with the CXCL4 and CXCL7 channel turned off. Therefore I was not influenced by positive staining for CXCL4 and CXCL7 within the synovium.

6.2 Cardiovascular disease and rheumatoid arthritis

Rheumatoid arthritis patients generally have a decreased life expectancy ranging from 3 to 18 years when compared to the general population (Van Doornum, 2002). The disease, itself, not only affects joints, but can also affect multiple organ systems leading to extra-articular disease manifestations. Frequent complications arising in patients with RA include the development of rheumatoid nodules which are observed in 15-20% of patients, cardiovascular disease including atherosclerosis, pericarditis and myocarditis, respiratory disease such as pulmonary hypertension, pneumonia and bronchitis, and renal disease. Approximately 40% of patients with RA may also suffer from mental illness such as depression. Whilst in attendance at a conference, a question was raised regarding whether or not both CXCL4 and CXCL7 could be predictors of adverse cardiovascular events rather than being predictors of early disease outcome as both chemokines are released in huge abundance following the activation of platelets.

Cardiovascular disease is the leading cause of death in RA patients whereby it is accountable for 35-50% of excess mortality (Satter et al, 2003). However, although a number of risk factors associated with the development of cardiovascular disease are shared between patients with RA and the general population, such as smoking, hypertension and obesity, patients with RA develop cardiovascular disease almost a decade earlier. Therefore the disease, itself, driven by chronic inflammation or its treatment may be attributed to this earlier onset. In a retrospective study of an inception cohort of RA patients in Rochester, MN, patients were found to have a significantly increased cardiovascular disease mortality rate compared to age and sex matched controls. Treatment of patients with glucocorticoids was also reported to drive premature atherosclerosis and increase cardiovascular mortality risk.

Both CXCL4 and CXCL7, as well as platelets, have been identified in atherosclerotic lesions (Pitsilos et al, 2003). CXCL4 was evident in human atherosclerotic carotid arteries and was reported to positively correlate with increasing lesion grade and clinical severity of disease. CXCL4 was observed in macrophages of early fatty streak atherosclerotic lesions and in foam cells in more advanced lesions, whereas CXCL7 was evident in advanced lesions, only. CXCL4 was also identified in calcified regions surrounding macrophages and in the neovasculature of the atherosclerotic lesion. Moreover CXCL4 has been reported to colocalise with oxidized LDL in foam cells (Nassar et al, 2002). Pitsilos et al (2003) identified that both CXCL4 and CXCL7 were not derived from newly incorporated platelets into the lesion, but instead from platelet secretion and retention of these chemokines in the lesions. It was suggested that CXCL4 may be internalised by endothelial cells and subsequently released into the surrounding plaque upon apoptosis or that CXCL4 may bind to the surface of monocytes and migrate into the vessel wall.

Little is known about the role of CXCL7 in atherosclerosis, however CXCL4 has been studied extensively and has been reported to exacerbate disease and drive its progression. $CXCL4^{-/-}$ mice have reduced atherosclerosis and furthermore deletion of CXCL4 in $ApoE^{-/-}$ mice led to a reduction in the number of atherosclerotic lesions, thus suggesting that elimination of CXCL4 is atheroprotective (Sachais et al, 2007). CXCL4 is capable of forming heterodimers with CCL5/RANTES and as a result can trigger monocyte arrest on the endothelium. Although CXCL4 alone cannot affect monocyte arrest on endothelial cells, in cooperation with CCL5 the result is greater than the effect of CCL5 alone (Gleissner and Ley, 2007). CXCL4 can prevent apoptosis of monocytes and promote differentiation to macrophages that lack surface expression for HLA-DR. CXCL4 differentiated macrophages also fail to upregulate the atheroprotective enzyme heme oxygenase-1 at the RNA and protein level thus drive atherosclerosis (Gleissner et al, 2010). CXCL4 can trigger phagocytosis and generation of ROS and may therefore trigger the uptake of oxidized LDL by macrophages thus driving foam cell formation. Esterification of oxidized LDL by macrophages is increased by CXCL4. Furthermore, CXCL4 has been shown to interfere with the binding, internalisation and degradation of LDL by the LDL-receptor, thus increasing the opportunity for oxidization to take place. CXCL4 can bind oxidized LDL and increase its binding to vascular cells and macrophages (Nassar et al, 2002).

In this thesis, I quantified CXCL4 and CXCL7 within the plasma taken from patients enrolled in the BEACON cohort and healthy controls. I also quantified sGPVI as a marker of platelet activation in the plasma of these individuals. The high levels of CXCL4 and CXCL7 that I observed in my study may be indicative of over-active platelets in these patients. This was also indicated by the high concentrations of sGPVI observed. Although I was unable to use

the results to distinguish between those patients who developed early RA from those who had a resolving disease course, it is possible that the levels of CXCL4 and CXCL7 may be used to predict future cardiovascular events in this cohort. Tracing of morbidity and mortality in the BEACON cohort is routine, but to answer these questions will require significant time for follow-up in order to provide a meaningful analysis. It would be interesting to analyse the changes in the expression of CXCL4 and CXCL7 over time to determine whether or not they are predictors of adverse outcome in RA.

6.3 FUTURE WORK

Following on from my findings that both CXCL4 and CXCL7 are elevated in synovial biopsies at an early stage of disease, it would be important to validate these findings in an independent cohort. Moreover, a longitudinal study to monitor the expression of both chemokines throughout the disease would be an interesting area to explore, as well as their potential to predict adverse cardiovascular events in RA. However, as I used patients who were DMARD and glucocorticoid naïve at the time of biopsy, it would be somewhat unethical to deny treatment to patients over a longer period of time. Another interesting area to explore would be to evaluate CXCL4 and CXCL7 as predictive markers of therapeutic outcome. Studies have suggested thus far that increased CXCL4 expression in the serum can predict a poor response to infliximab, which is a monoclonal antibody used during the treatment of autoimmune diseases which is directed against TNFα. However as of yet, the usefulness of CXCL7 in predicting response to therapy has not been carried out. Moreover, another interesting avenue to explore would be the levels of CXCL7 in the serum of psoriatic patients. Although only described briefly in this thesis, I did observe an increase in serum CXCL7 in

psoriatic arthritis patients compared to controls and RA patients. Therefore I could study this further in a much larger psoriatic arthritis cohort in order to address the main questions; does an increase in CXCL7 correlate with the severity of psoriatic arthritis and the skin lesions observed, can we use the expression of CXCL7 to predict arthritis in those patients presenting with psoriasis, and vice versa? Previously, an increase in CXCL4 has been shown to correlate with systemic sclerosis which like psoriatic arthritis is also characterised by skin lesions. As CXCL7 exists in a number of different isoforms, it may also be interesting to determine the exact isoform expressed within the synovium.

In order to study the functional role of both CXCL4 and CXCL7 in RA, I could utilise knockout mice crossed with a model for arthritis. I could also use these mice to study the therapeutic potential of targeting CXCL4 and CXCL7 in different models of RA. Within the University of Birmingham I have access to PF4-cre mice crossed with Rosa26-Stop-EYFP. In this model, any cells that express the PF4 transcript will be reported. A study is in place to induce arthritis in these mice and monitor the % EYFP cells in different leukocyte subsets at the peak of inflammation. Moreover, induction of systemic inflammation via injection of LPS and monitoring any alteration in the % of $EYFP^+$ cells in the different leukocyte populations will be studied. This study will be carried out by Dr Guillaume Desanti, a post-doctoral researcher based at The University of Birmingham. A group at Kings College London managed by Professor Bruce Hendry and colleagues have developed CXCL7/PPBP knockout mice for the study of renal injury, however publications describing this model are lacking. If I decide to study the effect of knocking out PPBP on arthritis development, then I would need to enquire on the possibility of housing some of these mice in Birmingham. Unfortunately I would not be able to study CXCL4L1 in the same way. The gene for CXCL4L1 is expressed

in humans and primates, only. There is no mouse equivalent of the gene and animal work carried out at the university is limited to studies on mice, rats and rabbits. One potential way in which I could explore the role of CXCL4L1 would be to perform knockdown experiments of the CXCL4L1 gene using small interfering RNA (SiRNA). This would enable functional assays to be carried out to further explore the role of CXCL4L1 in angiogenesis and lymphangiogenesis. I may also have the potential to collaborate with Dr Helen McGetterick at The University of Birmingham to study the role of CXCL4L1 in angiogenesis. Here I could explore the effect on CXCL4L1 expression when fibroblasts are co-cultured with blood endothelial cells. Another interesting area to explore would be to stain tissue sections from different disease groups to study the pattern of CXCL4L1 expression.

With regards to the validation of the In Situ Hybridization method, described in chapter 4, for the detection of single CXCL7/PPBP RNA molecules, I did try multiple troubleshooting techniques in order to validate the method. However, for CXCL7, the results so far were not entirely convincing. As a result, any future plans would involve stripping the protocol back to the beginning and attempting the optimisation for the heat pre-treatment and protease digestions steps again. Moreover, as I was not entirely convinced by the GAPDH expression across the tissue sections, largely due to its absence across large areas of tissue, I may therefore opt to combine multiple house-keeping genes to prepare a more robust positive control. Moreover in chapter 4, I studied the expression of CXCL4 and CXCL7 mRNA in $CD14^{+}$ monocytes, and in vitro differentiated macrophages under M1, M2 and Mo-DC culture conditions. A further area to explore would be the different monocyte subsets, sub-grouped based on their CD16 expression and their regulation of CXCL4 and CXCL7.

7 REFERENCES

ALETAHA, D., Neogi, T., Silman, A. J., Funovits, J., Felson, D. T., Bingham, III, C. O., Birnbaum, N. S., Burmester, G. R., Bykerk, V. P., Cohen, M. D., Combe, B., Costenbader, K. H., Dougados, M., Emery, P., Ferraccioli, G., Hazes, J. M .W., Hobbs, K., Huizinga, T. W. J., Kavanaugh, A., Kay, J., Kvien, T. K., Laing, T., Mease, P., Ménard, H. A., Moreland, L. W., Naden, R. L., Pincus, T., Smolen, J. S., Stanislawska-Biernat, E., Symmons, D., Tak, P. P., Upchurch, K. S., Vencovský, J., Wolfe, F., Hawker, G (2010). 2010 Rheumatoid arthritis classification criteria: An American College of Rheumatology/European League Against Rheumatism Collaborative Initiative. *Arthritis & Rheumatism* **62**: 2569-2581.

De ALMEIDA, D. E., Ling, S., Holoshitz, J (2011). New insights into the functional role of the rheumatoid arthritis shared epitope. *FEBS Letters* **585**: 3619-3626.

AL-TAMIMI. M., Arthur, J. F., Gardiner, E. E., Andrews, R. K (2011). Focusing on plasma glycoprotein VI. *Thrombosis and Haemostasis* **107**: 648-655.

AL-TAMIMI, M., Grigoriadis, G., Tran, H., Paul, E., Servadei, P., Berndt, M. C., Gardiner, E. E., Andrews, R. K (2011). Coagulation-induced shedding of platelet glycoprotein VI mediated by factor Xa. *Blood* **117**: 3912-3920.

AL-TAMIMI, M., Mu, F. T., Moroi, M., Gardiner, E. E., Berndt, M. C., Andrews, R. K (2009). Measuring soluble platelet glycoprotein VI in human plasma by ELISA. *Platelets* **20**: 143-149.

APPENZELLER-HERZOG, C., and Ellgaard, L (2008). The human PDI family: versatility packed into a single fold. *Biochemica et Biophysica Acta* **1783**: 535-548.

ARNETT, F. C., Edworthy, S. M., Bloch, D. A., McShane, D. J., Fries, J. F., Cooper, N. S., Healey, L. A., Kaplan, S. R., Liang, M. H., Luthra, H. S., Medsger, Jr, T. A., Mitchell, D. M., Neustadt, D. H., Pinals, R. S., Schaller, J. G., Sharp, J. T., Wilder, R. L, Hunder, G. G (1988). The American Rheumatism Association 1987 revised criteria for the classification of rheumatoid arthritis. *Arthritis & Rheumatism* **31**: 315-324.

AUERBACH, D. J., Lin, Y., Miao, H., Cimbro, R., DiFiore, M J., Gianolini, M. E., Furci, L., Biswas, P., Fauci, A. S., Lusso, P (2012). Identification of the platelet-derived chemokine CXCL4/PF-4 as a broad-spectrum HIV-1 inhibitor. *Proceedings of the National Academy of Science of the United States of America* **109**: 9569-9574.

BANCHEREAU, J., Briere, F., Caux, C., Davoust, J., Lebecque, S., Liu, Y-J., Pulendran, B., Palucka, K (2000). Immunobiology of dendritic cells. *Annual Review of Immunology* **18**: 768-811.

BARTOK, B., and Firestein, G. S (2010). Fibroblast-like synoviocytes: key effector cells in rheumatoid arthritis. *Immunological Reviews* **233**: 233-255.

BAUER, S., Jendro, M. C., Wadle, A., Kleber, S., Stenner, F., Dinser, R., Reich, A., Faccin, E., Gödde, S., Dinges, H., Müller-Ladner, U., Renner, C (2006). Fibroblast activation protein is expressed by rheumatoid myofibroblast-like synoviocytes. *Arthritis Research & Therapy* **8**: 1-11.

BEGOVICH, A. B., Carlton, V. E. H., Honigberg, L. A., Schrodi, S. J, Chokkaligam, A. P., Alexander, H. C., Ardlie, K. G., Huang, Q., Smith, A. M., Spoerke, J. M., Conn, M. T., Chang, M., Chang, S-Y. P., Saiki, R. K., Catanese, J. J., Leong, D. U., Garcia, V. E., McAllister, L. B., Jeffery, D. A., Lee, A. T., Batliwalla, F., Remmers, E., Criswell, L. A., Seldin, M. F., Kastner, D. L., Amos, C. I., Sninsky, J. J., Gregersen, P. K (2004). A missense

single-nucleotide polymorphism in a gene encoding a protein tyrosine phosphatase (*PTPN22*) is associated with rheumatoid arthritis. *The American Journal of Human Genetics* **75**: 330-337.

BERLANGA, O., Emambokus, N., Frampton, J (2005). GPIIb (CD41) integrin is expressed on mast cells and influences their adhesion properties. *Experimental Hematology* **33**: 403-412.

BERGMEIER, W., and Wagner, D. D (2007). "Inflammation". In Michelson, A. D. Platelets, Burlington Academic Press, UK.

BIEHL, M., Bunte, K., Schneider, P (2013). Analysis of flow cytometry data by matrix relevance learning quantization. *PLoS ONE* **8**: e59401.

BIGALKE, B., Haap, M., Stellos, K., Geisler, T., Seizer, P., Kremmer, E., Overkamp, D., Gawaz, M (2010). Platelet glycoprotein VI (GPVI) for early identification of acute coronary syndrome in patients with chest pain. *Thrombosis Research* **125**: e184-e189.

BIOMARKERS DEFINITIONS WORKING GROUP. Biomarkers and surrogate endpoints: preferred definitions and conceptual framework. *Clinical Pharmacology and Therapeutics* **69**: 89-95.

BLAIR, P., and Flaumenhaft (2009). Platelet α-granules: Basic biology and clinical correlates. *Blood Reviews* **23**: 177-189.

BLUM, D. L., Koyama, T., M'Koma, A. E., Iturrequi, J. M., Martinez-Ferrer, M., Uwamariya, C., Smith, J. A., Clark, P. E (2008). Chemokine markers predict biochemical recurrence of prostate cancer following prostatectomy. *Clinical Cancer Research* **14**: 7790-7797.

BOILARD, E., Blanco, P., Nigrovic, P. A (2012). Platelets: active players in the pathogenesis of arthritis and SLE. *Nature Reviews Rheumatology* **8**: 534-542.

BOILARD, E., Nigrovic, P. A., Larabee, K., Watts, G. F. M., Coblyn, J. S., Weinblatt, M. E., Massarotti, E. M., Remold-O'Donnell, E., Farndale, R. W., Ware, J., Lee, D. M (2010). Platelets amplify inflammation in arthritis via collagen-dependent microparticle production. *Science* **327**: 580-583.

Van, BON, L., Affandi, A. J., Broen, J., Christmann, R. B., Marijnissen, R. J., Stawski, L., Farina, G. A., Stifano, G., Mathes, A. L., Cossu, M., York, M., Collins, C., Wenink, M., Huijbens, R., Hesselstrand, R., Saxne, T., DiMarzio, M., Wuttge, D., Agarwal, S. K., Reveille, J. D., Assassi, S., Mayes, M., Deng, Y., Drenth, J. P. H., de Graaf, J., den Heijer, M., Kallenberg, C. G. M., Bijl, M., Loof, A., van den Berg, W. B., Joosten, L. A. B., Smith, V., de Keyser, F., Scorza, R., Lunardi, C., van Riel, P. L. C. M., Vonk, M., van Heerde, W., Meller, S., Homey, B., Beretta, L., Roest, M., Trojanowska, M., Lafyatis, R., Radstake, T. R. D. J (2014). Proteome-wide analysis and CXCL4 as a biomarker in systemic sclerosis. *The New England Journal of Medicine* **370**: 433-443.

BONINI, J. A., Martin, S. K., Dralyuk, F., Roe, M. W., Philipson, L. H., Steiner, D. F (1997). Cloning, expression, and chromosomal mapping of a novel human CC-chemokine receptor (CCR10) that displays high-affinity binding for MCP-1 and MCP-3. *DNA and Cell Biology* **16**: 1249-1256.

BORRONI, E. M., Mantovani, A., Locati, M., Bonecchi, R (2010). Chemokine receptors intracellular trafficking. *Pharmacology & Therapeutics* **127**: 1-8.

BORTHWICK, N. J., Akbar, A. N., Maccormac, L. P., Lowdell, M., Craigen, J. L., Hassan, I., Grundy, J. E (1997). Selective migration of highly differentiated primed T cells, defined by

low expression of CD45RB, across human umbilical vein endothelial cells: effects of viral infection on transmigration. *Immunology* **90**: 272-280.

BOWES, J., and Barton, A (2008). Recent advances in the genetics of RA susceptibility. *Rheumatology* **47**: 399-402.

BRANDT, E., van Damme, J., Flad, H-D (1991). Neutrophils can generate their activator neutrophil-activating peptide 2 by proteolytic cleavage of platelet-derived connective tissue-activating peptide III. *Cytokine* **3**: 311-321.

BRANDT, E., Petersen, F., Ludwig, A., Ehlert, J. E., Bock, L., Flad, H-D (2000). The β-thromboglobulins and platelet factor 4: blood platelet-derived CXC chemokines with divergent roles in early neutrophil regulation. *Journal of Leukocyte Biology* **67**: 471-478.

BRESNIHAN, B., Baeten, D., Firestein, G. S., Fitzgerald, O. M., Gerlag, D. M., Haringman, J. J., McInnes, I. B., Reece, R. J., Smith, M. D., Ulfgren, A-K., Veale, D. J., Tak, P. P., OMERACT 7 special interest group (2005). Synovial tissue analysis in clinical trials. *The Journal of Rheumatology* **32**: 2481-2484.

BURMESTER, G. R., Stuhlmuller, B., Keyszer, G., Kinne, R. W (1997). Mononuclear phagocytes and rheumatoid synovitis. Mastermind or workhorse in arthritis? *Arthritis & Rheumatology* **40**: 5-18.

CAGNARD, N., Letourneur, F., Essabbani, A., Devauchelle, V., Mistou, S., Rapinat, A., Decraene, C., Fournier, C., Chiocchia, G (2005). Interleukin-32, CCL2, PF4F1 and GFD10 are the one cytokine/chemokine genes differentially expressed by in vitro cultured rheumatoid and osteoarthritis fibroblast-like synoviocytes. *European Cytokine Network* **16**: 289-292.

CALAMINUS, S. D. J., Guitart, A., Sinclair, A., Schachtner, H., Watson, S. P., Holyoake, T. L., Kranc, K. R., Machesky, L. M (2012). Lineage tracing of Pf4-Cre marks hematopoietic stem cells and their progeny. *PLoS ONE* **7**: e51361.

CARTER, R. A., Campbell, I. K., O'Donnel, K. L., Wicks, I. P (2002). Vascular cell adhesion molecule-1 (VCAM-1) blockade in collagen-induced arthritis reduces joint involvement and alters B cell trafficking. *Clinical and Experimental Immunology* **128**: 44-51.

CASSETTA, L., Cassol, E., Poli, G (2011). Macrophage polarization in health and disease. *The Scientific World Journal* **11**: 2391-2402.

CAVANAGH, L. L., Boyce, A., Smith, L., Padmanabha, J., Filgueira, L., Pietschmann, P., Thomas, R (2005). Rheumatoid arthritis synovium contains plasmacytoid dendritic cells. *Arthritis Research and Therapy* **7**: R230-R240.

CAZZOLA, M and Novelli, G (2010). Biomarkers in COPD. *Pulmonary Pharmacology and Therapeutics* **23**: 493-500.

CHA, H-S., Bae, E-K., Koh, J-H., Chai, J-Y., Jeon, C. H., Ahn, K-S., Kim, J., Koh, E-M (2007). Tumour necrosis factor-alpha induces vascular endothelial growth factor-C expression in rheumatoid synoviocytes. *The Journal of Rheumatology* **34**: 16-19.

CHAPMAN, L. M., Aggrey, A. A., Field, D. J., Srivastava, K., Ture, S., Yui, K., Topham, D. J., Baldwin II, W. M., Morrell, C. N (2012). Platelets present antigen in the context of MHC class I. *Journal of Immunology* **189**: 916-923.

CHIMEN, M., McGettrick, H. M., Apta, B., Kuravi, S. J., Yates, C. M., Kennedy, A., Odedra, A., Alassiri, M., Harrison, M., Martin, A., Barone, F., Nayar, S., Hitchcock, J. R., Cunningham, A. F., Raza, K., Filer, A., Copland, D. A., Dick, A. D., Robinson, J., Kalia, N.,

Walker, L. S. K., Buckley, C. D., Nash, G. B., Narendran, P., Rainger, G. E (2015). Homeostatic regulation of T cell trafficking by a B cell-derived peptide is impaired in autoimmune and chronic inflammatory disease. *Nature Medicine* **21**: 467-475.

CHOW, A., Brown, B. D., Merad, M (2011). Studying the mononuclear phagocyte system in the molecular age. *Nature Reviews Immunology* **11**: 788-798.

CLEMETSON, K. J., Clemetson, J. M., Proudfoot, A. E. I., Power, C. A., Baggiolini, M., Wells, T. N. C (2000). Functional expression of CCR1, CCR3, CCR4, and CXCR4 chemokine receptors on human platelets. *Blood* **96**: 4046-4054.

COGNASSE, F., Hamzeh, H., Chavarin, P., Acquart, S., Genin, C., Garraud, O (2005). Evidence of Toll-like receptor molecules on human platelets. *Immunology & Cell Biology* **83**: 196-198.

COLONNA, M., Trinchieri, G., Liu, Y. J (2004). Plasmacytoid dendritic cells in immunity. *Nature Immunology* **5**: 1219-1226.

COMERFORD, I., Milasta, S., Morrow, V., Milligan, G., Nibbs, R (2006). The chemokine receptor CCX-CKR mediates effective scavenging of CCL19 in vitro. *European Journal of Immunology* **36**: 1904-1916.

COMERFORD, I., and Nibbs, R. J (2005). Post-translational control of chemokines: a role for decoy receptors? *Immunology Letters* **96**: 163-174.

CORNEC, D., Varache, S., Morvan, J., Devauchelle-Pensec, V., Berthelot, J-M., Le Henaff-Bourhis, C., Hoang, S., Martin, A., Chalès, G., Jousse-Joulin, S., Saraux, A (2012). Comparison of ACR 1987 and ACR/EULAR 2010 criteria for predicting a 10-year diagnosis of rheumatoid arthritis. *Joint Bone Spine **79**:581-585.*

CUSH, J. J (2007). Early rheumatoid arthritis-is there a window of opportunity? *The Journal of Rheumatology* **(Suppl) 80**: 1-7.

CUTBUSH, M., Mollison, P. L., Parkin, D. M (1950). A new human blood group. *Nature* **165**: 188-189.

DEL REY, M. J., Faré, R., Izquierdo, E., Usategui, A., Rodríguez-Fernández, J. L., Suárez-Fueyo, A., Cañete, J. D, Pablos, J. L (2014). Clinicopathological correlations of podoplanin (gp38) expression in rheumatoid synovium and its potential contribution to fibroblast platelet crosstalk. *PloS One* **9**: e99607.

DEMORUELLE, M. K., and Deane, K. D (2012). Treatment strategies in early rheumatoid arthritis and prevention of rheumatoid arthritis. *Current Rheumatology Reports* **14**: 472-480.

DI STEFANO, A., Caramori, G., Gnemmi, I., Contoli, M., Bristot, L., Capelli, A., Ricciardolo, F. L. M., Magno, F., Ennio D'Anna, S., Zanini, A., Carbone, M., Sabatini, F., Usai, C., Brun, P., Chung, K. F., Barnes, P. J., Papi, A., Adcock, I. M., Balbi, B (2009). Association of increased CCL5 and CXCL7 chemokine expression with neutrophil activation in severe stable COPD. *Thorax* **64**: 968-975.

EKWALL, A-K, H., Eisler, T., Anderberg, C., Jin, C., Karlsson, N., Brisslert, M., Bokarewa, M. I (2011). The tumour-associated glycoprotein podoplanin is expressed in fibroblast-like synoviocytes of the hyperplastic synovial lining layer in rheumatoid arthritis. *Arthritis Research and Therapy* **13**: R40.

EL-GEDAILY, A., Schoedon, G., Schneemann, M., Schaffner, A (2004). Constitutive and regulated expression of platelet basic protein in human monocytes. *Journal of Leukocyte Biology* **75**: 494-503.

ELZEY, B. D., Ratliff, T. L., Sowa, J. M., Crist, S. A (2011). Platelet CD40L at the interface of adaptive immunity. *Thrombosis Research* **127**:180-183.

ERDEM, H., Pay, S., Musabak, U., Simsek, I., Dinc, A., Pekel, A., Sengul, A (2007). Synovial angiostatic non-ELR CXC chemokines in inflammatory arthritides: does CXCL4 designate chronicity of synovitis? *Rheumatology International* **27**: 969-973.

FARR, M., Scott, D. L., Constable, T. J., Hawker, R. J., Hawkins, C. F., Stuart, J (1983). Thrombocytosis of active rheumatoid disease. *Annals of the Rheumatic Diseases* **42**: 545-549.

FILER, A (2013). The fibroblast as a therapeutic target in rheumatoid arthritis. *Current Opinion in Pharmacology* **13**: 413-419.

FLEISCHER, J., Grage-Griebenow, E., Kasper, B., Heine, H., Ernst, M., Brandt, E., Flad, H-D., Petersen, F (2002). Platelet Factor 4 inhibits proliferation and cytokine release of activated human T cells. *The Journal of Immunology* **169**: 770-777.

FRIIS, T., Engel, A., Beniksen, C., Larsen, L., Houen, G (2013). Influence of levamisole and other angiogenesis inhibitors on angiogenesis and endothelial cell morphology in vitro. *Cancers* **5**: 762-785.

FUCHSBERGER, M., Hochrein, H., O'Keeffe, M (2005). Activation of plasmacytoid dendritic cells. *Immunology and Cell Biology* **83**: 571-577.

GARDINER, E. E., Karunakaran, D., Shen, Y., Arthur, J. F., Andrews, R. K., Berndt, M. C (2007). Controlled shedding of platelet glycoprotein (GP)VI and GPIb-IX-V by ADAM family metalloproteinases. *Journal of Thrombosis and Haemostasis* **5**: 1530-1537.

GARDNER, L., Wilson, C., Patterson, A. M., Bresnihan, B., FitzGerald, O., Stone, M. A., Ashton, B. A., Middleton, J (2006). Temporal expression pattern of Duffy antigen in rheumatoid arthritis: up-regulation in early disease. *Arthritis & Rheumatology* **54**: 2022-2026.

GAUCHAT, J-F., Henchoz, S., Mazzei, G., Aubry, J-P., Brunner, T., Blasey, H., Life, P., Talabot, D., Flores-Romo, L., Thompson, J., Kishi, K., Butterfield, J., Dahinden, C., Bonnefoy, J-Y (1993). Induction of human IgE synthesis in B cells by mast cells and basophils. *Letters to Nature* **365**: 340-343.

GERDES, N., Zhu, L., Ersoy, M., Hermansson, A., Hjemdahl, P., Hu, H., Hansson, G. K., Nailin, L (2011). Platelets regulate $CD4^+$ T cell differentiation via multiple chemokines in humans. *Thrombosis and Haemostasis* **106**: 353-362.

GERLAG, D. M., Hollis, S., Layton, M., Vencovsky, J., Szekanecz, Z., Braddock, M., Tak, P. P., ESCAPE study group (2010). Preclinical and clinical investigation of a CCR5 antagonist, AZD5672, in patients with rheumatoid arthritis receiving methotrexate. *Arthritis & Rheumatism* **62**: 3154-3160.

GERLAG, D., and Tak, P. P (2005). Synovial biopsy. *Best Practice & Research. Clinical Rheumatology* **19**: 387-400.

GERLAG, D. M., and Tak, P. P (2008). Novel approaches for the treatment of rheumatoid arthritis: lessons from the evaluation of synovial biomarkers in clinical trials. *Best Practice & Research Clinical Rheumatology* **22**: 311-323.

GERLAG, D. M., and Tak, P. P (2009). How to perform and analyse synovial biopsies. *Best Practice & Research Clinical Rheumatology* **23**: 221-232.

GLEISSNER, C. A., Shaked, I., Little, K. M., Ley, K (2010). CXC Chemokine Ligand 4 induces a unique transcriptome in monocyte-derived macrophages. *The Journal of Immunology* **184**: 4810-4818.

GODESSART, N., and Kunkel, S. L (2001). Chemokines in autoimmune disease. *Current Opinion in Immunology* **13**: 670-675.

GORMAN, C. L., and Cope, A. P (2008). Immune-mediated pathways in chronic inflammatory arthritis. *Best Practice & Research Clinical Rheumatology* **22**: 221-238.

GREEN, C. J., ST, Charles, R., Edwards, B. F. P., Johnson, P. H (1989). Identification and characterization of PF4var1, a human gene variant of platelet factor 4. *Molecular and Cellular Biology* **9**: 1445-1451.

GREGERSEN, P. K., Silver, J., Winchester, R. J (1987). The shared epitope hypothesis. An approach to understanding the molecular genetics of susceptibility to rheumatoid arthritis. *Arthritis & Rheumatism* **30**: 1205-1213.

GUÉRY, L., and Hugues, S (2013). Tolerogenic and activatory plasmacytoid dendritic cells in autoimmunity. *Frontiers in Immunology* **59**: 1-11.

GUO, R., Zhou, Q., Proulx, S. T., Wood, R., Ji, R-C., Ritchlin, C. T., Pytowski, B., Zhu, Z., Wang., Y-J., Schwarz, E. M., Xing, L (2009). Inhibition of lymphangiogenesis and lymphatic drainage via vascular endothelial growth factor receptor 3 blockade increases the severity of inflammation in a mouse model of chronic inflammatory arthritis. *Arthritis & Rheumatism* **60**: 2666-2676.

HAMZEH-COGNASSE, H., Cognasse, F., Palle, S., Chavarin, P., Olivier, T., Delezay, O., Pozzetto, B., Garraud, O (2008). Direct contact of platelets and their released products exert different effects on human dendritic cell maturation. *BMC Immunology* **9**: 1-15.

HAO, N-B., Lü, M-H., Fan, Y-H., Cao, Y-L., Zhang, Z-R., Yang, S-M (2012). Macrophages in tumour microenvironments and the progression of tumors. *Clinical and Developmental Immunology* 2012:948098.

HARINGMAN, J. J., Gerlag, D. M., Smeets, T. J., Baeten, D., van den Bosch, F., Bresnihan, B., Breedveld, F. C., Dinant, H. J., Legay, F., Gram, H., Loetscher, P., Schmouder, R., Woodworth, T., Tak, P. P (2006). A randomized controlled trial with an anti-CCL2 (anti-monocyte chemotactic protein 1) monoclonal antibody in patients with rheumatoid arthritis. *Arthritis & Rheumatism* **54**: 2387-2392.

HARINGMAN, J. J., Gerlag, D. M., Zwinderman, A. H., Smeets, T. J. M., Kraan, M. C., Baeten, D., McInnes, I. B., Bresnihan, B., Tak, P. P (2005). Synovial tissue macrophages: a sensitive biomarker for response to treatment in patients with rheumatoid arthritis. *Annals of the Rheumatic Diseases* **64**: 834-838.

HARRY, R. A., Anderson, A. E., Isaacs, J. D., Hilkens, C. M. U (2010). Generation and characterisation of therapeutic tolerogenic dendritic cells for rheumatoid arthritis. *Annals of the Rheumatic Diseases* **69**: 2042-2050.

HASHIMOTO, D., Chow, A., Noizat, C., Teo, P., Beasley, M. B., Leboeuf, M., Becker, C. D., See, P., Price, J., Lucas, D., Greter, M., Mortha, A., Boyer, S. W., Forsberg, E. C., Tanaka, M., van Rooijen, N., García-Sastre, A., Stanley, E. R., Ginhoux, F., Frenette, P. S., Mered, M (2013). Tissue resident macrophages self-maintain locally throughout adult life with minimal contribution from circulating monocytes. *Immunity* **38**: 792-804.

HAYWOOD, L., and Walsh, D. A (2001). Vasculature of the normal and arthritic synovial joint. *Histology and Histopathology* **16**: 277-284.

HENN, V., Slupsky, J. R., Gräfe, Anagnostopoulos, I., Förster, R., Muller-Berghaus, G., Kroczek, R. A (1998). CD40 ligand on activated platelets triggers an inflammatory reaction on endothelial cells. *Nature* **391**: 591-594.

HILKENS, C. M. U., and Isaacs, J. D (2013). Tolerogenic dendritic cell therapy for rheumatoid arthritis: where are we now? *Clinical and Experimental Immunology* **172**: 148-157.

HIROHATA, S., Yanagida, T., Nagai, T., Sawada, T., Nakamura, H., Yoshino, S., Tomita, T., Ochi, T (2001). Induction of fibroblast-like cells from $CD34^+$ progenitor cells of the bone marrow in rheumatoid arthritis. *Journal of Leukocyte Biology* **70**: 413-421.

HITCHON, C. A and El-Gabalawy, H. S (2011). The synovium in rheumatoid arthritis. *The Open Rheumatology Journal* **5 (Suppl 1)** 107-114.

HOCHREIN, H., O'Keeffe, M., Wagner, H (2002). Human and mouse plasmacytoid dendritic cells. *Human Immunology* **63**: 1103-1110.

HOEK, R. M., de Launay, D., Kop, E. N., Yilmaz-Elis, A. S., Lin, F., Reedquist, K. A., Verbeek, J. S., Medof, M. E., Tak, P. P., Hamann, J (2010). Deletion of either CD55 or CD97 ameliorates arthritis in mouse models. *Arthritis and Rheumatism* **62**: 1036-1042.

IWAMOTO, T., Okamoto, H., Toyama, Y., Momohara, S (2008). Molecular aspects of rheumatoid arthritis: chemokines in the joints of patients. *The FEBS Journal* **275**: 4448-4455.

JACKMAN, R. P., Utter, G. H., Heitman, J. W., Hirschkorn, D. F., Law, J. P., Gefter, N., Busch, M. P., Norris, P. J (2011). Effects of blood sample age at the time of separation on measured cytokine concentrations in human plasma. *Clinical and Vaccine Immunology* **18**: 318-326.

JIANG, X., Trouw, L. A., van Wesemael, T. J., Shi, J., Bengtsson, C., Kallberg, H., Malstrom, V., Israelsson, L., Hreggvidsdottir, H., Verduijn, W., Klareskog, L., Alfredsson, L., Huizinga, T. W. J., Toes, R. E. M., Lundberg, K., van der Woude, D (2013). *Annals of the Rheumatic Diseases,* published online first [8 May 2014] doi: 10.1136/annrheumdis-2013-205109.

JOHNSON, Z., Proudfoot, A. E., Handel, T. M (2005). Interaction of chemokines and glycosaminoglycans: A new twist in the regulation of chemokine function with opportunities for therapeutic intervention. *Cytokine & Growth Factor Reviews* **16**: 625-636.

JOSEPH, J. E., Harrison, P., Mackie, I. J., Isenberg, D. A., Machin, S. J (2001). Increased circulating platelet-leukocyte complexes and platelet activation in patients with antiphospholipid syndrome. Systemic lupus erythematosus and rheumatoid arthritis. *British Journal of Haematology* **115**: 451-459.

JUNG, B. K., Cho, C. H., Moon, K. C., Hur, D. S., Yoon, J-A., Yoon, S-Y (2014). Detection of platelet-monocyte aggregates by the ADAM® image cytometer. *International Journal of Medical Sciences* **11**: 1228-1233.

KAKINUMA, T., and Hwang, S. T (2006). Chemokines, chemokine receptors, and cancer metastasis. *Journal of Leukocyte Biology* **79**: 639-651.

KANE, D., Veale, D. J., FitzGerald, O., Reece, R (2002). Survey of arthroscopy performed by rheumatologists. *Rheumatology (Oxford, England)* **41**: 210-215.

KANEKO, K., Miyabe, Y., Takayasu, A., Fukuda, S., Miyabe, C., Ebisawa, M., Yokoyama, W., Watanabe, K., Imai, T., Muramoto, K., Terashima, Y., Sugihara, T., Matsushima, K., Miyasaka, N., Nanki, T (2011). Chemerin activates fibroblast-like synoviocytes in patients with rheumatoid arthritis. *Arthritis Research and Therapy* **13**: R158.

KARATOPRAK, C., Uyar, S., Abanonu, G. B., Pehlevan, S. M., Okuroglu, N., Demirtunc, R (2012). The levels of *β*-thromboglobulin in female rheumatoid arthritis patients as activation criteria. *Rheumatology International* [Epub ahead of print]:12-15.

KASPER, B., and Petersen, F (2011). Molecular pathways of platelet factor 4/CXCL4 signaling. *European Journal of Cell Biology* **90**: 521-526.

KAVOUSANAKI, M., Makrigiannakis, A., Boumpas, D., Verginis, P (2010). Novel role of plasmacytoid dendritic cells in humans. *Arthritis & Rheumatism* **62**: 53-63.

KENNEDY, A., Fearon, U., Veale, D. J., Godson, C (2011). Macrophages in synovial inflammation. *Frontiers in Immunology* **2**: 1-9.

KOBILKA, B. K (2007). G protein coupled receptor structure and activation. *Biochimica et Biophysica Acta (BBA)- Biomembranes* **1768**: 794-807.

KOH, T. J., and DiPietro, L. A (2011). Inflammation and wound healing: The role of the macrophage. *Expert Reviews in Molecular Medicine* **13**: e23 1-14.

KOKKONEN, H., Söderström, I., Rocklöv, J., Hallmans, G., Lejon, K., Dahlqvist, S. R (2010). Up-regulation of cytokines and chemokines predates the onset of rheumatoid arthritis. *Arthritis & Rheumatism* **62**: 383-391.

KRAAN, M. C., Haringman, J. J., Post, W. J., Versendaal, J., Breedveld, F. C., Tak, P.P (1999). Immunohistological analysis of synovial tissue for differential diagnosis in early arthritis. *Rheumatology* **38**: 1074-1080.

KRIJGSVELD, J., Zaat, S. A., Meeldijk, J., van Veelen, P. A., Fang, G., Poolman, B., Brandt, E., Ehlert, J .E., Kuijpers, A. J., Engbers, G. H., Feijen, J., Dankert, J (2000). Thrombocidins, microbicidal proteins from human blood platelets, are C-terminal deletion products of CXC chemokines. *The Journal of Biological Chemistry* **275**: 20374-20381.

KUAN, W. P., Tam, L-S., Wong, C-K., Ko, F., W. S., Li, T., Zhu, T., Li, E. K (2010). CXCL 9 and CXCL 10 as sensitive markers of disease activity in patients with rheumatoid arthritis. *The Journal of Rheumatology* **37**: 257-264.

Van KUIJK, A. W., Vergunst, C. E., Gerlag, D. M., Bresnihan, B., Gomez-Reino, J. J., Rouzier, R., Verschueren, P. C., van der Leij, C., Maas, M., Kraan, M. C., Tak, P. P (2010). CCR5 blockade in rheumatoid arthritis: a randomised, double-blind, placebo-controlled clinical trial. *Annals of the Rheumatic Diseases* **69**: 2013-2016.

LAGURI, C., Arenzana-Seisdedos, F., Lortat-Jacob, H (2008). Relationships between glycosaminoglycan and receptor binding sites in chemokines- the CXCL12 example. *Carbohydrate Research* **343**: 2018-2023.

LANDE, R., Giacomini, E., Serafini, B., Rosicarelli, B., Sebastiani, G. D., Minisola, G., Tarantino, U., Riccieri, V., Valesini, G., Coccia, E. M (2004). Characterization and

recruitment of plasmacytoid dendritic cells in synovial fluid and tissue of patients with chronic inflammatory arthritis. *The Journal of Immunology* **173**: 2815-2824.

LASAGNI, L., Grepin, R., Mazzinghi, B., Lazzeri, E., Meini, C., Sagrinati, C., Liotta, F., Frosali, F., Ronconi, E., Alain-Courtois, N., Ballerini, L., Netti, G. S., Maggi, E., Annuziato, F., Serio, M., Romagnani, S., Bikfalvi, A., Romagnani, P (2007). PF-4/CXCL4 and CXCL4L1 exhibit distinct subcellular localization and a differentially regulated mechanism of secretion. *Blood* **109**: 4127-4134.

LASKE, C., Leyhe, T., Stransky, E., Eschweiler, G. W., Bueltmann, A., Langer, H., Stellos, K., Gawaz, M (2008). Association of platelet-derived soluble glycoprotein VI in plasma with Alzheimer's disease. *Journal of Psychiatric Research* **42**: 746-751.

LEBRE, M. C., Vergunst, C. E., Choi, I. Y. K., Aarrass, S., Oliveira, A. S. F., Wyant, T., Horuk, R., Reedquist, K. A., Tak, P. P (2011). Why CCR2 and CCR5 blockade failed and why CCR1 blockade might still be effective in the treatment of rheumatoid arthritis. *PLoS ONE* **6**: e21772.

LEE, D. M., Kiener, H. P., Agarwal, S. K., Noss, E. H., Watts, G. F. M., Chisaka, O., Takeichi, M., Brenner, M. B (2007). Cadherin-11 in synovial lining formation and pathology in arthritis. *Science* **315**: 1006-1010.

LEE, H. S., Irigoyen, P., Kern, M., Lee, A., Batliwalla, F., Khalili, H., Wolfe, F., Lum, R. F., Massarotti, E., Weisman, M., Bombardier, C., Karlson, E. W., Criswell, L. A., Vlietinck, R., Gregersen, P. K (2007). Interaction between smoking, the shared epitope, and anti-cyclic citrullinated peptide: a mixed picture in three large North American rheumatoid arthritis cohorts. *Arthritis & Rheumatism* **56**: 1745-1753.

LEFÈVRE, S., Knedla, A., Tennie, C., Kampmann, A., Wunrau, C., Dinser, R., Korb, A., Schnäker, E., Tarner, I., Robbins, P., Evans, C., Stürz, H., Steinmeyer, J., Gay S., Schölmerich, J., Pap, T., Müller-Ladner, U., Neumann, E (2009). Synovial fibroblasts spread rheumatoid arthritis to unaffected joints. *Nature Medicine* **15**: 1414-1420.

LEI, Y., and Takahama, Y (2012). XCL1 and XCR1 in the immune system. *Microbes and Infection* **14**: 262-267.

LEY, K (2003). The role of selectins in inflammation and disease. *Trends in Molecular Medicine* **9**: 263-268.

LI, J., Hsu, H-C., Mountz, J. D (2012). Managing macrophages in rheumatoid arthritis by reform or removal. *Current Rheumatology Reports* **14**: 445-454.

LIU, C. Y., Battaglia, M., Lee, S. H., Sun, Q-H., Aster, R. H., Visentin, G. P (2005). Platelet factor 4 differentially modulates $CD4^+CD25^+$ (regulatory) versus $CD4^+$ $CD25^-$ (nonregulatory) T cells. *The Journal of Immunology* **174**: 2680-2686.

MAIA, M., de Vriese, A., Janssens, T., Moons, M., van Landuyt, K., Tavernier, J., Lories, R. J., Conway, E. M (2010). CD248 and its cytoplasmic domain: a therapeutic target for arthritis. *Arthritis & Rheumatism* **62**: 3595-3606.

MAIER, M., Geiger, E. V., Henrich, D., Bendt, C., Wutzler, S., Lehnert, M., Marzi, I (2009). Platelet Factor 4 is highly upregulated in dendritic cells after severe trauma. *Molecular Medicine* **15**: 384-391.

MAMDOUH, Z., Chen, X., Plerini, L. M., Maxfield, F. R., Muller, W. A (2003). Targeted recycling of PECAM from endothelial surface-connected compartments during diapedesis. *Nature* **421**: 748-753.

MATHAN, T. S. M., Figdor, C. G., Buschow, S. I (2013). Human plasmacytoid dendritic cells: from molecules to intercellular communication network. *Frontiers in Immunology* **4**: 1-14.

MATSUBARA, J., Honda, K., Ono, M., Tanaka, Y., Kobayashi, M., Jung, G., Yanagisawa, K., Sakuma, T., Nakamoria, S., Sata, N., Nagai, H., Ioka, T., Okusaka, T., Kosuge, T., Tsuchida, A., Shimahara, M., Yasunami, Y., Chiba, T., Hirohashi, S., Yamada, T (2011). Reduced plasma level of CXC chemokine ligand 7 in patients with pancreatic cancer. *Cancer Epidemiology Biomarkers and Prevention* **20**: 160-171.

MATSUI, T., Akahoshi, T., Namai, R., Hashimoto, A., Kurihara, Y., Rana, M., Nishimura, A., Endo, H., Kitasato, H., Kawai, S., Takagishi, K., Kondo, H (2001). Selective recruitment of CCR6- expressing cells by increased production of MIP-3α in rheumatoid arthritis. *Clnincal Experimental Immunology* **125**: 155-161.

MAYEUX, R (2004). Biomarkers: Potential uses and limitations. *NeuroRX* **1**: 182-188.

MCINNES, I. B., and Schett, G (2007). Cytokines in the pathogenesis of rheumatoid arthritis. *Nature Reviews Immunology* **7**: 429-442.

MCLELLAN, A. D., and Kämpgen, E (2000). Functions of myeloid and lymphoid dendritic cells. *Immunology Letters* **72**: 101-105.

MEUWIS, M-A., Fillet, M., Geurts, P., de Seny, D., Lutteri, L., Chapelle, J-P., Bours, V., Wehenkel, L., Belaiche, J., Malaise, M., Louis, E., Merville, M-P (2007). Biomarker discovery for inflammatory bowel disease, using proteomic serum profiling. *Biochemical Pharmacology* **73**: 1422-1433.

MILLER, L. H., Mason, S. J., Clyde, D. F., McGinniss, M. H (1976). The resistance factor to Plasmodium vivax in blacks. The Duffy-blood- group genotype, FyFy. *The New England Journal of Medicine* **295**: 302-304.

MILLER, L. H., Mason, S. J., Dvorak, J. A., McGinniss, M. H., Rothman, IK (1975). Erythrocyte receptors for (Plasmodium knowlesi) malaria: Duffy blood group determinants. *Science* **15**: 561-563.

MOROI, M., Jung, S. M., Okuma, M., Shinmyozu, K (1989). A patient with platelets deficient in glycoprotein VI that lack both collagen-induced aggregation and adhesion. *The Journal of Clinical Investigation* **84**: 1440-1445.

MOSER, B., Wolf, M., Walz, A., Loetscher, P (2004). Chemokines: multiple levels of leukocyte migration control. *Trends in Immunology* **25**: 75-84.

MOSSER, D. M (2003). The many faces of macrophage activation. *The Journal of Leukocyte Biology* **73**: 209-212.

MÜLLER-LADNER, U., Kriegsmann, J., Franklin, B. N., Matsumoto, S., Geiler, T., Gay, R. E., Gay, S (1996). Synovial fibroblasts of patients with rheumatoid arthritis attach to and invade normal human cartilage when engrafted into SCID mice. *The American Journal of Pathology* **149**: 1607-1615.

MURRAY, P. J., and Wynn, T. A (2011). Protective and pathogenic functions of macrophage subsets. *Nature Reviews Immunology* **11**: 723-737.

MYLLYHARJU, J (2003). Prolyl 4-hydroxylase, the key enzymes of collagen biosynthesis. *Matrix Biology* **22**: 15-24.

NANKI, T., Urasaki, Y., Imai, T., Nishimura, M., Muramoto, K., Kubota, T., Miyasaka, N (2004). Inhibition of Fractalkine ameliorates murine collagen-induced arthritis. *The Journal of Immunology* **173**: 7010-7016.

National Institute for Health and Clinical Excellence (2009). Rheumatoid arthritis: The management of rheumatoid arthritis in adults [online].

NEUMANN, E., Khawaja, K., Müller-Ladner, U (2014). G protein-coupled receptors in rheumatology. *Nature Reviews Rheumatology* **10**: 429-436.

NIBBS, R., Graham, G., Rot, A (2003). Chemokines on the move: control by the chemokine "interceptors" Duffy blood group antigen and D6. *Seminars in Immunology* **15**: 287-294.

NIJENHUIS, S., Zendman, A. J. W., Vossenaar, E. R., Prujin, G. J. M., vanVenrooij, W. J (2004). Autoantibodies to citrullinated proteins in rheumatoid arthritis: clinical performance and biochemical aspects of an RA-specific marker. *Clinica Chimica Acta* **350**: 17-34.

NURDEN, A. T (2011). Platelets, inflammation and tissue regeneration. *Thrombosis and Haemostasis Supplement* **105 (Suppl 1)**: S13-S33.

O'HURLEY, G., Sjöstedt, E., Rahman, A., Li, B., Kampf, C., Pontén, F., Gallagher, W. M., Lindskog, C (2014). Garbage in, garbage out: A critical evaluation of strategies used for validation of immunohistochemical biomarkers. *Molecular Oncology* **8**: 783-798.

OKADA, Y., Wu, D., Trynka, G., Raj, T., Terao, C., Ikari, K., Kochi, Y., Ohmura, K., Suzuki, A., Yoshida, S., Graham, R. R., Manoharan, A., Ortmann, W., Bhangale, T., Denny, J. C., Carroll, R. J., Eyler, A. E., Greenberg, J. D., Kremer, J. M., Pappas, D. A., Jiang, L.,

Yin, J., Ye, L., Su, D-F., Yang, J., et al (2014). Genetics of rheumatoid arthritis contributes to biology and drug discovery. *Nature* **506**: 376-381.

PAMUK, G. E., Vural, Ö., Turgat, B., Demir, M., Pamuk, Ö. N., Çakir, N (2008). Increased platelet activation markers in rheumatoid arthritis: Are they related with subclinical atherosclerosis? *Platelets* **19**: 146-154.

PAP, T., Müller-Ladner, U., Gay, R. E., Gay, S (2000). Fibroblast biology: Role of synovial fibroblasts in the pathogenesis of rheumatoid arthritis. *Arthritis Research* **2**: 361-367.

PAPLOS, J. L., Santiago, B., Galindo, M., Torres, C., Brehmer, M. T., Blanco, F. J., Garcia-Lazaro, F. J (2003). Synoviocyte-derived CXCL12 is displayed on endothelium and induces angiogenesis in rheumatoid arthritis. *The Journal of Immunology* **170**: 2147-2152.

PARK, B., Lee, S., Kim, E., Cho, K., Riddell, S. R., Cho, S., Ahn, K (2006). Redox regulation facilitates optimal peptide selection by MHC class I during antigen processing. *Cell* **127**: 369-382.

PATTERSON, A. M., Siddall, H., Chamberlain, G., Gardner, L., Middleton, J (2002). Expression of the duffy antigen/receptor for chemokines (DARC) by the inflamed synovial endothelium. *The Journal of Pathology* **197**: 108-116.

PEASE, J. E., and Williams, T. J (2006). The attraction of chemokines as a target for specific anti-inflammatory therapy. *British Journal of Pharmacology* **147**: S212-S221.

PERTUY, F., Aguilar, A., Strassel, C., Eckly, A., Freund, J. N., Duluc, I., Gachet, C., Lanza, F., Léon, C (2015). Broader expression of the mouse platelet factor 4-cre transgene beyond the megakaryocyte lineage. *Journal of Thrombosis and Haemostasis* **13**: 115-125.

PERVUSHINA, O., Scheuerer, B., Reiling, N., Behnke, L., Schröder, J-M., Kasper, B., Brandt, E., Bulfone-Pas, S., Petersen, F (2004). Platelet Factor 4/CXCL4 induces phagocytosis and the generation of reactive oxygen metabolites in mononuclear phagocytes independently of Gi protein activation or intracellular calcium transients. *The Journal of Immunology* **173**: 2060-2067.

PETERSEN, F., Bock, L., Flad, H-D., Brandt (1999). Platelet factor 4-induced neutrophil-endothelial cell interaction: Involvement of mechanisms and functional consequences different from those elicited by interleukin-8. *Blood* **94**: 4020-4028.

PIQUERAS, B., Connolly, J., Freitas, H., Palucka, A. K., Banchereau, J (2006). Upon viral exposure, myeloid and plasmacytoid dendritic cells produce 3 waves of distinct chemokines to recruit immune effectors. *Blood* **107**: 2613-2618.

PLOW, E. F., Haas, T. A., Zhang, L., Loftus, J., Smith, J. W (2000). Ligand binding to integrins. *The Journal of Biological Chemistry* **275**: 21785-21788.

POLZER, K., Baeten, D., Soleiman, A., Distler, J., Gerlag, D. M., Tak, P. P., Schett, G., Zwerina, J (2008). Tumour necrosis factor blockade increases lymphangiogenesis in murine and human arthritic joints. *Annals of the Rheumatic Diseases* **67**: 1610-1616.

PORUK, K., E., Firpo, M. A., Huerter, L. M., Scaife, C. L., Emerson, L. L., Boucher, K. M., Jones, K. A., Mulvihill, S. J (2011). Serum platelets factor 4 is an independent predictor of survival and venous thromboembolism in patients with pancreatic adenocarcinoma. *Cancer Epidemiology, Biomarkers and Prevention* **19**: 2605-2610.

PRATESI, F., Teixeira, E. P., Sidney, J., Michou, L., Puxeddu, I., Sette, A., Cornelis, F., Migliorini, P (2013). HLA shared epitope and ACPA: Just a marker or an active player? *Autoimmunity Reviews* **12**: 1182-1187.

PRATS, A. C., van den Berghe, L., Rayssac, A., Ainaoui, N., Morfoisse, F., Pujol, F., Legonidec, S., Bikfalvi, A., Prats, H., Pyronnet, S., Garmy-Susini, B (2013). CXCL4L1-fibstatin cooperation inhibits tumor angiogenesis, lymphangiogenesis and metastasis. *Microvascular Research* **89**: 25-33.

RADSTAKE, T, R. D. J, Methods for the treatment or prevention of systemic sclerosis, United States patent application 0034234 A1, 2012.

Van RAEMDONCK, K., Berghmans, N., Vanheule, V., Bugatti, A., Proost, P., Opdenakker, G., Presta, M., van Damme, J., Struyf, S (2014). Angiostatic, tumor inflammatory and anti-tumor effects of CXCL4L47-70 and CXCL4L147-70 in an EFG-dependent breast cancer model. *Oncotarget* **5**: 10916-10933.

RAMAN, D., Sobolik-Delmaire, T., Richmond, A (2011). Chemokines in health and disease. *Experimental Cell Research* **317**: 575-589.

REICHARD, K. K., Hall, B. K., Corn, A., Foucar, M. K., Hozier, J (2006). Automated analysis of fluorescence in situ hybridization on fixed, paraffin-embedded whole tissue sections in B-cell lymphoma. *Modern Pathology* **19**: 1027-1033.

REIZIS, B., Bunin, A., Ghosh, H. S., Lewis, K. L., Sisirak, V (2011). Plasmacytoid dendritic cells: Recent progress and open questions. *Annual Review of Immunology* **29**: 163-183.

RENSHAW, B. R., Fanslow, W. C. 3rd., Armitage, R. J., Campbell, K. A., Liggitt, D., Wright, B., Davison, B. L., Maliszewski, C. R (1994). Humoral immune responses in CD40 ligand-deficient mice. *The Journal of Experimental Medicine* **180**: 1889-1900.

REPARON-SCHUIJT, C. C., van Esch, W. J., van Kooten, C., Rozier, B. C., Levarht, E. W., Breedveld, F. C., Verweij, C. L (2000). Regulation of synovial B cell survival in rheumatoid arthritis by vascular cell adhesion molecule 1 (CD106) expressed on fibroblast-like synoviocytes. *Arthritis & Rheumatism* **43**: 1115-1121.

RICHEZ, C., Schaeverbeke, T., Dumoulin, C., Dehais, J., Moreau, J-F., Blanco, P (2008). Myeloid dendritic cells correlate with clinical response whereas plasmacytoid dendritic cells impact autoantibody development in rheumatoid arthritis patients treated with infliximab. *Arthritis Research and Therapy* **11**: R100.

RIFAI, N., Gillette, M. A., Carr, S. A (2006). Protein biomarker discovery and validation: the long and uncertain path to clinical utility. *Nature Biotechnology* **24**: 971-983.

ROSEN, S. D., and Bertozzi, C. R (1994). The selectins and their ligands. *Current Opinion in Cell Biology* **6**: 663-673.

ROT, A (2005). Contribution of Duffy antigen to chemokine function. *Cytokine & Growth Factor Reviews* **16**: 687-694.

ROT, A., and von Andrian, U. H (2004). Chemokines in innate and adaptive host defense: Basic chemokinese grammar for immune cells. *Annual Review of Immunology* **22**: 891-928.

ROVIN, B. H., Song, H., Birmingham, D. J., Hebert, L.A., Yung Yu, C., Nagaraja, H. N (2005). Urine chemokines as biomarkers of human systemic lupus erythematosus activity. *Journal of the American Society of Nephrology* **16**: 467-473.

SAALBACH, A., Wetzig, T., Haustein, U. F., Anderegg, U (1999). Detection of human soluble Thy-1 in serum by ELISA. *Cell and Tissue Research* **298**: 307-315.

SALMON, M., Scheel-Toellner, D., Huissoon, A. P., Pilling, D., Shamsadeen, N., Hyde, H., D'Angeac, A. D., Bacon, P. A., Emery, P., Akbar, A. N (1997). Inhibition of T cell apoptosis in the rheumatoid synovium. *Journal of Clinical Investigation* **99**: 439-446.

SCHAFFNER, A., Rhyn, P., Schoedon, G, Schaer, D. J (2005). Regulated expression of platelet factor 4 in human monocytes-role of PARs as a quantitatively important monocyte activation pathway. *Journal of Leukocyte Biology* **78**: 202-209.

SCHENK, B. I., Petersen, F., Flad, H-D., Brandt, E (2002). Platelet derived chemokines CXC chemokine ligand (CXCL) 7, connective tissue-activating peptide III, and CXCL4 differentially affect and cross-regulate neutrophil adhesion and transendothelial migration. *The Journal of Immunology* **169**: 2602-2610.

SCHEUERER, B., Ernst, M., Dürrbaum-Landmann, I., Fleischer, J., Grage-Griebenow, E., Brandt, E., Flad, H-D., Petersen, F (2000). The CXC-chemokine platelet factor 4 promotes monocyte survival and induces monocyte differentiation into macrophages. *Blood* **95**: 1158-1166.

SCHMIDT, S., Moser, M., Sperandio, M (2013). The molecular basis of leukocyte recruitment and its deficiencies. *Molecular Immunology* **55**: 49-58.

SCHROHL, A-S., Würtz, S., Kohn, E., Banks, R. E., Nielsen, H. J., Sweep, F. C. G. J., Brünner, N (2008). Banking of biological fluids for studies of disease-associated protein biomarkers. *Molecular & Cellular Proteomics* **7**: 2061-2066.

SCHULZ, C., Gomez Perdiguero, E., Chorro, L., Szabo-Rogers, H., Cagnard, N., Kierdorf, K., Prinz, M., Wu, B., Jacobsen, S. E., Pollard, J. W., Frampton, J., Liu, K. J., Geissmann, F (2012). A lineage of myeloid cells independent of Myb and hematopoietic stem cells. *Science* **336**: 86-90.

SEMPLE, J. W., Italiano Jr, J. E., Freedman, J (2011). Platelets and the immune continuum. *Nature Reviews Immunology* **11**: 264-274.

SHI, J., van de Stadt, L. A., Levarht, E. W. N., Huizinga, T. W. J., Hamann, D., van Schaardenburg, D., Toes, R. E. M., Trouw, L. A (2013). Anti-carbamylated protein (anti-CarP) antibodies precede the onset of rheumatoid arthritis. *Annals of the Rheumatic Diseases,* published online first [13 December 2013] doi: 10.1136/annrheumdis-2013-204154.

SILMAN, A. J., and Pearson, J. E (2002). Epidemiology and genetics of rheumatoid arthritis. *Arthritis Research* **4 (Suppl 3)**: S265-S272.

SMITH, E., McGettrick, H. M., Stone, M. A., Shaw, J. S., Middleton, J., Nash, G. B., Buckley, C. D., Rainger, G. E (2008). Duffy antigen receptor for chemokines (DARC) and CXCL5 are essential for the recruitment of neutrophils in a multi-cellular model of the RA synovium. *Arthritis & Rheumatology* **58**: 1968-1973.

SMITH, N. L. D., Bromley, M. J., Denning, D. W., Simpson, A., Bowyer, P (2015). Elevated levels of the neutrophil chemoattractant pro-platelet basic protein in macrophages from individuals with chronic and allergic aspergillosis. *The Journal of Infectious Diseases* **211**: 651-660.

SONE, H., Kawakami, Y., Sakauchi, M., Nakamura, Y., Takahashi, A., Shimano, H., Okuda, Y., Segawa, T., Suzuki, H., Yamada, N (2001). Neutralization of vascular endothelial growth

factor prevents collagen-induced arthritis and ameliorates established disease in mice. *Biochemical and Biophysical Research Communications* **281**: 562-568.

SPLAWSKI, J. B., Fu, S. M., Lipsky, P. E (1993). Immunoregulatory role of CD40 in human B cell differentiation. *Journal of Immunology* **150**: 1276-1285.

SPRINGER, T. A (1994). Traffic signals for lymphocyte recirculation and leukocyte emigration: The multistep paradigm. *Cell* **76**: 301-314.

STEINMAN, R. M., Nussenzweig, M. C (2002). Avoiding horror autotoxicus: the importance of dendritic cells in peripheral T cell tolerance. *Proceedings of the National Academy of Science of the United States of America* **99**: 351-358.

STÖGER, J. L., Gijbels, M. J., van der Velden, S., Manca, M., van der Loos, C. M., Biessen, E. A., Daemen, M. J., Lutgens, E., de Winther, M. P (2012). Distribution of macrophage polarization markers in human atherosclerosis. *Atherosclerosis* **225**: 461-468.

STRAND, V., Kimberly, R., Isaacs, J. D (2007). Biologic therapies in rheumatology: lessons learned, future directions. *Nature Reviews Drug Discovery*. **6**: 75-92.

STRUYF, S., Salogni, L., Burdick, M. D., Vandercappellen, J., Gouwy, M., Noppen, S., Proost, P., Opdenakker, G., Parmentier, M., Gerard, C., Sozzani, S., Strieter, R. M., van Damme, J (2011). Angiostatic and chemotactic activities of the CXC chemokine CXCL4L1 (platelet factor-4 variant) are mediated by CXCR3. *Blood* **117**: 480-488.

SULLIVAN, D. P., Seidman, M. A., Muller, W. A (2013). Poliovirus receptor (CD155) regulates a step in transendothelial migration between PECAM and CD99. *The American Journal of Pathology* **182**: 1031-1042.

SWIECKI, M., and Colonna, M (2010). Unraveling the functions of plasmacytoid dendritic cells during viral infections, autoimmunity and tolerance. *Immunological Reviews* **234**: 142-162.

SZEKANECZ, Z., Kim, J., Koch, A. E (2003). Chemokines and chemokine receptors in rheumatoid arthritis. *Seminars in Immunology* **15**: 15-21.

SZEKANECZ, Z., and Koch, A. E (2001). Chemokines and angiogenesis. *Current Opinion in Rheumatology* **13**: 202-208.

SZEKANECZ, Z., and Koch, A. E (2007). Macrophages and their products in rheumatoid arthritis. *Current Opinion in Rheumatology* **19**: 289-295.

TAK, P. P., Thurkow, E. W., Daha, M. R., Kluin, P. M., Smeets, T. J. M., Meinders, A. E., Breedveld, F. C (1995). Expression of adhesion molecules in early rheumatoid synovial tissue. *Clinical Immunology and Immunopathology* **77**: 236-242.

TAKAKUBO, Y., Takagi, M., Maeda, K., Tamaki, Y., Sasaki, A., Asano, T., Fukushima, S., Kiyoshige, Y., Orui, H., Ogino, T., Yamakawa, M (2008). Distribution of myeloid dendritic cells and plasmacytoid dendritic cells in the synovial tissues of rheumatoid arthritis. *The Journal of Rheumatology* **35**: 1919-1931.

TANG, F., Du, Q., Liu, Y-J (2010). Plasmacytoid dendritic cells in antiviral immunity and autoimmunity. *Science China Life Sciences* **53**: 172-182.

TARRANT, T. K., and Patel, D. D (2006). Chemokines and leukocyte trafficking in rheumatoid arthritis. *Pathophysiology* **13**: 1-14.

TESCH, G., Amur, S., Schousboe, J. T., Siegel, J. N., Lesko, L. J., Bai, J. P. F (2010). Successes achieved and challenges ahead in translating biomarkers into clinical applications. *The AAPS Journal* **12**: 243-253.

THOMAS, R., Street, S., Ramnoruth, N., Pahau, H., Law, S., Brunck, M., Hyde, C., O'Sullivan, B., Capini, C., Tran, A., Ng, J., Paul, S (2011). [LB0004] Safety and preliminary evidence of efficacy in a phase I clinical trial of autologous tolerising dendritic cells exposed to citrullinated peptides (Rheumavax) in patients with rheumatoid arthritis. *Annals of the Rheumatic Diseases* **70 (Suppl3)**: 169.

TROCMÉ, C., Marotte, H., Baillet, A., Pallot-Prades, B., Garin, J., Grange, L., Miossec, P., Tebib, J., Berger, F., Nissen, M. J., Juvin, R., Morel, F., Gaudin, P (2009). Apolipoprotein A-I and platelets factor 4 are biomarkers for infliximab response in rheumatoid arthritis. *Annals of the Rheumatic Diseases* **68**: 1328-1333.

VÄÄNÄNEN, H. K., Zhao, H., Mulari, M., Halleen, J. M (2000). The cell biology of osteoclast function. *Journal of Cell Science* **113**: 377-381.

VANDERCAPPELLEN, J., Leikens, S., Bronckaers, A., Noppen, S., Ronsse, I., Dillen, C., Belleri, M., Mitola, S., Proost, P., Presta, M., Struyf, S., van Damme, J (2010). The COOH-terminal peptide of platelet factor-4 variant (CXCL4L1/PF-4var$^{47-70}$) strongly inhibits angiogenesis and suppresses B16 melanoma growth in vivo. *Molecular Cancer Research* **8**: 322-334.

VANDERCAPPELLEN, J., Noppen, S., Verbeke, H., Put, W., Conings, R., Gouwy, M., Schutyser, E., Proost, P., Sciot, R., Geboes, K., Opdenakker, G., van Damme, J., Struyf (2007). Stimulation of angiostatic platelet factor-4 variant (CXCL4L1/PF-4var) versus

inhibition of angiogenic granulocyte chemotactic protein-2 (CXCL6/GCP-2) in normal and tumoral mesenchymal cells. *Journal of Leukocyte Biology* **82**: 1519-1530.

VERBEKE, H., De Hertogh, G., Li, S., Vandercappellen, J., Noppen, S., Schutyser, E., El-Asrar, A. A., Opdenakker, G., Van Damme, J., Geboes, K., Struyf, S (2010). Expression of angiostatic platelet factor-4var/CXCL4L1 counterbalances angiogenic impulses of vascular endothelial growth factor, interleukin-8/CXCL8, and stromal cell-derived factor 1/CXCL12 in esophageal and colorectal cancer. *Human Pathology* **41**: 990-1001.

VERGUNST, C. E., Gerlag, D. M., Lopatinskaya, L., Klareskog, L., Smith, M. D., van den Bosch, F., Dinant, H. J., Lee, Y., Wyant, T., Jacobson, E. W., Baeten, D., Tak, P. P (2008). Modulation of CCR2 in rheumatoid arthritis: a double-blind, randomized, placebo-controlled clinical trial. *Arthritis & Rheumatism* **58**: 1931-1939.

VERGUNST, C. E., van de Sande, M. G. H., Lebre, M. C., Tak, P. P (2005). The role of chemokines in rheumatoid arthritis and osteoarthritis. *Scandinavian Journal of Rheumatology* **34**: 415-425.

VIEIRA-DE-ABREU, A., Campbell, R. A., Weyrich, A. S., Zimmerman, G. A (2012). Platelets: versatile effector cells in hemostasis, inflammation, and the immune continuum. *Seminars in Immunopathology* **34**: 5-30.

VORDENBÄUMEN, S., Joosten, L. A. B., Friemann, J., Schneider, M., Ostendorf, B (2009). Utility of synovial biopsy. *Arthritis Research & Therapy* **11**: 256.

WALLACE, G. R., Curnow, S.J., Wloka, K., Salmon, M., Murray, P. I (2004). The role of chemokines and their receptors in ocular disease. *Progress in Retinal and Eye Research* **23**: 435-448.

WANG, Z., and Huang, H (2013). Platelet factor 4 (CXCL4/PF-4): an angiostatic chemokine for cancer therapy. *Cancer Letters* **331**: 147-153.

WIJEYEWICKREMA, L. C., Gardiner, E. E., Moroi, M., Berndt, M. C., Andrews, R. K (2007). Snake venom metalloproteinases, crotarhagin and alborhagin, induce ectodomain shedding of the platelet collagen receptor, glycoprotein VI. *Thrombosis and Haemostasis* **98**: 1285-1290.

WILKINSON, B., and Gilbert, H. F (2004). Protein disulfide isomerase. *Biochemica et Biophysica Acta* **1699**: 35-44.

WOOLEY, P. H., Schaefer, C., Whalen, J. D., Dutcher, J. A., Counts, D. F (1997). A peptide sequence from platelet factor 4 (CT-112) is effective in the treatment of type II collagen induced arthritis in mice. *Journal of Rheumatology* **24**: 890-898.

WOOLLEY, D. E., and Tetlow, L. C (2000). Mast cell activation and its relation to proinflammatory cytokine production in the rheumatoid lesion. *Arthritis Research* **2:** 65-74.

WURSTER, T., Poetz, O., Stellos, K., Kremmer, E., Melms, A., Schuster, A., Nagel, E., Joos, T., Gawaz, M., Bigalke, B (2013). Plasma levels of soluble glycoprotein VI (sGPVI) are associated with ischemic stroke. *Platelets* **24**: 560-565.

YANG, J., Zhang, L., Yu, C., Yang, X-F., Wang, H (2014). Monocyte and macrophage differentiation: circulation inflammatory monocyte as biomarker for inflammatory disease. *Biomarker Research* **2**:1.

YEE, J., Sadar, M. D., Sin, D. D., Kuzyk, M., Xing, L., Kondra, J., McWilliams, A., Man, S. F. P., Lam, S (2009). Connective Tissue-Activating Peptide III: A novel blood biomarker for early lung cancer detection. *Journal of Clinical Oncology* **27**: 2787-2792.

YEO, L (2011). Characterisation of cytokine expression in early synovitis and established rheumatoid arthritis. PhD thesis, University of Birmingham.

ZARBOCK, A., Polanowska-Grabowska, R. K., Ley, K (2007). Platelet-neutrophil-interactions: Linking hemostasis and inflammation. *Blood Reviews* **21**: 99-111.

ZHOU, D., Huang, C., Lin, Z., Zhan, S., Kong, L., Fang, C., Li, J (2014). Macrophage polarization and function with emphasis on the evolving roles of coordinated regulation of cellular signalling pathways. *Cellular Signalling* **26**: 192-197.

ZHU, L., Huang, Z., Stålesen, R., Hansson, G. K., Li, N (2014). Platelets provoke distinct dynamics of immune responses by differentially regulating $CD4^+$ T-cell proliferation. *Journal of Thrombosis and Haemostasis* **12**: 1156-1165.

ZIMMERMAN, G. A., and Weyrich, A. S (2010). Arsonists in rheumatoid arthritis. *Science* **327**: 528-529.

8 APPENDIX

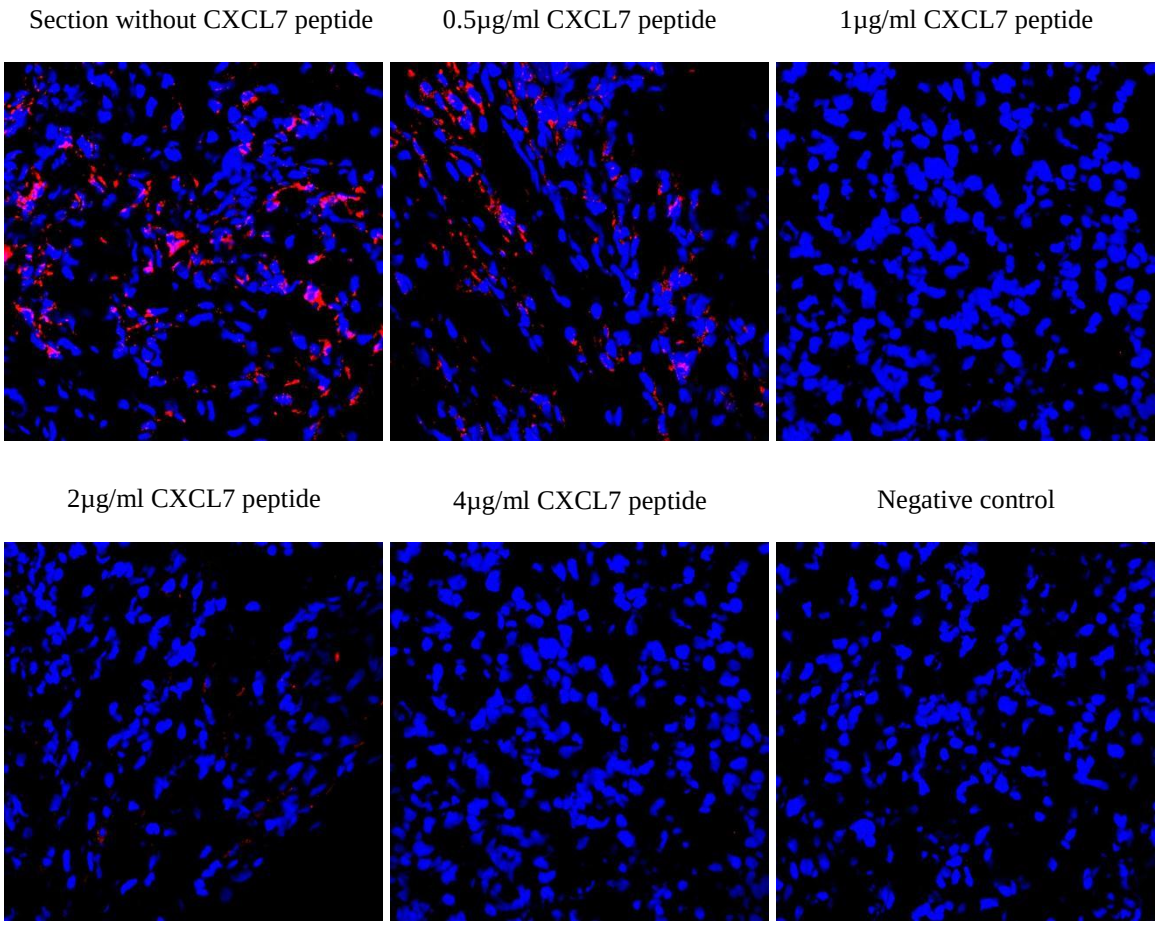

Figure 8.1 Validation of the CXCL7 antibody for immunofluorescence. CXCL7 antibody was incubated overnight with increasing concentrations of CXCL7 peptide. The CXCL7-peptide complex was used to stain a section of rheumatoid synovium taken from a patient undergoing joint replacement. The CXCL7 chemokine was successfully inhibited when incubated with the CXCL7 peptide. Nuclei were counterstained with Hoechst 33258 (blue). Images were taken at x400 total magnification using the Zeiss LSM 510-UV confocal.

Biopsy code	Age	Sex	Joint	Disease duration (weeks)	Diagnosis	RF	CCP
H03.8	70	F	Knee	1820	RA	P	NA
H03.10	78	M	Hip	1040	RA	NA	NA
H03.11	57	M	Knee	936	RA	NA	NA
H03.12	69	F	Knee	2288	RA	N	N
H04.5	72	F	Hip	1040	RA	NA	NA
H04.10	77	M	Knee	1144	RA	P	NA
H04.12	48	F	Knee	780	RA	N	N
H04.17	57	F	Knee	260	RA	NA	NA
H04.18	61	F	Hip	832	RA	N	N
H07.2	74	F	Elbow	1040	RA	N	N
H07.6	NA	NA	NA	NA	RA	NA	NA
H13.03	71	M	Elbow	780	RA	P	P
H13.12	68	M	MCP	21	RA	p	P

Table 8.1 Patient clinical information collected from those with longstanding disease who had undergone joint replacement surgery. Synovial biopsies were used widely throughout chapter 3 and chapter 5. Abbreviations used throughout the tables; CCP, Cyclic Citrullinated Peptide; RF, Rheumatoid Factor; N, Negative; P, Positive; and NA, Not Available.

Outcome	Age	Sex	Biopsied joint	Symptom duration (weeks)	CCP	RF	ESR	CRP	Global	SWJ28	TJC28	DAS28 baseline
Early RA	50	M	Knee	4	P	P	31	26	28	11	13	5.70
Early RA	70	F	Knee	5	N	N	68	26	96	5	4	6.04
Early RA	48	F	Knee	2	N	N	4	102	16	6	8	3.46
Early RA	59	M	Knee	6	N	N	14	22	54	20	4	4.98
Early RA	74	F	Knee	9	P	N	20	32	62	3	3	4.42
Early RA	51	M	Knee	8	P	P	61	97	75	NA	NA	6.67
Early RA	63	M	Knee	8	N	N	2	0	70	NA	NA	2.31
Early RA	60	F	Ankle	11	P	P	32	45	46	NA	NA	4.32
Early RA	44	F	Ankle	5	N	N	18	10	32	2	3	3.84
Early RA	56	M	MCP	10	N	P	5	0	50	21	14	5.21
Established RA	46	M	Knee	150	P	P	34	7	75	16	13	6.66
Established RA	69	F	Knee	52	N	N	11	0	52	7	7	4.63
Established RA	57	M	Knee	14	P	P	56	16	50	14	21	7.13
Established RA	58	M	Knee	16	P	P	7	0	33	7	7	4.05
Established RA	63	F	Knee	26	P	P	35	0	60	NA	NA	5.19
Established RA	72	M	Knee	38	N	N	53	43	70	16	21	7.45
Established RA	65	F	Knee	156	P	P	72	81	28	12	3	5.33

Outcome	Age	Sex	Biopsied joint	Symptom duration (weeks)	CCP	RF	ESR	CRP	Global	SWJ28	TJC28	DAS28 baseline
Established RA	22	F	Knee	52	N	N	81	79	89	6	6	6.38
Established RA	62	F	Ankle	16	P	P	40	5	16	2	4	4.32
Established RA	65	M	Ankle	53	N	N	50	10	29	NA	NA	4.95
Established RA	60	F	Ankle	45	N	P	70	112	6	NA	NA	5.20
Early Resolving	32	M	Knee	7	N	N	10	10	35	1	1	2.94
Early Resolving	33	M	Knee	4	N	N	51	14	83	9	12	6.69
Early Resolving	74	M	Knee	5	N	N	45	13	55	23	0	4.78
Early Resolving	37	F	Knee	7	N	N	7	0	NA	2	8	3.34
Early Resolving	28	M	Knee	6	N	N	18	8	99	1	2	4.48
Early Resolving	45	F	Knee	1	N	N	4	0	83	5	5	4.01
Early Resolving	35	M	Knee	2	N	N	51	7	33	1	1	4.05
Early Resolving	81	F	Ankle	7	N	N	60	52	50	11	16	6.73
Early Resolving	55	M	Ankle	6	N	N	2	6	91	5	4	3.51
Early non-RA	69	M	Knee	7	N	N	44	38	85	NA	NA	5.58
Early non-RA	41	M	Knee	2	N	N	50	25	50	4	2	4.79
Early non-RA	43	F	Knee	2	P	N	97	70	86	10	11	7.15
Early non-RA	39	F	Ankle	8	N	N	27	15	83	NA	NA	4.72
Early non-RA	34	M	Ankle	9	N	N	21	22	40	NA	NA	3.53

Outcome	Age	Sex	Biopsied joint	CCP	RF
Normal	49	F	Knee	N	N
Normal	42	M	Knee	N	N
Normal	38	F	Knee	N	N
Normal	16	M	Knee	N	N
Normal	41	F	Knee	N	N
Normal	41	F	Knee	N	N
Normal	42	M	Knee	N	N
Normal	23	M	Knee	N	N
Normal	44	M	Knee	N	N

Table 8.2 Patient clinical information from those used during the study of the expression of CXCL4 and CXCL7 in tissue biopsies.
*Abbreviations used throughout the tables; CCP, Cyclic Citrullinated Peptide; RF, Rheumatoid Factor; ESR, Erythrocyte Sedimentation Rate; CRP, C-Reactive Protein; Global, Global Arthritis Score; SWJ28, Swollen Joint Count of 28 joints; TJC28, Tender Joint Count of 28 joints; DAS28 baseline, Disease Activity Score of 28 joints baseline; N, Negative; P, Positive; F, Female; M, Male; and NA, Not Available.

Diagnosis	Symptom duration (weeks)	CCP	RF	ESR	CRP	Global	TJC 28	SJC 28
RA	257.1	1	48.4	18	0	10	5	6
RA	628.4	19	334	5	0	86	22	3
RA	12.0	>340	71.1	30	0	34	3	2
RA	42.0	1.1	0	5	8	68	8	5
RA	57.3	1	0	NA	0	25	3	1
RA	10.1	1	0	NA	48	59	4	1
RA	35.1	27	39	41	8	17	8	1
RA	7.9	0.8	29.8	8	10	82	8	5
RA	30.7	>340	115	34	6	49	0	0
RA	4.1	0.6	0	30	56	91	12	10
RA	53.1	158	127	30	5	37	4	2
RA	207.6	4.6	0	30	24	64	5	1
Unclassified inflammatory arthritis	NA	1	0	27	34	49	5	4
Unclassified inflammatory arthritis	17.4	0.9	11.5	38	0	75	5	11
Unclassified inflammatory arthritis	104.4	1.1	0	2	0	72	8	2
Unclassified inflammatory arthritis	628.4	1.6	0	12	30	100	1	1
Unclassified inflammatory arthritis	19.4	1.8	0	26	11	58	2	2
Unclassified inflammatory arthritis	22.4	0.4	0	2	0	20	1	1
Unclassified inflammatory arthritis	47.6	0.9	0	15	6	47	3	0
Unclassified inflammatory arthritis	22.3	2.8	0	NA	50	36	1	0
Unclassified inflammatory arthritis	22.3	0.5	0	0	0	30	2	2
Unclassified inflammatory arthritis	13.6	2	29.8	43	18	24	7	1
Unclassified inflammatory arthritis	22.0	1.5	21.5	123	132	80	1	1
Unclassified inflammatory arthritis	16.0	1	0	NA	13	45	7	3
Unclassified inflammatory arthritis	321.9	0.8	0	13	3	51	2	2

Diagnosis	Symptom duration (weeks)	CCP	RF	ESR	CRP	Global	TJC 28	SJC 28
Unclassified inflammatory arthritis	104.3	Not Done	0	2	1	18	18	7
Unclassified inflammatory arthritis	11.7	8	33.2	8	6	51	7	5
Psoriatic arthritis	16.1	0.9	0	16	14	79	4	0
Psoriatic arthritis	5.7	1.2	0	40	13	53	16	15
Psoriatic arthritis	32.9	0.4	14.2	2	0	23	7	5
Psoriatic arthritis	102.3	0.7	0	5	0	29	2	0
Psoriatic arthritis	51.0	Not Done	72.2	35	6	93	22	21
Psoriatic arthritis	8.4	1.7	0	2	0	14	14	10
Psoriatic arthritis	8.7	1	0	5	4	78	4	0
Psoriatic arthritis	22.3	1.2	0	37	20	65	2	1
Inflammatory arthralgia	109.3	0.9	0	2	8	11	1	0
Inflammatory arthralgia	18.4	>340	261	26	13	50	1	0
Inflammatory arthralgia	6.9	0.9	0	2	5	68	14	0
Inflammatory arthralgia	12.0	227	234	2	0	5	1	0
Inflammatory arthralgia	43.6	0.5	63	-9	0	21	1	0
Inflammatory arthralgia	14.7	1	0	27	12	51	3	0
Inflammatory arthralgia	39.9	1	0	2	0	49	0	0
Inflammatory arthralgia	13.0	Not Done	Not Done	NA	0	58	5	0
Inflammatory arthralgia	10.1	1.9	11	NA	6	69	4	0
Inflammatory arthralgia	17.0	1.4	0	NA	5	59	0	0
Inflammatory arthralgia	441.7	0.8	231	5	5	25	0	0
Inflammatory arthralgia	42.4	0.8	0	26	NA	75	8	0
Inflammatory arthralgia	NA	1.4	0	5	7	25	5	0
Inflammatory arthralgia	17.9	0.9	NA	NA	NA	70	6	0

Diagnosis	Symptom duration (weeks)	CCP	RF	ESR	CRP	Global	TJC 28	SJC 28
Inflammatory arthralgia	36.3	1.3	0	17	4	3	2	0
Inflammatory arthralgia	25.1	1	NA	20	15	54	2	0
Inflammatory arthralgia	117.6	1.3	NA	-9	8	80	1	0
Palindromic rheumatism	17.6	161	20	8	12	9	1	0
Palindromic rheumatism	11	>340	13.1	5	18	20	0	0
Diagnosis not given	260.9	>340	70.6	27	0	NA	15	17

Table 8.3 Patient clinical information collected from those used during the plasma ELISA experiments. Abbreviations used throughout the tables; CCP, Cyclic Citrullinated Peptide; RF, Rheumatoid Factor; ESR, Erythrocyte Sedimentation Rate; CRP, C-Reactive Protein; Global, Global Arthritis Score; SWJ28, Swollen Joint Count of 28 joints; TJC28, Tender Joint Count of 28 joints; N, Negative; P, Positive; and NA, Not Available.

Line	Diagnosis	Site	Gender	RF	CCP	ESR	CRP	Age	Disease duration (years)	Disease duration (weeks)	DAS28	SJC28	TJC28
ST01SY	Osteoarthritis	Knee	F	NA	NA	33	0	63	8	-	NA	NA	NA
ST02SY	Osteoarthritis	Knee	F	NA	NA	32	11	67	8	-	NA	NA	NA
ST04SY	Osteoarthritis	Hip	M	NA	NA	10	10	71	7	-	NA	NA	NA
ST08SY	Osteoarthritis	NA	M	NA	NA	NA	NA	73	10	-	NA	NA	NA
ST09SY	Osteoarthritis	Knee	F	NA	NA	NA	NA	72	30	-	NA	NA	NA
RA02SY	J Rep Est RA	Knee	F	P	NA	70	46	52	20	-	4.39	2	2
RA05SY	J Rep Est RA	Knee	F	P	NA	63	62	62	20	-	6.84	11	9
RA12SY	J Rep Est RA	Hip	F	P	NA	21	21	32	3	-	4.77	14	1
RA16SY	J Rep Est RA	Knee	F	P	NA	37	33	30	15	-	6.50	19	12
BX087	Early Resolving	Ankle	M	NA	N	37	28	27	-	4	3.76	2	2
BX127	Established RA	Ankle	F	P	N	70	112	60	-	45	5.20	10	5
BX128	Established RA	Wrist	F	P	P	NA	NA	51	-	36	NA	NA	NA
BX130	Early RA	Ankle	F	P	N	NA	NA	61	-	12	NA	NA	NA

Table 8.4 Clinical information collected from patients used in Figure 5.9. Abbreviations used throughout the tables; J Rep Est RA, Joint replacement established RA; CCP, Cyclic Citrullinated Peptide; RF, Rheumatoid Factor; ESR, Erythrocyte Sedimentation Rate; CRP, C-Reactive Protein; DAS28, Disease Activity Score in 28 joints; SWJ28, Swollen Joint Count of 28 joints; TJC28, Tender Joint Count of 28 joints; N, Negative; P, Positive; and NA, Not Available.

Line	Diagnosis	Site	Gender	RF	CCP	ESR	CRP	Age	Disease duration (years)	Disease duration (weeks)	DAS28	SJC28	TJC28
RA05SY	J Rep Est RA	Knee	F	P	NA	63	62	62	20	-	6.84	11	9
RA06SY	J Rep Est RA	Knee	M	P	NA	54	75	60	30	-	6.4	11	12
RA07SY	J Rep Est RA	Knee	F	P	NA	NA	NA	71	-	52	NA	NA	NA
RA11SY	J Rep Est RA	Knee	F	P	NA	NA	NA	62	-	1040	NA	NA	NA
RA18SY	J Rep Est RA	Knee	M	P	NA	57	45	47	23	-	3.8	1	1
BX070	Normal	Knee	M	N	N	NA	NA	44	NA	NA	NA	0	0
BX081	Normal	Knee	F	N	N	NA	NA	58	NA	NA	NA	0	0
BX082	Normal	Knee	F	N	N	NA	NA	49	NA	NA	NA	0	0
BX083	Normal	Knee	M	N	N	NA	NA	42	NA	NA	NA	0	0
BX094	Normal	Knee	F	NA	NA	NA	NA	46	NA	NA	NA	NA	NA

Table 8.5 Clinical information collected from patients used in Figure 5.10. Abbreviations used throughout the tables; J Rep Est RA, Joint replacement established RA; CCP, Cyclic Citrullinated Peptide; RF, Rheumatoid Factor; ESR, Erythrocyte Sedimentation Rate; CRP, C-Reactive Protein; DAS28, Disease Activity Score in 28 joints; SWJ28, Swollen Joint Count of 28 joints; TJC28, Tender Joint Count of 28 joints; N, Negative; P, Positive; and NA, Not Available.

ARD Online First, published on April 9, 2015 as 10.1136/annrheumdis-2014-206921

OPEN ACCESS

EXTENDED REPORT

Expression of chemokines CXCL4 and CXCL7 by synovial macrophages defines an early stage of rheumatoid arthritis

L Yeo,[1] N Adlard,[1] M Biehl,[2] M Juarez,[1] T Smallie,[1] M Snow,[3] C D Buckley,[1] K Raza,[1,4] A Filer,[1,5] D Scheel-Toellner[1]

Handling editor Tore K Kvien

▶ Additional material is published online only. To view please visit the journal online (http://dx.doi.org/10.1136/annrheumdis-2014-206921).

[1]Rheumatology Research Group, Centre for Translational Inflammation Research, College of Medical and Dental Sciences, University of Birmingham, Birmingham, UK
[2]Johann Bernoulli Institute for Mathematics and Computer Science, University of Groningen, University of Groningen, Groningen, The Netherlands
[3]Royal Orthopaedic Hospital NHS Foundation Trust, Birmingham, UK
[4]Sandwell and West Birmingham Hospitals NHS Trust, Birmingham, UK
[5]University Hospitals Birmingham NHS Foundation Trust, Birmingham, UK

Correspondence to
Dr D Scheel-Toellner, Rheumatology Research Group, Centre for Translational Inflammation Research, College of Medical and Dental Sciences, University of Birmingham, Birmingham -B15 2TT, UK; d.scheel@bham.ac.uk

LY, NA, KR, AF and DS-T contributed equally.

Received 31 October 2014
Revised 18 February 2015
Accepted 7 March 2015

To cite: Yeo L, Adlard N, Biehl M, *et al*. *Ann Rheum Dis* Published Online First: [*please include* Day Month Year] doi:10.1136/annrheumdis-2014-206921

ABSTRACT

Background and objectives For our understanding of the pathogenesis of rheumatoid arthritis (RA), it is important to elucidate the mechanisms underlying early stages of synovitis. Here, synovial cytokine production was investigated in patients with very early arthritis.

Methods Synovial biopsies were obtained from patients with at least one clinically swollen joint within 12 weeks of symptom onset. At an 18-month follow-up visit, patients who went on to develop RA, or whose arthritis spontaneously resolved, were identified. Biopsies were also obtained from patients with RA with longer symptom duration (>12 weeks) and individuals with no clinically apparent inflammation. Synovial mRNA expression of 117 cytokines was quantified using PCR techniques and analysed using standard and novel methods of data analysis. Synovial tissue sections were stained for CXCL4, CXCL7, CD41, CD68 and von Willebrand factor.

Results A machine learning approach identified expression of mRNA for CXCL4 and CXCL7 as potentially important in the classification of early RA versus resolving arthritis. mRNA levels for these chemokines were significantly elevated in patients with early RA compared with uninflamed controls. Significantly increased CXCL4 and CXCL7 protein expression was observed in patients with early RA compared with those with resolving arthritis or longer established disease. CXCL4 and CXCL7 co-localised with blood vessels, platelets and $CD68^+$ macrophages. Extravascular CXCL7 expression was significantly higher in patients with very early RA compared with longer duration RA or resolving arthritis

Conclusions Taken together, these observations suggest a transient increase in synovial CXCL4 and CXCL7 levels in early RA.

INTRODUCTION

The rheumatoid synovium is characterised by a complex inflammatory infiltrate, which can either be highly structured with distinct features of lymphoid neogenesis or comprise a more diffuse infiltrate. There is considerable evidence that cytokines produced by the synovial infiltrate play an important role in the orchestration of both the development and the resolution of synovial inflammation.[1] Since there is evidence that therapeutic outcome in rheumatoid arthritis (RA) is influenced by the time elapsed before initiation of therapy, there is a considerable clinical need to diagnose patients with early disease.[2–4] Due to the important role of cytokines in the regulation of the inflammatory infiltrate and the need to understand and diagnose early RA, this study systematically addresses the level of mRNA expression of a wide range of cytokines in the early stages of synovial inflammation.

In order to capture a population of patients in a time frame close to the onset of clinically apparent joint inflammation, patients with at least one clinically swollen joint were seen within 12 weeks of the onset of any symptom attributed, by the assessing rheumatologist, to an inflammatory arthritis. At this time, among a range of other investigations performed within the Birmingham Early Inflammatory Arthritis Cohort (BEACON), ultrasound-guided biopsies were taken. At an 18-month follow-up visit, patients who had progressed to RA as classified according to the 1987 American College of Rheumatology (ACR) criteria[5] or had resolving disease were identified for this study. Furthermore, patients from the same clinic who were disease-modifying antirheumatic drug (DMARD) naive but had synovitis for >12 weeks, as well as patients attending a clinic due to mechanical joint problems without any clinically observed inflammation, were investigated as control groups.

Profiling of cytokine mRNA expression led to the finding that the chemokines CXCL4 and CXCL7 are expressed during the earliest phase of RA, but not in patients with resolving arthritis or established RA. We found that both chemokines, which are classically regarded as platelet-derived chemokines, were also expressed on macrophages in the synovium, implicating a previously undescribed role for this cell type in the earliest clinically evident stages of RA.

PATIENTS AND METHODS

Study participants

Patients with early arthritis were seen in the BEACON cohort; details of this clinic have been reported previously.[6] Patients were eligible for the early arthritis cohort if they had at least one clinically swollen joint, were seen within 12 weeks of the onset of any symptom attributed by the assessing rheumatologist to an inflammatory arthritis and had not been treated with either DMARD or glucocorticoids prior to referral. Patients underwent a 68-joint clinical examination.[7] Patients with a joint amenable to ultrasound-guided biopsy[8] were recruited for this study. Following the biopsy, patients were followed

for up to 18 months. Patients were identified for inclusion in the study if they were classified as having RA according to 1987 ACR criteria,[5] or a resolving arthritis defined as the absence of clinically apparent synovial swelling at final assessment with no DMARDs or glucocorticoids having been used for the previous three months. A small number of patients developed chronic inflammatory diseases of the joint other than RA (table 1). As a control group, we included patients with RA with disease duration (defined as the time from the onset of any symptom attributed by the assessing rheumatologist to an inflammatory arthritis) of >12 weeks who fulfilled the 1987 ACR criteria[5] at the time of biopsy. Similarly to patients with early arthritis, those with RA of >12 weeks' duration were all DMARD and glucocorticoid naive and synovial tissue was obtained by ultrasound-guided biopsy. As a further control group, we included 'uninflamed controls' who underwent knee arthroscopy because of unexplained joint pain. None of these subjects showed inflammatory or degenerative joint pathology upon physical examination or arthroscopy. All researchers involved in the investigation of biopsies either at mRNA or protein level were blinded to patient outcome throughout the study.

Ultrasound-guided synovial biopsy

Prior to biopsy, joints were assessed using a Siemens Acuson Antares scanner (Siemens, Bracknell, UK) and multifrequency (5–13 MHz) linear array transducers; for details, see Filer *et al*.[7] Ultrasound-guided biopsy was used to collect tissue from multiple regions within knee, ankle or metacarpophalangeal (MCP) joints in which there was evidence of grey-scale synovitis. Ultrasound guidance was used to introduce a single portal through which tissue was sampled using custom manufactured 2.0 mm cutting-edged forceps or a 16 g core biopsy needle (MCP joint).[9] Frozen blocks were assembled for processing from six individual biopsies in order to overcome synovial heterogeneity.[8 10–12]

Synovial tissue cytokine mRNA real-time PCR analysis

TaqMan low-density real-time PCR arrays (Applied Biosystems, Paisley, UK) were designed to determine expression of 117 cytokines and cytokine-related molecules (for full details, see online supplementary table S1). RNA was extracted from synovial tissue sections using an RNeasy RNA extraction kit (Qiagen, Crawley, UK). RNA from synovial tissue used in the low-density array for genes with non-intron spanning primers was treated with DNase (Qiagen). A reaction mixture containing RNA, QuantiTect-RT Master Mix (Qiagen) and QuantiTect Reverse Transcriptase (Qiagen, Crawley, UK) was added to a TaqMan low-density array microfluidic card. Six times more RNA was loaded into microfluidic cards designed for weakly expressed genes and genes with non-intron spanning primers (see online supplementary table S1). Reverse transcription and real-time PCR was performed in a 7900HT Real-Time PCR System (Applied Biosystems). Relative gene expression (RQ) was expressed as $2^{-\Delta Ct}$, where ΔCt represents the difference in Ct between glyceraldehyde-3-phosphate dehydrogenase and the target gene. Validation experiments established the reproducibility of quantitation and a combination of positive controls from anti-CD3/anti-CD28-activated lymphocytes and commercially available control mRNA from human cell lines representing different tissues (Stratagene) were used to ascertain that all cytokines listed could be detected.

GMLVQ analysis of cytokine mRNA profiles

Cytokine mRNA data were log-transformed and all zero values were replaced by 0.00002, the smallest non-zero expression value in the data. This yielded 117 log-transformed expression values per patient. These data were analysed by applying a combination of principal component analysis and learning vector quantisation (LVQ), a distance-based classification technique, which determines class representatives from a set of example data in an iterative training process. Example data corresponded to the individual cytokine profiles observed within the four classes of patients. Matrix relevance LVQ identifies a suitable distance measure, which is discriminative with respect to the different classes. The specific technique used was generalised matrix relevance LVQ (GMLVQ), a variant that optimises the distance measure with respect to its discriminative power.[13] Further details on this methodology can be found in online supplementary method 1.

Immunofluorescence

Frozen sections from synovial biopsies taken from patients with resolving arthritis, early RA and established RA were stained with antibodies specific for CXCL4 (Abcam, UK) or CXCL7

Table 1 Demographic and clinical characteristics of study participants used for cytokine and chemokine mRNA real-time PCR low-density arrays

	Uninflamed	Resolving arthritis	Early RA	Established RA
Number	10	9	17	12
Symptom duration (weeks); median (IQR)	na	5 (2–9)	6 (4–9)	38 (27–52)
Female; n (%)	5 (50)	3 (33)	12 (71)	6 (50)
Age years; median (IQR)	43 (37–48)	40 (30–69)	53 (48–59)	60 (48–67)
RF and/or anti-CCP positive; n (%)	na	0 (0)	8 (47)	7 (58)
Global disease-related variables				
CRP; median (IQR)	na	10 (8–22)	12 (5–32)	17 (7–52)
ESR; median (IQR)	na	24 (8–48)	25 (14–58)	28 (12–55)
DAS28; median (IQR)	na	4.1 (3.4–4.6)	4.7 (4.2–6.0)	5.4 (4.7–6.6)
Biopsied joint-related variables				
Joint biopsied				
Ankle; n (%)	0 (0)	3 (33.3)	4 (24)	2 (17)
Knee; n (%)	10 (100)	6 (66.6)	10 (59)	10 (83)
MCP joint; n (%)	0 (0)	0 (0)	3 (18)	0 (0)

CCP, cyclic citrullinated peptide; CRP, C-reactive protein; DAS28, Disease Activity Score in 28 Joints; ESR, erythrocyte sedimentation rate; MCP, metacarpophalangeal; na, not available; RF, rheumatoid factor.

(Novus Biologicals, UK), and CD41 (Dako, UK), CD68 (Thermo Scientific Pierce, UK) and von Willebrand factor (vWF) (Dako, UK). Staining with isotype-matched, species-matched and concentration-matched negative controls was performed in parallel. Secondary antibodies used were goat antirabbit Chromeo 494 (Abcam, UK), Cy3-conjugated streptavidin (Jackson Immunoresearch, USA), goat antimouse Alexa Fluor 488 (Jackson Immunoresearch, USA) and goat antimouse Cy5 (Southern Biotechnology, USA). Immunofluorescence was visualised using a Zeiss LSM 780 Zen Confocal and analysed using Zeiss imaging software (Zeiss, Germany). Five to six 2×2 tile scans were taken from each section at ×400 total magnification. Regions were drawn around tissue; areas with folding or bleeding into tissue caused during biopsy collection/processing were excluded from analysis. As readout, pixels per unit area were calculated.

RESULTS

Study participants

Details of study participants used for cytokine mRNA profiling and immunofluorescence studies are shown in tables 1 and 2, respectively. The symptom durations of patients with early arthritis highlight that this population was captured very soon after the onset of their clinically apparent disease (median 5 weeks for those with resolving disease and 6 weeks for those with early RA in the patients who provided samples for cytokine mRNA profiling; median 6 weeks for those with resolving disease and 7 weeks for those with early RA in the patients who provided samples for immunofluorescence studies).

Synovial cytokine mRNA expression profiles in early arthritis

The mRNA expression of a panel of 117 cytokines and related molecules was assessed in synovial biopsies using low-density real-time PCR arrays. Subject groups investigated were patients with resolving arthritis (n=9), patients with very early RA (n=17), patients with established RA (>3 months' symptom duration; n=12) and uninflamed control subjects (n=10). Twenty-two genes were identified as being differentially expressed between subject groups by Kruskal–Wallis and Dunn's post-test analysis, shown in figure 1A. Eighteen of these genes were more highly expressed in patients with established RA compared with the uninflamed controls. Of interest, both CXCL4 and CXCL7 mRNA levels were found to be significantly elevated in patients with early RA compared with uninflamed controls, and showed a trend towards higher expression in early RA compared with patients with resolving arthritis. Intriguingly there was also a trend towards higher expression in early RA compared with established RA, suggesting an increase in CXCL4 and CXCL7 levels in the early phase of disease in patients whose arthritis persisted versus those whose arthritis resolved. No significant differences were observed in CXCL4 and CXCL7 expression between cyclic citrullinated peptide (CCP)-positive and CCP-negative patients in either the early RA or established RA groups (see online supplementary figure S2). When cytokine and chemokine mRNA expression was ranked by their difference in expression between resolving arthritis and early RA groups, CXCL4 and CXCL7 were ranked highly in showing differential expression between the two groups (figure 1B).

Machine learning classification selection of differentiating cytokines and chemokines

We applied a novel strategy of multivariate analysis to test whether combinations of gene expression signals rather than individual cytokine mRNA signals could distinguish synovium from patients with self-limiting arthritis from those with early-stage RA. Matrix relevance GMLVQ analysis was applied to the cytokine mRNA data to achieve classification of samples by determining a discriminative distance measure that characterises differences between subject groups. For classification of the established RA and uninflamed groups, analysis of the obtained relevance matrix revealed that the 10 most informative genes in discriminating patients with established RA from uninflamed controls were CXCL7, CXCL4, IL1B, MST1, CCL20, IL8, LGALS12, LTA, CXCL13 and OSM (figure 2A). Receiver-operating characteristic (ROC) analysis was used to assess the performance of classifier models for group classification. For the established RA and uninflamed group classification, GMLVQ yielded an area under the curve (AUC) of 0.996 (figure 2B). For classification of the early RA and resolving arthritis groups, the 10 most informative genes corresponded to CXCL7, CXCL4, MST1, CCL20, LGALS12, IL8, IL1B, CXCL1, LTA and IL1RN (figure 2C). ROC analysis yielded

Table 2 Demographic and clinical characteristics of study participants used for detection of CXCL4 and CXCL7 by immunofluorescence

	Resolving arthritis	Early RA	Established RA	Early non-RA
Number	9	10	11	5
Symptom duration (weeks); median (IQR)	6 (3–7)	7 (4.8–9.3)	45 (16–53)	7 (2–8.5)
Female; n (%)	3 (33)	5 (50)	6 (55)	2 (40)
Age, years; median (IQR)	37 (33–65)	58 (50–65)	62 (57–65)	41 (37–56)
RF and/or anti-CCP positive; n (%)	0 (0)	4 (40)	6 (55)	1 (20)
Global disease-related variables				
CRP; median (IQR)	8 (3–13.5)	26 (7.5–58)	10 (0–79)	25 (18.5–54)
ESR; median (IQR)	18 (5.5–51)	19 (4.75–39.25)	50 (34–70)	44 (24–73.5)
DAS28; median (IQR)	4.1 (3.4–5.7)	4.7 (3.8–5.8)	5.2 (4.6–7.5)	4.8 (4.1–6.4)
Biopsied joint-related variables				
Joint biopsied				
Ankle; n (%)	2 (22)	2 (20)	3 (27)	2 (40)
Knee; n (%)	7 (78)	7 (70)	8 (73)	3 (60)
MCP joint; n (%)	0 (0)	1 (10)	0 (0)	0 (0)

Early non-RA group: psoriatic arthritis n=2, sarcoidosis n=1, ankylosing spondylitis n=1, unclassified n=1.
CCP, cyclic citrullinated peptide; CRP, C-reactive protein; DAS28, Disease Activity Score in 28 Joints; ESR, erythrocyte sedimentation rate; MCP, metacarpophalangeal; na, not available; RF, rheumatoid factor.

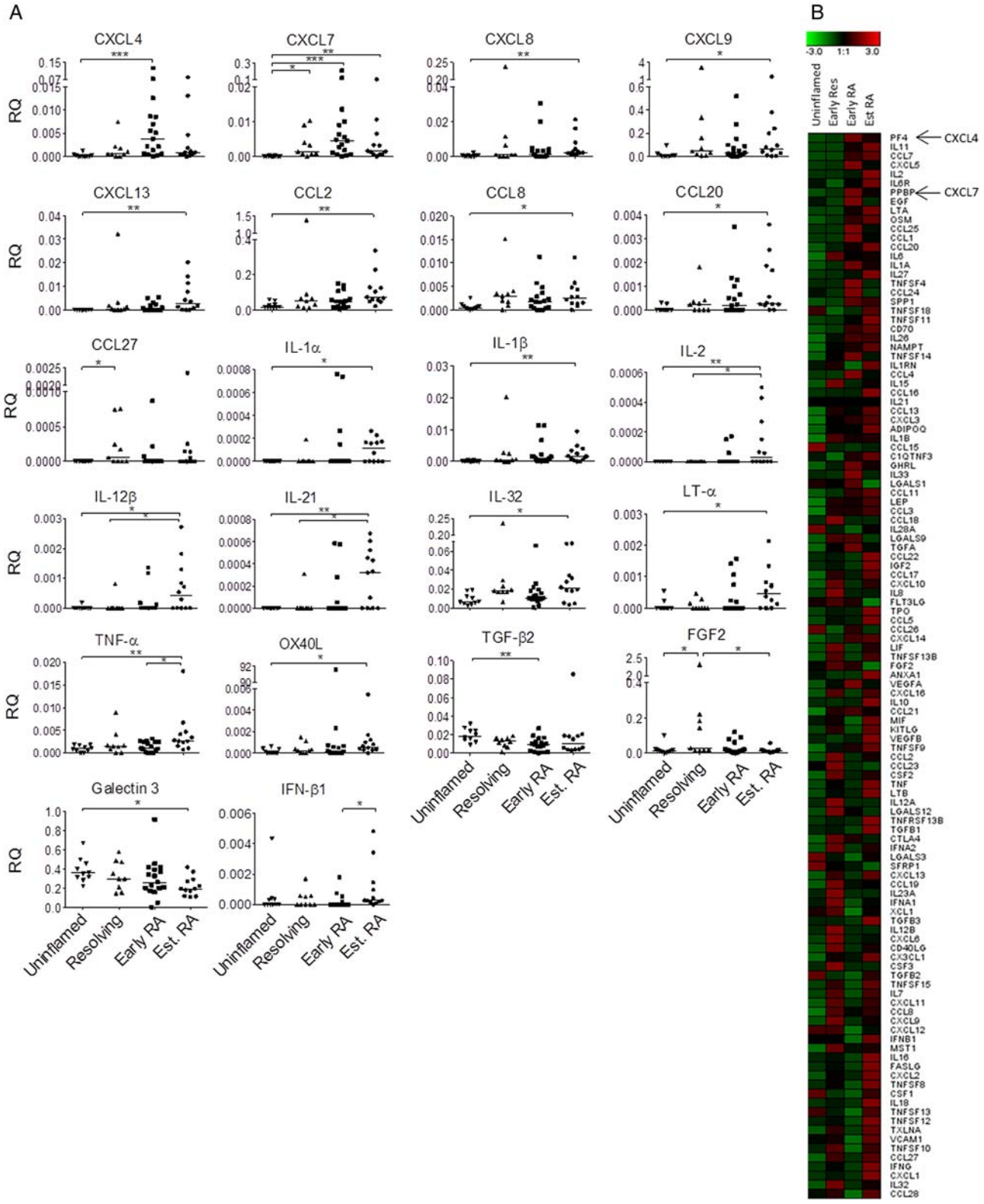

Figure 1 Cytokine and chemokine mRNA expression in synovial biopsies from uninflamed controls and patients with resolving arthritis, early rheumatoid arthritis (RA) and established RA. (A) Synovial tissue sections were assessed from uninflamed controls (n=10) and patients with resolving arthritis (n=9), early RA (n=17) and established RA (n=12). Data for genes for which the Kruskal–Wallis and Dunn's post-test showed significant difference between the four groups are shown. * p<0.05, ** p<0.01, ***p<0.001. (B) Cytokine and chemokine genes were ranked by difference in mRNA expression between resolving arthritis and early RA groups. Means of each group are represented in the heat map. Green represents low and red high relative expression (z-score of mean expression levels).

an AUC of 0.764 (figure 2D). In both cases, CXCL4 and CXCL7 played dominant roles in terms of discriminative power.

CXCL4 and CXLC7 protein expression in synovial tissue

Since cytokine mRNA profiling suggested an upregulation of CXCL4 and CXCL7 expression in patients with early RA, we

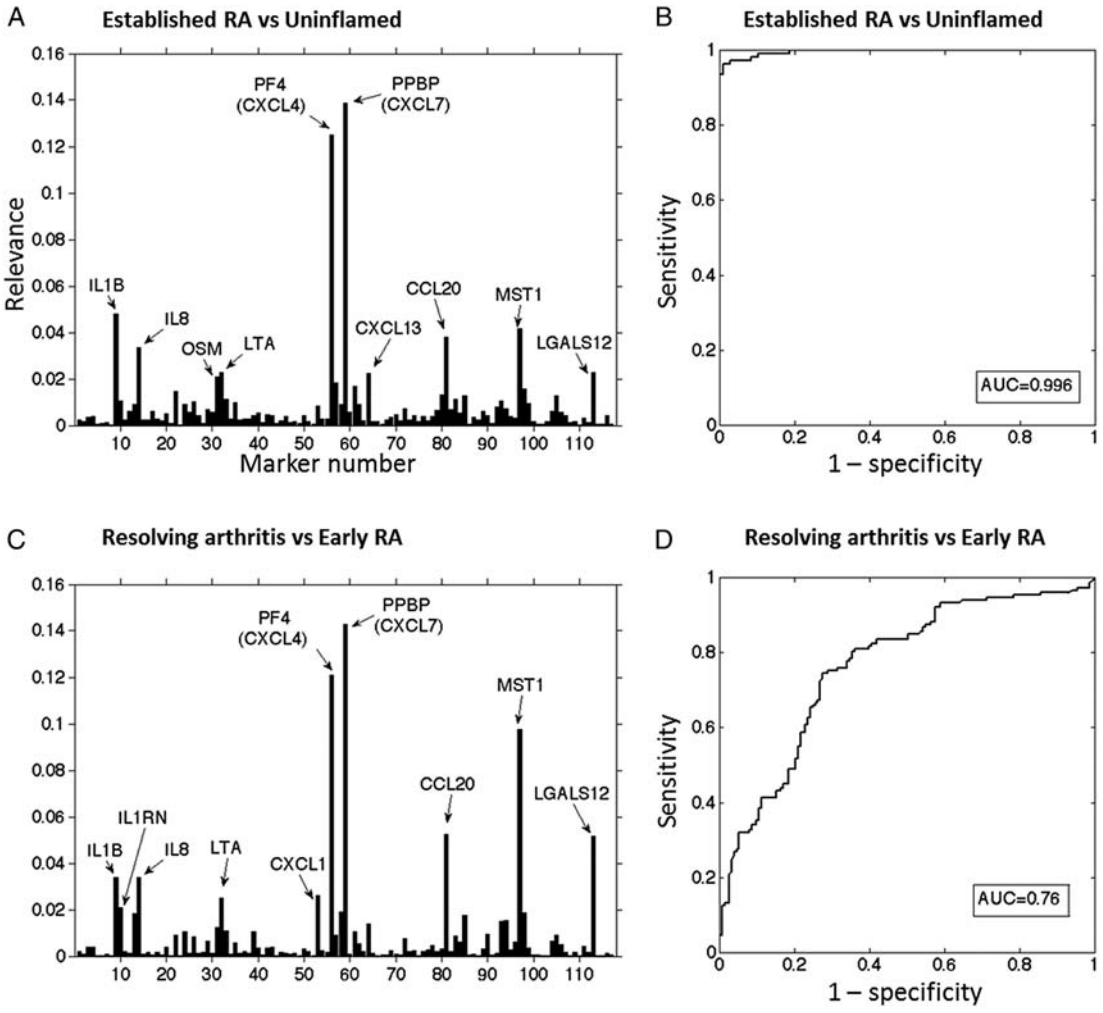

Figure 2 Generalised matrix relevance learning vector quantisation-based discrimination of subject groups (A) All 117 cytokine/chemokine genes used to classify uninflamed controls versus patients with established rheumatoid arthritis (RA). The 10 genes most informative in discriminating groups are indicated. (B) Receiver-operating characteristic (ROC) characteristics of the obtained classifiers for uninflamed controls and patients with established RA. (C) Classification cytokine mRNA signals in resolving arthritis versus patients with early RA. The 10 genes most informative in discriminating groups are indicated. (D) ROC characteristics of the obtained classifiers for patients with resolving arthritis and early RA. AUC, area under the curve.

next sought to test whether expression of these chemokines was also elevated at the protein level. CXCL4 and CXCL7 were stained in synovial tissue sections from patients with resolving arthritis (n=9), early RA (n=10) and established RA (n=11), and staining was visualised by immunofluorescence. Representative images of staining of CXCL4 and CXCL7 in the synovium are shown in figure 3A, B. Synovial tissue sections were co-stained for CD68 to identify macrophages, CD41 to identify platelets and vWF to identify vascular endothelial cells. Both CXCL4 and CXCL7 were found to be expressed in the synovium of all subject groups examined. However, expression of both CXCL4 and CXCL7 was significantly elevated in patients with early RA compared with patients with resolving arthritis (CXCL4 and CXCL7; $p<0.05$) and patients with established RA (CXCL4 and CXCL7; $p<0.05$; figure 3C), which supported the findings made at the mRNA level. Quantification of protein levels of CD41, which is specifically expressed by platelets, did not show significant differences (data not shown). The groups of patients investigated in the cytokine mRNA profiling and those tested for immunofluorescence studies were partially overlapping. Protein data from seven patients who were not investigated in the mRNA study also showed a higher level of CXCL4 and CXCL7 protein expression in the patients with early RA compared with those with established disease (see online supplementary figure S3A and B). A small number of patients developed chronic inflammatory joint diseases other than RA (table 2). Their CXCL4 and CXCL7 levels are shown in online supplementary figures S3C, D.

In the synovium of all subject groups studied, CXCL4 and CXCL7 staining was found to co-localise with CD68 staining, indicating an association of both of these chemokines with macrophages (figure 4A, B). As expected, CXCL4 and CXCL7 staining was also observed on CD41-expressing platelets (figure 3). To further investigate this finding, synovial tissue samples were stained for vWF and expression of CXCL4 and CXCL7 was quantified inside and outside of the vasculature. Quantification of positive pixels showed that CXCL4 and CXCL7 were found predominantly outside the vasculature (figure 5A, B). In addition, the specificity of the CXCL7 staining was confirmed by inhibition of staining with preincubation of the antibody with recombinant CXCL7 (see online supplementary figure S1).

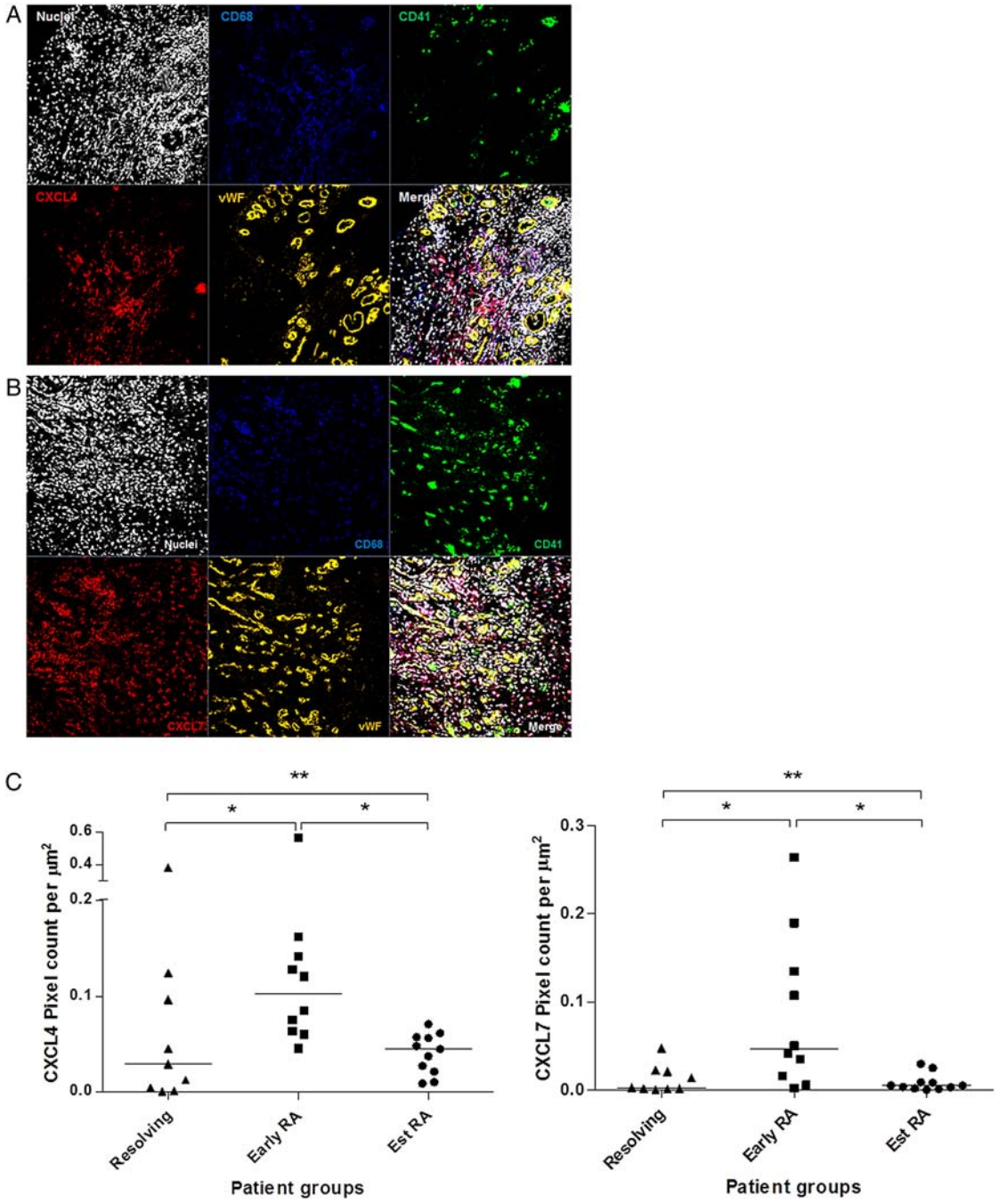

Figure 3 Immunofluorescence staining of CXLC4 and CXCL7 in synovial tissue sections. (A) Synovial tissue staining of CXCL4 (red), CD68 (blue), CD41 (green) and von Willebrand factor (vWF) (orange). (B) Synovial tissue staining of CXCL7 (red), CD68 (blue), CD41 (green) and vWF (orange). Nuclear counterstain is shown. Images are representative of early rheumatoid arthritis (RA) synovium (n=10). No staining was observed using isotype and concentration-matched negative controls. Images were taken at ×40 magnification. (C) Quantification of CXCL4 and CXCL7 staining, calculated as the number of pixels per μm^2 over 6× 2×2 tile scans at ×40 magnification, in synovial tissue sections from patients with resolving arthritis (n=9), early RA (n=10) and established RA (n=11). Patients with early RA showed a significantly higher level of CXCL4 ($p<0.05$) and CXCL7 ($p<0.05$) compared with patients with resolving arthritis and established RA. Kruskal–Wallis and Dunn's post-test; * $p<0.05$, ** $p<0.01$.

DISCUSSION

In this study, we have identified two chemokines, CXCL4 and CXCL7, which are expressed in the earliest clinically apparent stage of RA. They were predominantly detected on macrophages infiltrating the synovium, indicating a previously undescribed role for this cell type in contributing to RA pathogenesis in the very early phase of disease.

Macrophages are found in large numbers throughout the rheumatoid synovium. Type A synoviocytes are macrophage-derived cells that constitute part of the healthy synovial lining while large numbers of activated macrophages are found in the inflammatory infiltrate in the sublining and at the pannus–cartilage interface. The origin of these cells is a matter of debate; they could derive from the proliferation of tissue-based macrophages or from circulating monocytes entering from the blood stream.[14–17] Macrophages are important contributors to inflammation and joint destruction due to their production of proinflammatory mediators and tissue-degrading enzymes.

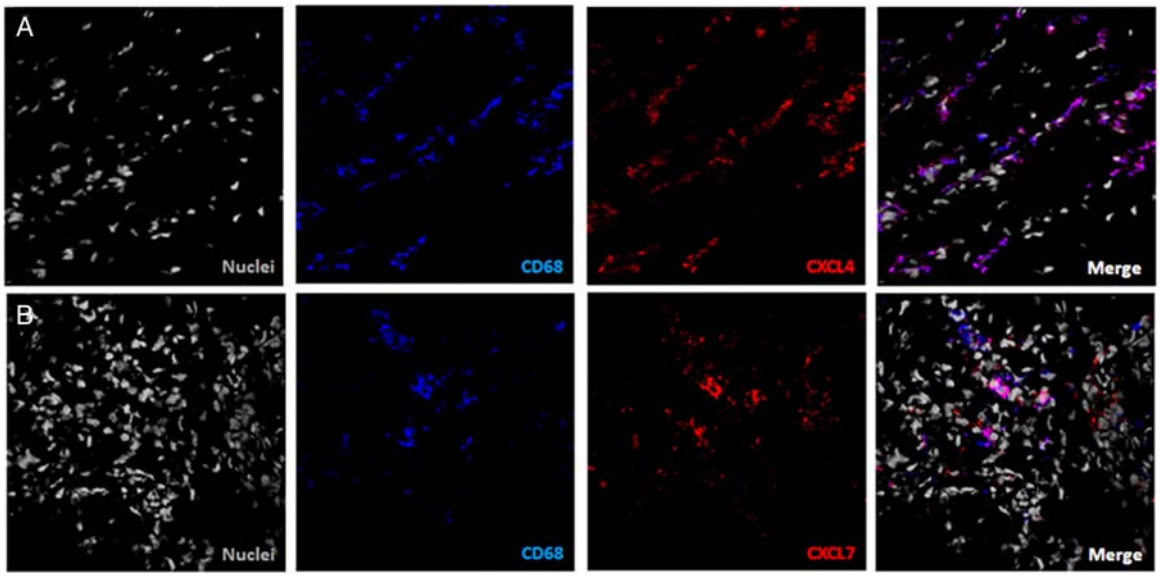

Figure 4 Co-localisation of CXCL4 and CXCL7 with CD68-positive cells. (A) Synovial tissue staining of CXCL4 (red) and CD68 (blue) and (B) staining of CXCL7 (red) and CD68 (blue) showed co-localisation of both cytokines with macrophages. Image representative of rheumatoid arthritis synovium (n=10).

Furthermore, the number of synovial macrophage has been found to correlate with joint erosion in RA while changes in the numbers of CD68+ macrophages correlate with therapeutic success of a range of therapies.[18–20]

CXCL4 is chemotactic for neutrophils, fibroblasts and monocytes, prevents monocyte apoptosis, induces differentiation of monocytes into macrophages and enhances monocyte phagocytosis and oxygen radical production.[21–24] CXCL7 is involved in neutrophil chemotaxis and activation, and activates connective tissue cells.[25] The functions described for CXCL4 and CXCL7 suggest that in RA these chemokines could not only exacerbate synovial inflammation but also promote its chronicity by attracting monocytes to the inflamed tissue and activating them following recruitment to the synovium. Our finding that CXCL4 and CXCL7 are highly expressed during the first 12 weeks of synovitis in patients who develop RA but are found at lower levels in longer duration RA may reflect local pathological changes occurring during this critical phase, which has been described as the therapeutic 'window of opportunity'. A similar phenomenon was recently reported by van Bon *et al*,[26] who demonstrated high levels of CXCL4 expression in patients at an early stage of systemic sclerosis.

Previous studies have suggested roles for CXCL4 and CXCL7 in RA. Elevated levels of CXCL7 have been reported in the serum, synovial fluid and synovial tissue of patients with RA.[27 28] While CXCL7 promotes angiogenesis, CXCL4 has an antiangiogenic effect.[29] The elevated expression of the angiostatic chemokine CXCL4 during the early phase of disease may reflect an attempt to prevent or minimise the first signs of angiogenesis that takes place in the RA synovium.

In our study, CXCL4 and CXCL7 expression in the synovium was found to be predominantly localised to CD68+ macrophages, with less co-localisation observed with platelets. Where CXCL4 and CXCL7 expression was seen to co-localise with platelets in the synovium, this was mainly confined to vessel thrombi. The genes for CXCL4 and CXCL7 are located in a

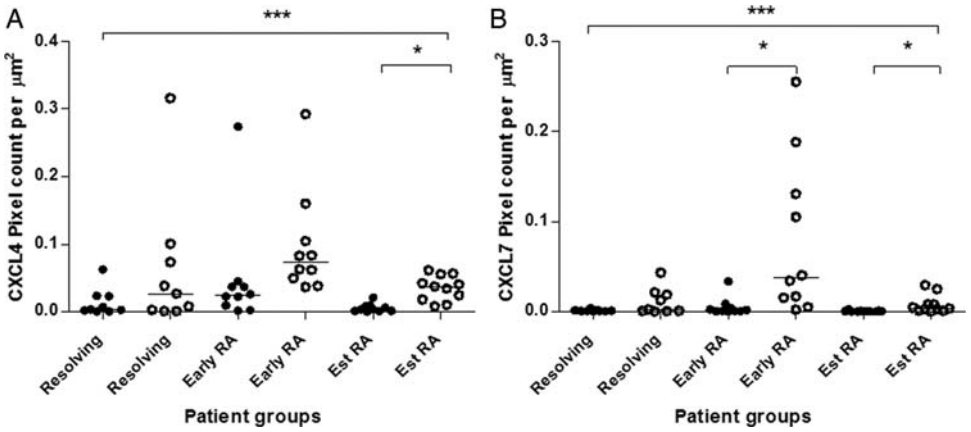

Figure 5 Expression of CXCL4 and CXCL7 in the synovium is predominantly found outside the vasculature. Staining of CXCL4 and CXCL7 in synovial tissue sections was quantified inside and outside of the vasculature, as assessed by co-staining with von Willebrand factor. Expression of both chemokines was significantly elevated outside the vasculature. RA, rheumatoid arthritis. Kruskal–Wallis test, Dunn's post-test; *p<0.05, ***p<0.001.

gene cluster comprising several CXC chemokines in a locus on chromosome 4,[30 31] which was once considered to be megakaryocyte-specific. However, other studies have reported that expression of these chemokines is not restricted to the megakaryocyte lineage. A recent study using a PF4-Cre mouse model reported that CXCL4 could be produced by both myeloid and lymphoid lineages, with CXCL4 transcripts detected in adult haematopoietic stem cells.[32] In a similar reporter gene model, CXCL4 expression was shown in mature murine macrophages.[33] Furthermore, Schaffner *et al*[34] reported expression of CXCL4 by human monocytes and found that CXCL4 expression was upregulated upon monocyte activation. Intriguingly, a recent study reported CXCL4 expression by activated T cells that limited Th17 differentiation.[35] Monocytes have been described to constitutively transcribe and translate CXCL7, which is processed intracellularly into several derivatives known to have signalling and effector functions.[36] Together this evidence is supportive of our finding that CXCL4 and CXCL7 is associated with and may be produced directly by macrophages in the synovium during very early RA.

Interest in chemokines in RA has been revived by findings such as detection of citrullinated chemokines in RA synovial fluid that have enhanced chemotactic activity[37] and the prospect of using antichemokine targeting for therapeutic purposes.[38 39] We have interpreted the high levels of CXCL4 and CXCL7 found in early RA compared with resolving arthritis or established RA to represent a transient upregulation of these cytokines based on a cross-sectional analysis of samples; it would be interesting to confirm the transient nature of this upregulation in a longitudinal study. However, the ethical implications would make an observational study of the evolution of synovial tissue pathology from early to established RA in the absence of therapeutic intervention impossible to conduct in patients. In the future, it will be important to investigate whether the production of CXCL4 and CXCL7 observed in the synovium in early RA is reflected by elevated levels in plasma samples. Future use of these chemokines as biomarkers for prediction of progression to RA will depend on replication in other independent cohorts.

Twitter Follow Nichola Adlard at @Nichola_Adlard

Acknowledgements We gratefully acknowledge the excellent technical support by Ms Holly Adams.

Contributors LY, NA, KR, AF and DS-T contributed equally to the article. LY and NA have performed most of the experimental work and have contributed to planning, data analysis, and writing of the project and manuscript. MB and TS have performed computational analysis of the data. MJ and MS have contributed unique clinical samples. DS-T, KR, AF and CDB have designed, managed and analysed the project and have written the manuscript. All authors have read and agreed the final version of the manuscript.

Funding This report is independent research supported by the National Institute for Health Research/Wellcome Trust Clinical Research Facility at University Hospitals Birmingham NHS Foundation Trust. We gratefully acknowledge funding from an Arthritis Research UK PhD studentship (Ref 19593) supporting NA and a Medical Research Council PhD studentship supporting LY (Ref G0700023-2/1). AF was supported by an Arthritis Research UK Clinician Scientist Award 18547. MB held a visiting fellowship funded by the Institute of Advanced Studies, University of Birmingham, during which the computational analysis was completed. The Arthritis Research UK Rheumatoid Arthritis Pathogenesis Centre of Excellence is part-funded by Arthritis Research UK through grant number 20298. Furthermore, we received funding from European Community's Collaborative project FP7-HEALTH-F2-2012-305549 'Euro—TEAM'.

Competing interests None.

Patient consent Obtained.

Ethics approval West Midlands Black Country REC.

Provenance and peer review Not commissioned; externally peer reviewed.

REFERENCES

1 McInnes IB, Schett G. Cytokines in the pathogenesis of rheumatoid arthritis. *Nat Rev Immunol* 2007;7:429–42.
2 Raza K, Buckley CE, Salmon M, *et al*. Treating very early rheumatoid arthritis. *Best Pract Res Clin Rheumatol* 2006;20:849–63.
3 van der Linden MP, le Cessie S, Raza K, *et al*. Long-term impact of delay in assessment of patients with early arthritis. *Arthritis Rheum* 2010;62:3537–46.
4 Nell VP, Machold KP, Eberl G, *et al*. Benefit of very early referral and very early therapy with disease-modifying anti-rheumatic drugs in patients with early rheumatoid arthritis. *Rheumatology (Oxford)* 2004;43:906–14.
5 Arnett FC, Edworthy SM, Bloch DA, *et al*. The American Rheumatism Association 1987 revised criteria for the classification of rheumatoid arthritis. *Arthritis Rheum* 1988;31:315–24.
6 Raza K, Breese M, Nightingale P, *et al*. Predictive value of antibodies to cyclic citrullinated peptide in patients with very early inflammatory arthritis. *J Rheumatol* 2005;32:231–8.
7 Filer A, de Pablo P, Allen G, *et al*. Utility of ultrasound joint counts in the prediction of rheumatoid arthritis in patients with very early synovitis. *Ann Rheum Dis* 2011;70:500–7.
8 Scire CA, Epis O, Codullo V, *et al*. Immunohistological assessment of the synovial tissue in small joints in rheumatoid arthritis: validation of a minimally invasive ultrasound-guided synovial biopsy procedure. *Arthritis Res Ther* 2007;9:R101.
9 Kelly S, Humby F, Filer A, *et al*. Ultrasound-guided synovial biopsy: a safe, well-tolerated and reliable technique for obtaining high-quality synovial tissue from both large and small joints in early arthritis patients. *Ann Rheum Dis* 2015;74:611–17.
10 Schumacher HR, Kitridou RC. Synovitis of recent onset. A clinicopathologic study during the first month of disease. *Arthritis Rheum* 1972;15:465–85.
11 Freeston JE, Wakefield RJ, Conaghan PG, *et al*. A diagnostic algorithm for persistence of very early inflammatory arthritis: the utility of power Doppler ultrasound when added to conventional assessment tools. *Ann Rheum Dis* 2010;69:417–19.
12 van de Sande MG, Gerlag DM, Lodde BM, *et al*. Evaluating antirheumatic treatments using synovial biopsy: a recommendation for standardisation to be used in clinical trials. *Ann Rheum Dis* 2011;70:423–7.
13 Schneider P, Biehl M, Hammer B. Adaptive relevance matrices in learning vector quantization. *Neural Comput* 2009;21:3532–61.
14 Edwards JC, Willoughby DA. Demonstration of bone marrow derived cells in synovial lining by means of giant intracellular granules as genetic markers. *Ann Rheum Dis* 1982;41:177–82.
15 Smith MD. The normal synovium. *Open Rheumatol J* 2011;5:100–6.
16 Jenkins SJ, Hume DA. Homeostasis in the mononuclear phagocyte system. *Trends Immunol* 2014;35:358–67.
17 Schulz C, Gomez Perdiguero E, Chorro L, *et al*. A lineage of myeloid cells independent of Myb and hematopoietic stem cells. *Science* 2012;336:86–90.
18 Tak PP, Smeets TJ, Daha MR, *et al*. Analysis of the synovial cell infiltrate in early rheumatoid synovial tissue in relation to local disease activity. *Arthritis Rheum* 1997;40:217–25.
19 Mulherin D, Fitzgerald O, Bresnihan B. Synovial tissue macrophage populations and articular damage in rheumatoid arthritis. *Arthritis Rheum* 1996;39:115–24.
20 Smeets TJ, Kraan MC, van Loon ME, *et al*. Tumor necrosis factor alpha blockade reduces the synovial cell infiltrate early after initiation of treatment, but apparently not by induction of apoptosis in synovial tissue. *Arthritis Rheum* 2003;48:2155–62.
21 Flad HD, Grage-Griebenow E, Scheuerer B, *et al*. The role of cytokines in monocyte apoptosis. *Res Immunol* 1998;149:733–6.
22 Scheuerer B, Ernst M, Durrbaum-Landmann I, *et al*. The CXC-chemokine platelet factor 4 promotes monocyte survival and induces monocyte differentiation into macrophages. *Blood* 2000;95:1158–66.
23 Fricke I, Mitchell D, Petersen F, *et al*. Platelet factor 4 in conjunction with IL-4 directs differentiation of human monocytes into specialized antigen-presenting cells. *FASEB J* 2004;18:1588–90.
24 Xia CQ, Kao KJ. Effect of CXC chemokine platelet factor 4 on differentiation and function of monocyte-derived dendritic cells. *Int Immunol* 2003;15:1007–15.
25 Castor CW, Ritchie JC, Scott ME, *et al*. Connective tissue activation. XI. Stimulation of glycosaminoglycan and DNA formation by a platelet factor. *Arthritis Rheum* 1977;20:859–68.
26 van Bon L, Affandi AJ, Broen J, *et al*. Proteome-wide analysis and CXCL4 as a biomarker in systemic sclerosis. *N Engl J Med* 2014;370:433–43.

27 Castor CW, Andrews PC, Swartz RD, *et al*. Connective tissue activation. XXXVI. The origin, variety, distribution, and biologic fate of connective tissue activating peptide-III isoforms: characteristics in patients with rheumatic, renal, and arterial disease. *Arthritis Rheum* 1993;36:1142–53.
28 Castor CW, Smith EM, Hossler PA, *et al*. Connective tissue activation. XXXV. Detection of connective tissue activating peptide-III isoforms in synovium from osteoarthritis and rheumatoid arthritis patients: patterns of interaction with other synovial cytokines in cell culture. *Arthritis Rheum* 1992;35:783–93.
29 Strieter RM, Polverini PJ, Kunkel SL, *et al*. The functional role of the ELR motif in CXC chemokine-mediated angiogenesis. *J Biol Chem* 1995;270:27348–57.
30 Tunnacliffe A, Majumdar S, Yan B, *et al*. Genes for beta-thromboglobulin and platelet factor 4 are closely linked and form part of a cluster of related genes on chromosome 4. *Blood* 1992;79:2896–900.
31 Zhang C, Thornton MA, Kowalska MA, *et al*. Localization of distal regulatory domains in the megakaryocyte-specific platelet basic protein/platelet factor 4 gene locus. *Blood* 2001;98:610–17.
32 Calaminus SD, Guitart AV, Sinclair A, *et al*. Lineage tracing of Pf4-Cre marks hematopoietic stem cells and their progeny. *PLoS ONE* 2012;7:e51361.
33 Pertuy F, Aguilar A, Strassel C, *et al*. Broader expression of the mouse platelet factor 4-cre transgene beyond the megakaryocyte lineage. *J Thromb Haemost* 2015;13:115–25.
34 Schaffner A, Rhyn P, Schoedon G, *et al*. Regulated expression of platelet factor 4 in human monocytes—role of PARs as a quantitatively important monocyte activation pathway. *J Leukoc Biol* 2005;78:202–9.
35 Shi G, Field DJ, Ko KA, *et al*. Platelet factor 4 limits Th17 differentiation and cardiac allograft rejection. *J Clin Invest* 2014;124:543–52.
36 El-Gedaily A, Schoedon G, Schneemann M, *et al*. Constitutive and regulated expression of platelet basic protein in human monocytes. *J Leukoc Biol* 2004;75:495–503.
37 Yoshida K, Korchynskyi O, Tak PP, *et al*. Citrullination of ENA-78/CXCL5 results in conversion from a non-monocyte recruiting to a monocyte recruiting chemokine. *Arthritis Rheumatol* 2014;66:2716–27.
38 Koch AE. Chemokines and their receptors in rheumatoid arthritis: future targets? *Arthritis Rheum* 2005;52:710–21.
39 Szekanecz Z, Koch AE. Macrophages and their products in rheumatoid arthritis. *Curr Opin Rheumatol* 2007;19:289–95.

Expression of chemokines CXCL4 and CXCL7 by synovial macrophages defines an early stage of rheumatoid arthritis

L Yeo, N Adlard, M Biehl, M Juarez, T Smallie, M Snow, C D Buckley, K Raza, A Filer and D Scheel-Toellner

Ann Rheum Dis published online April 9, 2015

Notes